DOE/NV/10039-3
(DE81030487)

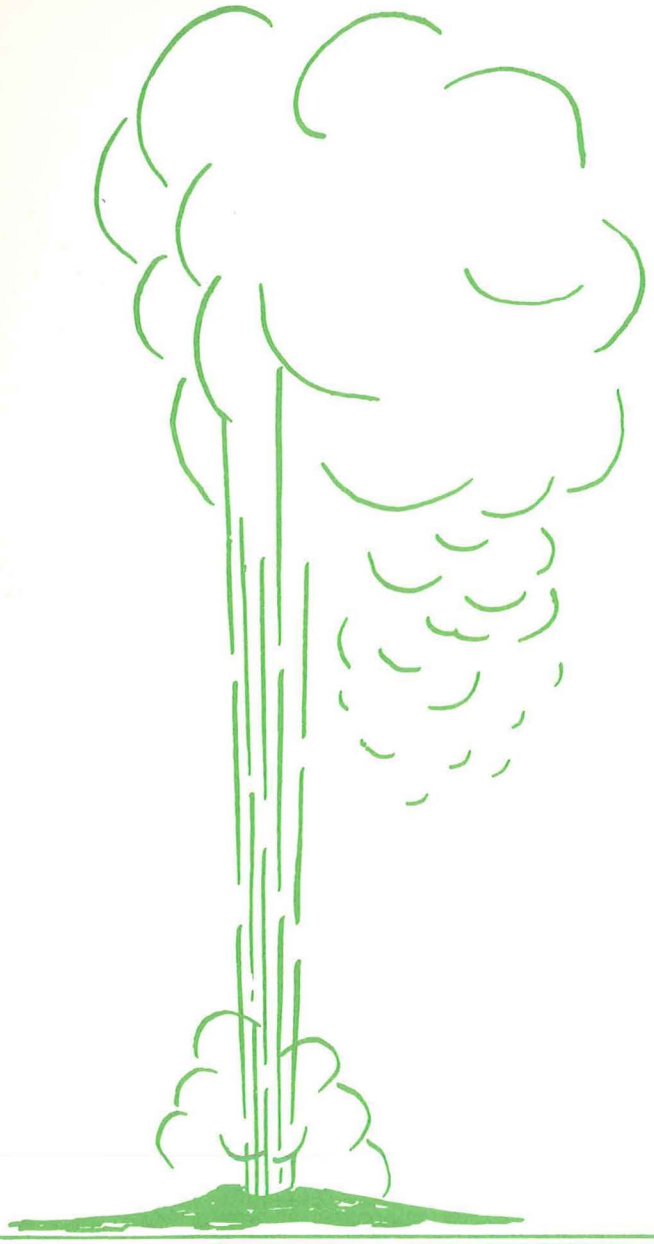

LOW-TO-MODERATE TEMPERATURE GEOTHERMAL RESOURCE ASSESSMENT FOR NEVADA: AREA SPECIFIC STUDIES

Final Report for the Period June 1, 1980–August 30, 1981

By
Dennis T. Trexler
Brian A. Koeing
Thomas Flynn
James L. Bruce
George Ghusn, Jr.

Work Performed Under Contract No. AC08-79NV10039

Nevada Bureau of Mines and Geology
University of Nevada
Reno, Nevada

U. S. DEPARTMENT OF ENERGY
Geothermal Energy

DISCLAIMER

Available from the National Technical Information Service, U. S. Department of Commerce, Springfield, Virginia 22161.

Price: Printed Copy A11
Microfiche A01

Codes are used for pricing all publications. The code is determined by the number of pages in the publication. Information pertaining to the pricing codes can be found in the current issues of the following publications, which are generally available in most libraries: *Energy Research Abstracts, (ERA); Government Reports Announcements* and Index (*GRA* and I); *Scientific and Technical Abstract Reports (STAR);* and publication, NTIS-PR-360 available from (NTIS) at the above address.

DOE/NV/10039-3
(DE81030487)
Distribution Category UC-66a

LOW-TO-MODERATE TEMPERATURE GEOTHERMAL RESOURCE ASSESSMENT FOR NEVADA, AREA SPECIFIC STUDIES

Final Report
June 1, 1980 - August 30, 1981

DENNIS T. TREXLER, BRIAN A. KOENIG,
THOMAS FLYNN, JAMES L. BRUCE,
GEORGE GHUSN, JR.

Nevada Bureau of Mines and Geology
University of Nevada
Reno, Nevada

Prepared for the

U.S. DEPARTMENT OF ENERGY
DIVISION OF GEOTHERMAL ENERGY
UNDER CONTRACT DE-AC08-79NV10039

ABSTRACT

The Hawthorne study area is located in Mineral County, Nevada and surrounds the municipality of the same name. It encompasses an area of approximately 310 sq. km (120 sq. mi), and most of the land belongs to the U.S. Army Ammunition Plant. The energy needs of the military combined with those of the area population (over 5,000 residents) are substantial. The area is classified as having a high potential for direct applications using the evaluation scheme described in Trexler and others (1979).

A variety of scientific techniques was employed during area-wide resource assessment. General geologic studies demonstrate the lithologic diversity in the area; these studies also indicate possible sources for dissolved fluid constituents. Geophysical investigations include aeromagnetic and gravity surveys which aid in defining the nature of regional, and to a lesser extent, local variations in subsurface configurations. Surface and near-surface structural features are determined using various types of photo imagery including low sun-angle photography. An extensive shallow depth temperature probe survey indicates two zones of elevated temperature on opposite sides of the Walker Lake basin. Temperature-depth profiles from several wells in the study area indicate significant thermal fluid-bearing aquifers. Fluid chemical studies suggest a wide spatial distribution for the resource, and also suggest a meteoric recharge source in the Wassuk Range. Finally, a soil-mercury survey was not a useful technique in this study area.

Two test holes were drilled to conclude the area resource assessment, and thermal fluids were encountered in both wells. The western well has measured temperatures as high as 90°C (194°F) within 150 meters (500 ft) of the surface. Temperature profiles in this well indicate a negative temperature gradient below 180 meters (590 ft). The eastern hole had a bottom hole temperature of 61°C (142°F) at a depth of only 120 meters (395 ft). A positive gradient is observed to a total depth in the well.

Several conclusions are drawn from this study: the resource is distributed over a relatively large area; resource fluid temperatures can exceed 90°C (194°F), but are probably limited to a maximum of 125°C (257°F); recharge to the thermal system is meteoric, and flow of the fluids in the near surface (<500 m) is not controlled by faults; heat supplied to the system may be related to a zone of partially melted crustal rocks in the area 25 km (15 mi) south of Hawthorne.

***

Geothermal fluids in the Paradise Valley study area in north central Nevada range in temperature from 40° to 70°C (106° to 158°F), and discharge at moderate rates from tuffa-cemented sediment mounds. Discharge occurs at or near the intersection of linear and curvilinear features which were identified on both Landsat imagery and contoured gravity data. Steep gravity gradients were identified near thermal fluid discharge areas, but could not be correlated with fault scarps on the surface. Soil-mercury surveys were largely inconclusive because of interference from sources of detrital mercury from nearby mines. Two-meter depth temperature probe surveys indicate that thermal fluids do not influence the temperature regime outside the immediate area of discharge. Two groups of thermal fluids were identified on the basis of chemical and stable-light isotope compositions. Both groups of thermal fluids have limited compositional variation and are also chemically distinct from the geothermal fluids. Chemical geothermometers are used to predict a maximum temperature of 94°C (202°F)for thermal fluids near the town of Golconda. Thermal fluids are isotopically lighter than surrounding non-thermal fluids and probably originated as precipitation at

elevations above 2500 meters (8200 ft). Isothermal temperature gradients were measured in wells adjacent to thermal fluids. Temperature measurements in wells outside the area of thermal fluid discharge show positive geothermal gradients of approximately 35°C/km. Combined data sets suggest that geothermal fluids in Paradise Valley are deeply-circulating meteoric waters heated by average basin and range geothermal gradients. Heated fluids rise at or near the intersection of lineaments, probably fault zones, and discharge from vertical pipes of tuffa-cemented sediments that extend deep into the subsurface.

***

A geothermal assessment study of the southern Carson Sink, Nevada was requested by the U.S. Department of Energy following an inquiry by the U.S. Navy to study the feasibility of establishing a district space heating system at the Fallon Naval Air Station. Geological and geochemical data were collected and field studies were undertaken to evaluate an area greater than 600 sq. km (232 sq. mi). Tasks conducted during this program include aerial image analysis, microgravity survey, soil-mercury survey, fluid chemistry studies, and temperature gradient studies of existing wells.

A shallow geothermal anomaly was identified using temperature gradient techniques in the eastern portion of the study area with approximately 70°C (158°F) fluid temperatures at depths less than 50 meters (164 ft). A gravity survey indicated that this resource exists along a basin and range fault, substantiating the theory that the geothermal fluids migrate along fault planes. The soil-mercury survey showed an area of anomalously high mercury values directly above and slightly north of the resource in

an area of high geothermal gradients. This suggests that a deeper, hotter resource exists beneath the shallow, moderate temperature resource.

***

During the statewide assessment phase of study to update the geothermal resources map, 23 new fluid chemistries and temperatures were added to the file; several wells and springs throughout the state are not listed in the file because they could not be found or because they were inaccessible.

ACKNOWLEDGMENTS

Much of the work in the Hawthorne study area was completed thanks to the help of U.S. Army Ammunition Plant personnel including Mr. Ralph Beeman, Mr. Cliff Cichowlaz, Mr. Frank Peterson, Mr. Ken Ramsy, and Mr. Jim Ryan. Also, valuable information and assistance was provided by Mr. Frank Sousa and Mr. Bob Milsap of the Hawthorne Utilities District. A special thanks also goes to Mr. Gene Terry of the El Capitan Motel-Casino for his time, advice and cooperation. Finally, a special thanks goes to the Honorable Robert List for taking the time to visit our project during the drilling phase.

In the Paradise Valley study area, much of the data was obtained thanks to the cooperation, assistance, and support of land owners and ranchers including Ms. Anne Zelinsky and Mr. Ron Parratt of the Southern Pacific Land Company, Mrs. Kirk Day of Winnemucca, Mr. Stanley Klauman, Mr. Jim Cress of the Nevada Department of Highways, and especially Dr. and Mrs. Gary Thrasher of the Nevada First Corporation, and Mr. Carl Segerstrom of Golconda. We also appreciate the efforts of Mr. Robert Whitney for his help with the aerial photographs as well as Mr. H. Markley McMahon, publisher, and Mr. Rex Bovee, reporter, both of the Humboldt Sun for their news-coverage of our work.

In the southern Carson Sink study area, a special thanks is extended to the Geothermal Utilization Division of the Naval Weapons Center, China Lake, California, Union Oil Company of California, the Truckee-Carson Irrigation District, the Fallon Naval Air Station and all the private landowners, too numerous to name here, who gave us permission to collect geologic samples on their properties.

A special thanks goes to Mr. Allen Evolokimo who provided field assistance during the statewide assessment phase of the study, and to Mr. Dennis M. Grover who drove all the way to Sands Springs Valley from Reno to pick up one fluid sample.

And finally, a very special thank you to Mr. Cameron Covington and Ms. Heather Dolan whose assistance, guidance, and patience steered us through seemingly insurmountable odds during the preparation of this report.

TABLE OF CONTENTS

TABLE OF CONTENTS

LIST OF FIGURES

LIST OF TABLES

INTRODUCTION

by DENNIS TREXLER

INTRODUCTION

Geothermal resource assessment in Nevada was conducted by the State Assessment Team for the U.S. Department of Energy, Division of Geothermal Energy over the past three years. The first phase of this cooperative program focused on statewide evaluation of geothermal resources. In meeting these needs, a 1:500,000 scale map entitled "Geothermal Resources of Nevada and their Potential for Direct Utilization", NVO/1556-1 (Trexler and others, 1979), was prepared and published. The map depicts technical resource information for more than 300 springs and wells throughout the state and evaluates 40 large areas with potential for geothermal development based upon a numerical evaluation scheme.

The second phase of the cooperative program was a two year contract for area specific investigations to stimulate geothermal development. These area specific studies employ geological, geophysical and geochemical surveys and are designed to expand the data base of the regional assessment, provide more detailed resource information, and develop and test scientific exploration methods for low-to-moderate temperature geothermal resources.

The first year of area specific studies began in May, 1979 in two study areas: the Big Smoky Valley in central Nevada, and Carson-Eagle Valleys in west-central Nevada. The two areas were selected on the basis of their high potential for the development of industrial process heat and residential space heating, respectively. The results of these investigations were reported in the first annual report, "Assessment of the Geothermal Resources of Carson-Eagle Valleys and Big Smoky Valley, Nevada", Report No. DOE/NV/10039-2, May, 1980. An additional study area, Caliente, was added in November, 1979 at the request of DOE. Limited resource evaluation included geologic reconnaissance, two-meter depth temperature probe survey, soil

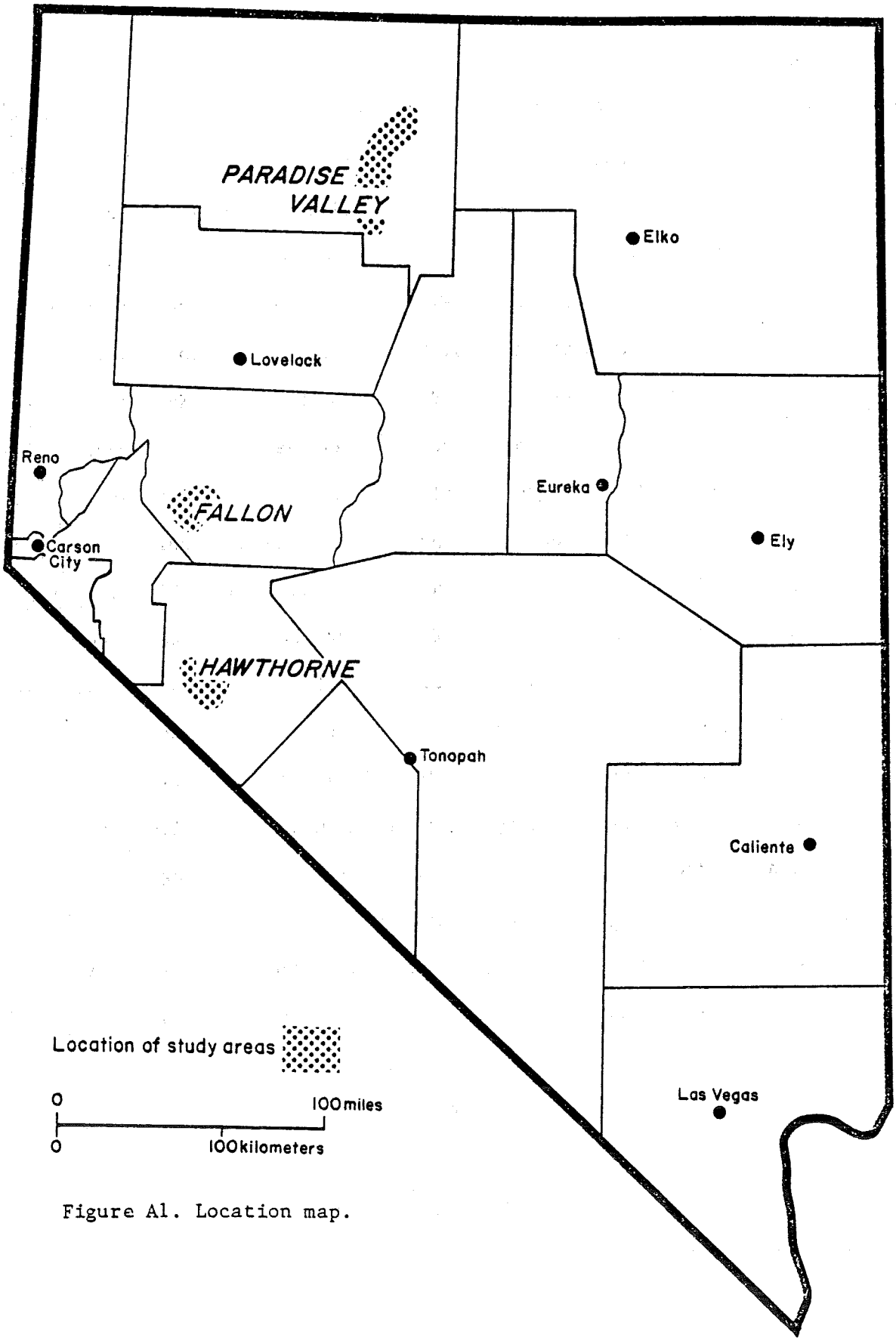

Figure A1. Location map.

mercury, and fluid geochemistry techniques. The results of this investigation and the selection of two sites for reservoir confirmation wells were reported in "Assessment of Geothermal Resources of Caliente, Nevada", DOE/NV/10039-1.

During the second year of area specific studies, three locations were investigated to determine their potential for low-to-moderate temperature geothermal resources. These areas are Hawthorne, located in west-central Nevada, Paradise Valley in north-central Nevada, and the Fallon Naval Air Station located in the southern Carson Sink of west-central Nevada. The Paradise Valley and Hawthorne study areas received the full compliment of exploration and assessment techniques, while less extensive investigations were performed in the Fallon area because of previous geothermal exploration work by the Navy. The location of the three areas is presented in Figure A1.

Regional definition of the nature of the resource, its extent, and controls on the extent are the primary objectives of the research. The program is organized around the completion of nine tasks that pertain to resource evaluation. Each of these work units is briefly described below.

1. Gather and examine existing information including geological, geophysical and hydrological literature, chemical data, lithologic and well completion logs, and appropriate aerial imagery.

2. Acquire relatively detailed information on the subsurface configuration through the use of gravity surveys employing station spacings of approximately 1/2 mile.

3. Collect and analyze soil samples for mercury content on regional (approximately one-mile spacing) and smaller grids.

4. Obtain low sun-angle photography at a scale of 1:24,000 for use in studying subtle geomorphologic manifestations, particularly faults.

5. Conduct shallow-depth temperature probe surveys to determine the

near surface thermal regime on both regional (1 mile grid) and smaller more localized grids.

6. Sample thermal and non-thermal groundwaters and, if possible, meteoric waters, and analyze for bulk chemical and stable light isotopic composition.

7. Collect and examine bulk rock samples for mineralogic composition. Analyze selected samples for whole rock chemical composition if appropriate. Compare rock mineralogic and chemical composition with the chemical composition and mineral equilibria of sampled fluids.

8. Based on the data obtained from 1-7 above, select sites for drilling three to five 100-250 meter temperature gradient holes. Determine lithology, temperature profile, and fluid chemical composition where possible.

9. Prepare a report detailing the results of the study.

In addition to the area specific resource tasks identified above, a tenth work element was initiated which included collecting and analyzing fluid samples, measuring physical and chemical parameters, and preparing input to the U.S. Geological Survey GEOTHERM data file for springs and wells lacking these data.

BASELINE DATA

The investigations began with a review of all pertinent literature including topographic maps, geologic reports, geologic maps, Bouguer gravity maps, theses, lithologic well logs, and water resource reports. This provided a general understanding of the areas as well as an initial direction for the area specific studies.

Samples of thermal and non-thermal waters were collected from several sources in the study areas. Garside and Schilling (1979) provided chemical

data for thermal springs and wells. Additional water quality data were collected from the files of the Consumer Health Protection Services, a Division of the Nevada Department of Health in Carson City. These data pertain to non-thermal waters and include only the major dissolved constituents.

Lithologic logs for residential and agricultural water wells are available for public inspection in the Office of the State Engineer, Carson City. Although most logs were difficult to read, they were helpful in determining the distribution and depth of many warm water aquifers. Data from oil and natural gas exploration in Railroad Valley in southeastern Nevada are, unfortunately, of little value in this study. Also, data from mineral and geothermal exploration holes are largely proprietary.

GEOLOGIC RECONNAISSANCE

Geologic reconnaissance consisted of identifying important rock stratigraphic units and structures in the field. No large-scale geologic mapping was required because most of this work has already been performed.

Much of the reconnaissance was incorporated into other phases of the program such as the gravity and low sun-angle photo surveys. In the Paradise Valley area, several previously unmapped faults were identified on low sun-angle photographs and verified during geologic reconnaissance. In addition, hydrothermally altered areas were examined for evidence of recent thermal spring deposits and hydrothermally-cemented sediments.

Several representative samples of the major rock units were collected for petrographic examination. Thin sections were used to investigate possible genetic affinities among various lithologies.

GRAVITY

Gravity measurements were taken to obtain useful subsurface structural information. This choice was based in part on the results of other investigators working the Basin and Range region.

One of the earliest studies was carried out in the Virginia City and Mt. Rose, Nevada quadrangles by Thompson and Sandberg (1958). Their study combined gravity data with density measurements of the surrounding sedimentary, volcanic and metamorphic rocks. From their data, the authors were able to calculate the thickness of sedimentary rocks in several basins. A more regional survey was completed by Thompson (1959) in the area between Hazen and Austin, Nevada. These measurements depicted a series of north-south trending horsts and grabens bordered by normal faults along which several thousand feet of vertical displacement had occurred. Stewart (1971) also used regional gravity data to characterize the Basin and Range horst and graben structures for several areas in north-central Nevada. He interpreted the steep gravity gradients which occur near the Basin-Range interface as an indication of normal faulting. Goldstein and Paulsson (1979) integrated gravity data with seismic and deep electrical resistivity surveys in Grass Valley and Buena Vista Valley, Nevada. They were also able to estimate a basement configuration, fault patterns, and depth to the Paleozoic basement.

An additional reason for using gravity measurements was the relatively high rating assigned to the technique by Goldstein (1977) for area-specific studies.

In the three study areas, 721 gravity stations were occupied. Readings were made with a Worden gravimeter with a scale range of 80 milligals. Vertical control was maintained to $\pm$0.1 ft using an HP electronic transit. Station

spacing ranged from 0.5 to 1.0 mile. The instrument was allowed to thermally equilibrate (as judged by an unchanging reading over a five minute interval) for 15-20 minutes before making an initial measurement at the first station of a loop. A second reading was taken at the initial station as the termination measurement of the loop to establish instrument drift. Loop duration ranged from two to six hours with the smaller interval used as frequently as conditions permitted.

AERIAL PHOTOGRAPHY AND LANDSAT IMAGE ANALYSIS

Three aerial photographic techniques were used in the study areas: moderate to high altitude imagery, low altitude photography along selected flight lines, and low sun-angle photography. Landsat imagery at 1:250,000 scale, 1:120,000 U2 black and white photography, and 1:60,000 scale black and white U.S.G.S. aerial mapping photography were used under the first technique. This imagery identified regional trends possibly related to the location of geothermal occurrences within the area. Low sun-angle photography was flown at a scale of 1:24,000 along selected flight lines in the Paradise Valley and Hawthorne study areas, and low sun-angle photography at a scale of 1:40,000 was flown for the Fallon area. Aerial photography was flown in October to maximize sun-angle illumination; the photos were taken with 60% forelap and 20% sidelap to allow for stereoscope examination. In an earlier study, Trexler and others (1978) demonstrated the usefulness of the low sun-angle photographic technique in delineating near-surface structural features associated with known geothermal occurrences in Nevada.

FLUID SAMPLING

Samples of thermal and non-thermal fluids were collected in each study area for analysis of major dissolved constituents, minor and trace dissolved species, and oxygen and hydrogen-stable light isotopes. The goal was to gather information on the nature and possible flow paths of fluids recharging the geothermal systems. This approach has been used with good results by several previous investigators including White (1968), Ellis and Mahon (1977), and Cusicanqui and others (1975). A chemical data base was also compiled using sampling and analysis procedures which were uniformly applied to each area.

Two fluid samples were collected at each site; one contained a 250 ml aliquot and the second an 80-100 ml aliquot. The larger sample was topped-off to reduce atmospheric interaction, and preserved in a raw state for the analysis of anions. After filtration to remove particulate matter larger than 5 microns, a sufficient quantity of reagent grade nitric acid was added to bring the pH of the smaller sample to a value of approximately two. These steps were taken to insure reliable cation data. Additionally, a 125 ml sample was collected in glass bottles for isotopic analysis. Sample caps were dipped in hot paraffin prior to application and the top portion of the vessel was immersed in the wax to form an airtight seal.

Subsequent to collection, raw and isotopic samples were promptly shipped to laboratories for analysis. Values for SiO_2 are derived from an undiluted sample using an induction-coupled plasma or atomic absorption technique.

TEMPERATURE PROBE SURVEYS

Temperature anomalies located near the ground surface can be mapped using thermistor probes buried to a depth of one to two meters. These surveys

are most effective when probes are buried to depths at which diurnal effects are insignificant, approximately 1.5 m (Birman, 1969). However, temperature probes to a depth of 1 m effectively delineate high temperature gradients in areas of known geothermal activity (Kintzinger, 1956; Olmstead, 1977).

Subsurface temperature surveys have been used to locate groundwater (Birman, 1969; Cartwright, 1966) to estimate thermal stresses on the walls of underground buildings (Singer and Brown, 1956), and to locate subsurface leaks in barge canals (Kappelmeyer, 1957).

In this study, temperature probes buried to depths of 1.5 - 2 m were used to delineate areas of anomalous temperature highs. General purpose, vinyl-tipped thermistor probes were used. The probes are 3 m in length and are equipped with a standard phone-jack.

Small diameter holes (8-9 cm) were drilled to various depths with a trailer-mounted gasoline-powered auger; a thermistor probe encased in a 2 m section of PVC pipe was emplanted. Spacing between probes varied from 0.25 - 1 mile depending on the size of the area under investigation.

Field tests indicate that reliable temperature measurements may be taken within 24 hours of the installation. This short reading interval is applicable only to those areas where relatively unconsolidated materials permit drilling times of 10-15 minutes per hole or less. In general, the holes were allowed two to four days to equilibrate.

SOIL-MERCURY SURVEYS

Soil-mercury surveys are reliable in geothermal energy exploration. The basic principle behind the method is that mercury is generally volatile above 80°C; since many geothermal systems are higher than 80°C at depth, mercury is released from the rock. The vaporized mercury then migrates upward untilit encounters absorbent clays which capture the mercury.

Sampling this clay soil layer provides the sample base for the analysis. After collection, the samples are oven-dried at about 40-60°C to remove excess moisture. The samples are then sieved to a minus 80 mesh (180 micron) fraction, and analyzed with a Jerome gold film mercury detection machine. Background values are determined from this data base. Anomalous regions are then studied to determine the relationship of soil mercury values to the hypothesized geothermal system (i.e., structure controls, areal extent, etc.).

TEMPERATURE GRADIENT DRILLING

Gradient drilling was implemented during the final quarter of the project as a technique to analyze selected areas for low-to-moderate temperature resources. Drill sites were selected based upon the data gathered from field and analytical techniques, and also based upon the availability of land.

Three gradient holes were drilled in the Paradise Valley study area, each to a total depth of 132 m (400 ft). The holes were cased with 2" diameter schedule 40 PVC. Casing in GDS-1 was open, while PVC was capped and water was added during installation in the remaining two holes. Two gradient holes were drilled in the Hawthorne area, one to 265 m (800 ft), and a second to 132 m (400 ft). Both holes were cased using 3" pipe, and closed at the bottom to retain a column of water. A complete discussion of maximum temperatures and gradients is presented in the Paradise Valley and Hawthorne sections of this report.

HAWTHORNE STUDY AREA

by BRIAN A. KOENIG

INTRODUCTION

The Hawthorne study area is located in west-central Nevada approximately 40 miles from the California border. It encompasses an area of nearly 120 square miles and includes a large proportion of the land belonging to the U.S. Army Ammunition Plant as well as the communities of Hawthorne and Babbitt (fig. B1). The local population which exceeds 5000, and that of the Military Reservation make up a strong basis for geothermal energy development, particularly in the area of direct applications such as space heating and/or cooling.

No surface manifestations of geothermal activity have been identified in the study region to date. Information on the nature and distribution of the resource was obtained from several wells drilled within and near the city of Hawthorne. Thermal fluids were first discovered in the area during the 1940's and 1950's when wells were drilled on property which belonged to the Navy. Temperatures ranged from a minimum of 16°C along the range front near the southwest shore of Walker Lake to a maximum of 51.5°C in a hole two miles northwest of the city. A well drilled approximately one mile southwest of Hawthorne and 1/2 mile from a warm (34°C) city well encountered thermal fluids at 99°C. These temperatures were recorded within the past two years, indicating a strong resource potential in the area.

Representatives from both the government and private sectors have expressed interest in exploitation and development of geothermal resources over the past few years. DOE and private resource evaluation teams completed a cooperative study on engineering and economic feasibility of geothermal resources in the area. The study was initiated at the request of owners of the El Capitan Casino and the Mineral County Commissioners in a joint effort to utilize hot fluids produced from the well located on Casino-owned property.

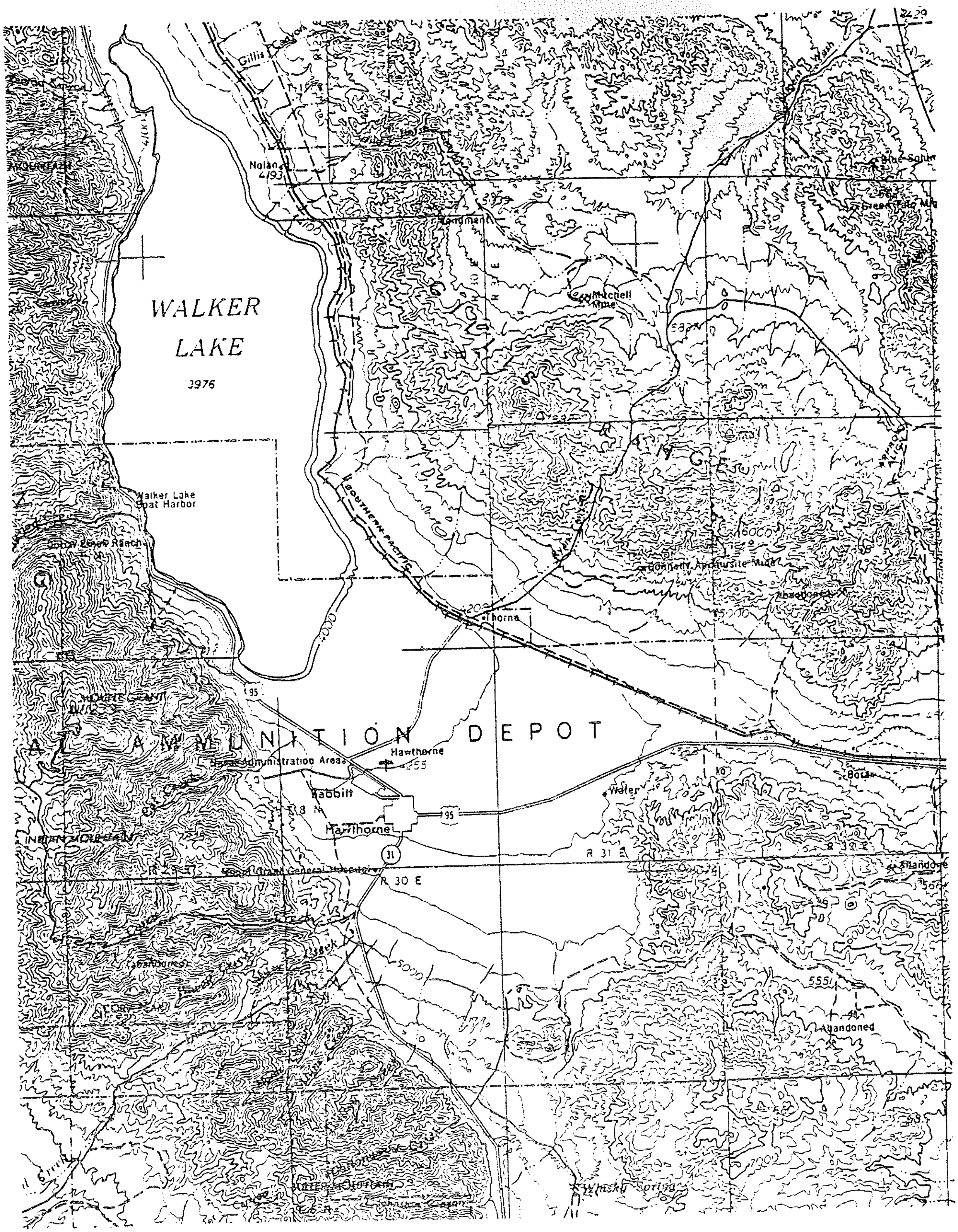

Figure B1. Hawthorne study area.

Personnel of the Hawthorne Army Ammunition Plant have also expressed an interest in utilizing geothermal resources as a result of the discovery of shallow depth (175 m), moderate temperature (90°C) fluids on Army land. Efforts are in progress to obtain funding for continued development and/or exploration in the Hawthorne area.

GENERAL GEOLOGY

The study area lies within the Walker Lake Basin. Although similar to other Basin and Range valleys, it is located in a zone of topographic discordance. Ranges to the south and west of the zone exhibit northwesterly trends while those north and east have northeast orientations. Within the zone, orientations are diverse and follow arcuate patterns. This zone was labeled the Walker Lane by Locke and others (1940). Some investigators interpret this feature to represent a zone of large scale right-lateral displacement. A discussion of various theories regarding the nature and timing of events within the zone is given by Stewart (1980, p. 86-87). Most characteristics discussed in the following paragraphs are presented graphically in a geologic map, Figure B2. It is a generalization from the maps of Ross (1961) and Stewart and Carlson (1978).

Rocks exposed within the area range in age from Triassic to Holocene, and a variety of lithologies is present. The Wassuk Range which forms the study area's western boundary is largely composed of intermediate intrusive rocks. Although compositions from diorite to granite are observed, the majority of rocks are granodiorite to quartz monzonite. The diorite rocks are directly associated with metavolcanic rocks of the Excelsior formation as defined by Muller and Ferguson (1936). Ross (1961, p. 28) suggests that the diorites are partly the result of assimilation of the metavolcanic rocks during intrusion

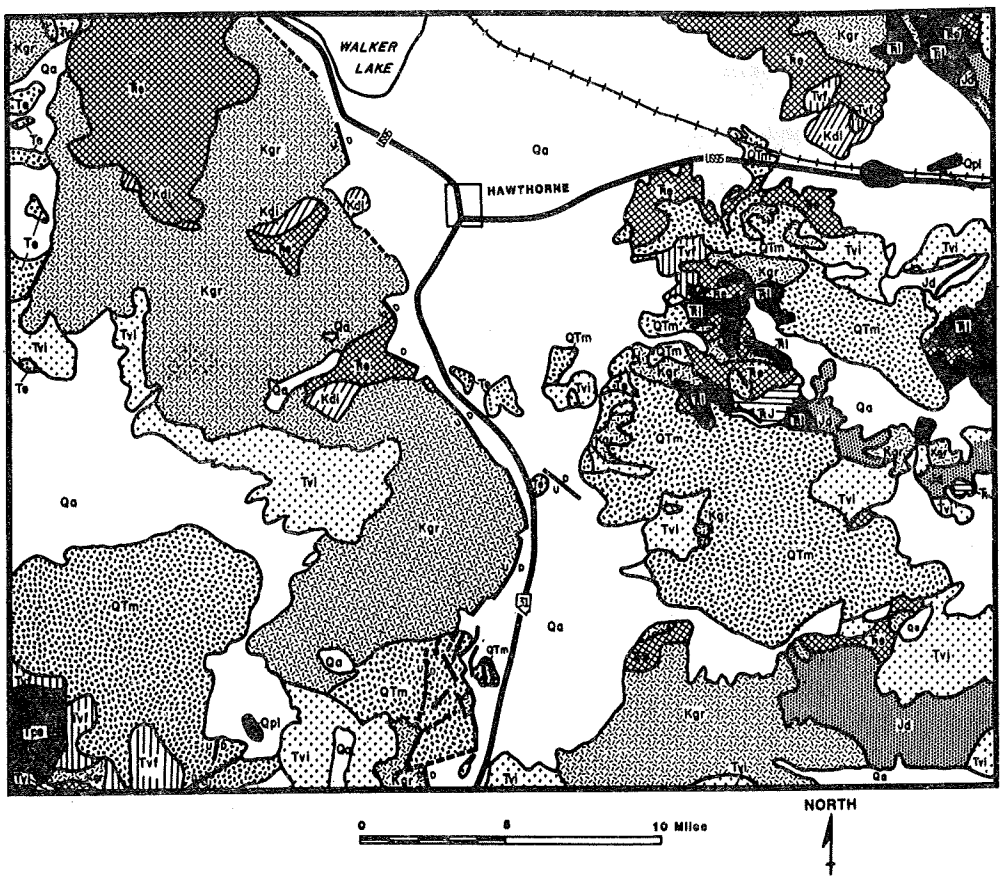

EXPLANATION

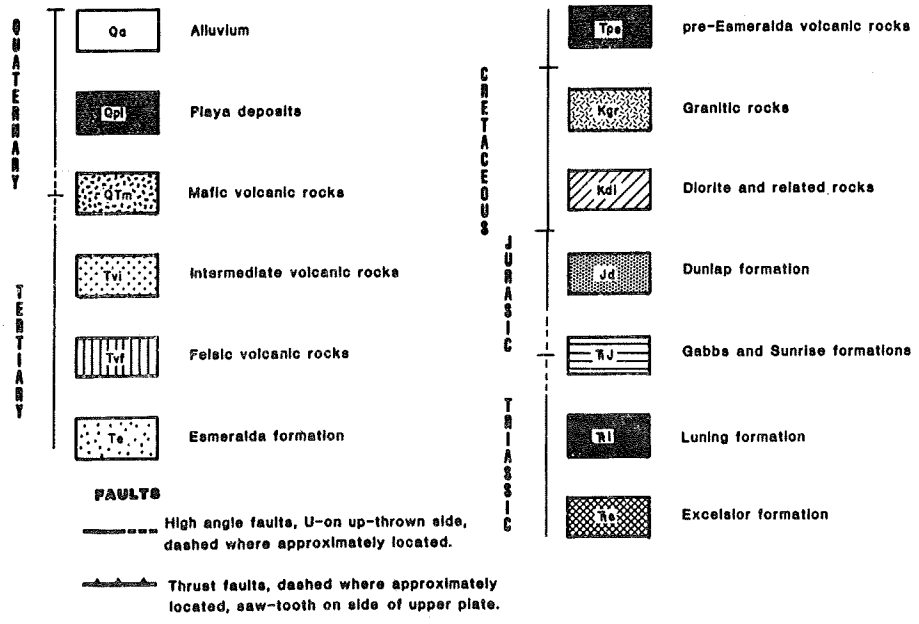

Figure B2. Generalized geologic map of the Hawthorne study area and surrounding region.

of the granites. He also proposes (Ross, 1961, p. 30) that the granitic rocks are probably related to the Sierra Nevada Batholith complex. The Excelsior formation rocks and associated diorites appear to be roof pendants on the granites. In the Lucky Boy Mine area, marble and phyllites are locally present in the Excelsior formation. These lithologies are probably the result of contact metamorphism during intrusion of granitic rocks. The western front of the Wassuk Range at the latitude of the study area is made up of intermediate volcanic rocks of Tertiary age. South of the primary study area, recent mafic volcanic rocks are present in the range. This rock type is found in the Aurora Crater and Mud Spring Volcano immediately west of the Wassuk Range. The former is dated at 250,000 years and the latter is determined to be even younger (Stewart, 1980, p. 109).

A group of low hills is located immediately north of Whiskey Flat in the southern portion of the study area. These hills are largely covered by Quaternary alluvium owing to their near central location in the valley, however, only limited outcrops are present. Ross (1961) labels these features as the Tertiary Esmeralda formation. Field checking confirms that the northern two groups of hills are composed of tuffaceous and lacustrine sediments as Ross' map suggests. The southernmost hill appears to be composed of a dark copper-bearing rock similar to the metavolcanic rocks of the Excelsior formation.

The eastern boundary of the study region is formed by the Garfield Hills. In their western extent, the mountains consist largely of the same units described for the Wassuk Range. However, volcanic rocks of Tertiary and especially Quaternary age dominate in this area. Only limited exposures of the Mesozoic granites are observed. Sizable outcrops of Excelsior formation rocks are present in the northwest part of the range. Rock units not seen in the Wassuk Range include limestone, shales, sandstones, and conglomerates of the Luning,

Gabbs and Sunrise, and Dunlap formations of Mesozoic age and Tertiary felsic volcanic rocks. Quaternary alluvial deposits cover the valley floor and are occasionally found in topographic lows within the ranges.

Structurally, the Wassuk Range is similar to several other large mountain ranges in Nevada. Its eastern flank is well defined by frontal faults, particularly in the vicinity of Hawthorne. The eastern slope is steep and has deeply incised canyons. Elevation changes as much as 1500 feet per mile occur where Mt. Grant adjoins Walker Lake. Conversely, the western slope exhibits a notably more gentle grade with clearly defined frontal faults only locally evident. Recent faulting along the eastern front is evidenced by scarps cutting alluvium. Ross (1961, p. 56) notes that south of the study area in the vicinity of Powell Canyon, movement is distributed along several faults. Some of these faults are antithetic. Examination of low sun-angle photography suggests that a similar structural configuration exists in the study area (see section on "Aerial Imagery").

Structure of the Garfield Hills is documented in great detail by Ferguson and Muller (1949). A well-defined period of Mesozoic orogeny is recorded by the attitude and juxtaposition of beds in the Excelsior, Luning, and Dunlap formations. Types of documented orogenic events include folding, uplift, rapid erosion and deposition, thrust faulting, and intrusion. Following the Mesozoic intrusion, large volumes of Tertiary and Quaternary volcanic rocks were extruded, particularly in the western part of the range. Unlike the well-defined frontal fault patterns of the eastern slope of the Wassuk Range, range front scarps are essentially absent from the Garfield Hills. Relief of the range is subdued above the surrounding alluvium. Data supporting recent fault movement are not apparent.

AEROMAGNETIC DATA

An aeromagnetic survey was performed in 1967 for the U.S. Geological Survey. Two separate elevations, 9000 and 11,000 feet barometric were used in the aerial survey and both are found within the study area. Only a general discussion is appropriate since the survey was not flown drape and the effects of terrain were not taken into consideration. A segment of the map (U.S. Geological Survey, 1971) is reproduced as Figure B3.

From an overall perspective, the contours make up a collection of isolated closures and linear patterns. The most prominent feature of the area is the linear pattern which trends east-southeast within the Garfield Hills. This feature assumes a southeasterly orientation where it traverses the Walker Lake Basin. Position of the linear pattern compared with topographic and geologic maps indicates that it follows a depression primarily filled with alluvium. Regions of contour closure located north and south of the linear pattern tend to correlate with topographic highs and/or outcrops of mafic to intermediate volcanic rocks. Similarly, closure correlated with rock type are observed along the western front of the Wassuk Range. A more subtle pattern is observed in the vicinity of Mt. Grant, extending eastward to Hawthorne and southward to the vicinity of the Lucky Boy Mine. Relative differences between highs and lows are small within this region. A broad, rather non-descript zone is present west of Babbitt. These poorly-defined patterns may result from the large mass of relatively uniform granitic rocks which form the Wassuk Range.

Generally, information on this map provides little additional data compared to other sources such as topographic and geologic maps.

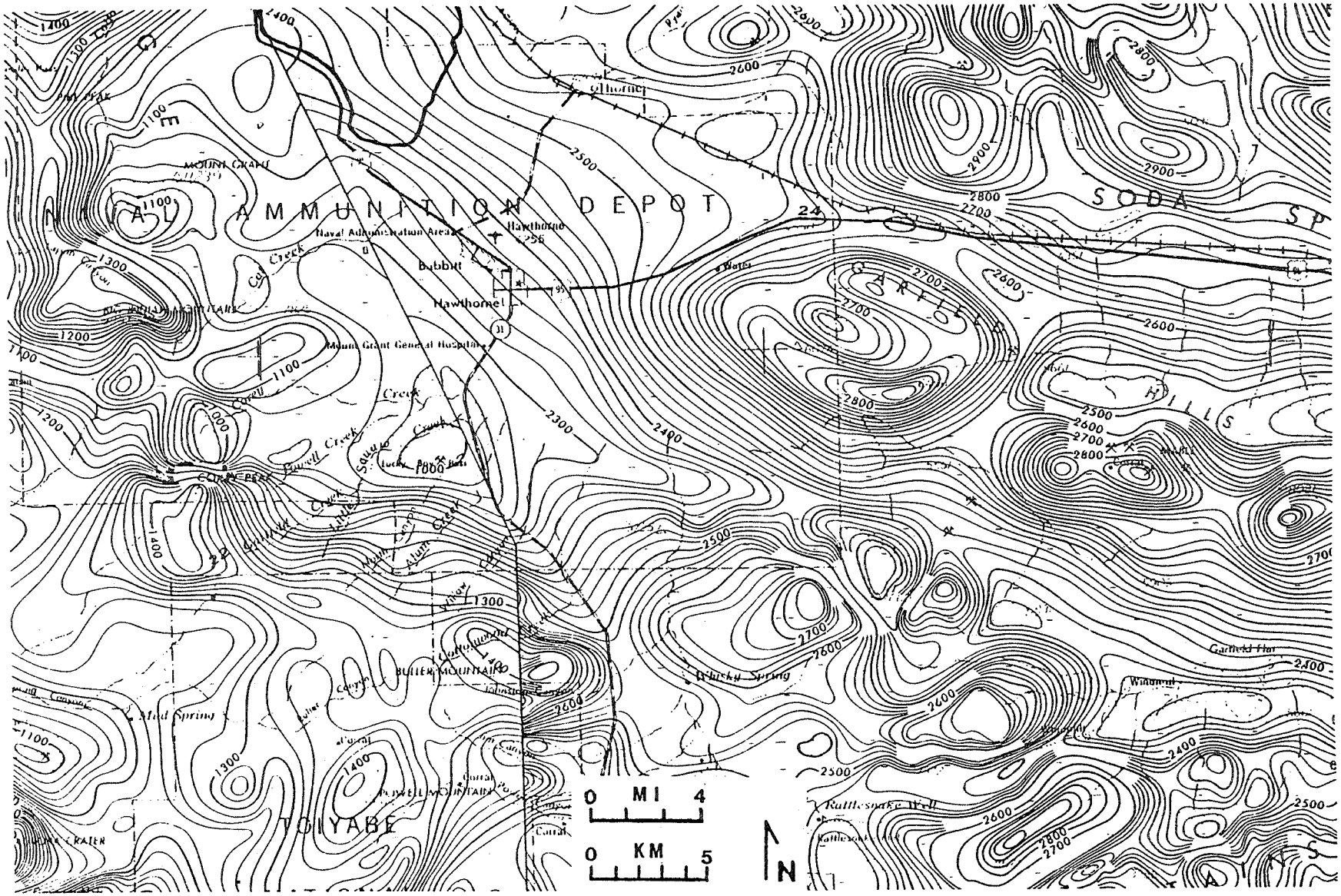

Figure B3. A portion of the U.S. Geological Survey aeromagnetic map (U.S. Geological Survey, 1971). Contours in Gammas.

LITERATURE SEARCH

Existing data sources were examined prior to commencement of field studies. Geology of the area is discussed in Ferguson and Muller (1949), Locke and others (1940), Muller and Ferguson (1936), Ross (1961), Speed (1977b), and Stewart (1980). Regional geophysical data for gravity is available in the form of a 1:250,000 scale map and accompanying tables (Healey and others, 1980). Aeromagnetic data in a 1:250,000 scale map is available from the U.S. Geological Survey (1971). Hydrology and hydrogeology are discussed in Everett and Rush (1967) and VanDenburgh and Rush (1975). A preliminary report on geothermal resources contains a compilation of fluid chemistry (Bohm and Jacobson, 1977). Further information on lithology and chemistry for wells located on the military reservation are available from records at the Ammunition Plant. Well records filed with the State Engineer's office were also examined.

SHALLOW TEMPERATURE SURVEY

Over 90 holes were drilled to an approximate depth of two meters, and thermistor probes were implanted. The probes remained undisturbed for a minimum of 24 hours before readings were taken. Previous work using this technique demonstrated that 24 hours is sufficient to obtain temperatures within 0.1°C of those recorded after the hole returns to a thermal equilibrium state. Locations of the probe holes are depicted in Figures B4 and B5 where the numbers correspond to those listed in Table B1.

This study was completed during three separate trips to the field in September, October and December, 1980. Therefore, the data represent measurements taken at three points along the changing curve of the annual wave, the effects of which penetrate to depths greater than two meters. To compensate

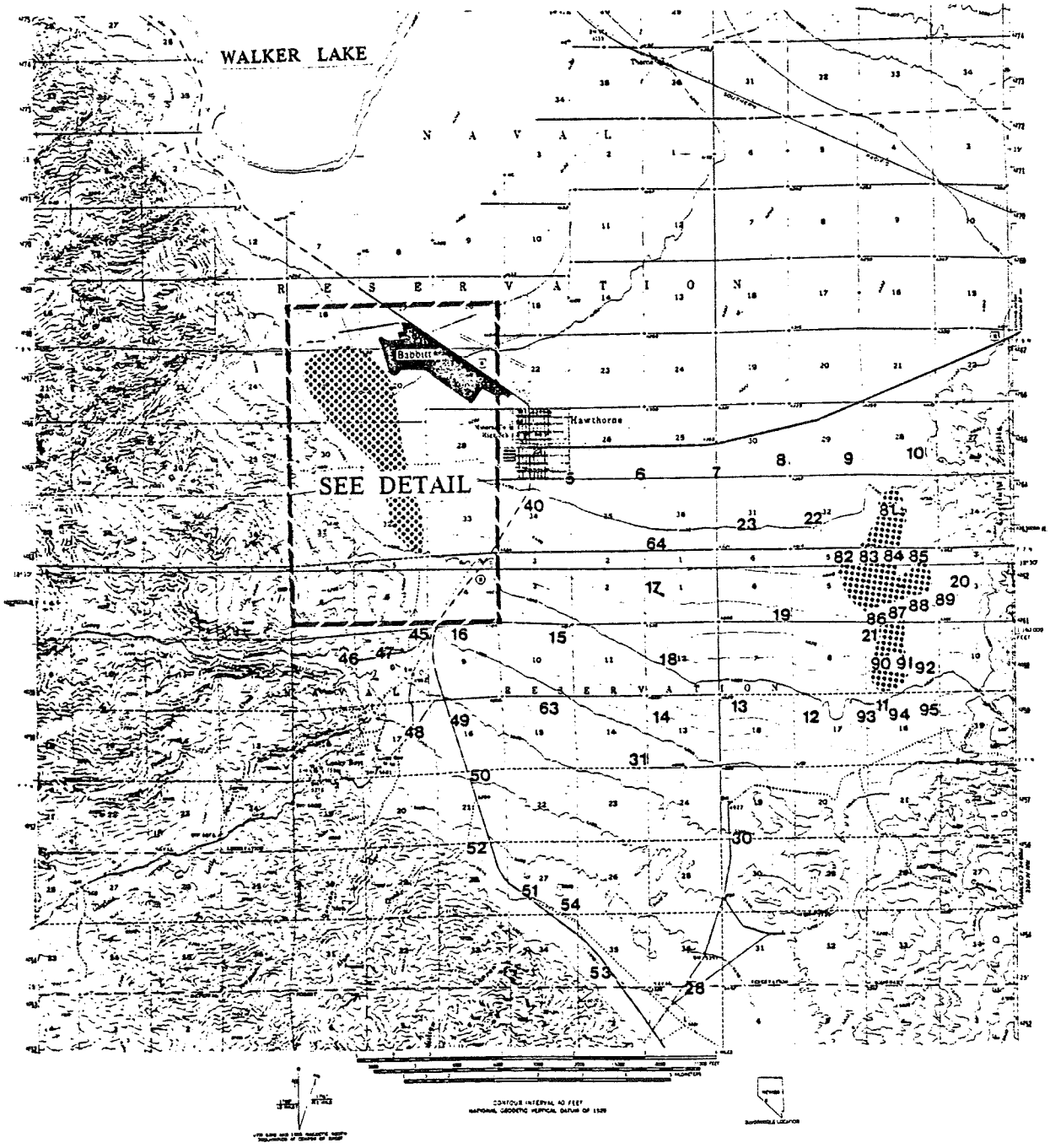

Figure B4. Two-meter temperature probe locations. Stippling indicates area of elevated temperatures. See Figure B5 for detail.

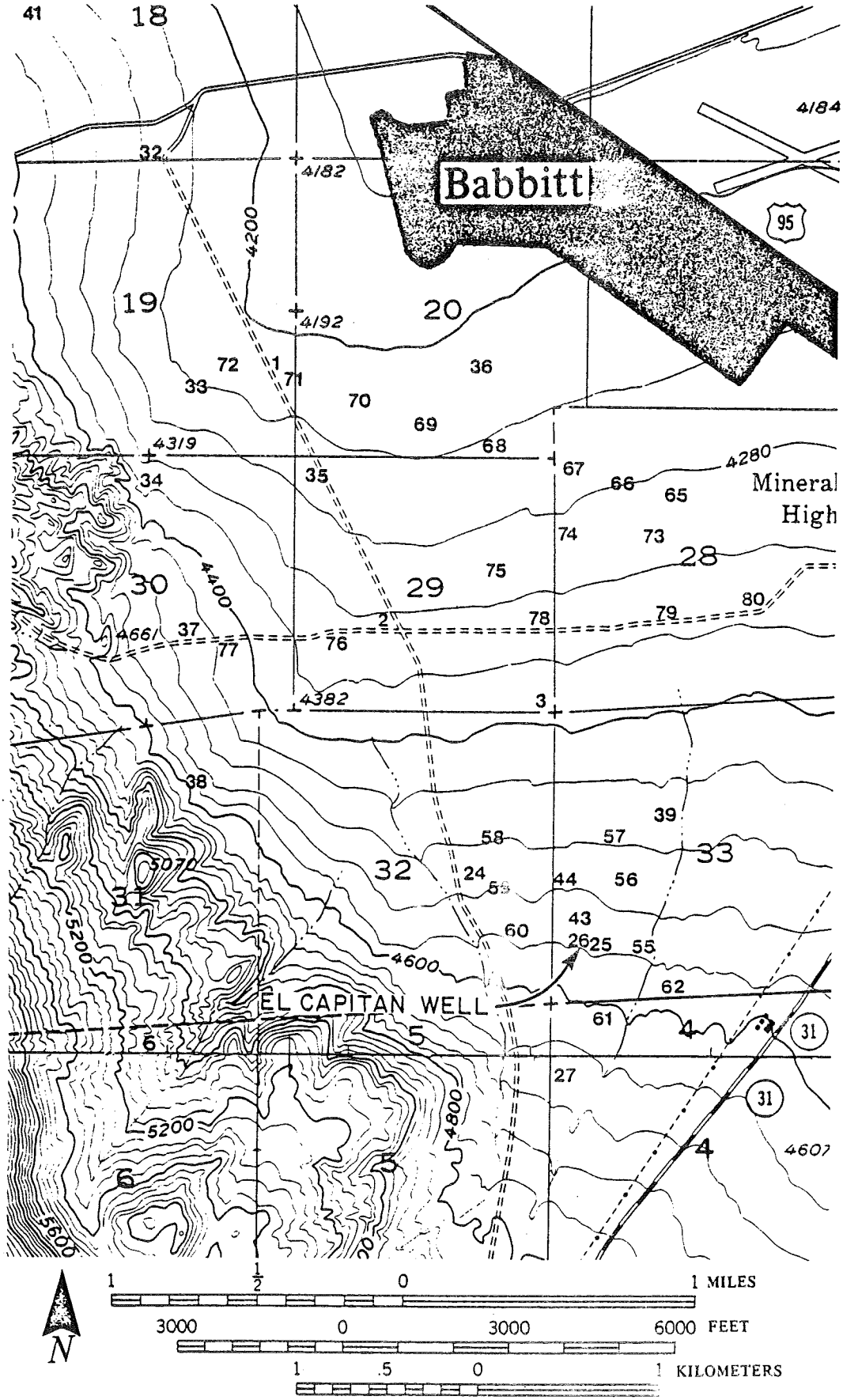

Figure B5. Detail of temperature probe locations.

Table B1. Temperature Probe Data

Probe #	Date of Reading	Measured Temp (°C)	Correction Factor	Corrected Temp (°C)
1	27 Sept.	22.8	N/A	N/A
2	27 Sept.	23.9		
2	1 Oct.	23.75		
2	17 Oct.	23.3		
2	3 Dec.	18.25		
3	27 Sept.	23.4		
4	27 Sept.	21.0		
5	27 Sept.	22.4		
6	27 Sept.	19.8		
7	27 Sept.	21.0		
7	1 Oct.	20.9		
7	17 Oct.	20.6		
8	27 Sept.	21.1		
9	27 Sept.	22.0		
10	27 Sept.	22.3		
11	27 Sept.	22.2		
12	27 Sept.	21.1		
13	27 Sept.	21.1		
14	27 Sept.	20.5		
15	27 Sept.	20.8		
16	27 Sept.	20.9		
17	27 Sept.	21.5		
18	27 Sept.	20.9		
19	27 Sept.	21.8		
20	27 Sept.	20.8		
21	27 Sept.	22.3		
22	27 Sept.	21.2		
23	27 Sept.	21.2		
24	27 Sept.	22.6		
25	27 Sept.	23.3		
26	27 Sept.	24.7		
27	27 Sept.	22.0		
28	27 Sept.	18.2		
29	27 Sept.	18.9		
30	27 Sept.	19.9	N/A	N/A
31	27 Sept.	Probe Damaged	-	-
31	18 Oct.	20.25	+0.5	20.75
32	17 Oct.	22.8	+0.5	23.3
33	17 Oct.	23.9	+0.5	24.4
34	17 Oct.	21.0	+0.5	21.5
35	17 Oct.	23.35	+0.5	23.85
36	17 Oct.	24.3	+0.5	24.8
37	17 Oct.	23.65	+0.5	24.15
38	18 Oct.	21.8	+0.5	22.3
39	18 Oct.	22.3	+0.5	22.8
40	18 Oct.	20.75	+0.5	21.25
41	17 Oct.	19.8	+0.5	20.3
42	No Station	-	-	-
43	18 Oct.	24.0	+0.5	24.5
44	18 Oct.	23.3	+0.5	23.8
45	18 Oct.	23.3	+0.5	23.8

Table B1. Temperature Probe Data (Cont.)

Probe #	Date of Reading	Measured Temp (°C)	Correction Factor	Corrected Temp (°C)
46	18 Oct.	18.8	+0.5	19.3
47	18 Oct.	19.2	+0.5	19.7
48	18 Oct.	19.95	+0.5	20.45
49	18 Oct.	20.7	+0.5	21.2
50	18 Oct.	20.7	+0.5	21.2
51	18 Oct.	17.15	+0.5	17.65
52	18 Oct.	19.3	+0.5	19.8
53	18 Oct.	18.7	+0.5	19.2
54	18 Oct.	18.75	+0.5	19.25
55	18 Oct.	21.6	+0.5	22.1
56	18 Oct.	22.55	+0.5	23.05
57	18 Oct.	22.75	+0.5	23.25
58	18 Oct.	23.2	+0.5	23.7
59	18 Oct.	23.1	+0.5	23.6
60	18 Oct.	23.6	+0.5	24.1
61	18 Oct.	24.95	+0.5	25.45
62	18 Oct.	21.1	+0.5	21.6
63	18 Oct.	20.2	+0.5	20.7
64	None	None	-	-
65	3 Dec.	16.7	+5.7	22.4
66	3 Dec.	17.7	+5.7	23.4
67	3 Dec.	18.5	+5.7	24.2
68	3 Dec.	17.3	+5.7	23.0
69	3 Dec.	16.8	+5.7	22.5
70	3 Dec.	17.3	+5.7	23.0
71	3 Dec.	16.4	+5.7	22.1
72	3 Dec.	18.5	+5.7	24.2
73	3 Dec.	18.75	+5.7	23.95
74	3 Dec.	17.8	+5.7	23.5
75	3 Dec.	17.0	+5.7	22.7
76	3 Dec.	17.2	+5.7	22.9
77	3 Dec.	17.6	+5.7	23.3
78	3 Dec.	18.3	+5.7	24.0
79	3 Dec.	18.6	+5.7	24.3
80	3 Dec.	15.9	+5.7	21.6
81	4 Dec.	17.95	+5.7	23.65
82	4 Dec.	17.0	+5.7	22.7
83	4 Dec.	17.0	+5.7	22.7
84	4 Dec.	16.5	+5.7	22.2
85	4 Dec.	17.15	+5.7	22.85
86	4 Dec.	17.3	+5.7	23.0
87	4 Dec.	17.9	+5.7	23.6
88	4 Dec.	18.7	+5.7	24.4
89	4 Dec.	17.9	+5.7	23.6
90	4 Dec.	17.5	+5.7	23.2
91	4 Dec.	16.0	+5.7	21.7
92	4 Dec.	17.4	+5.7	23.1
93	4 Dec.	16.4	+5.7	22.1
94	4 Dec.	16.9	+5.7	22.6
95	4 Dec.	17.4	+5.7	23.1

for this problem, selected probes were left undisturbed from one measurement period to the next. For example, probe namber 2 was implanted at the inception of the two-meter temperature study and removed at the study's termination. Probe number 7 was in place for the first two measurement periods. Based on the recorded temperature differences between the probes remaining in place over time and the probes removed early, correction factors were calculated to permit comparison of all data. The modified data appear as corrected temperatures in Table B1.

This technique was systematically applied to the Hawthorne study area. Probes were first placed at intervals of one per square mile. The distribution of temperatures recorded during the initial phase provided a basis for selection of detailed study areas. Probe spacings as small as 250 meters (820 ft) were employed during the detailed study. This methodology established the presence of two regions of elevated temperature indicated by the stippled patterns in Figure B5. In addition, a trend of increasing temperatures exists, progressing from the southern extent of the study area to the central portion. Temperatures recorded in the immediate vicinity of a hot well in the study area (El Capitan Well - 99°C) were some of the highest measured during the study.

Isotherm configurations interpreted from temperature probe data are presented in Figures B6 and B7. Regions depicted in these figures approximately correspond to those delineated by stippling in Figure B4. The accuracy of interpreted isotherms is questionable in the western region (fig. B6). Patterns do not conform to linear arrangements which are usually associated with the upward flow of thermal fluids along fault zones. Instead, the data suggest broad zones with a limited temperature variation (3°C) and localized, irregularly shaped highs. In some locations within this region, measured temperatures varied abruptly over small distances. These characteristics make proper placement of isotherms problematical even with probe spacings as small as 250 m

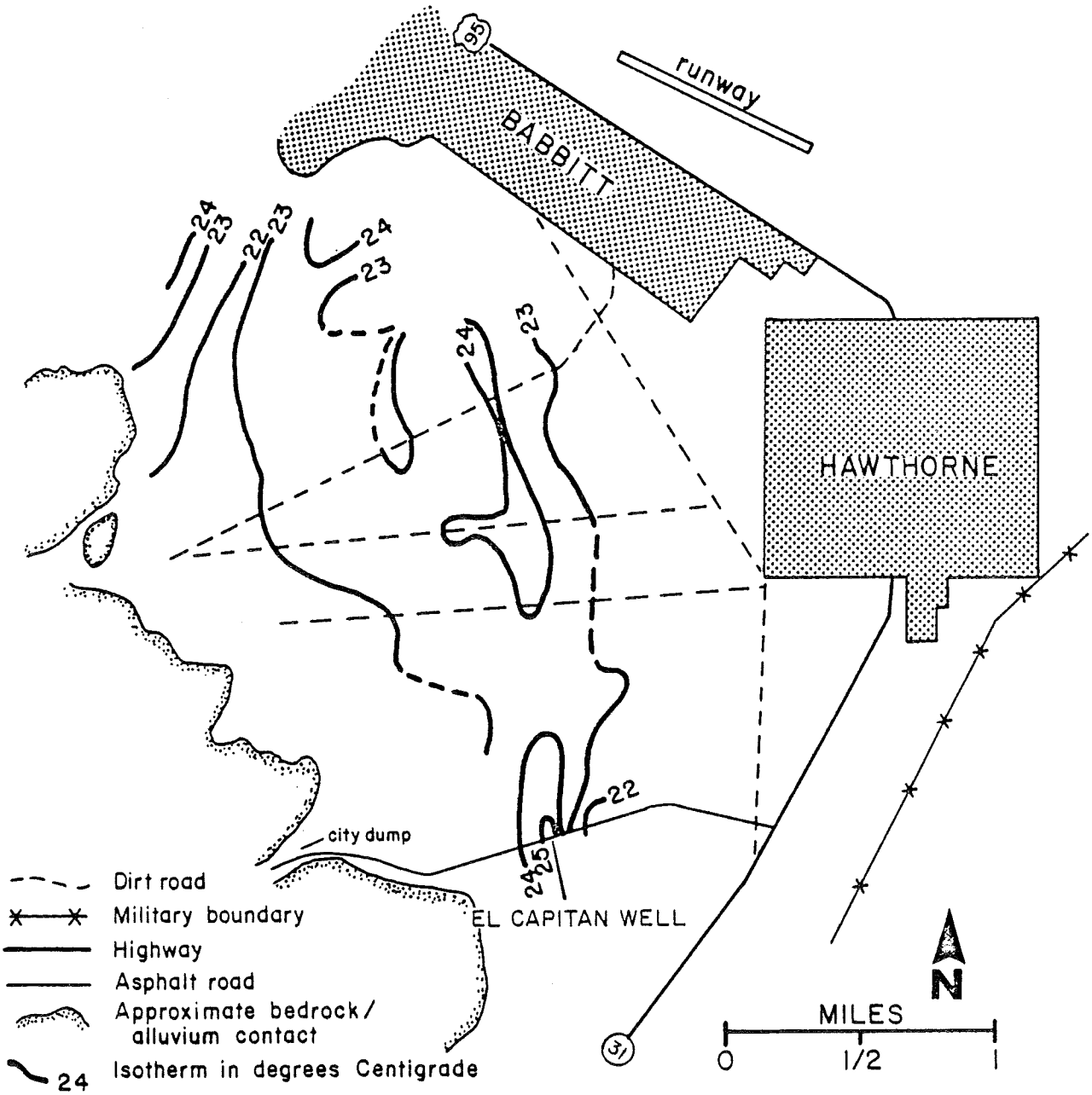

Figure B6. Possible isotherm configurations at a depth of two meters, see text for detail.

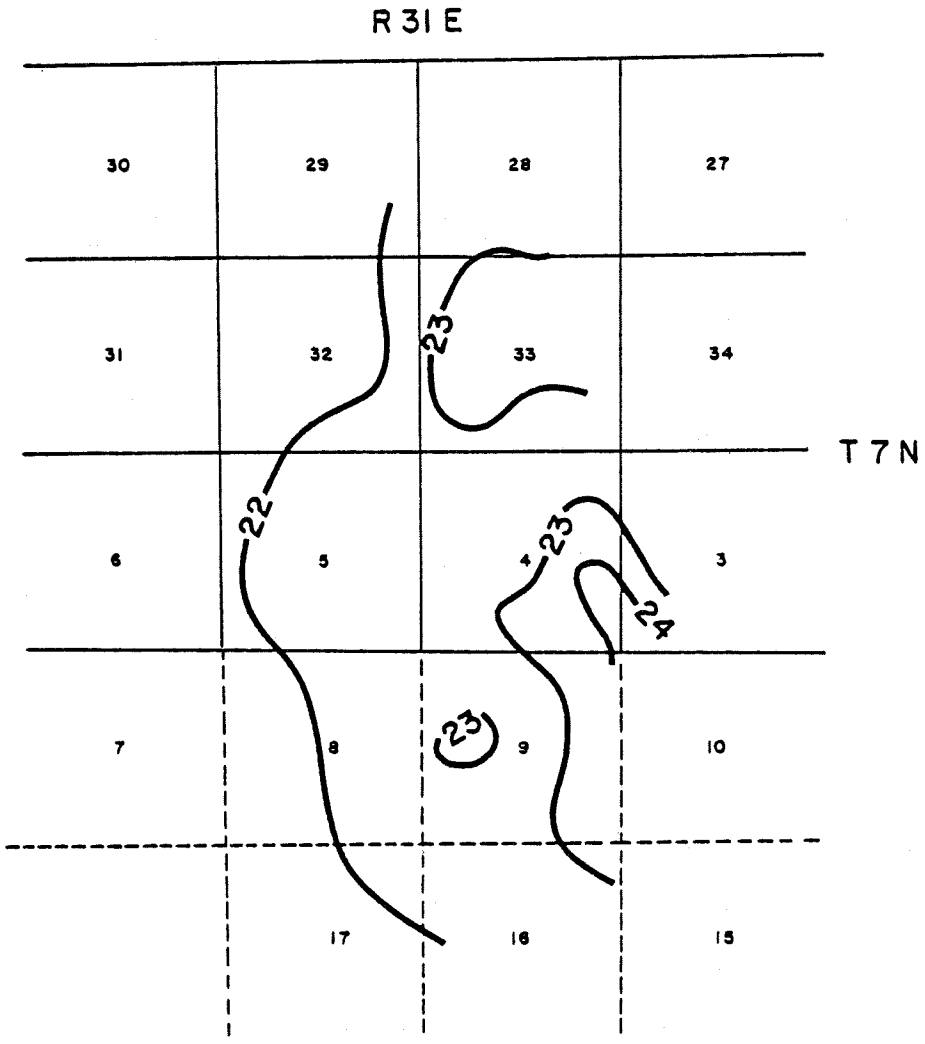

Figure B7 Two-meter isotherm configuration interpreted from two-meter depth temperature probe study, eastern segment of study area.

(820 ft). The irregular shape and localization of areas with elevated temperatures may be partially due to interpretation. It should also be noted that the accuracy of individual probes is $\pm 0.5^{\circ}C$.

Figure B7 details the inferred two-meter depth isotherms for the eastern region. Characteristics of the patterns here are similar to those observed to the west. Well-defined linears are absent, and isolated irregularly-shaped zones of elevated temperature are once again present. Abrupt temperature variations over short distances were not detected, however, sampling-density was lower for this area.

Despite limitations outlined above, the shallow-depth temperature probe study clearly delimits regions of elevated temperature in the study area. This is particularly meaningful in Hawthorne since there are no surface manifestations of geothermal resources. The selection of test hole drill sites was largely based upon data obtained from this technique.

PHOTO IMAGERY

Imagery used to examine the Hawthorne study area ranged in scale from 1:24,000 to 1:250,000. Two forms of 1:250,000 scale color imagery, false color computer-enhanced Landsat, and natural color Skylab were employed. Black and white photography included U-2, Army Map Service Missions, and a low sun-angle mission flown for our study. Scales of the three sets of photographs are 1:120,000, 1:60,000 and 1:24,000, respectively. The smaller scale photographs were used to search for regional structural features and to examine the areal distribution of rock types. Fault locations and linear and curvilinear features were investigated on the larger scale imagery.

Examination of Skylab and Landsat photographs reveals only a limited

number of regional-scale linear features surrounding the study area. The most conspicuous linear alignment occurs along the trend of the Walker Lane (Locke and others, 1940) and is particularly apparent in the Gillis and Gabbs Valley ranges. Range front boundaries on the eastern slope of the Wassuk Range are also clearly visible. An analysis of lineaments (Rowan and Wetlaufer, 1975) concluded that there are few regional features in the area. In addition, there was little correlation between photo image linears and faults mapped by Steward and Carlson (1974). Ekren and others (1976) describe a very extensive regional linear which they name the Pancake Range Lineament. This feature traverses the Garfield Flat and Whiskey Flat and passes south of the detailed study area. The feature is actually an S-shaped curvilinear in this region and, therefore, does not present a single orientation. Late Tertiary and Quaternary extrusive rocks may mask the presence of regional-scale linears in the region.

Low sun-angle photography was flown over most of the area bounded by U.S. Highway 95 to the north and a topographic rise separating Walker Lake Basin from Whiskey Flat to the south. The Garfield Hills and Wassuk Range are the eastern and western boundaries, respectively. This imagery provided the greatest amount of detailed information on the location and direction of offset along faults, as well as the nature and orientation of other features in the area.

Linear and curvilinear features interpreted from low sun-angle photographs are shown in Figure B8. The majority of these linears represent traces of faults or suspected faults; however, some depict drainage paths or topographic features which do not appear to be directly related to faulting. All features appear to fall into one of three general orientations: a NW-SE trend defined by the bounding faults of the eastern flank of the Wassuk Range and other

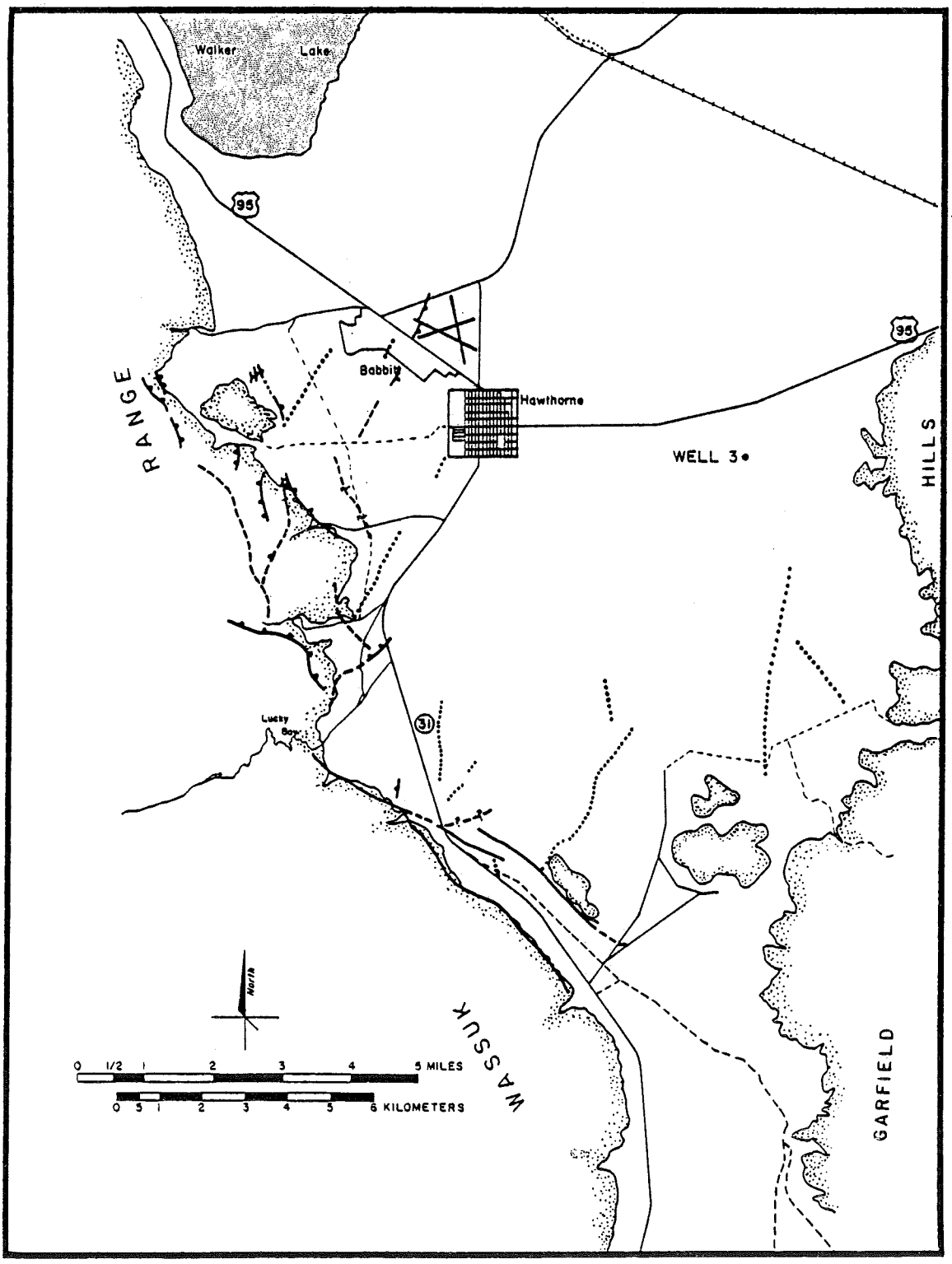

Figure B8. Linear and curvilinear features interpreted from low sun-angle photography in the Hawthorne study area.

subparallel faults; a NE-SW attitude exhibited by faults and drainages in the valley's western area; and a N-S textural grain represented in the south-central portion of the valley. Range front fault traces and escarpments are notably absent in alluvium along the western front of the Garfield Hills.

The eastern frontal zone of the Wassuk Range exhibits well-defined fault traces unlike the western front of the Garfield Hills. These faults are both present in bedrock and alluvium. There are good examples of scarps in alluvium in the region between the mouth of Cat Creek and the airfield runways east of Babbitt (figs. B9, B10). It is likely that some movement has taken place following the last high stand of Lake Lahontan approximately 12,000 years B.P., since some of these scarps lie below this level. Fault scarps are not co-located with wells containing thermal water with one exception where the well was deliberately sited along the fault trace.

A large number of faults in bedrock and alluvium is present along the Wassuk front approximately three miles west of Hawthorne. A complex of horsts and grabens appears to be present within this zone. Faults with blocks downthrown toward the range and the valley are a phenomenon also observed in the vicinity of Powell Canyon (Ross, 1961, p. 56).

U-2 and AMS photography provided little additional information. In certain instances, 1:60,000 scale AMS imagery aided in delineating contacts between certain rock units.

TEMPERATURE PROFILING OF WELLS

Measurements of temperature as a function of depth were completed in four wells in the Walker Lake Basin. Two profiles were taken from existing holes at the Army Ammunition Plant, and the remaining pair was acquired from geothermal test wells. A third profile in one of the Army Plant wells was abandoned when

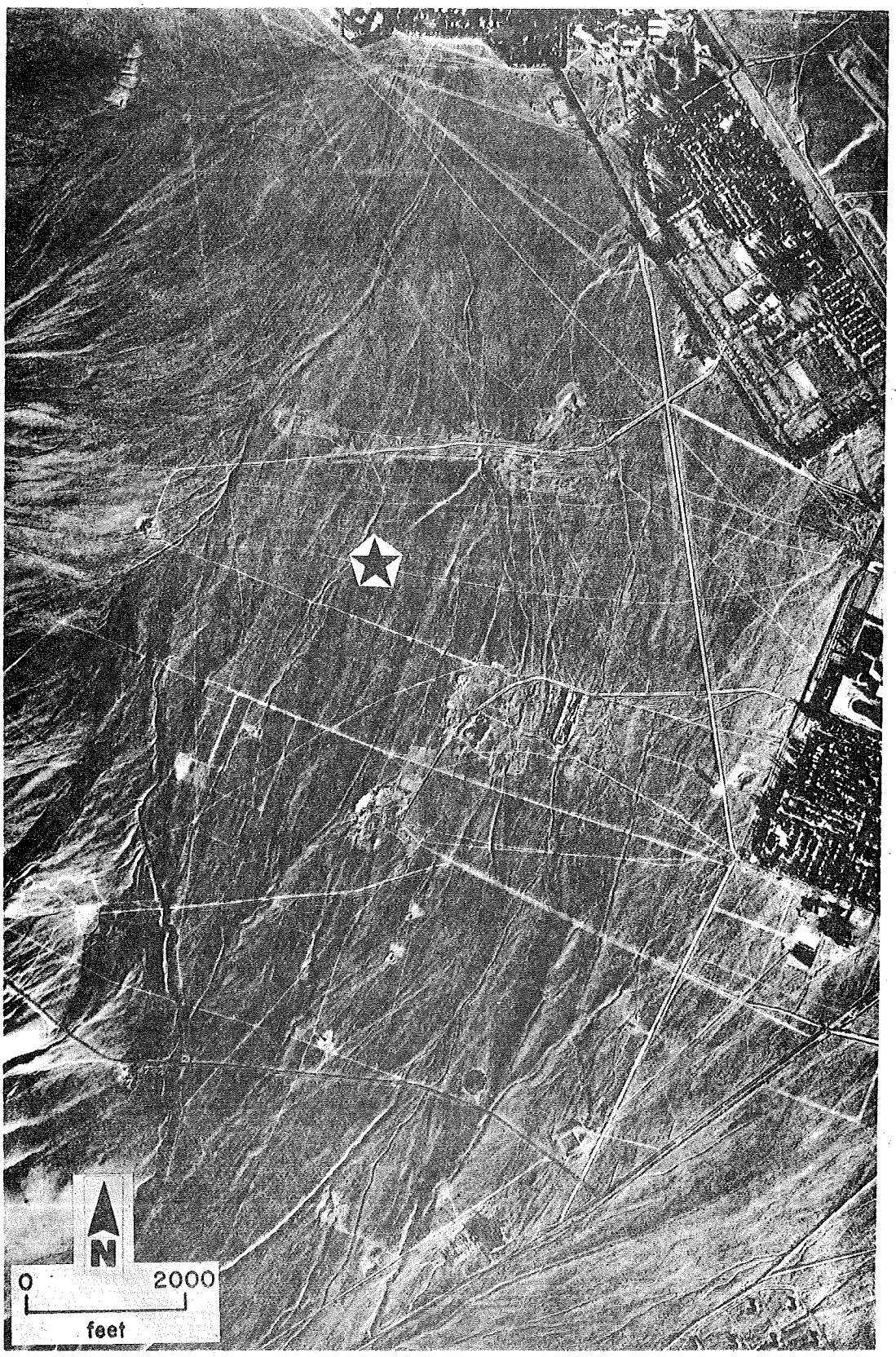

Figure B9. Fault scarps in alluvium west of Hawthorne; star indicates location of test well HHT-1.

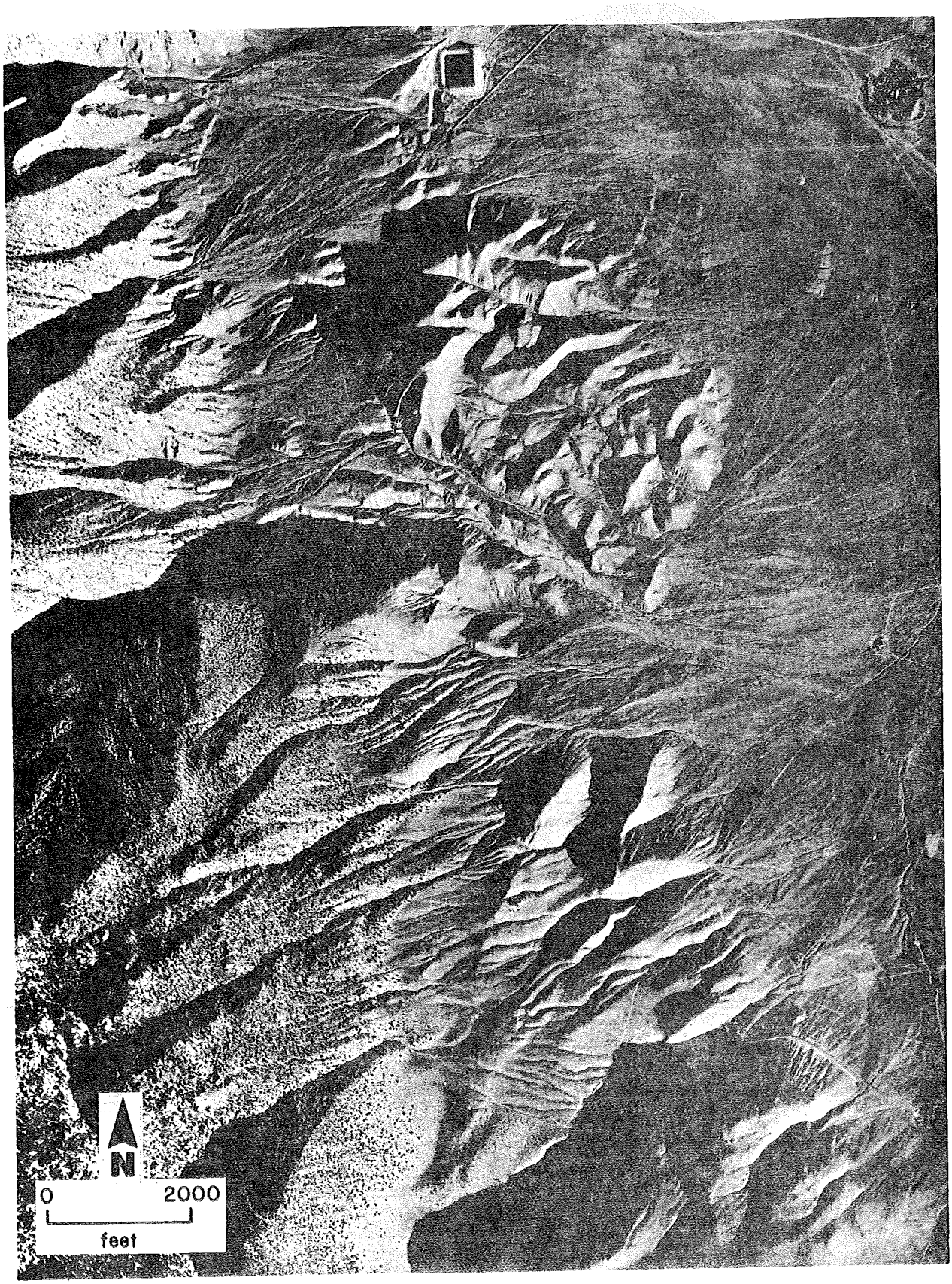

Figure B10. Fault scarps bounding the eastern front of the Wassuk Range west of Hawthorne.

the probe became entangled. Data from the two thermal wells formerly on Navy land are presented in Table B2. Fluids in both wells are essentially isothermal and are around the same temperature. These holes are separated by a distance of nearly 11 km (7 mi) and are located near opposite sides of the Walker Lake Basin (fig. B11, HAAP5 and HAAP 3).

Two geothermal test wells drilled and cased with three-inch diameter threaded pipe were filled with water for the purpose of temperature profiling. Their designations are HHT-1 and HHT-2; their locations are shown in Figure B11. Leaks developed at threaded pipe couplings causing water loss. At HHT-1 which is drilled to a total depth of 255 m (800 ft), temperature profiling was limited to the interval between approximately 73 m (240 ft) and TD. Only the bottom 17 m (55 ft) of the 120-meter (395 ft) HHT-2 contained fluid at the time of profiling.

Three separate temperature profiles were completed on test well HHT-1. The first was performed one week after well completion and is labeled "23 April 81" in Figure B12. Three intervals, each with a lower gradient than the overlying interval, were found at 82-98 m (270-320 ft), 98-122 m (320-400 ft), and 122-146 m (400-480 ft). From 146-177m (480-580 ft) temperatures were essentially isothermal and attained the maximum temperature recorded in the well. A distinct temperature reversal occurs below 177 m (580 ft). Although the temperature probe was calibrated before use, it would not stabilize for some readings due to a leak in the cable shield. In spite of these problems it is believed that temperatures recorded during profiling were within ± 5 degrees centigrade of those actually present. Furthermore, the shape of the curve is accurate.

A second set of profiles was performed on HHT-1 three weeks following completion. The first of these labeled "6 May 18" in Figure B11 represents conditions in the well before the addition of 416 liters (110 gal) of water.

Table B2. Temperature data from Hawthorne Army Ammunition Plant, wells 3 and 5.

HAAP well No. 3* 4 Dec. 1980

Depth in ft.	Temperature °C
260	39.7
280	40.0
300	40.1
320	40.0
340	39.9
360	40.1
380	40.2
400	40.3
420	40.3
440	40.3
452	40.3

*well pumped immediately prior to measurement

HAAP well No. 5 2 Dec. 1980

Depth in ft.	Temperature °C
210	40.3
220	40.5
240	40.7
260	40.8
280	40.8
300	40.8
320	40.8
340	40.8
360	40.8
380	40.8
400	40.8

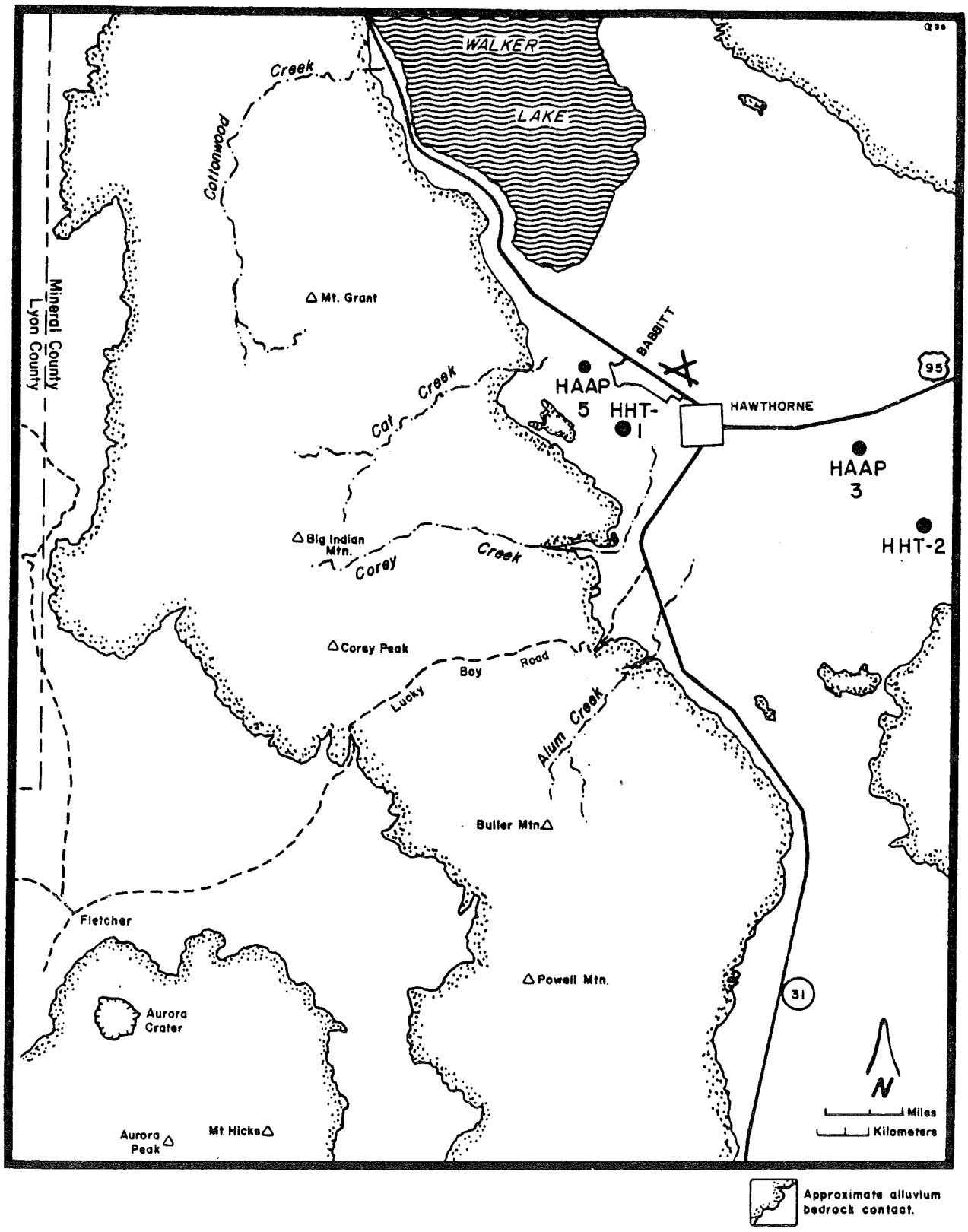

Figure B11. Location of wells profiled for temperature.

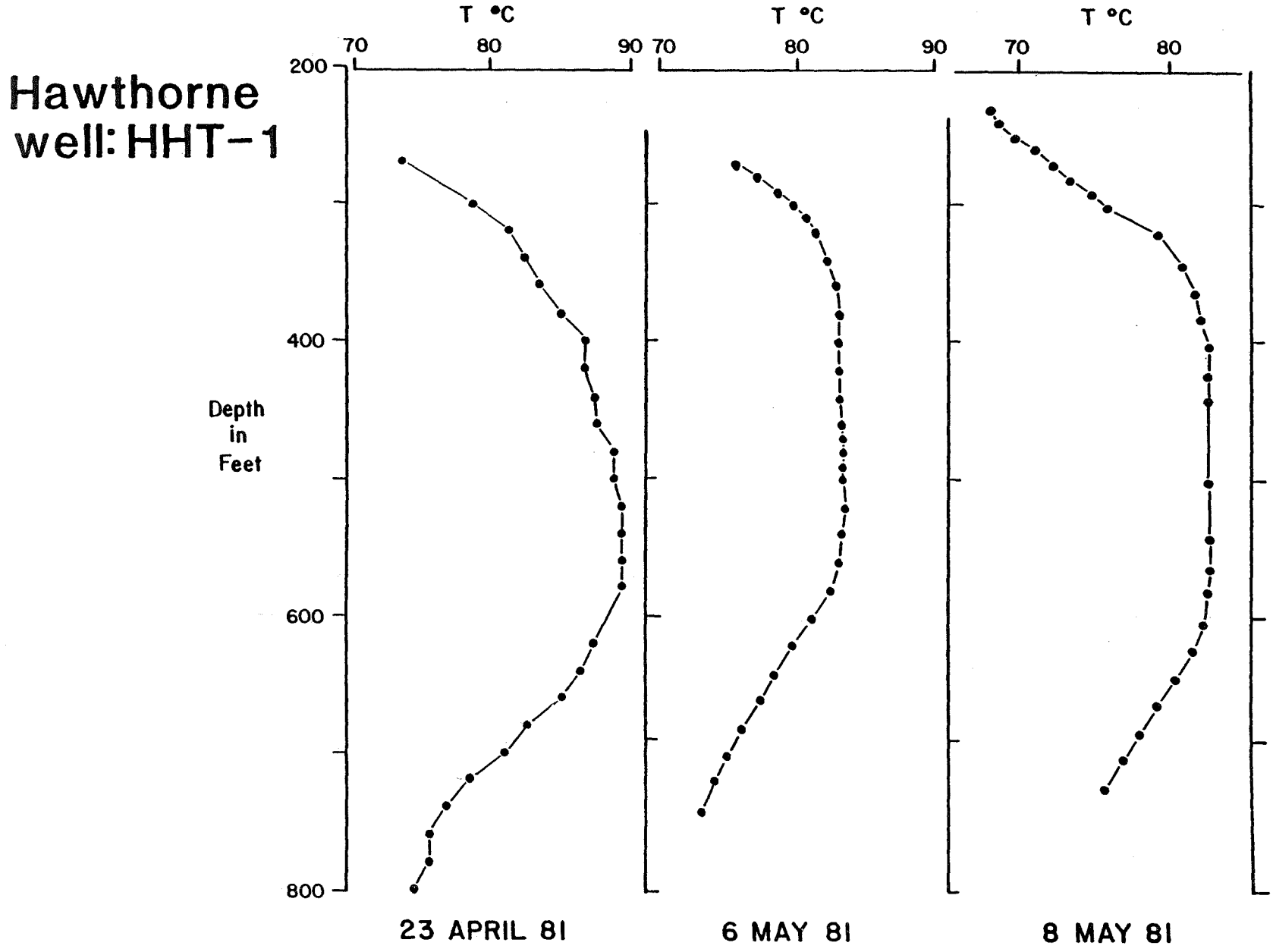

Figure B12. Temperature profiles of test well HHT-1.

A second curve labeled "8 May 81" was drawn from data collected 24 hours after the addition of water. The level of well water was increased only 11m (36 ft) after this addition.

General characteristics of all three profiles are similar. Each has a zone of positive gradient, an isothermal layer, and a segment in which the temperature decreases with depth. There are, however, certain notable differences. Isothermal zones of the second and third curves are approximately twice the thickness of that encountered during the first measurement period. Gradients in the zones where temperature decreases with increasing depth are lower for the 6-May and 8-May curves. Maximum temperatures encountered during the first profile are $6^{o}C$ greater than those of subsequent measurements. And lastly, the shape of the profile above isothermal layers of the latter curves is convex as opposed to the linear-to-concave shape of the same region of the 23 April plot.

A combination of factors is probably responsible for changes between the profiling periods. Poor transfer between thermal and non-thermal fluids and the well casing is perhaps the most influential factor. HHT-1 was drilled using mud to prevent caving of alluvial materials. During drilling, the mud became noticeably thicker due to high temperatures. It is likely that the mud formed a relatively impermeable wall cake after standing since it was not flushed before insertion of the casing. The steel casing is a second important factor. If exposed to a hot zone such as that which appears to be present in HHT-1, the casing tends to conduct heat in both directions, particularly if external thermal sources or sinks were insulated by the mud cake suggested above. Thickness of the isothermal layer tends to increase and the magnitude of the negative gradient decreases. These changes follow the pattern observed in HHT-1 over time. Other influential factors include the upward migration of heat via well-bore convection, and the lack of cold shallow

groundwater as noted during the drilling of HHT-1. The lack of cool groundwaters at levels less than 63 m (200 ft) is documented in well logs from the surrounding area.

One profile was completed on test hole HHT-2, and the data are plotted in Figure B13. Water loss problems were severe at this site limiting the length of the profile. Little can be deduced about temperature-depth relationships at this location due to limited data. Because the temperature is over 60°C at less than 122 m (400 ft) below the surface and the gradient is definitely positive, deeper drilling at this site may be warranted.

SOIL-MERCURY SURVEY

Sixty-four soil samples were collected for analysis of soil-mercury content in the Hawthorne study area. Samples were collected from an average depth of 25 cm (2 ft) and dried at 30°C (54°F) before being analyzed on a gold-film apparatus. The analytical results are listed in Table B3. Collection locations and sample numbers used in the table correspond directly to those used for two-meter temperature probes (see figs. B4 and B5).

Variations in the data are due to several factors. The highest measured value, 127 ppb, is suspect. It occurred at sample location 30, an area of possible contamination. Also, errors associated with operation of the analytical apparatus, and sample in homogeneities limit precision at any selected site to $\pm$15%. If the 127 ppb value is excluded based on contamination, the statistical parameters for the remaining data are $\bar{X}$ = 18 ppb, σ = 8 ppb. Since 3σ represents 99.7% of the area under a normal distribution curve, it is reasonable to adopt the mean plus or minus 3σ as the bounds for "normal" values. Using this formula and excluding the previously discussed high value, 43 ppb becomes the minimum for anomalous points.

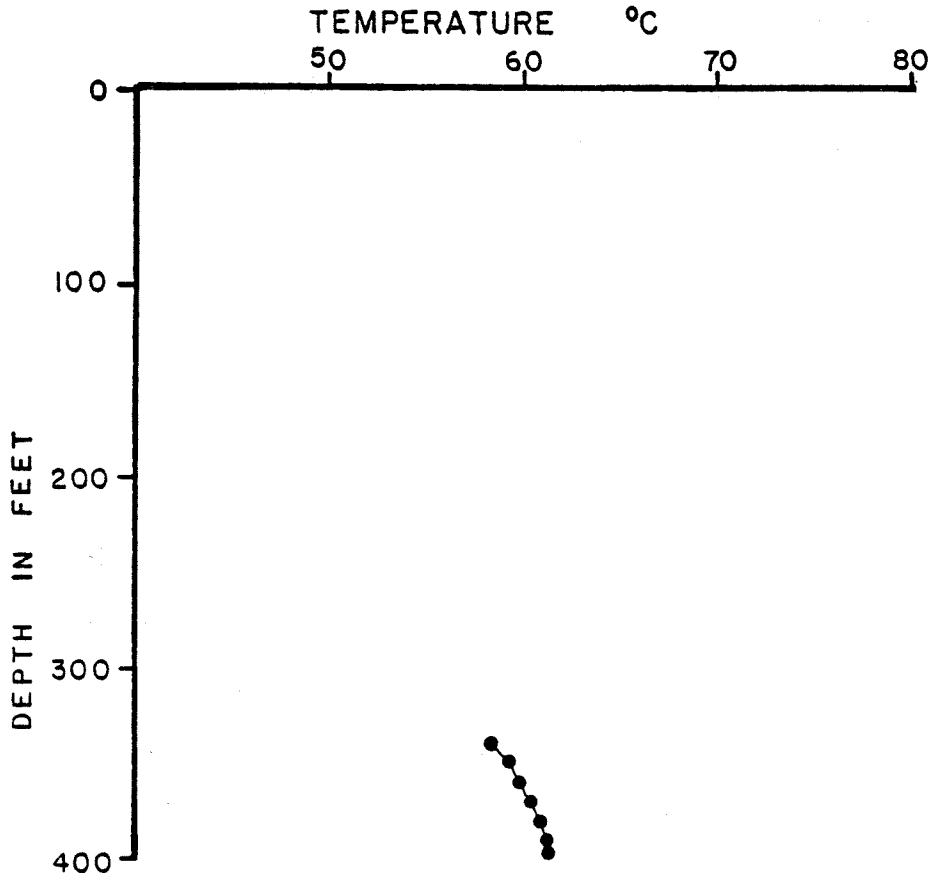

Figure B13. Temperature-depth relationships in test hole HHT-2, profiled May 7, 1981.

Table B3. Results of Hawthorne soil-mercury survey.

Sample #	Mercury Conc. (ppb)	Sample #	Mercury Conc. (ppb)
1	38	28	15
2	18	29	13
3	22	30	127
4	19	31	16
5	38	36	14
6	22	38	16
7	13	39	28
8	16	40	24
9	23	41	19
10	17	43	18
11	20	44	14
12	19	45	15
13	16	46	19
14	17	47	20
15	14	49	12
16	16	51	9
17	12	52	18
18	12	53	11
19	13	54	21
20	13	55	17
21	24	56	27
23	58	57	12
24	14	58	11
25	13	59	14
26	18	60	15
27	15	63	17
		64	20

The soil-mercury data confirm that this technique is not useful for resource exploration in the Hawthorne study area. Only one data point is considered both valid and anomalous (fig. B14). Rather than suggesting trends which define regional anomalies, the data reflect a relatively narrow range of background values. In addition, neither the anomalous point or even the high "normal" values are co-located with points of elevated temperature recorded during the shallow-depth temperature probe study. Finally, data gathered on a small grid spacing, approximately 244 m (800 ft) in the immediate vicinity of the 99° C El Capitan well, are essentially all at background levels. One of the lowest recorded values occurs adjacent to the well.

FLUID GEOCHEMISTRY

Fifteen water samples were collected and analyzed for bulk chemistry and oxygen and hydrogen-stable light isotopic composition to help explain the nature of thermal fluids and flow and/or recharge paths. Results of the analyses for major and minor dissolved constituents are presented in Table B4. Data reported for samples taken during the present study are designated using the letters "HAW" followed by a one or two digit number. Data taken from literature sources are indicated by other appropriate alphanumeric combinations.

Two problems are associated with the analyses results for the HAW series. Silica concentrations reported by the analysts of the HAW series are consistently lower than those reported in the literature although both samples were taken from the same fluid source. For example, two measurements of silica made on fluid extracted from the same location, HAW-6, in May and August, 1980 revealed values of 78 and 74 ppm, respectively. Our sample taken in October, 1980 contained only 40.8 ppm according to the results reported to us. The problem again is apparent when comparing reported values in the two SiO_2

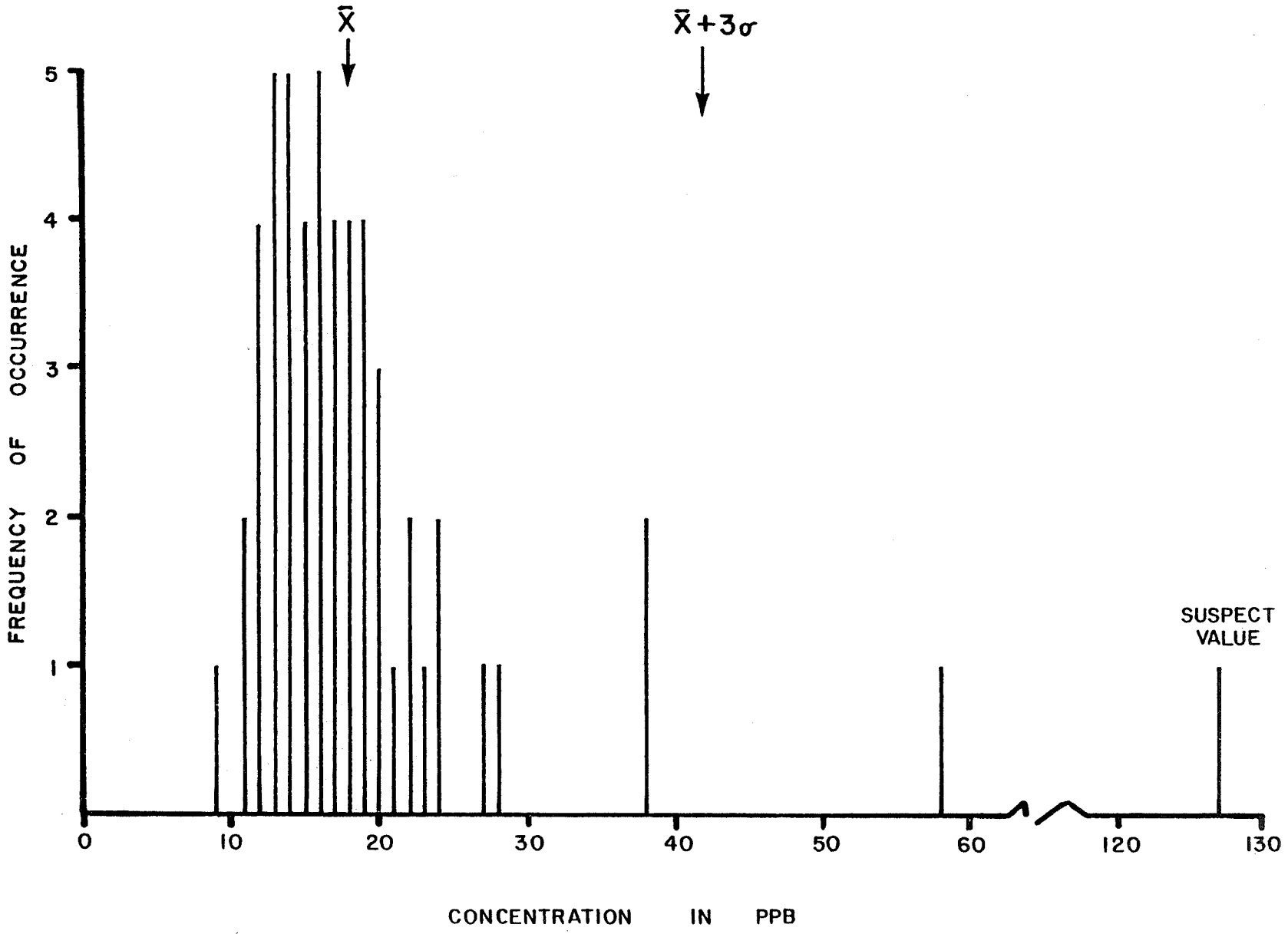

Figure B14. Frequency of occurrence vs. soil-mercury content in ppb.

Table B4. Fluid Chemistry in the Hawthorne study area.

Sample Designation	Temp. C°	pH	Ca	Mg	Na	K	Li	Sr	Al	Cl	SO_4	CO_3	HCO_3	NO_3	F	B	SiO_2 This Study	SiO_2 Other Study	Cation/ Anions (Equiv.)
HAW-1 (HAAP #1)	42/51	7.4	66.9	4.33	185	8	0.17	1.03	<0.3	68.9	384	0	43.9	0.24	1.96	1.12	18.8	31.8‡	1.12
HAW-2 (HAAP #5)	41	7.4	42.9	0.41	276	10	0.60	1.11	<0.3	89.2	491	0	51.2	0.10	7.48	2.27	32.3	50HAAP	1.10
HAW-3 (HAAP #6)	/24	7.3	87.0	17.9	165	7	0.04	0.555	<0.3	85.8	369	0	85.4	0.41	1.61	1.59	13.9	23.8‡	1.17
HAW-4 (HAAP #3)	40.8/	8.1	42.3	4.74	242	16	0.22	0.426	<0.3	105	350	0	117	<0.05	5.15	2.79	38.1	54‡	1.11
HAW-5 (HAAP #4)	/23	7.5	128	26.3	95	6	0.03	0.160	<0.3	95.5	325	0	100	0.96	0.747	1.40	16.3	30‡	1.15
HAW-6 (El Cap)	97/	7.4	40.4	0.08	260	11	0.50	1.46	<0.3	85.2	436	0	95.2	<0.05	7.28	2.19	40.8	76DRI	1.02
HAW-7 (Alum Cr)	6.5/	3.2	186	91.3	26	3	0.06	0.553	109	6.8	1390	0	0	1.34	1.89	0.112	39.0		1.02
HAW-8 (Cottonwood Cr) 4800'	9.7/	7.4	40.2	8.06	18	2	<0.01	0.208	<0.3	6.0	34.1	0	109.8	<0.05	0.315	0.049	14.2		1.29
HAW-9 (Cottonwood Cr) 7500'	6.9/	7.5	35.1	6.85	12	1	<0.01	0.126	<0.3	3.63	12.0	0	100	<0.05	0.097	0.036	10.9		1.42
HAW-10 (Cottonwood Cr) 9000'	3.1/	7.3	28.6	6.81	9	2	<0.01	0.140	<0.3	3.06	4.51	0	102.5	1.15	0.085	0.027	15.4	39HAAP	1.20
HAW-12 (Coreyville)	5.7/	7.1	24.9	4.13	13	3	<0.01	0.170	<0.3	5.88	10.2	0	90.3	<0.05	0.092	0.041	12.4		1.19

Table B4. Fluid chemistry in the Hawthorne study area (Cont.)

Sample Designation	Temp. C°	pH	Ca	Mg	Na	K	Li	Sr	Al	Cl	SO_4	CO_3	HCO_3	NO_3	F	B	SiO_2 This Study	SiO_2 Other Study	Cation/ Anions (Equiv.)
HAW-13 (Cottonwood Spr)	14.7/	7.9	160	27.8	69	6	0.02	0.957	<0.3	45.8	177	0	390.4	<0.05	0.710	0.131	18.5		1.17
HAW-14 (HHO 5)	35.0/	7.4	99.4	13.4	82	6	0.02	0.987	<0.3	21.4	272	0	136.6	1.59	0.179	0.103	14.9	25‡	1.14
HAW-15 (Corey Canyon Well)	11.1/	7.5	87.4	14.1	28	4	0.02	0.669	<0.3	16.0	96.9	0	180.6	1.54	0.163	0.067	9.5		1.03
HAW-16 (Walker Warm Spr)	34.5/	7.2	27.9	0.66	212	3	0.40	1.23	<0.3	4.44	68.2	0	43.9	0.18	7.89	1.83	21.3		1.29
BLM* (Whiskey Flat Windmill)	/43	--	6.0	0.9	116		--		--	64	109	9	47	0.1	4.8	--		37	--
6/31 b2 * (Whiskey Flat Irrigation)	/11	8.1	30	13	44		--		--	38	93	0	90	--	--	--		--	--
NAD2‡	/27.5	7.5	82	9.7	187.5	11.9	--	--	--	85.6	405	0	134	--	1.09	--		58.4	--
NAD7‡	/21	8.6	18.2	0.25	135	4.4	--	--	--	60.4	204	0	61	--	3.35	--		136	--
NAD8‡	/26.5	7.4	74	8.4	137.5	7.4	--	--	--	52.9	193	0	259	--	2.85	--		43.9	--

* = Data from Everett, D.E. and Rush, F.E. (1967)
‡ = Data from Bohm, B.W. and Jacobson, R.L. (1977)
HAAP = Data from Hawthorne Army Ammunition Plant records.
DRI = Data from files of Desert Research Institute, University of Nevada System, Reno.

Data preceded by a slash were extracted from a source independent of our work.

columns in Table B4. Lengthy discussions with the analysts together with reanalysis of several samples failed to produce any satisfactory explanation of this problem. Due to this unusual situation, all silica concentrations from our study should be considered suspect.

In addition to low silica values, several analyses from the HAW sample series exhibit relatively poor ionic balances. Ordinarily this would imply that an important species was omitted from the analysis suite. However, the analysis suite was comprehensive. The completeness of the analytical suite and the composition of probable source rocks for dissolved constituents argue strongly against omission error. Reanalysis of several samples produced similar values. Literature data describing the same fluid sources indicate lower calcium and higher bicarbonate values than our analyses. Such differences bias the ionic balances toward the cation side, which is also the nature of the imbalance observed in our data.

The sampling program design makes it possible to trace changes in fluid composition moving down the hydrologic gradient. For example, samples HAW-10,HAW-9, HAW-8 were collected at elevations of 2743 m (9000 ft), 2286 m (7500 ft), and 1463 m (4800 ft) along Cottonwood Creek. Data presented in Table B4 indicate that concentrations of most dissolved constituents increase with decreases in elevation for Cottonwood Creek waters. Sample HAW-12 represents meteoric surface water collected near the source of Corey Creek. HAW-15 and HAW-13 are groundwaters from progressively lower elevations. Once again, decreasing elevation corresponds to higher concentrations of dissolved constituents. These trends suggest that significant increases in the concentration of dissolved species take place simply with migration down the hydraulic gradient. It is also generalized from Table B4 that groundwaters contain notably higher levels of dissolved constituents than surface fluids at the same elevation.

Gross chemical characteristics of fluids in the study area and surrounding region are shown in the form of a trilinear plot in Figure B15. The cutoff for designation as a thermal fluid is arbitrarily set at 25°C. Sample compositions tend to fall into one of three groups with respect to cations. One of these assemblages is located near the Na+K apex and includes samples 2, 4, 5, 16, NAD7, and BLM. A second more calcium and magnesium-rich collection is defined by numbers 1, 3, NAD8, and NAD2. And finally, samples 5, 8, 10, 12, 13, 14, and 15 constitute a third group. The latter group consists primarily of cool surface waters and groundwaters. If anions are used for comparison, waters can be described as those which lie above the 50% SO_4 line, and those which fall below it. Decreasing elevation apparently correlates to decreasing relative CO_3 + HCO_3 content as demonstrated by meteoric surface waters (10, 12, 8) and groundwaters that are probably directly related to these surface fluids (13, 15). This phenomenon is also partially a result of increasing SO_4 content as elevation decreases.

The colinear arrangement of selected points in Figure B15 suggests that some water compositions may result from mixing. Samples 1, NAD2 and 8 define one line. In addition to being colinear, the relative spacing of the points and their sequence along the line is maintained in all three segments of the plot. This further substantiates the mixing hypothesis. The same situation also exists for samples 6, NAD8 and 12. A further test of the hypothesis could be made if stable light isotopic data were available for all samples. Unfortunately, samples from sites NAD2 and NAD8 could not be obtained during the study period.

Modified Stiff diagrams provide a method of depicting areal variations of bulk chemistry. This format is used in Figure B16. The shape of the symbols in Figure B16 suggests that certain waters are similar. For example,

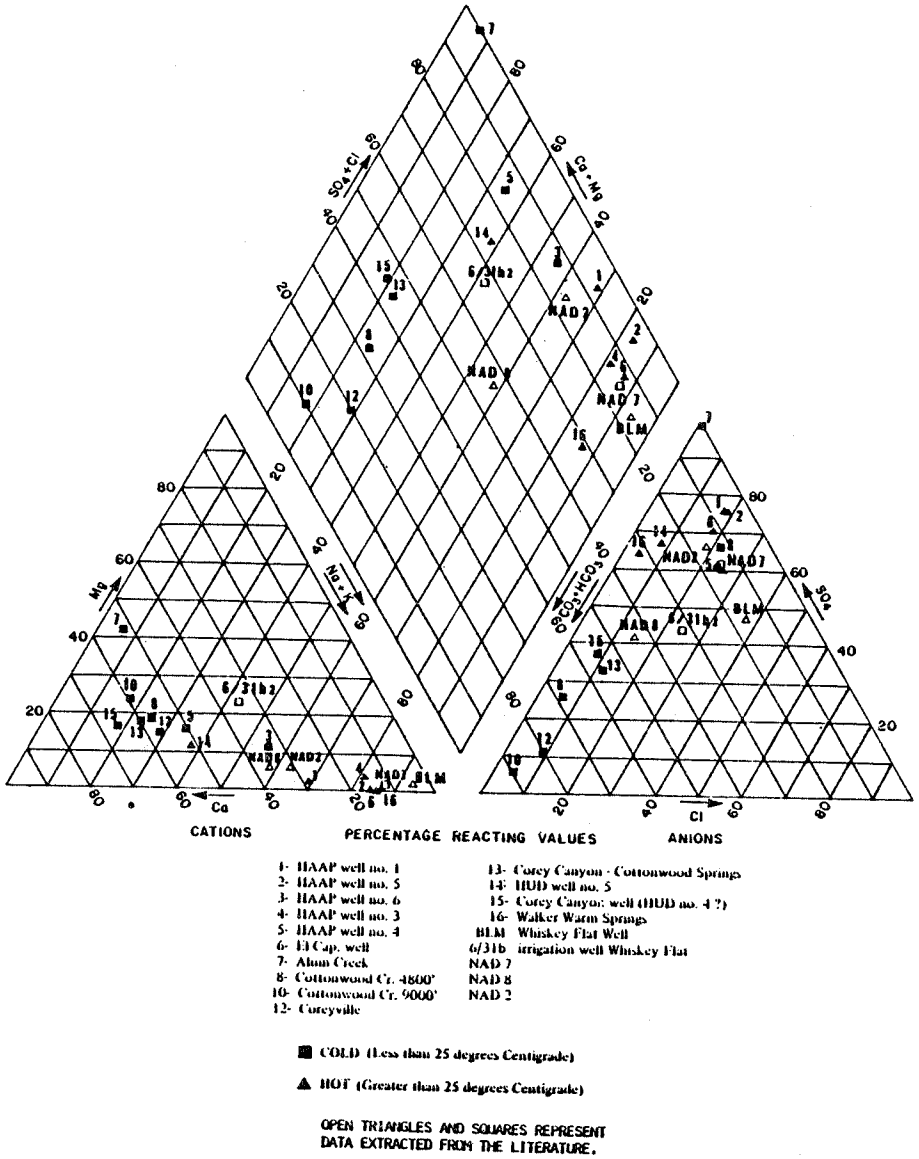

Figure B15. Chemical characteristics of thermal and non-thermal fluids in the Hawthorne study area. Numbers refer those in Table B4.

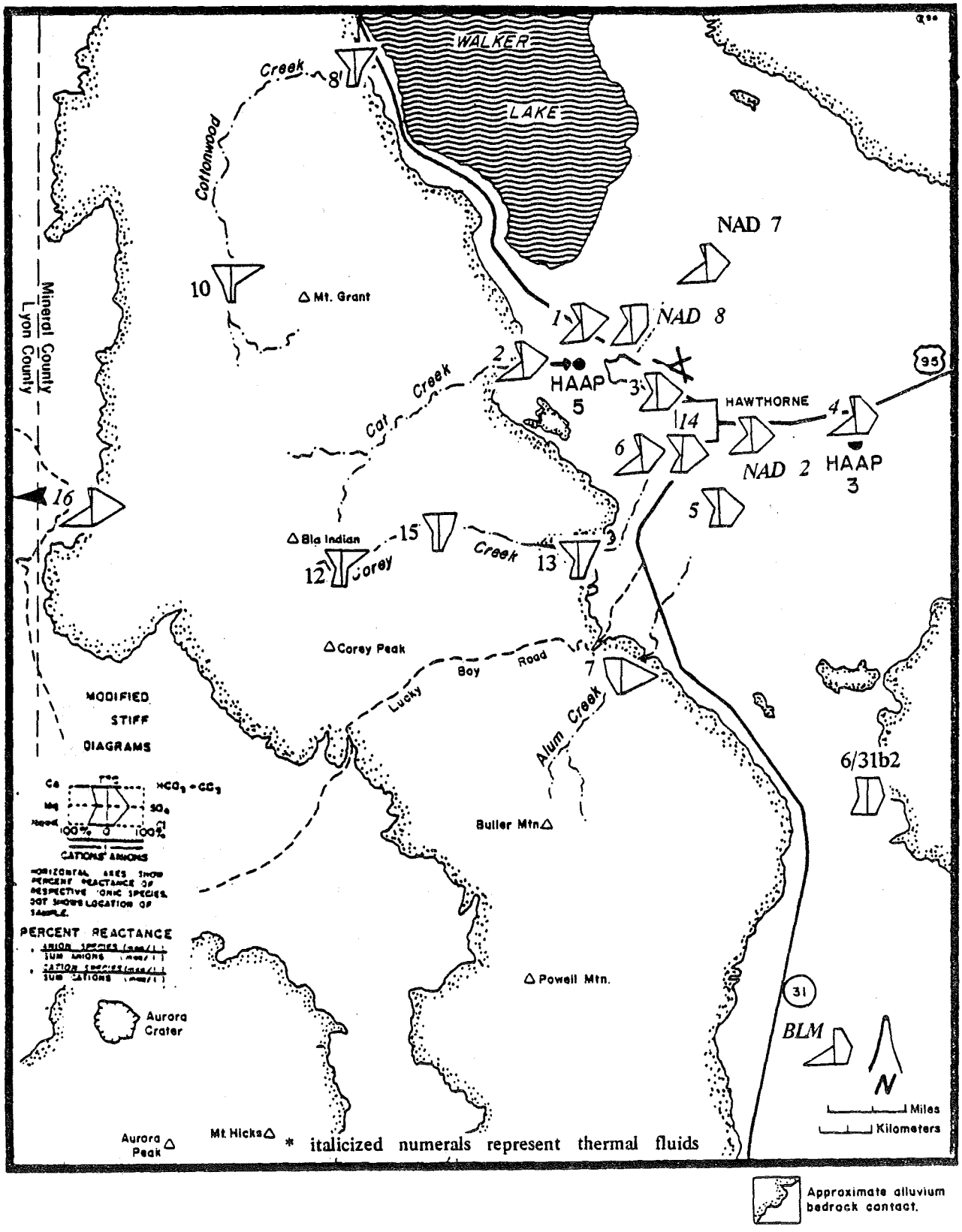

Figure B16. Chemical variations in fluids sampled throughout the Hawthorne study area. Numbers refer to those in Table B4.

samples 2, 4, 6, 16, and NAD7 exhibit marked parities although they are widely spatially distributed. Differences between groundwaters in the Wassuk Range and those of the Whiskey Flat are delineated by comparing symbols 13 and 15 to number 6/31b2. Lastly, the anomalous composition of surface waters in Alum Creek is indicated by symbol 7. Field examination of the rocks through which Alum Creek flows demonstrates that a zone of intense hydrothermal alteration exists near the headwater. Clay minerals are present in large quantities and sulfides are also found in the altered rocks. The low pH (3.2) and high aluminum content of the stream waters probably result from acids released during sulfide weathering.

Trace Constituents

Trace element concentrations may be useful to a limited extent as a tool to distinguish thermal from non-thermal fluids in the Hawthorne area. Concentrations of boron, fluoride, lithium, and strontium are plotted for most samples in Figure B17. Lithium maintains a clear distinction between concentration level in hot versus cold waters. For boron, fluoride and strontium, cold water concentrations are present which approximate or exceed those of hot fluids. Sample 14 is noteworthy because levels of all four trace constituents are comparable to those observed in cold fluids, even though a temperature of 35^{o}C was measured at the sample site.

Stable Light Isotopes

Data on the hydrogen and oxygen stable light isotopic compositions for 15 study area fluids are listed in Table B5 and plotted in Figure B18. The point labeled "3" in Figure B18 exhibits a relatively large ^{18}O shift relative to the meteoric water line and compared to other samples. This shift is not the result of water-rock interaction; it was caused when the sealed

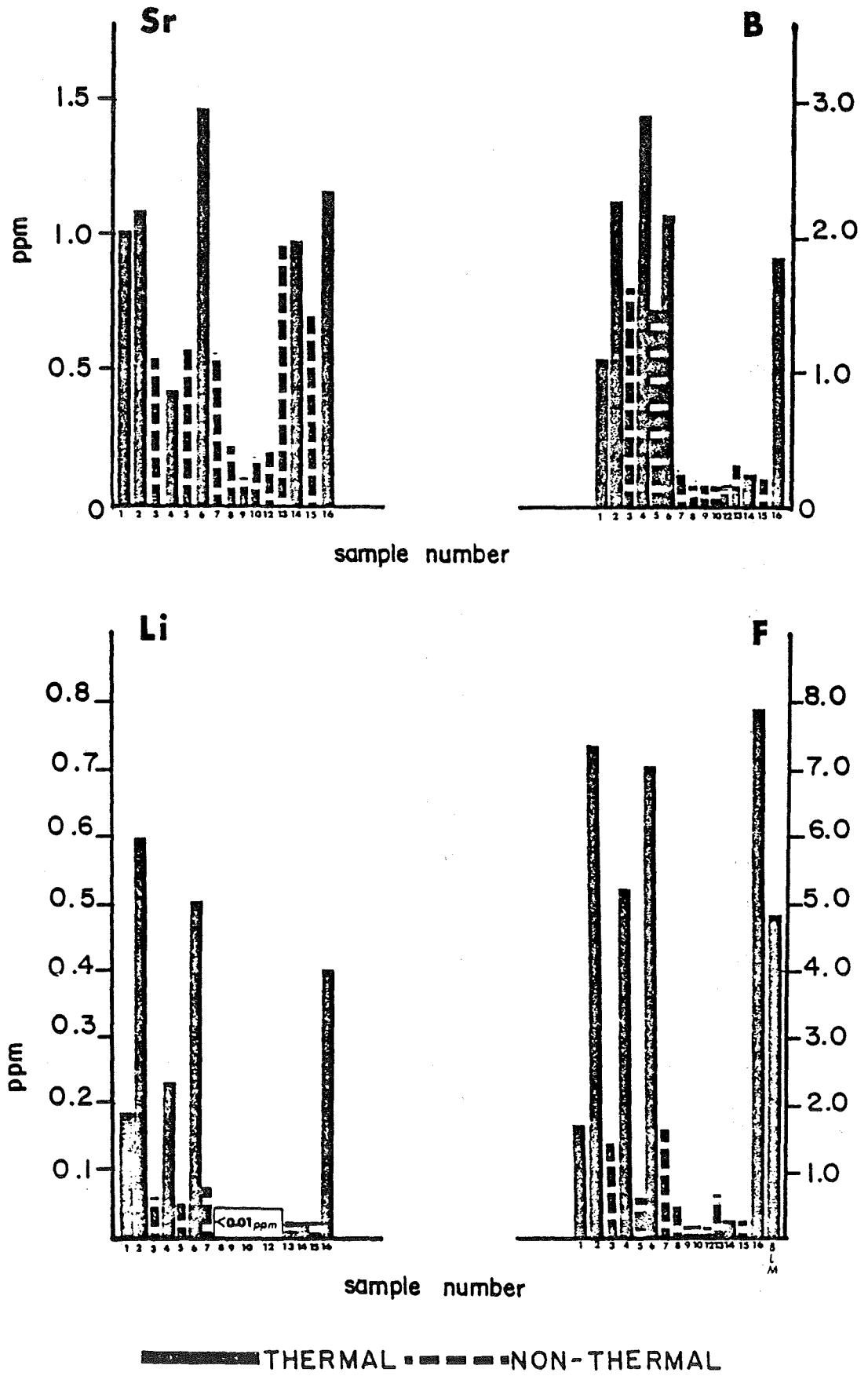

Figure B17. Trace element compositions of samples from the Hawthorne area.

Table B5. RESULTS OF FLUID ISOTOPIC ANALYSIS, HAWTHORNE AREA

SAMPLE DESIGNATION	$\delta^{18}O$ °/oo	δD °/oo
HAW-1	-15.2	-126.
-2	-15.3	-127.
-3	-13.6	-124.
-4	-15.6	-123.
-5	-15.3	-132.
-6	-15.4	-130.
-7	-14.8	-116./-117.*
-8	-15.2	-119.
-9	-15.3/-15.5*	-115.
-10	-16.1	-124.
-11	-16.2	-127.
-12	-15.7	-119.
-13	-15.1	-123.
-14	-15.2	-122.
-15	-15.2	-124.
-16	-16.2	-133./-131.*
-17	-15.8	-124.

* Values separated by slashes represent duplicate analyses of a single sample.

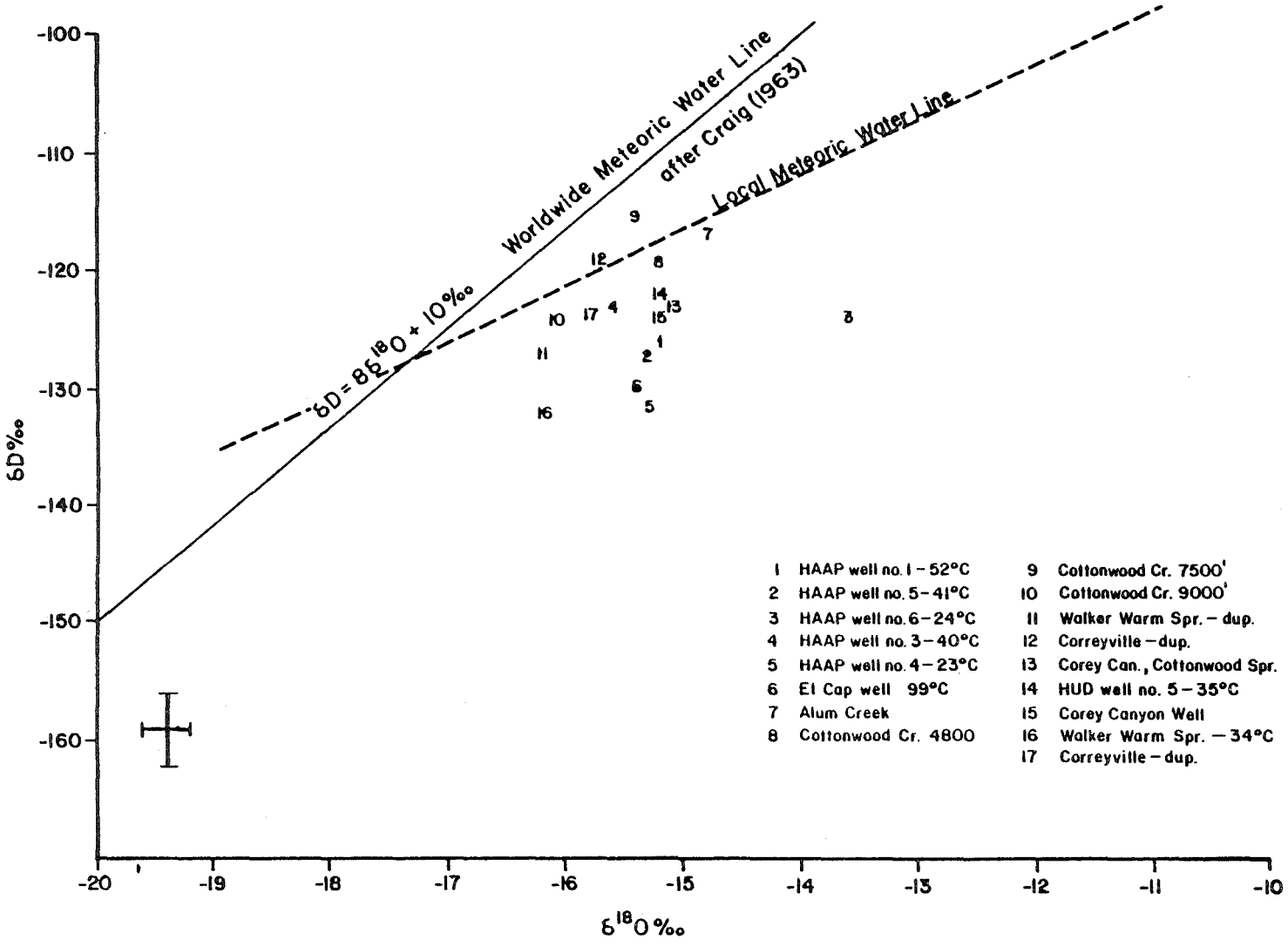

Figure B18. Stable light isotopic composition of Hawthorne area waters – reference SMOW.

sample bottle cracked before analysis and exposed the fluid to atmospheric oxygen. Since the deuterium value should not be significantly affected by this process, it may be used for discussion purposes. Error limits reported by the analysts are $\pm 3^{o}/oo$ for deuterium and $\pm 0.2^{o}/oo$ for oxygen. These limits are depicted to scale in Figure B18 as a cross in the lower left-hand corner of the plot.

In general, the location of points in Figure B18 shows a relatively small variation among many of the waters, and the deviation shrinks even further when analytical error limits are considered. Samples 11 and 16, and samples 12 and 17 are analyses of duplicate aliquots collected during a single visit. Waters 7, 8, 9, and 10 are taken from surface streams with 8, 9 and 10 representing different elevations along the same water body. Number 10 was collected at the highest elevation 2744 m (9000 ft) and exhibits the isotopically lightest signature. However, samples 8 and 9 are indistinguishable within analytical error limits even though they differ by approximately 823 m (2700 ft) in collection-point elevation. This situation may reflect the nature of infeed waters at different elevations along the main creek.

Data derived from samples of meteoric surface waters in the Hawthorne area suggest that the slope of the worldwide meteoric water line given by Craig (1963) may not be appropriate for use in this region. A line with a slope calculated from linear regression of the Hawthorne data (samples 7, 8, 9, 10, 12, and 17) is shown in Figure B18 as the "local meteoric water line". This line has a slope approximately equal to 5 indicating that the local system may be a "closed basin" with respect to meteoric water cycles. Craig (1963) found similar slope lines for meteoric waters collected in Africa. The slope is the result of a complex isotopic exchange process that occurs in areas with high evaporation rates. Because Hawthorne area meteoric

surface waters can be correlated with such a well-defined line, the "local" line will be used for discussion purposes.

Most of the waters sampled during the study period appear to be isotopically directly related to local meteoric waters of the type sampled in the Wassuk Range (fig. B18). However, a few fluids do stand apart. The isotope data of Table B5 have been plotted in terms of δD-Cl plots (fig. B19) as a means of highlighting the similarities and differences between sampled fluids. One of the most striking features of the plot is the clear distinction in chloride content between various sample groups. Samples 1, 2, 3, 4, 5, and 6 taken from wells drilled in alluvium contain notably higher chloride levels than other fluids. This implies that the well waters obtain chloride from an alluvial source or follow a different recharge path than other area groundwaters. Sample 14 was collected from a well drilled in alluvium located approximately 1 km east of the sample 6 site. Its Cl content places it in a relatively low level group similar to other groundwater (sample 15). These relationships support the hypothesis that different recharge paths are responsible for the high chloride values of samples 1-6. Sample 13, a spring water from Corey Canyon, possesses an intermediate chloride level possibly derived from a recharge path similar to that which feeds the wells of the high chloride group.

Deuterium values for the 15 waters do not appear to be systematically related to chloride content (fig. B19). Changes in the heavy hydrogen isotope can be correlated with variations in recharge elevation. Waters collected from elevations less than 2300 meters (samples 7, 8 and 9) have δD values less than $120^{o}/oo$ and are labeled "group I" in Figure B19. Samples 12, 17 and 10 collected at 2400 and 2700 meters are placed into a second group (II, fig. B19) along with related groundwaters and well waters. An

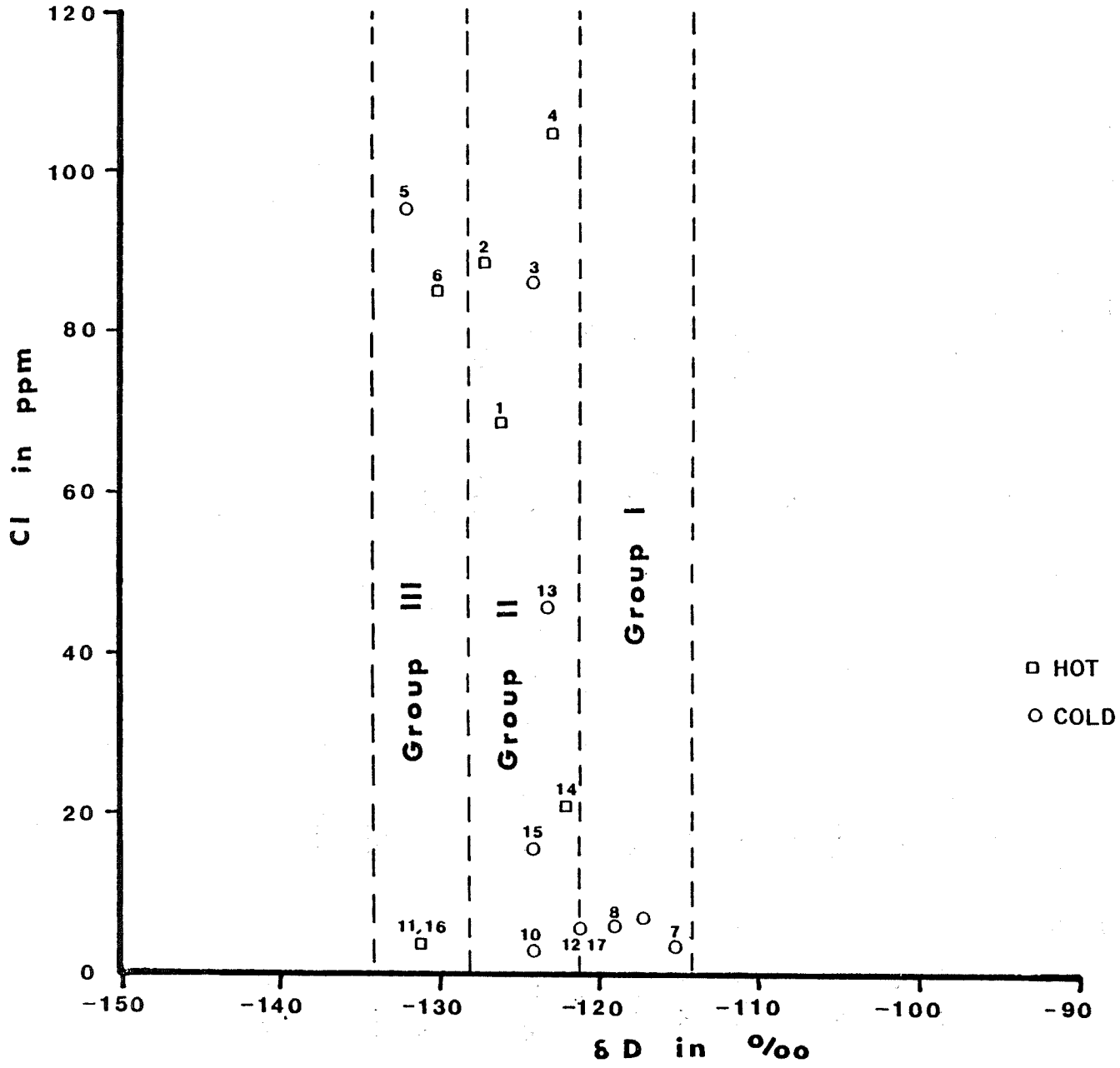

Figure B19. δD-Cl diagram for selected regional fluids.

elevation functional relationship identifies a third group in which isotopically lighter recharge is occurring. Samples 11, 16, 6, and 5 (fig. B19) define this group. Elevations greater than 2700 meters are limited to relatively small portions of the Wassuk Range and the Sierra Nevada which are several kilometers to the west of the study area. Thus, possible recharge regions are areally restricted and may be the same for fluids collected from spatially widely distributed sources. Fluid ^{18}O compositons fall into a relatively narrow range spanning only 1.4°/oo (fig. B18). Maximum "oxygen shifts" occur for samples 5 and 6 and are approximately 2.5°/oo if the plotted values are true values. However, if analytical error limits are taken into consideration, the apparent shift may be as little as 1.6°/oo. Sample 6 was collected from a well that produces fluids with a temperature greater than 99°C. Therefore, the "shift" may represent that expected for area thermal fluids. Carbonates are present in the regional section but only to a very limited extent in the vicinity of the Lucky Boy Mine. It is possible, although unlikely, that they contribute to the oxygen "shift" since this would require a recharge path which opposes the regional hydrologic gradient.

There is no clear definition of recharge and/or reservoir processes due to the limited range of isotopic compositions, uncertainties introduced by analytical error limits, and general lack of well-defined trends in isotopic compositions. All fluids appear to be related to meteoric recharge from the Wassuk Range. The limited "oxygen shift" observed in a few fluids could result from short circulation times, relatively low temperature (<150°C) water-rock interaction, high water/rock ratios, or a combination of these factors.

Chemical Geothermometers

Many approaches to predict subsurface fluid temperatures use fluid composition and the temperature dependence of specific reactions. Perhaps the most widely known and universally applied of these chemical geothermometers are those developed by Fournier and Rowe (1966) and Fournier and Truesdell (1973). Values calculated from concentrations of silica, sodium, potassium, and calcium using the equations given by Fournier in Rybach and Muffler (1980, p. 13) are shown for selected study area fluids in Table B6. Historical data for silica were used for computation purposes because of analytical uncertainties previously discussed. Samples HAW-4 and BLM each have two values for the cation geothermometer. Numbers following the slash are computed with a magnesium correction factor after the procedure developed by Fournier and Potter (1979).

The most conspicuous feature of the data in Table B6 is the generally moderate maximum temperatures indicated by both the silica and cation geothermometers. Nine of the ten samples listed have calculated maximum temperatures below 125°C. Sample NAD7 is the only exception. Fluids from this well contain the highest silica level of any recorded for the entire region. Silica concentration in NAD7 is nearly a factor of two greater than that recorded in the hottest well (HAW-6, 99°C) in the area. There are three possible explanations of this phenomenon: the historically reported silica value is erroneous; the silica phase which controls the concentration is not quartz; and the silica value is real and regulated by quartz equilibrium. The first explanation must be considered since no other data are available to substantiate or refute it. Furthermore, samples taken during the study which generated the NAD7 value notably disagree with silica data acquired during other investigations. Table 3

Table B6. Calculated Geothermometers for fluids in the Hawthorne Study Area.

Sample Designator	Quartz No. Steam Loss	Quartz Maximum Steam Loss	Chalcedony	Amorphous Silica	Na-K-Ca	Measured Temperature	-Cristo-Balite	B-Cristo-Balite
HAW-1	81.8	85.2	50.6	-30.9	71.8	51	32.0	-13.5
HAW-2	101.8	102.6	71.9	-14.0	93.6	41	51.4	4.7
HAW-3	70.1	74.9	38.3	-40.6	61.2	24	20.7	-23.9
HAW-4	105.4	105.7	75.8	-10.9	158.8/112*	41	55.0	8.0
HAW-5	79.4	83.1	48.1	-32.9	44.6	23	29.6	-15.6
HAW-6	122.4	120.2	94.2	3.8	97.7	97	71.8	23.9
HAW-14	72.0	76.6	40.3	-39.0	47.8	35	22.5	-22.2
BLM	88.3	90.8	57.4	-25.5	152.5/107*	43	38.2	- 7.7
NAD 2	109.2	108.9	79.8	- 7.7	80.3	28	58.7	11.5
NAD 7	155.1	147.7	130.5	33.2	77.0	21	100.0	55.5
NAD 8	95.8	97.4	65.5	-19.1	64.3	27	45.6	- 0.8

*Na-K-Ca Value with Magnesium Correction of Fournier and Potter (1979)

of Bohm and Jacobson (1977) under the heading NAD1 offers an example of this. The contention that quartz does not control silica level in NAD7 is supported by the large discrepancy between the quartz and the cation geothermometer temperatures. No evidence supports the hypothesis that the reported value for NAD7 is real and quartz-controlled.

If the data in Table B6 are considered with respect to agreement between silica and cation geothermometer temperatures, the samples fall into two groups. Group one contains samples HAW-1, HAW-2, HAW-3, HAW-4, and BLM and shows closest agreement between quartz and Na-K-Ca temperatures. Samples HAW-5, HAW-6, HAW-14, NAD2, and NAD8 form a second collection. Comparison of chalcedony and cation numbers yields the smallest disparity between calculated temperatures for the second group. NAD7 does not fall into either assemblage which casts greater doubt on the validity of the reported silica value. The significance of the groups is not clear, however, it is interesting to note that both the chalcedony and cation temperatures for HAW-6 are within 5°C of temperatures measured during pumping at a rate of 2500 1/min (660 gpm). This may suggest that the two groups are the result of different recharge paths, one controlled by chalcedony and another regulated by equilibria with quartz.

Source for $SO_4^=$.

Sulfate is a major dissolved constituent in all study area groundwaters. The highest measured level, 1390 ppm, occurs in a sample collected from Alum Creek. This correlation may indicate the source for the constituent in area waters. Field examination of the rocks through which Alum Creek flows demonstrates that a highly altered zone is present in granitic rocks near the headwater. The zone contains disseminated sulfides. When placed in contact with oxygenated surface waters, these minerals react to produce sulfuric acid and release iron. Rock minerals, particularly feldspars, are then attacked

by the acid, releasing aluminum and calcium into the solution. This mechanism accounts for the high calcium, aluminum and sulfate content and low pH observed in Alum Creek waters. Although not shown in Table B4, the iron content of the creek is also at least two orders of magnitude higher than any other water sampled. High iron content further substantiates the oxidation-acid production hypothesis. Similar zones containing sulfides may exist at other locations below the surface in granitic rocks of the Wassuk Range.

Granitic rocks are not the only lithologic type known to contain sulfides. Disseminated pyrite is present in a hand specimen collected near the mouth of North Canyon. Lithologic type is metavolcanic, and the rocks are part of the loosely-defined Excelsior formation discussed by Ross (1961). This rock type is also present over much of the study region as roof pendants on Mesozoic granites. Its presence in the subsurface is unconfirmed although suspected based upon areal distribution.

Buried evaporites or oxidation of H_2S are other possible sources for the sulfates. A gypsum deposit is present along the western slope of the Wassuk Range approximately 48 km (30 mi) north-northwest of Hawthorne. Similar deposits may be present along the recharge path of sampled groundwaters. Calcium-to-sulfate mole ratios calculated from analysis of thermal fluids are notably different from 1. This suggests that gypsum or anhydrite is not likely to be a major source of $SO_4^{=}$. Hydrogen sulfide is not present as a detectable odor in any sampled fluid. In addition, the pH of all area groundwaters is neutral to basic. Therefore, it is highly unlikely that near-surface oxidation of the gas is a source of sulfate. Deep subsurface sulfate contributions from H_2S oxidation are indeterminate.

GRAVITY SURVEY

A detailed gravity survey using a grid spacing of approximately 0.8 km (0.5 mi) was conducted in the Southern Walker Lake Basin to obtain subsurface structural information. Existing data in the form of a 1:250,000 scale map contoured with a 5 milligal interval (Healey and others, 1980) was not useful. Data from the survey conducted for this project is shown as a complete Bouguer contour map in Figure B20. The subcontractor performing the work failed to tie his work into any known gravity base stations in the area. The values selected for contouring were chosen with regard to the reduction program. These limitations permit only relative changes to be discussed and prohibit correlation with regional absolute gravity data.

Several prominent characteristics are noted on the regional scale map depicted in Figure B20. A strong north-northwesterly linear trend does not parallel the Walker Lane described by Locke and others (1940) and instead, corresponds to the general attitude of the contours seen on the 1:250,000 scale map by Healey and others (1980). It may represent a second or third order phenomenon related to Walker Lane tectonics or the imprint of a later tectonic event upon Walker Lane trends. This trend ends at a point which is the convergence of a south-southwesterly and southeasterly trend located in the southern extent of the study area. The southeasterly direction parallels the Walker Lane. The contours also define a relatively broad region of limited variation and localized highs and low closures. The region of limited variation covers most of the basin. General assymetry of the valley is suggested by steep gradients found along the eastern front of the Wassuk Range which contrast with gradual gradients bounding the western Garfield Hills.

Figure B21 suggests several relationships between thermal well locations, surface fault traces, and subsurface configuration defined by gravity. Fault

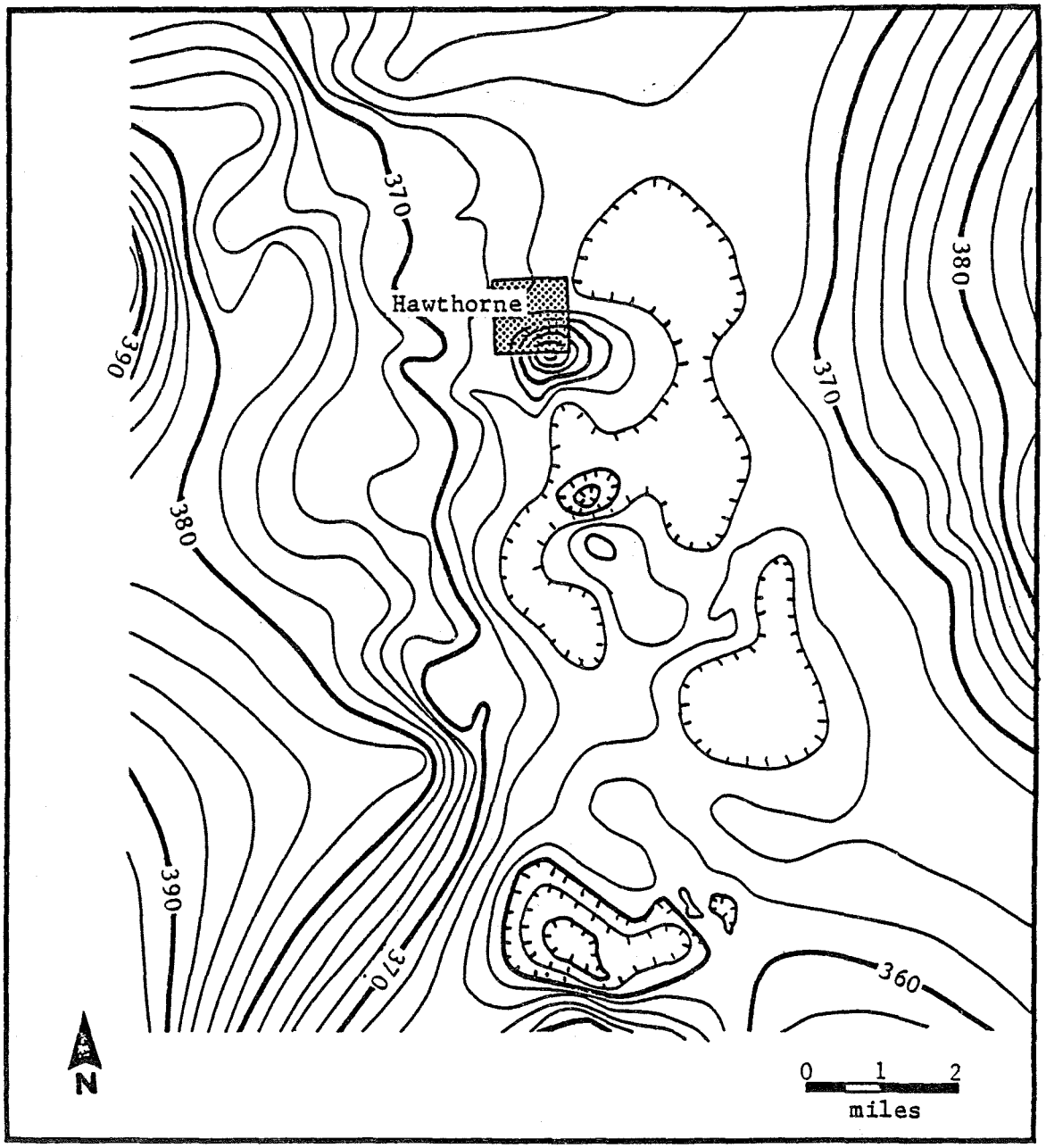

Figure B20. Complete Bouguer gravity map for the Hawthorne study area.

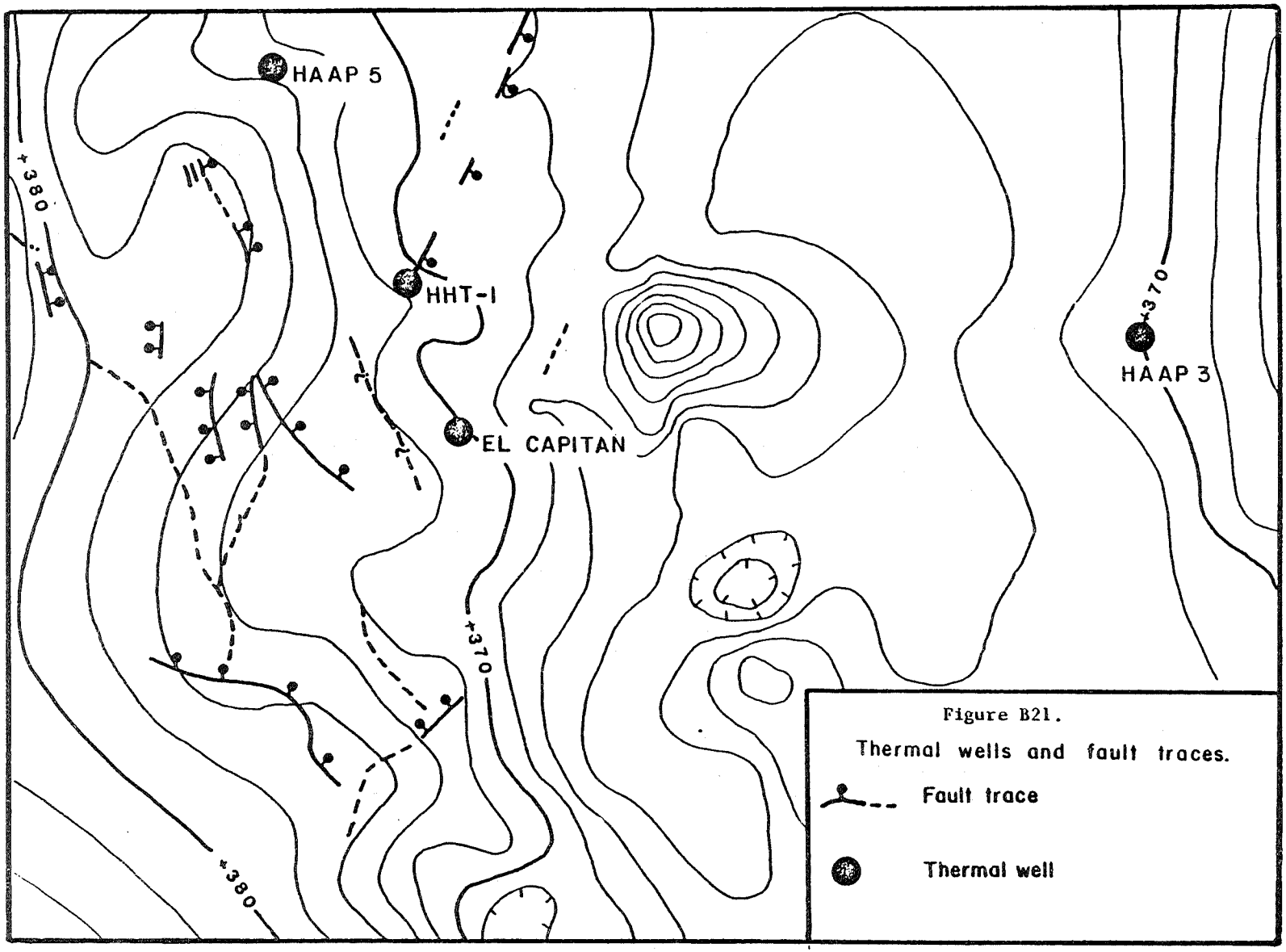
HAAP 5
HHT-1
EL CAPITAN
HAAP 3
+380
+370
+370
+380
Thermal wells and fault traces.
Fault trace
Thermal well

Figure B21.

and suspected fault traces shown in the figure are those observed on low sun-angle photographs. Although several traces parallel or subparallel gravity contours, others cross gravity lines at angles between 45 and 90 degrees. This suggests that these contours are probably controlled by subsurface topographic changes in bedrock materials as opposed to vertical fault displacement. The hottest test hole, HHT-1, is sited in a location where these circumstances exist. On the other hand, the El Capitan well (99°C) is sited along contours which are subparallel to traces of a fault and a suspected fault. This is in direct opposition to the situation described for HHT-1. Both wells are located in a region of gradual change in gravity between Hawthorne and the steep front of the Wassuk Range. A third well containing thermal fluids is shown in Figure B21 (HAAP #5). It is located in an area where gravity contours have a marked inflection which is not co-located with any surface fault traces. These inflections appear to be correlated with the location of thermal fluids, and are one of the criteria for siting the second test well, HHT-2.

A high closure occurring in the southeast corner of Hawthorne is one of the most curious features on the contour map shown in Figure B21. This feature is unlike any other observed in the region of the gravity survey. A dense object of limited areal extent is inferred. The magnitude of this relative high is equal to values measured at elevations of 1768 m (5800 ft) along the Wassuk front. Possible explanations for the phenomenon include an erosional or tectonic remnant of bedrock, an intrusive igneous body in the valley fill, a buried mafic volcanic center, or densification of allivium by deposition related to hydrothermal activity. A two-meter depth temperature probe implaced near the southeast corner of the city measured a higher temperature than other probes in the area. However, a 183 m (600 ft) city well which is nearly co-located with the center of the gravity high produces

cold groundwaters. The relationship of this feature to area geothermal phenomena, if any, is uncertain.

TEST HOLE DRILLING

A total of 366 m (1200 ft) of 15 cm (6 in) hole was allotted for the test hole drilling program in the southern Walker Lake Basin. A variable-depth drilling program was developed based upon the general absence of shallow groundwaters (100 m/328 ft) and the known depth to thermal fluids in the El Capitan well (180 m/590 ft). Under this program, two or three holes would be drilled depending on the temperatures observed during drilling.

The full 244 m (800 ft) length allotted to drilling in the area west of Hawthorne was expended in a single hole. Drilling a 122 m (400 ft) hole near the Garfield Hills used up the remaining footage. Locations of the test holes are NW¼, NE¼, SE¼, Sec. 29, T8N, R30E (HHT-1, 244 m) and SW¼, SE¼, Sec. 4, T7N, R31E (HHT-2, 112 m) (fig. B22).

Site selection involved the following considerations in order of decreasing importance: comparison of data generated from different exploration techniques, land status for acquiring permission to drill, and site accessibility. In choosing a location for test hole HHT-1 a comparison was made between the two-meter isotherm patterns and fault scarps in alluvium west of Hawthorne (fig. B23). An irregular, somewhat linear segment of 24°C line forms an intersection with a fault trace in the alluvium approximately 1.6 km west of the city limit. Chemical similarity of fluids taken from thermal wells was another factor in drill site selection. These parities are shown in Figure B24 by modified Stiff diagram symbols labeled"2" and "6". A simple Bouguer gravity contour map indicating a distinct inflection in gravity contours was also used in the site selection process. Permission

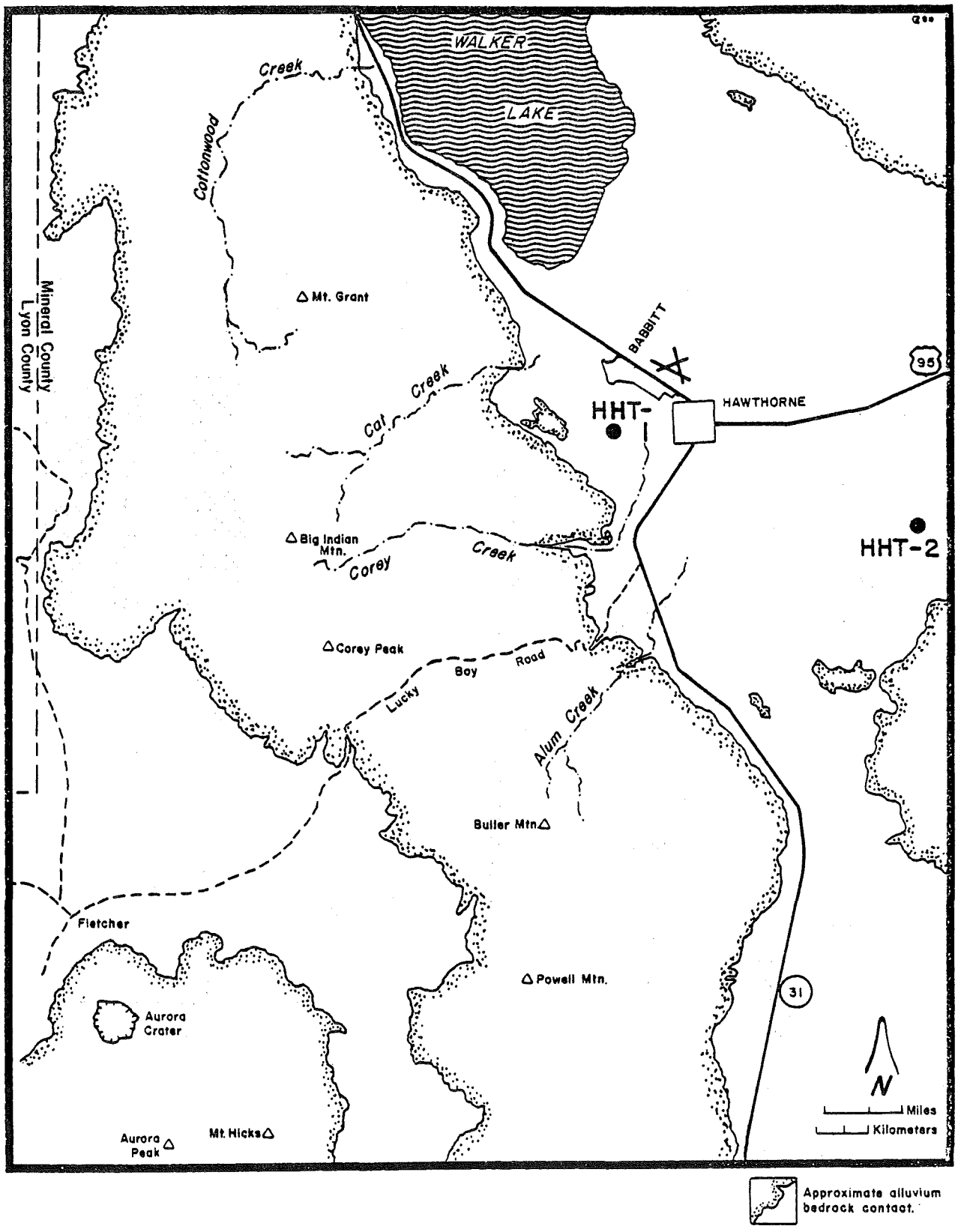

Figure B22. Location of test hole drill sties.

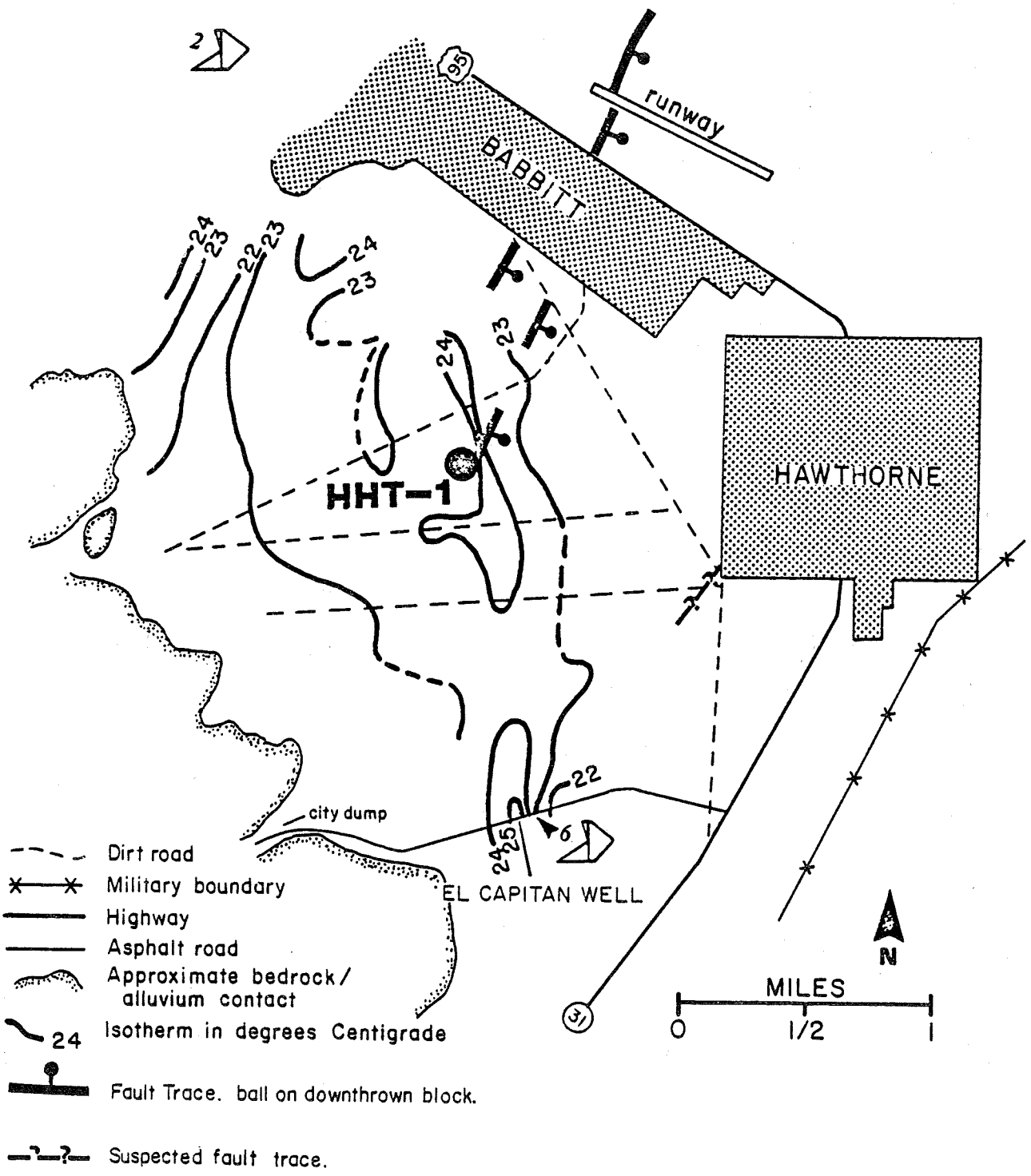

Figure B23. Correlation of isotherm high with fault trace in alluvium.

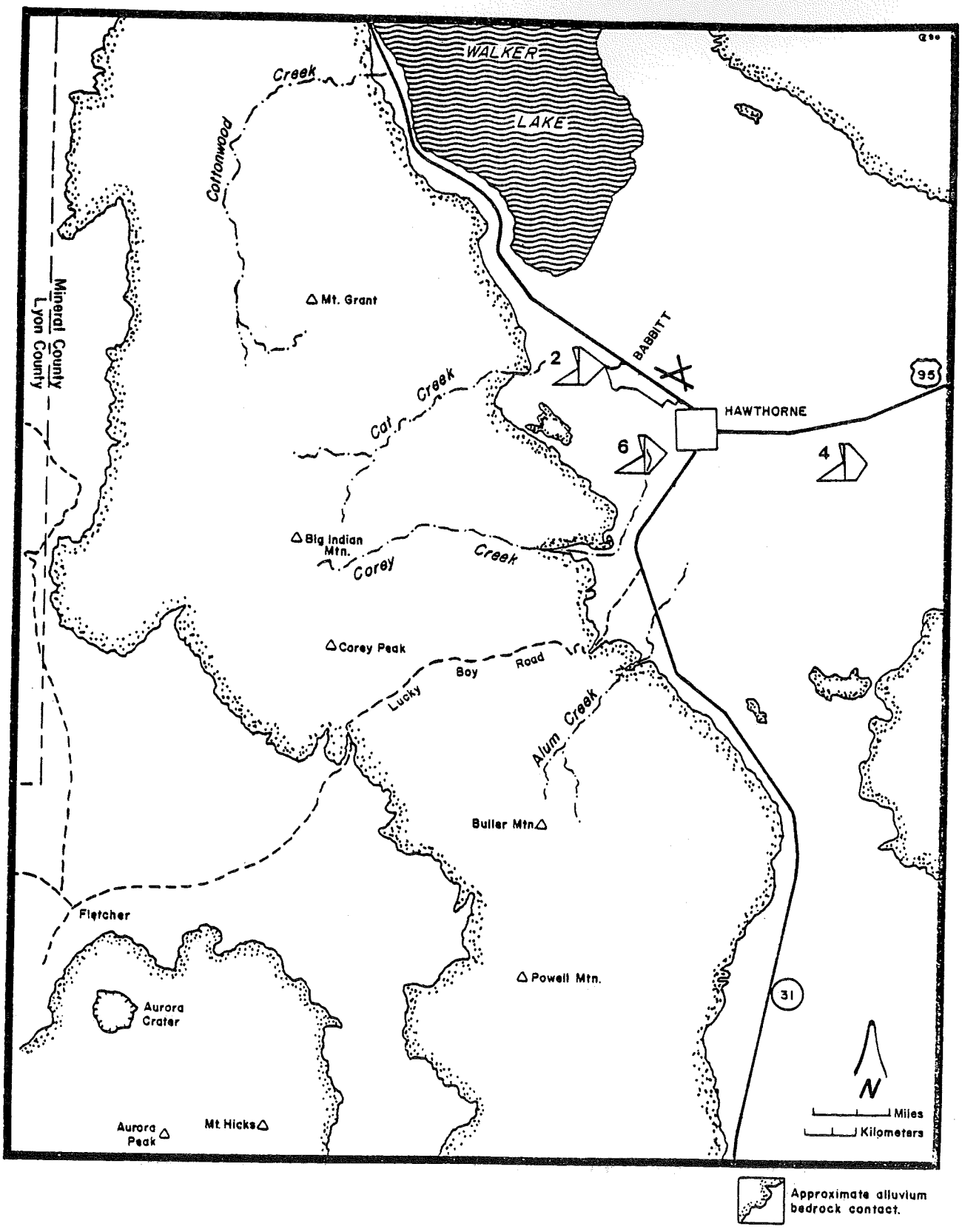

Figure B24. Chemical similarities between thermal wells.

to drill on U.S. Army property was obtained prior to site selection, and a network of dirt roads provided easy access.

Site selection for test hole HHT-2 relied heavily upon two-meter isotherm patterns and marked inflections in the gravity contours. Chemical evidence for a possible thermal fluid source is given by the similarity of fluid composition between western thermal wells such as numbers 2 and 6, and the eastern thermal well 4 on Figure B24. This site is also located on U.S. Army property, and is accessible via a paved road.

Both test holes encountered thermal fluids. A discussion of temperature depth relationships in these wells is given in the section titled "Temperature Profiling of Wells."

Return Temperatures

Two probes capable of measuring 100°C were used to monitor input mud temperatures (mud pit) and outlet mud temperatures (surface casing perimeter) as drilling progressed. Temperature records generated from this procedure were used to construct the return temperature-versus-depth profiles shown in Figures B25 and B26. Temperature measurements were taken primarily for drilling safety since no blow-out preventer was used. A return temperature of 75°C was chosen as a cutoff. Because this temperature was never attained, it was assumed that fluid temperatures above the cutoff were not encountered, however, this assumption was incorrect. Temperature profiles measured in the wells after casing (figs. B12, B13) indicate that return temperatures are from 32° - 40°C lower than maximum recorded temperatures.

Lithologic Descriptions

Both HHT-1 and HHT-2 were completed to total depth in alluvium. The rock types which compose the alluvial fill vary somewhat from one side of

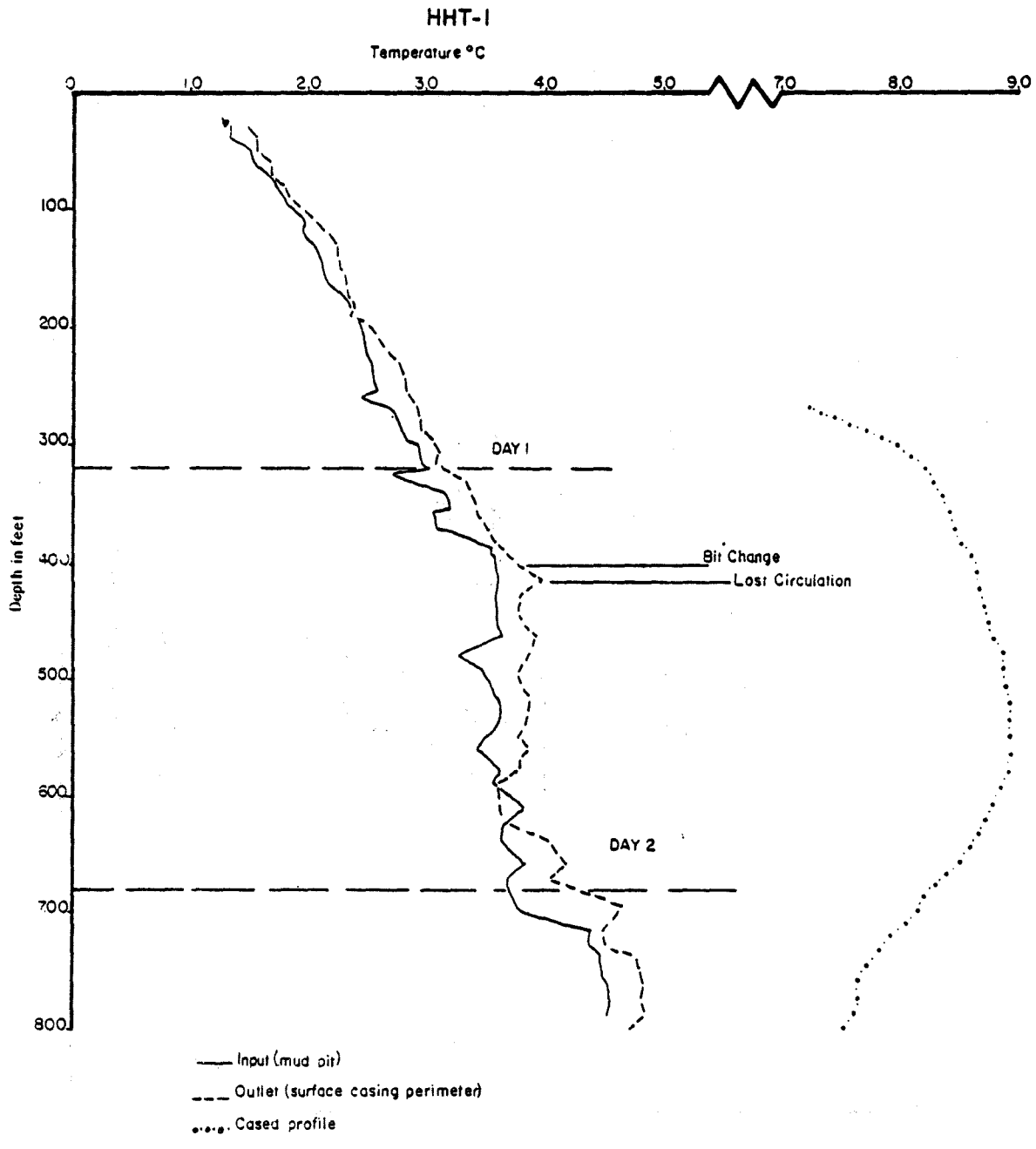

Figure B25. Return temperatures vs. depth of drilling

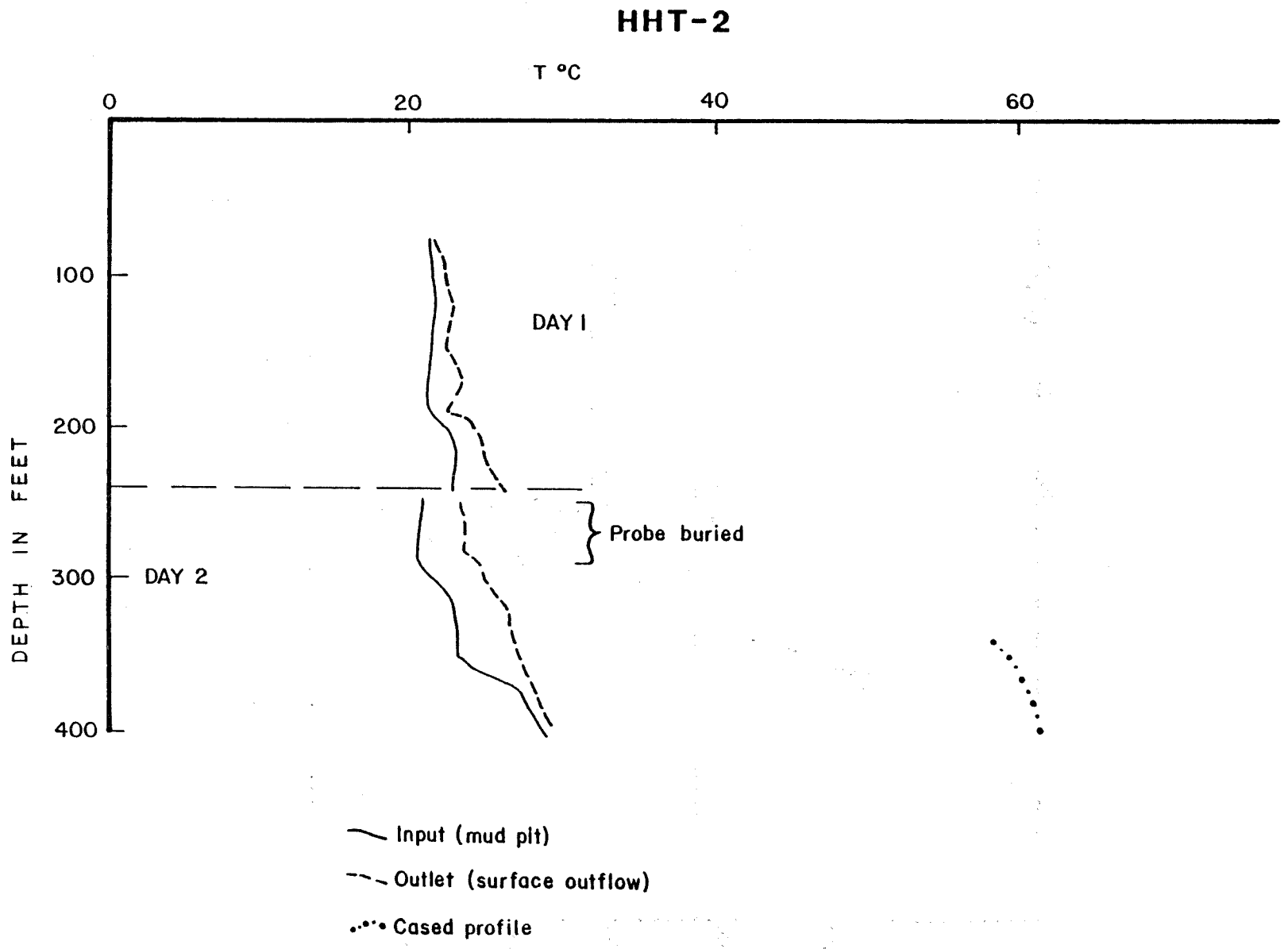

Figure B26. Mud return temperatures vs.drilling depth.

the valley to the other (figs. B27 and B28). This reflects that differing source regions supply the materials. Rock types from HHT-1 can be directly related to the intermediate intrusive and metavolcanic rocks of the Wassuk Range. Lithologies present in HHT-2 are rich in basic to acidic flow rocks and tuffs and tuffaceous sediments.

An interesting correlation is noted if clay content is plotted versus depth in the two test holes (fig. B29). In both cases, clay content is less than or equal to five percent to a depth of approximately 67 m (220 ft). Beyond this point, a marked increase occurs to approximately 76 m (250 ft) where both curves begin a rapid decrease. A second zone of relatively high clay content is found in both holes between 92 and 122 m (300-400 ft). At approximately 122 m, a zone in which both white and brown cohesive clays is observed in HHT-1 and HHT-2. These correlations suggest a uniform depositional environment in the basin. Unfortunately, no other sufficiently detailed lithologic descriptions are available for comparison.

SUMMARY

General Geology

The study area lies within a region of physiographic and structural discordance termed the Walker Lane by Locke and others (1940). Its eastern boundary is the Garfield Hills which record an intense period of orogeny during the Mesozoic era. The Wassuk Range forms a western boundary and is a west-dipping tectonically-tilted block. Ages of rocks exposed within the area vary from Triassic to Holocene, and a variety of lithologies is present. Rock types include intermediate intrusive, metavolcanic, limited marble and phyllite, mafic to intermediate flows, intermediate to felsic tuffs,

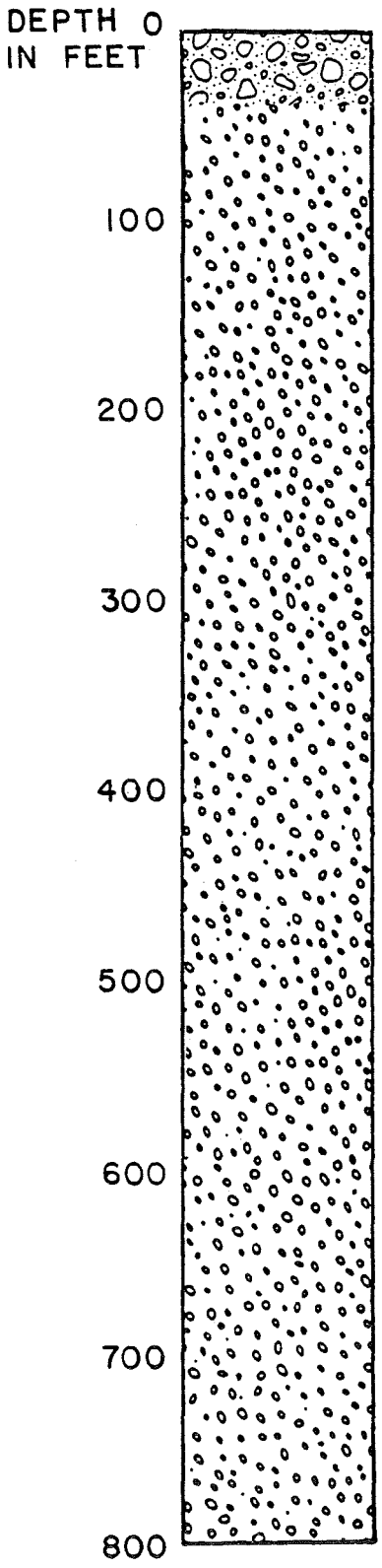

HHT-1

Alluvial materials consisting of: Angular to subangular fragments of decomposing intermediate intrusive rocks containing - quartz, plagioclase, k-feldspar, biotite and/or hornblende; fragments of more mafic intrusives probably diorite; fragments of basic rock such as diabase (probably the result of mixing during intrusion of the granitic rock); epidote color mineral; and fragments of metavolcanic rocks from Excelsior formation of the Wassuk Range. Many of the intermediate intrusive fragments are heavily iron stained from mafic mineral decomposition. Size of the fragments is variable from <1-30 mm above 40' and generally <5 mm from 50' to TD. Between 780' and 800' all material was <2 mm. Clay content was variable from <5% up to >70% by visual volume estimate. Occassional cobble to boulder size fragments encountered during drilling.

Figure B27. Lithologic log and description - test hole HHT-1.

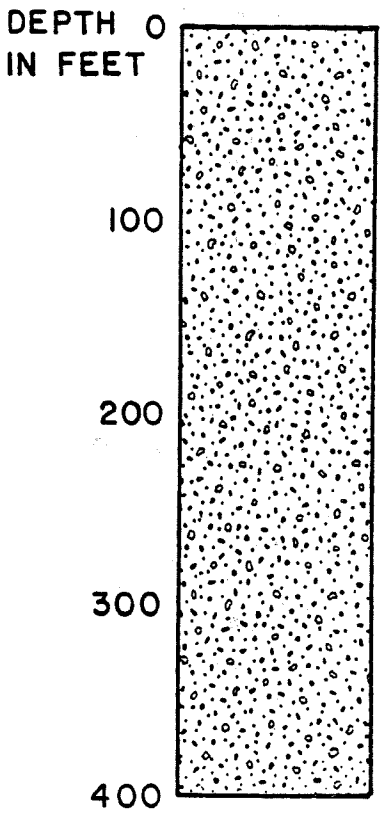

HHT-2

Alluvium, angular to subrounded fragments composed in varying proportions of: quartz, k-feldspar, DG, mafic volcanics (basalt?), light colored fine-grained tuff containing biotite flakes, fine grained poorly sorted tuffaceous sediment, reddish-purple aphanitic volcanics (andesite), red porphyritic rhyolite, green and brown chert, and epidote. Above 30 ft. some pebble size frags, from 30-220 ft. 2 mm-10 mm, 220-400 ft.<5 mm. Occasional cobble and/or boulder size material encountered during drilling. Clay content variable from 5% to >70% by visual estimate.

Figure B28. Lithologic log and description - test hole HHT-2.

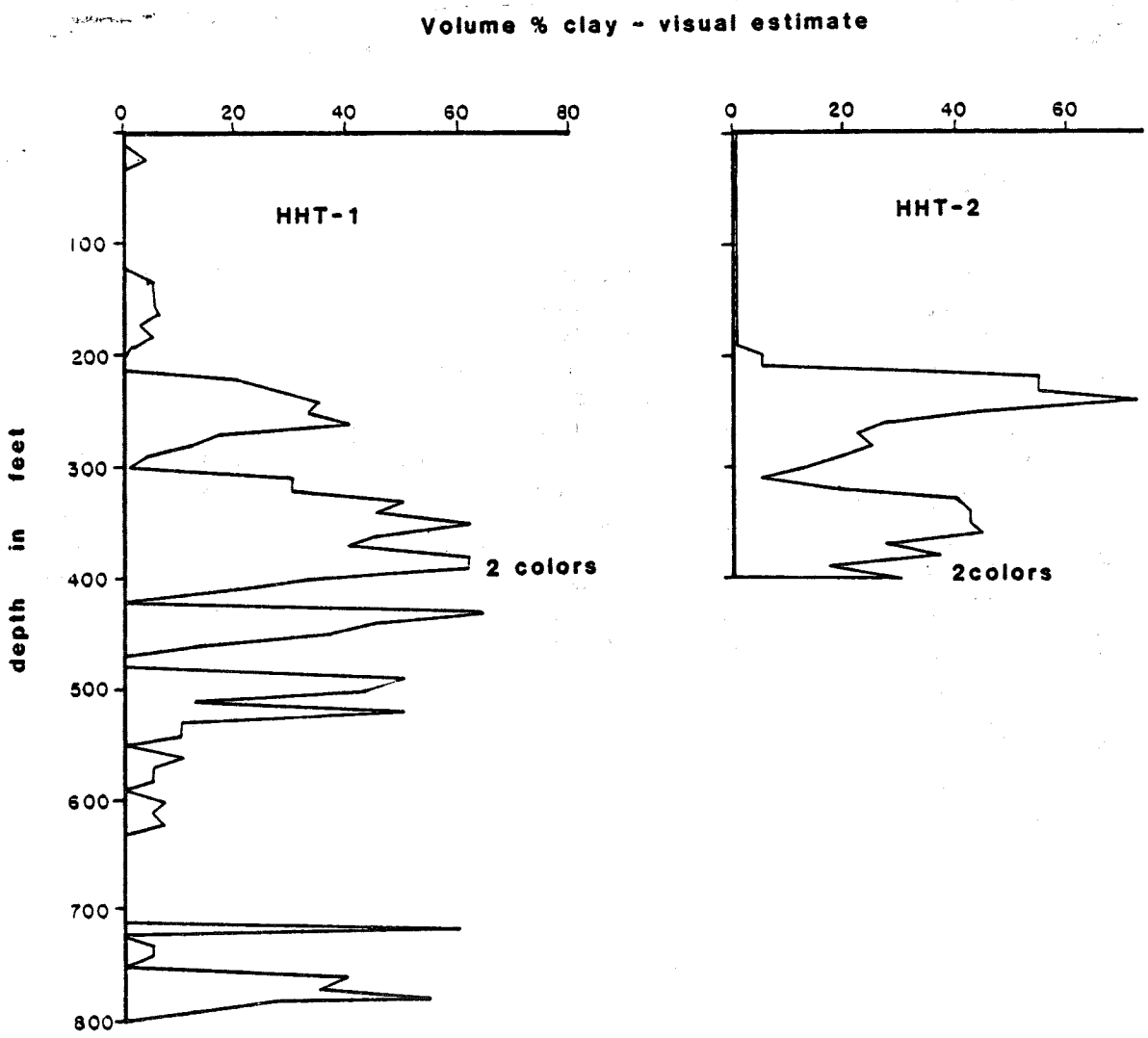

Figure B29. Clay content as a function of depth, HHT-1 and HHT-2.

tuffaceous sediments, and clastic sediments.

Aeromagnetic Map

High and low closures on the map generally follow the outcrop patterns of volcanic rocks or topographic features. This is probably in part an effect of the non-drape method of data collection. Within the vicinity of the city of Hawthorne, the contour patterns record only subtle changes.

Shallow Depth Temperature Survey

This study involved the emplacement of over 90 two-meter probes on both regional and reduced scales. Two regions of elevated temperatures were delineated. They are located in the Hawthorne vicinity along the eastern front of the Wassuk Range and western front of the Garfield Hills, respectively. The regions are composed of broad zones of limited temperature variation and contain irregular non-linear localized highs as indicated by isotherm configurations.

Photo Imagery

Both B & W and color imagery were examined. Scales from 1:24,000 to 1:250,000 were used. Identified regional features are limited to Walker Lane linears and frontal structures of the eastern Wassuk Range. Low sun-angle photography proved most useful. It demonstrated the presence of three general linear trends: NW-SE, NE-SW and N-S. There is also a lack of fault traces and escarpments along the western front of the Garfield Hills.

Soil-Mercury Survey

This technique was not useful for exploration in the Hawthorne area. No trends were observed and only a single anomalous value was measured. Low background values were recorded in the immediate vicinity of the El Capitan

well which contains 99°C fluids.

Temperature Profiling of Wells

Two previously existing wells and two test holes drilled for this study were profiled. The two existing wells proved to be essentially isothermal over vertical distances of 60 meters. They are separated by nearly 11 km and have nearly identical temperatures. Temperature depth relationships in our 244-meter test hole HHT-1 demonstrate the presence of three distinct zones at increasing depths: a positive gradient zone, an isothermal zone, and a negative gradient zone.

Gravity Survey

A relatively closely spaced grid of 0.8 km was employed during data collection. Several features are distinguishable. Many area attitudes follow a strong NNW trend. This trend does not follow the Walker Lane but does correspond to the general orientation of contours shown on the 1:250,000 scale regional map of Healey and others (1980). A Walker Lane trend is present within the southern portion of the survey. Like the aeromagnetic patterns, gravity contours indicate a region of subtle variations in the vicinity of Hawthorne. Some of the gravity contour trends parallel surface fault traces while others are clearly discordant. Hot well locations correspond to both of these circumstances. Hot well locations also correspond to inflections in contours. Finally, an area of high closure exists under Hawthorne which may be explained by an erosional or tectonic bedrock remnant, an igneous intrusive, a buried mafic volcanic center, or densification related to mineral deposition.

Fluid Geochemistry

Fifteen samples were collected and analyzed for bulk chemical and stable light isotopic composition. Numerous functional relationships can be described

from the data. Concentrations for the majority of dissolved constituents increase when moving down the hydrologic gradient. Groundwaters contain higher total dissolved solids than surface waters collected at the same elevations. Waters tend to fall into several groups based upon cation or anion relative percents. Certain spatially widely separated fluids exhibit marked chemical similarities. There is a distinction between cold groundwaters in the Wassuk Range and those in Whiskey Flat. Lithium content may also be useful for distinguishing thermal and non-thermal fluids.

Isotopically, the fluids exhibit a limited compositional range. Most waters seem to be related to meteoric recharge in the Wassuk Range. Only limited ^{18}O "shifts" are observed. This could result from short circulation times, a temperature <150°C for water-rock interaction, a high water to rock ratio, or a combination of these factors. Geothermometers suggest an upper limit of 125°C for equilibration temperatures.

High sulfate content of thermal fluids is probably related to the oxidation of sulfide minerals found in granitic and/or metavolcanic rocks within the area.

Test Hole Drilling and Associated Lithologies

Two test holes were drilled to test for the presence of geothermal fluids and to determine temperature-depth relationships. Thermal fluids were encountered in both wells. HHT-1 in the area west of Hawthorne shows a maximum temperature of 90°C, and HHT-2 near the Garfield Hills shows a maximum of 61°C. Each well is completed in alluvium. They have similar clay content versus depth relations, and both possess a two-color clay zone at approximately the same level. These similarities suggest a uniform depositional history for alluvium on both sides of the valley.

CONCLUSIONS

Four important parameters characterize geothermal resources in the Hawthorne study area. Greater knowledge of these parameters will aid resource exploration and development in the future. They are:

1) areal distribution of thermal fluids,
2) recharge paths and associated fluid chemical variations,
3) subsurface controls on fluid flow, and
4) heat source.

These variables are all part of a complex system and are not independent.

Waters with anomalous heat content are found over a wide area in the southern Walker Lake Basin and surrounding region. The majority of these fluids occurs in wells drilled in alluvium; however, HAW-16 is an exception. It occurs as a thermal spring of low flow rate in a narrow canyon along the Walker River west of the Wassuk Range. This location places the spring approximately 18 km to the west of the "cluster" of thermal fluids found in wells of the Army Ammunition Plant. Another hot water labeled "BLM" is also widely separated from the "cluster". Like the fluids farther north, it is a well-water in alluvium although it is located nearly 18 km from the main grouping of thermal waters. Some of these fluids exhibit notable chemical similarities in addition to above-normal temperatures. Similarities between mode of occurrence, measured temperatures, and bulk and isotopic composition suggest that some of the thermal fluids may be related to a common and possibly widespread source.

Concordance and discordance are both evident when comparing bulk chemical compositions and measured temperatures of thermal waters. These similarities and contrasts are probably the result of differing recharge paths of various fluids. For example, if fluid HAW-6 (99°C) represents a relatively unchanged sample of the geothermal fluid source, then waters such as HAW-2 (41°C) and

HAW-4 (41°C) are probably from the same source. This conclusion is based upon the chemical similarity of fluids from three wells. Recharge to this group probably occurs along very similar lithologic paths. Temperature disparities could result from simple conductive cooling. Fluids areally distributed between the waters discussed above, such as HAW-3 and NAD2, are relatively enriched in calcium and magnesium, and relatively depleted in sodium. However, their anion compositions are comparable to those of HAW-6, HAW-2 and HAW-4. The majority of wells in the "cluster" around Hawthorne follow a similar pattern of consistency in anionic composition coupled with variable calcium, magnesium and sodium concentrations. If HAW-6 is a parent fluid, it seems reasonable that the relative enrichment of Ca and Mg in other fluids is a function of water-rock interaction along different recharge/flow paths within the alluvium. The mixing of various fluids might also explain the compositional variations. However, lack of a well-defined end member which could produce such changes argues against this hypothesis.

Parameters which govern fluid movement and distribution in the near surface (<500 m) environment of the Hawthorne geothermal resource cannot be clearly deduced from available data. As previously discussed, the resource appears to be present over a large region although, with one exception, it does not exhibit any surface manifestations. No direct correlations between range front faults and geothermal fluids are demonstrated within the detailed study area. Orientations of fault scarps in alluvium in the area west of Hawthorne do not correlate with isotherm patterns from the two-meter probe study. Also, there are no anomalously high soil-mercury concentrations or trends related to fault locations. Reliable temperature profiles from thermal wells where they were completed indicate relatively thick (60 m) zones of hot fluids. These facts all support a type of control on fluid distribution which is not primarily high-angle faults. Rather, it is postulated

that lateral movement along permeable zones within the alluvium is the primary control. A possible scenario might include initial movement upward along range-bounding or subparallel faults driven by forced convection; rising thermal fluids contacting a zone within which lateral permeability exceeds that in the vertical direction; followed by lateral transport down the hydraulic gradient. Parameters which govern permeability within alluvium are presently indeterminate. One possible explanation is movement of fluid in the vicinity of the alluvium-bedrock interface. This hypothesis is based upon two observed phenomena. The temperature-depth profile in test hole HHT-1 possesses a reversal from positive to negative gradient near the 180 m (600 ft) level. This may be the result of drilling into a relatively impermeable bedrock layer. However, owing to the similarities between alluvium and bedrock apparent in chip samples, this cannot be demonstrated in the lithologic log. Secondly, there is a marked contrast in temperatures and chemistries between samples HAW-6 and HAW-14. The wells are nearly identical in depth, apparently completed to total depth in alluvium and located within 1 km of each other along an east-west line. HAW-14 might not be deep enough to reach hotter fluids found in HAW-6 due to increasing depth to the interface of valley fill and bedrock when moving toward the center of the valley. No further confirming evidence can be cited due to a lack of detailed lithologic logs for the area, and the uncorrelated nature of gravity data.

Many low-to-moderate temperature geothermal systems in Nevada seem to be related to deep circulation of meteoric waters in a region of normal or above normal crustal gradient. This may also be valid for Hawthorne area fluids although other heat sources are possible. The presence of relatively young (<250,000 yrs) extrusions of mafic rock in the area of Aurora Crater suggests that subsurface igneous bodies may also supply heat. It is inferred

from chemical evidence that Hawthorne fluids are probably moderately-heated (<150°C) meteoric waters that have not experienced extensive high temperature water-rock interaction. If this assumption is correct, then rocks which transfer heat to the Hawthorne fluids are probably, in turn, heated by conductive and or convective processes associated with relatively remote igneous bodies in the subsurface. There is geophysical evidence for the existence of igneous bodies. Van Wormer and Ryall (1980) determined that the configuration P-wave residuals in the vicinity of the Adobe Hills is consistent with a region of partial melting in the crust. This region extends to the northeast. The authors also postulate an upper mantle source below the Excelsior Mountains. Phenomena of this magnitude could easily provide elevated subsurface temperatures necessary to produce heating with limited circulation of fluid at depth. It would also explain the extensive areal distribution of geothermal fluids.

The remote possibility of an intrusive igneous body in the valley fill is suggested by certain patterns in the detailed gravity survey. Presently there are insufficient data to refute or confirm such a hypothesis.

Suggestions for Further Study

A considerable amount of information has been compiled from this study regarding the nature and distribution of geothermal resources in the Hawthorne area. A better understanding of the distribution of thermal fluids in the near surface (<600 m) is of primary importance in siting future production wells for direct applications. Depending upon funding availability, several approaches could be taken including accurate temperature-depth profiles of all accessible wells, drilling a deeper test hole (600 m) with accurate and detailed lithologic and borehole logging, and completing a deep electrical resistivity survey that may provide a 3-dimensional picture of the distribution of hot waters.

PARADISE VALLEY STUDY AREA

by THOMAS FLYNN

GEOGRAPHIC SETTING, HISTORICAL NOTES

The Paradise Valley study area is located in Humboldt County near the cities of Winnemucca and Golconda in northwest Nevada (fig. C1). The area of interest includes approximately 1800 km^2 and is bounded on the south by the Humboldt River, on the west and north by the Santa Rosa Range, and on the east by the Hot Springs Range and the Osgood Mountains. Elevation of the valley floor ranges from 1311 to 1342 m (4300-4400 ft) above sea level, and peaks in the surrounding ranges rise to approximately 2592 (8500 ft) above sea level.

Principal drainage is the south-flowing Little Humboldt River which empties into the west-flowing Humboldt River near the southern border of the study area. Annual rainfall in Humboldt County ranges from 5 to 10 inches per year; most of the precipitation occurs in the winter months. Daily temperatures range from 30 to 40°C during the summer and from 10 to -30°C during the winter.

Agriculture is the principal economic activity in this area, and includes large potato and alfalfa farms as well as livestock production. Two major railroad lines, the Western Pacific and the Southern Pacific, service Winnemucca and Golconda and are located along the banks of the Humboldt River near the southern border of the study area.

In 1884 The Pacific Tourist (Adams and Bishop, 1884) made reference to the town of Golconda in a travel guide of northern Nevada, and presented what may be the earliest report on geothermal activity in the area. The report describes Golconda as:

> "...a little town ... that has one or two stores, a hotel, several adobe houses, and the usual railroad conveniences. It also is the location of some eight or ten hot mineral springs, which are passed on the right side of the tracks, just after leaving town. These waters vary in temperature from cool or tepid water, to that which is boiling hot. The swimming bath - an excavation in the ground - is supplied with tepid water and is said to be very exhilarating. The Boiling Spring is utilized by the farmers in the valley in scalding their swine. The

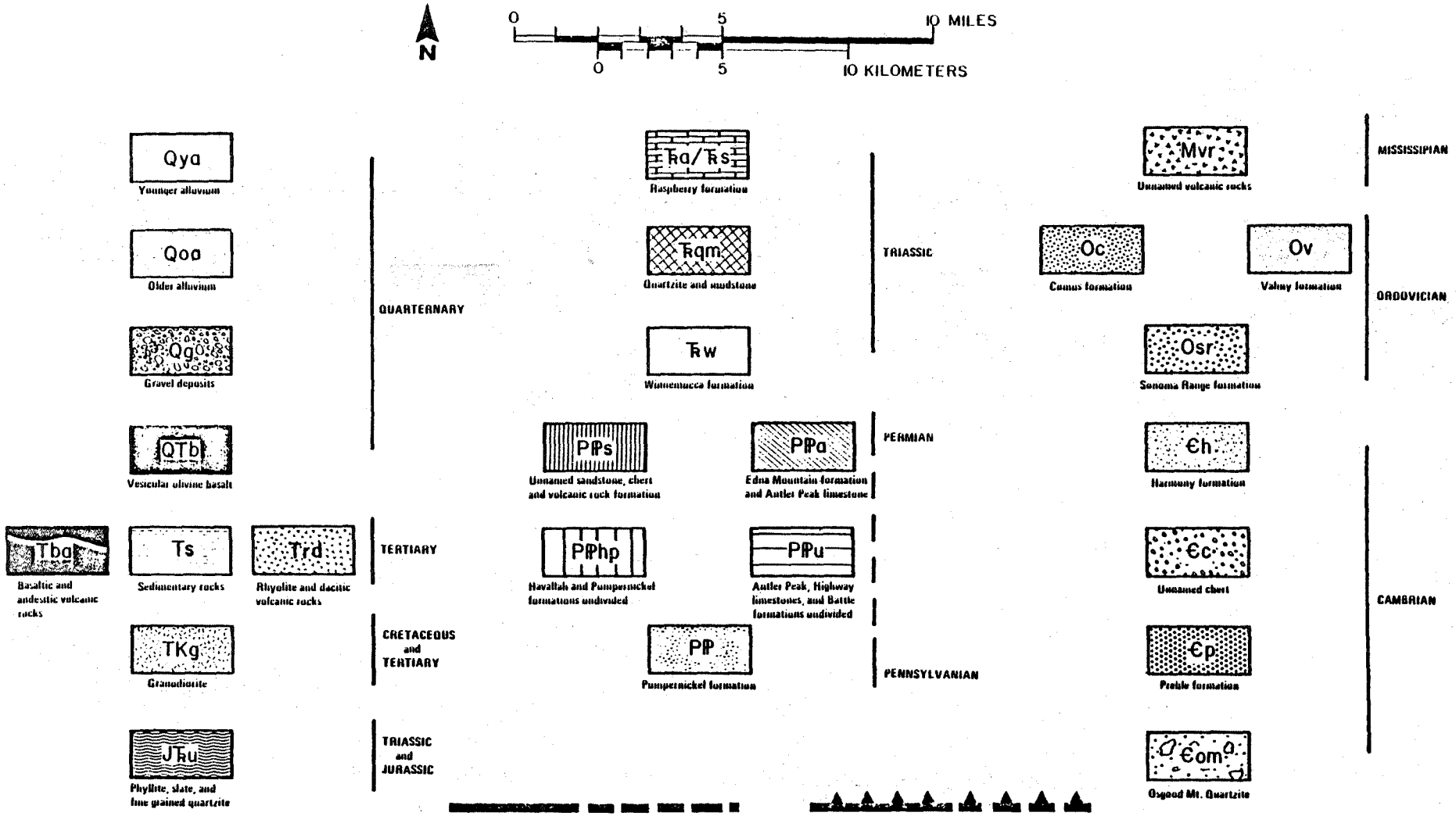
N
0
5
10 MILES
0
5
10 KILOMETERS
Qya
Younger alluvium
Qoa
Older alluvium
Qg
Gravel deposits
QTb
Vesicular olivine basalt
Tbg
Basaltic and andesitic volcanic rocks
Ts
Sedimentary rocks
Trd
Rhyolite and dacitic volcanic rocks
TKg
Granodiorite
JTRu
Phyllite, slate, and fine grained quartzite
QUARTERNARY
TERTIARY
CRETACEOUS and TERTIARY
TRIASSIC and JURASSIC
TRa/TRs
Raspberry formation
TRqm
Quartzite and sandstone
TRw
Winnemucca formation
PPPs
Unnamed sandstone, chert and volcanic rock formation
PPPa
Edna Mountain formation and Antler Peak limestone
PPPhp
Havallah and Pumpernickel formations undivided
PPPu
Antler Peak, Highway limestones, and Battle formations undivided
PPP
Pumpernickel formation
TRIASSIC
PERMIAN
PENNSYLVANIAN
Mvr
Unnamed volcanic rocks
Oc
Comus formation
Ov
Valmy formation
Osr
Sonoma Range formation
Ch
Harmony formation
Cc
Unnamed chert
Cp
Preble formation
Com
Osgood Mt. Quartzite
MISSISSIPIAN
ORDOVICIAN
CAMBRIAN
High-Angle Fault
Normal, reverse or strike-slip. Dashed where approximated.
Thrust Fault
Teeth on upper plate. Dashed where approximated.

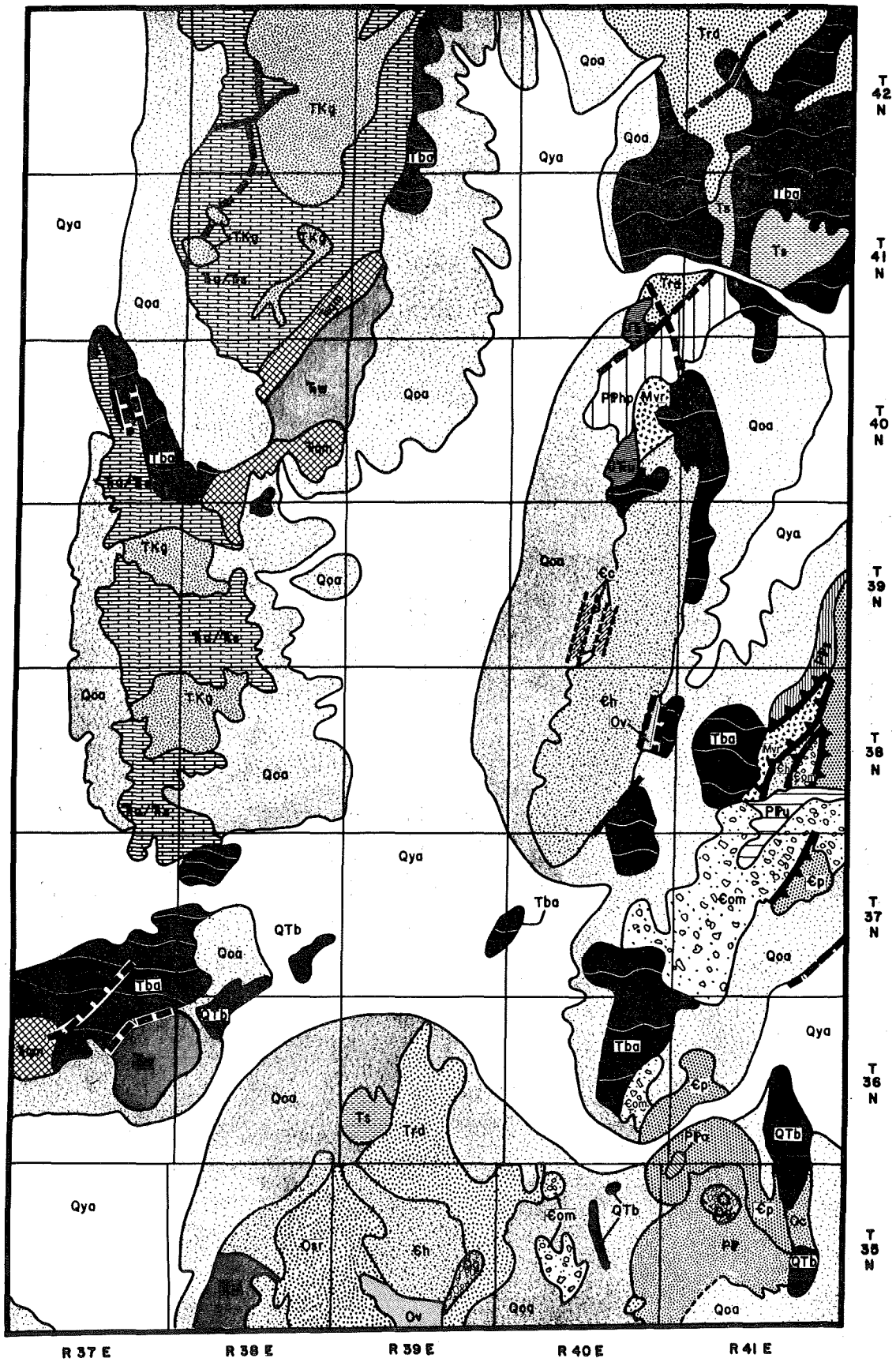

Figure C1. Generalized geologic map of the Paradise Valley study area (modified after Willden, 1964).

> water is said to be hot enough to boil an egg in one minute ... The water flowing from the hot spring is used for irrigation purposes, and the owners of the spring have a monopoly on early vegetable 'garden truck', raising early radishes, lettuce, onions, etc., before their season, by the warmth produced from the hot water. Sunday excursion trains are run from Winnemucca to accomodate parties who desire to enjoy the luxury of these springs."

More recent reports (Miller, 1953) indicate that the Golconda hot springs were used for recreational and agricultural purposes until early in the twentieth century. In 1940 a well was drilled by Tungsten Properties, Ltd. near the Golconda hot springs to provide water for a mill and chemical plant that treated ore from a tungsten-iron-manganese mine four miles east of Golconda (NBMG files). The well was drilled to a total depth of 53 m (175 ft) and, when pumped at 1703 liters per min. (450 gpm), produced water at a temperature of 74°C (165°F). Another well located at the tungsten mine was drilled to a depth of 78 m (265 ft) and encountered 62°C (143°F) water at a depth of 67 m (220 ft).

At present there is no commercial use of geothermal fluids in the Golconda-Paradise Valley area. Also, historical records do not indicate that any other hot springs in the study area were ever used for commercial activity.

GEOLOGY AND TECTONIC FRAMEWORK

Humboldt County historically has been an important source of gold, tungsten, mercury, and silver (Willden, 1964), and much geologic information in the Paradise Valley study area is derived from mineralogical investigations. Mineral deposits are widespread in this area; however, the principal mining areas are located in the Osgood Mountains and in the Hot Springs Range. In addition to mining-related studies, the geologic record has been supplemented by intensive regional geology studies of a nearly-continuous column of rocks extending from the Quaternary to the late Precambrian. The only exception is rocks from the Silurian and Devonian

periods which are exposed several miles east of the study area.

Figure C1 and the accompanying explanation is a generalized geologic map modified after Willden (1964). The map illustrates the spatial distribution and lithology of major rock units. It also shows the location of some major faults associated with Paleozoic and Mesozoic tectonic activity as well as high-angle Basin and Range faults. Table C1 describes the important rock units in this area.

The following narrative summarizes relevant geologic events for the Paradise Valley study area.

Paleozoic Era

Three major depositional provinces existed in central Nevada from early Cambrian through middle Devonian time. The most comprehensive report on the geology of this area is presented in Stewart (1980). Using data from Erickson and Marsh (1974), Ferguson and Muller (1951), Ferguson, Roberts and Muller (1952), Siberling (1975), and Willden (1964), Stewart uses a series of palinspastic maps that show the areal extent of these depositional provinces and how they vary over time. The easternmost province known as the Eastern Assemblage is interpreted as a north-trending miogeosyncline characterized by extensive accumulations of shallow-water marine carbonates. This province extended east from central Nevada as far as eastern Utah and parts of western Colorado. A second depositonal province, the Western Assemblage, was located in what is now western Nevada and eastern California in a configuration that was roughly parallel to the miogeosyncline. This area is interpreted as a eugeosyncline and is characterized by massive accumulations of siliceous shales, cherts, greenstones, and volcanic rocks. A third smaller depositonal province known as the Transitional Assemblage was located between the eastern and western depositional provinces and consisted of interbedded shale and limestone deposits.

Table C1. Lithologic descriptions and ages of selected geologic formations in the Paradise Valley study area (after Willden, 1964)

Age	Symbol	Lithology
Quaternary	Qya	Younger alluvium: includes playa, dune and stream deposits and deposits of Lake Lahontan.
	Qoa	Older alluvium: includes alluvial fans and some upland alluvial deposits.
	Qg	Gravel deposits: includes bench deposits and landslide deposits.
	QTb	Vesicular olivine basalts.
Tertiary	Ts	Sedimentary rocks: includes shale, sandstone, conglomerate, tuff, and diatomaceous shale.
	Trd	Rhyolitic and dacitic volcanic rocks: locally includes some more basic rocks and some interbedded sedimentary rocks.
	Tba	Basaltic and andesitic volcanic rocks: locally includes more silicic rock types and sedimentary rocks.
Cretaceous and Tertiary	Tkg	Granodiorite: used for all quartz-bearing igneous rocks that pre-date Tertiary intrusive rocks; principally granodiorite with local compositional variations to quartz diorite and quartz monzonite.
Triassic and Jurassic	JTR u	Phyllitic slate and fine-grained quartzite.
Triassic	TR a, TR s	Raspberry formation: includes Andorno and Singas formations - slate and some phyllite, limestone and quartzite lenses locally abundant.
	TR gm	Quartzite and mudstone: thickness 2000 to 4000 feet, correlative unit in the Santa Rosa Range named O'Neill formation by Compton (1940).
	TR w	Winnemucca Formation: shale and sandstone locally metamorphosed to slate and quartzite - contains lesser amounts of limestone and dolomite.

Table C1. (Cont.)

Age	Symbol	Lithology
	PPhp	Havallah formation and Pumpernickel formation undivided: Havallah is slate and quartzite with some chert, limestone, greenstone, graywacke, and conglomerate; Pumpernickel described below.
	PPs	Unnamed sandstone, chert and volcanic rock formation - present only in the Osgood Mountains.
Pennsylvanian	PPa	Edna Mountain formation and Antler Peak limestone: Edna Mtn. formation is sandstone quartzite and slate with a few beds of limestone; Antler Peak consists of massive to thin-bedded limestone - sandy and pebbly layers are locally common, shaly beds in upper part.
	PPu	Antler Peak limestone, Highway limestone, and Battle formation: Antler Peak described above; Battle formation is divided into three parts: lower part is red, medium to thick-bedded coarse conglomerate; middle part is interbedded red conglomerate, sandstone, calcareous shale, and shale; upper part consists of pebble and granular conglomerate interbedded with sandstone, shale, calcareous shale, and limestone.
	Pp	Pumpernickel formation: consists of greenstone, dark chert and dark argillite with variable amounts of interbedded limestone and clastic sediments.
Mississippian	Mvr	Unnamed volcanic rocks: consists of altered fine-grained andesites, altered pyroclastics and altered pillow lavas; also contains limestones, calcareous sandstone and shale, siliceous shale, and chert.
	Oc	Comus formation: relatively thick layers of interbedded limestone, dolomite and shale; also with thinner beds of sand and chert nodules.
Ordovician	Ov	Valmy formation: lower unit is at least 4000 feet thick and consists of pure quartzite, dark chert and siliceous shale with significant amounts of greenstone; upper unit is at least 3000 feet thick and consists largely of thin-bedded chert interbedded with dark shale and some greenstone.
	Osr	Sonoma Range formation: consists of dark chert, siliceous argillite and slate, altered andesitic lava, limestone lenses, pillow basalts, and quartzite.

Table C1. (Cont.)

Age	Symbol	Lithology
Cambrian	€h	Harmony formation: composed predominately of feldspathic graywacke and feldspathic quartzite with some feldspathic pebble conglomerate and shale.
	€c	Unnamed chert unit: contains minor amounts of siliceous shale and limestone.
	€p	Preble formation: consists of shale in the lower unit, interbedded limestone and shale in the middle unit, and shale in the upper unit.
	€om	Osgood Mountain quartzite: consists of tan, gray, brown, and purple-colored bedded quartzite with shale partings; thickness estimated to be 5000 feet.

This pattern of deposition remained virtually unchanged until the onset of the Antler Orogeny in the late Devonian period. During this orogeny which ended in early Mississippian, Western Assemblage siliceous rocks were thrust eastward along the Robert's Mountain Thrust as much as 145 km (90 mi) over coeval carbonates of the Eastern Assemblage.

Several tectonic models have been suggested to explain this orogenic episode including gravity sliding of "allochthonus" (not-in-place) units from the newly formed Antler Highland (Ketner, 1977) and island arc-continental collisions (Burchfield and Davis, 1972; Silberling, 1975; and Poole, 1974). Evidence for the existence of the Antler Highland is derived largely from the absence of late Devonian age rocks west of the Robert's Mountain Allochthon (thrust sheet), and also from syn- and post-tectonic coarse, clastic deposits (conglomerates and arkosic sandstones) on both the east and west sides of the thrust sheet. Proponents of plate tectonics models cite the presence of volcanogenic rocks in the Western Assemblage as evidence for an island arch which may have persisted offshore the North American continent throughout much of the Paleozoic era (Stewart, 1980).

Post-Antler Orogeny depositional patterns reflect some patterns developed in the Early Paleozoic era. The Eastern Assemblage, although not as extensive as formerly, continued to accumulate shallow water carbonates in a bank extending from eastern Nevada to Colorado. In central Nevada, however, the Antler Highland contributed coarse clastics to a deep water zone just west of the carbonate province, while siliceous and volcanic rock types accumulated just west of the Antler Highland (Stewart, 1980).

This pattern of deposition persisted until the Sonoma Orogeny of late Permian to early Triassic age. The Sonoma Orogeny is similar to the Antler Orogeny and resulted in the eastward lateral movement (thrusting) of deep water siliceous and coarse clastic rocks over coeval shallow water carbonates.

Several models have been suggested to explain the juxtaposition of siliceous rocks over the carbonates. The most recent models outlined in Stewart (1980) propose that an east-dipping plate located under the offshore island arc (Antler Highland) began to accelerate toward the continent. This resulted in the landward migration of the island arc and the obduction or over-thrusting of siliceous sediments over the carbonate deposits on the continental margin. Alternatively, Speed (1977) proposed the emplacement of the siliceous sediments over the continental carbonate rocks along the top of a west-dipping plate which was subducted under the island arc just west of the continental margin. Although the exact mechanism is still uncertain, the orogeny is recognized by superposition of Pennsylvanian and Permian age deep water siliceous sediments (Havallah and Pumpernickel formations) over shallow water carbonate rocks of the same age (Antler Peak and Edna Mountain limestones).

Mesozoic Era

Triassic sediments in western Nevada occur in two depositional provinces. In the study area, the Winnemucca Formation has been interpreted as a shallow shelf deposit consisting of shale with subordinate amounts of limestone, dolostone and sandstone. Further north in the Santa Rosa Range, the Raspberry Formation has been assigned to a deep-water basinal province consisting of pelites, sandstones and some limestone conglomerates. These sediments are thought to post-date the Sonoma Orogeny.

Upper Triassic to lower Jurassic sedimentary rocks occur at the north end of Hot Springs Range and on the west side of Santa Rosa Range. These sediments consist of pelites, shales and fine-grained quartzites which have all been affected by both regional and contact metamorphism associated with igneous activity during the Cretaceous period. These metamorphic rocks apparently represent a continuation of depositional patterns that began in the mid-Triassic.

Cretaceous sedimentary rocks are rare in Nevada. These widely scattered deposits consist of pebble conglomerates, phyllites, slates, and fresh-water limestones. Plutonic rocks of Cretaceous age are, however, widespread throughout Nevada and are well exposed in the Santa Rosa Range and Osgood Mountains.

Compositionally, these rocks are primarily granodiorites; locally, they may consist of quartz diorite and quartz monzonite. All of the granodiorites in the study area are considered to be a continuation of the Sierra Nevada Batholith (Moore, 1969).

Emplacement of these plutonic rocks was accompanied by regional metamorphism, folding and faulting, as well as contact metamorphism of Triassic sedimentary rocks. The influence of significant amounts of water as well as rapid heating during the metamorphic event are largely responsible for the characteristic mineral assemblages now exposed in the Triassic sediments in the Santa Rosa Range (Compton, 1960).

Tertiary Era

Sedimentary rocks ranging in age from 17 m.y. to 6 m.y. are exposed in the northeast corner of the study area. They include interbedded deposits of shales, mudstones, conglomerates, and volcanic tuffs.

Two important events occurred in central Nevada approximately 17 m.y. BP which helped shape present topographic features: tectonic forces changed from compressional to tensional, and volcanic rock compositons shifted from rhyolitic and calc-alkaline to basalt and basaltic andesites.

The onset of extensional tectonics produced widespread block faulting throughout the Basin and Range province. Vertical displacement along high-angle normal faults (60^{o}) varies from area to area, but most estimates range from 1800 to 4600 m (6000 - 15,000 ft) (Stewart, 1980). The exact nature of faulting is still uncertain although several models have been proposed (Stewart,

1980; p. 110).

A shift from acidic to basic type volcanic rocks accompanied Basin and Range faulting. Basalt andesites of Tertiary age occur throughout the study area with extensive outcrops in the Osgood Mountains, the Hot Springs Range and the Santa Rosa Range.

Quaternary age deposits constitute the largest single rock type in the area. Older alluvial deposits are located adjacent to the mountain ranges and consist of coarse alluvial fan deposits and debris slides. Younger alluvial deposits include lacustrine sediments from Lake Lahontan, stream gravels, playa deposits, and sand dunes. Much evidence of earlier Basin and Range faulting has been obscured by these younger Quaternary deposits.

A vescular olivine basalt tentatively dated at less than 6 m.y. is exposed in the south and west parts of the study area. These basalts may be related to similar age basalts that crop out in northwestern Humboldt County and northern Lander County immediately to the south.

GEOTHERMAL OCCURRENCES

Geothermal fluids ($T>20^{o}C$) occur throughout the study area (fig. C2), however, this investigation focused on three areas located on the east side of the valley. None of the fluids have temperatures greater than $70^{o}C$, but they all have a significant potential for direct use such as space heating or industrial process heating applications (Trexler and others, 1979).

Two separate spring sites occur in the town of Golconda: a small spring located near the center of town (Golconda Hot Spring) and a series of 10 to 12 larger and hotter springs just north of town (Segerstrom's Hot Springs). None of these springs is currently in use although a thermal well near Segerstrom Springs once supplied water to an ore processing plant. Temperaure profiles for this and another nearby well (fig. C3) were isothermal and therefore do not suggest the presence of a deeper, hotter reservoir.

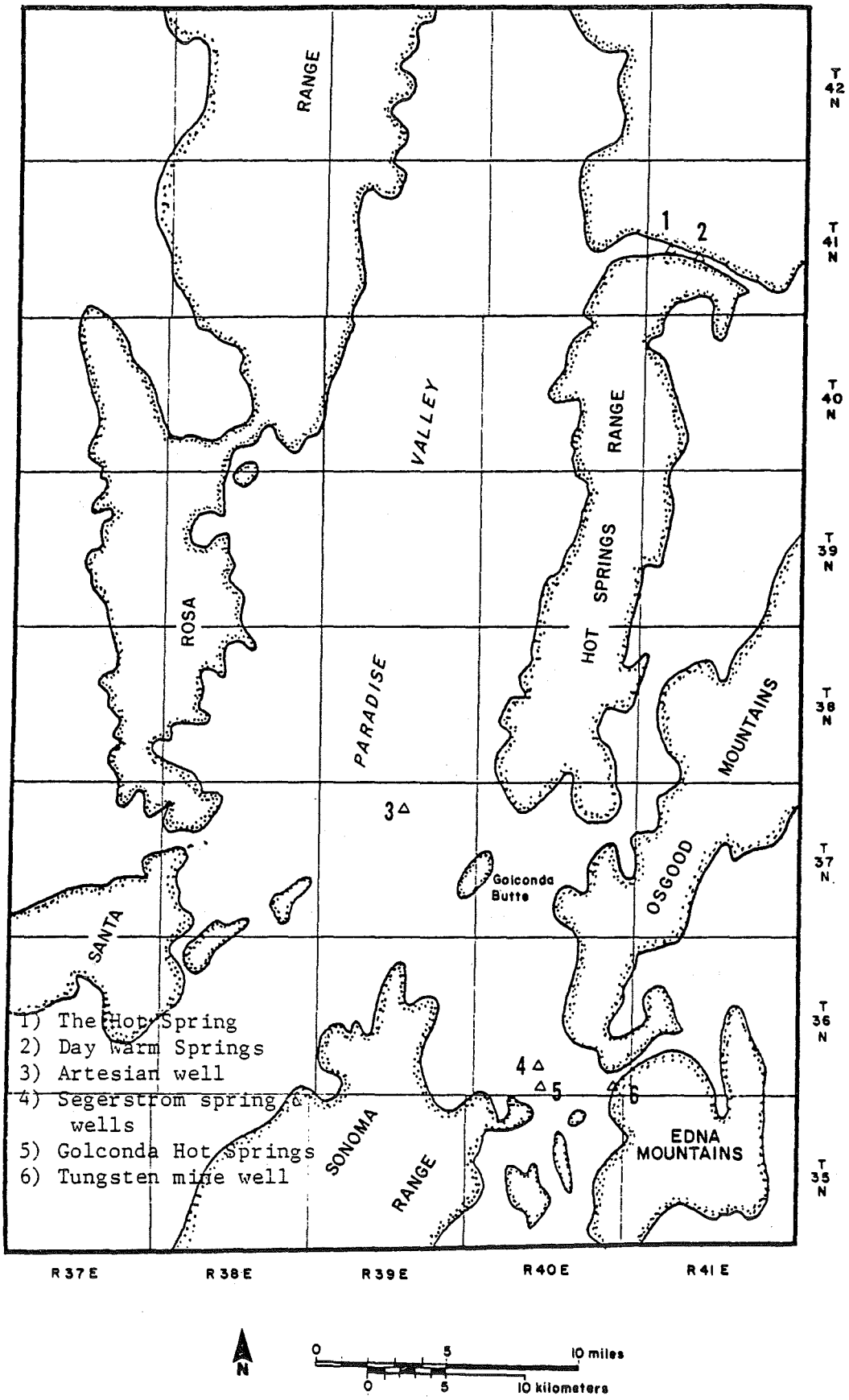

Figure C2. Principal geothermal occurrences in the Paradise Valley study area.

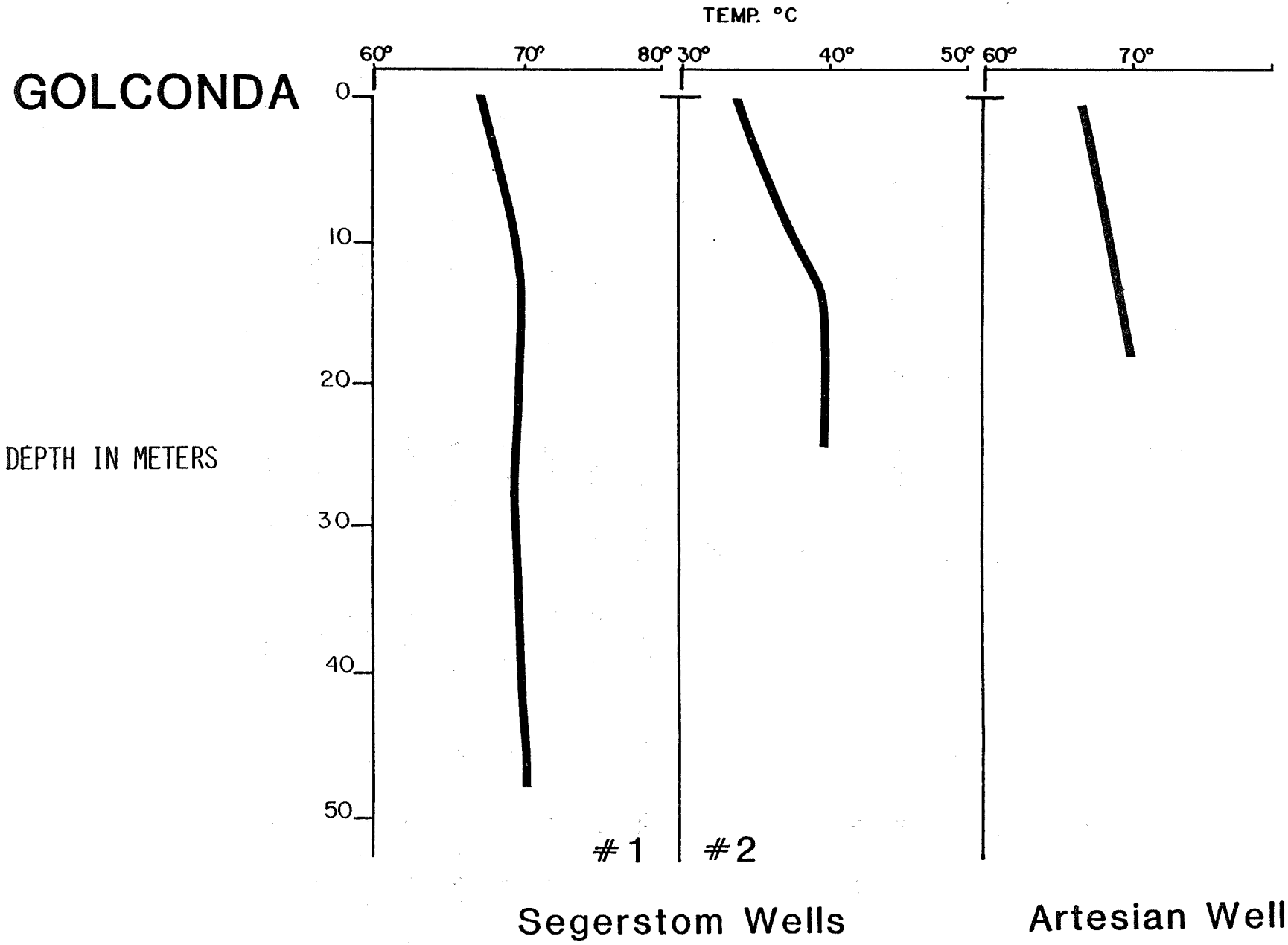

Figure C3. Temperature profiles of existing thermal wells.

The artesian hot well (fig. C2) was once the site of a small thermal spring. The well flows at a rate of 1 to 2 GPM and is located on a small mound, presumably a tuffa deposit rising several meters above the surrounding ground. A temperature profile taken for this well (fig. C3) shows an isothermal configuration similar to those measured near Golconda.

The third area located at the north end of the valley consists of two separate springs. The first is listed on the topographic sheet as The Hot Springs. The second is not designated on the map and is unnamed. This spring is now referred to as Day Warm Springs. The name is taken from the owner of the land, Mrs. Kirk Day of Winnemucca.

GRAVITY SURVEY

Gravity surveys are used extensively throughout regions of the Basin and Range province to characterize major geologic structures (Stewart, 1971) and to determine depth-of-valley fill (Thompson and Sandberg, 1958). The strategy for the Paradise Valley study area consisted of assembling existing gravity data and combining these data with results of a valley-wide gravity survey. The combined data sets would then be used to identify major geologic structures and trends, estimate depth-to-basement, and locate range-bounding faults that may act as structural controls for rising geothermal fluids.

Existing data were limited to the Bouguer gravity map of the Winnemucca Quadrangle (Erwin, 1974). Only the extreme southern end of the study area is included on this 1:250,000 map. Gravity data are presented in 5 milligal contours which, although useful on a regional scale, could not be used in this study.

A gravity survey of the study area was completed in January, 1981. The survey covered approximately 1700 km^2 (650 mi^2) and included 255 new gravity

stations. Station-spacing varied from 1 to 2 km. Closer spacing was used in areas adjacent to thermal springs to enhance the resolution of data and to minimize interpolation between stations. Results of the gravity survey are shown in Figure C4 which illustrates the complete Bouguer gravity map.

On the complete Bouguer gravity map, the contour interval is 2 milligals and the total gravity relief is 42 milligals. Three major trends can be identified on this map. The first is a north-northeast trending feature which consists of a series of aligned narrow basins flanked on both sides by parallel and closely-spaced gravity contours. The second feature appears as a series of northwest-trending gravity contours in the north-central portion of the map. This trend is also faintly defined at the south end of the map near points 1 and 2. The third major feature is located near point 3 and trends east-west across the map.

In additon to structural trends, Figure C4 also delineates several large gravity highs which correspond to mountain ranges. One notable exception is the gravity high located north of point 2. This feature is probably a former outcrop of Tertiary age basaltic andesite now buried beneath alluvial fill.

A depth-to-basement calculation was computed for several of the gravity lows in Figure C4 using the formula published by Thompson and Sandberg (1958). A density of 2.67 gm/cm^3 was used for basement rocks and a value of 2.00 gm/cm^3 was selected for unconsolidated alluvial material. Based on these assumptions, the deepest portion of the valley lies just north of the map center and contains 1.5 to 2 km (5000 - 6000 ft) of alluvial fill. This is roughly comparable to the topographic relief between the valley floor and the highest surrounding mountain peaks.

Vertical displacement along range-bounding faults is often identified by steep gradients in gravity contours. Gravity gradients were computed for several locations and the values range from 0 milligals/km to greater than

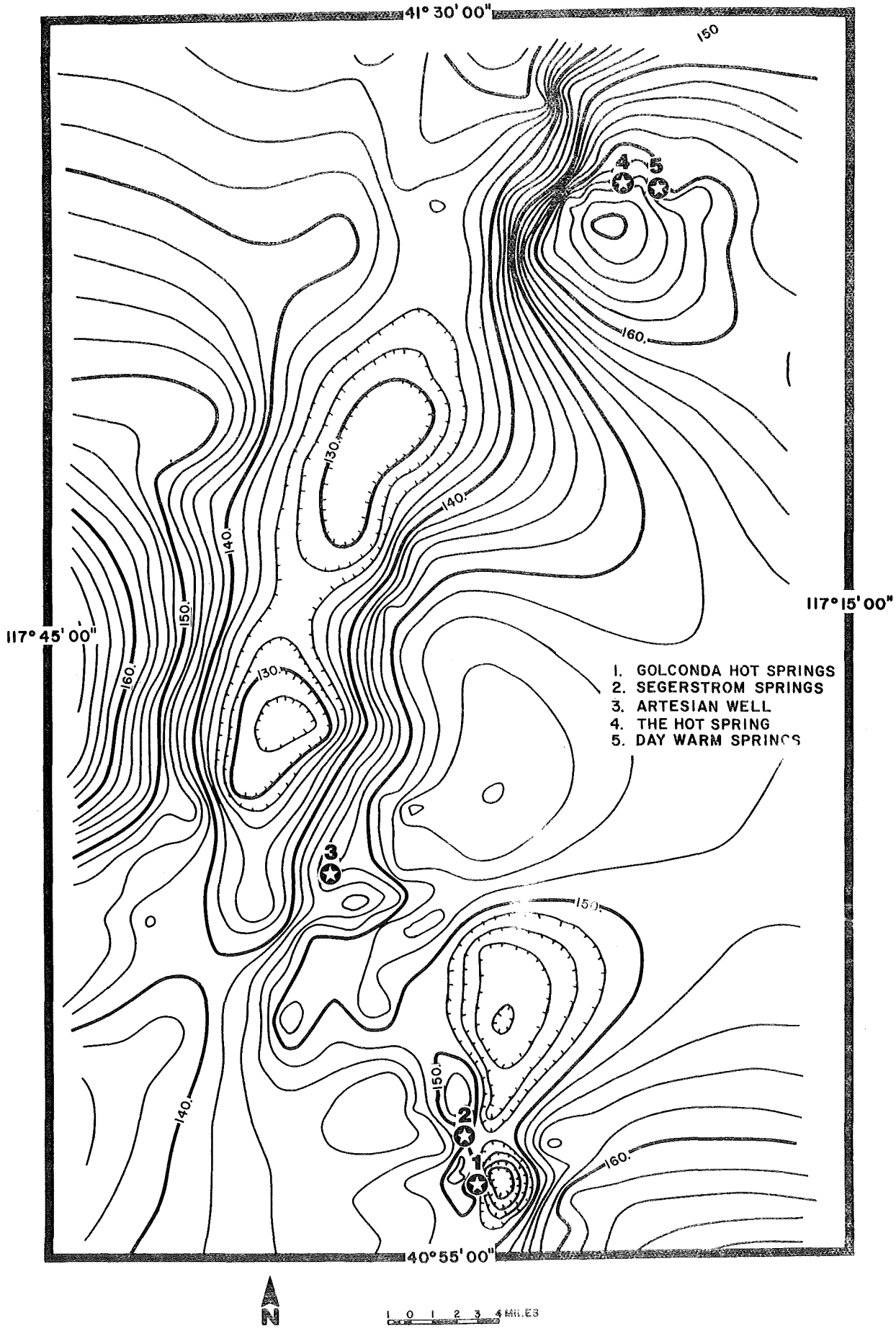

Figure C4. Complete Bouguer gravity map of the Paradise Valley study area.

7 milligals/km. The following values were computed for those areas adjacent to thermal fluids:

Golconda Area (1,2)	7.5 mgal/km
Artesian Well (3)	2.5 mgal/km
The Hot Spring (4)	4.1 mgal/km

Although these values represent considerable vertical displacement (as much as 100 m/mgal), no surface indications of recent faults correspond to the steep gravity gradients. Steep gravity gradients probably represent displacement along buried faults, but the exact location of these faults cannot be ascertained by these data.

In addition to steep gravity gradients, thermal springs are also co-located with the intersection of major trends in the gravity contours. Springs 1 and 2, for example, occur near the intersection of northeast and northwest trends while spring 3 is adjacent to the intersection of east-west and northeast trending features. Such a configuration may correspond to the orthogonal intersection of fault zones. Increased permeability in the vicinity of these intersections may enhance the flow of rising thermal fluids (Trexler and others, 1978; Trexler and others, 1980; Flynn and others, 1980).

AERIAL PHOTOGRAPHY, SATELLITE IMAGERY AND LINEAMENT ANALYSIS

Three data sets were used in a lineament analysis of the Paradise Valley study area. These data sets were 1:60,000 scale black and white vertical air photos, 1:250,000 scale false color NASA Landsat satellite imagery, and 1:24,000 scale low sun-angle (LSAP) air photos.

In 1954 the Army Map Service (AMS) Mission 109 was conducted in Paradise Valley and included nine east-west flight lines. This data set shows all large scale structural features in the study area, however, most subtle features have been obscured by Quaternary age deposits from Lake Lahontan and by sand dunes

that cover most of the southern half of the study area.

False-color NASA Landsat satellite imagery from the U.S. Geological Survey EROS Data Center was much more useful for gross-lineament analysis than the AMS photos. The Landsat image was printed at a scale of 1:250,000, the same as the Humboldt County Geologic Map (Willden, 1964). This facilitated correlation with geologic structures and topographic features. In addition, extensive coverage of NASA Landsat imagery permitted a large-scale lineament analysis that included features beyond the boundary of the study area.

Lineament trends identified on Landsat imagery roughly correspond to two major lineament trends in north-central Nevada. The first is the Midas Trench (Rowan and Wetlaufer, 1973) which trends northeast and extends from Lake Tahoe to the Nevada-Idaho border. The second is the Oregon-Nevada lineament (Stewart and others, 1975) which trends north-northeast and extends from Robert's Mountain to the Oregon-Idaho-Nevada border.

The prominent north-northwest and northwest lineaments trend roughly in the same direction as the Oregon-Nevada lineament (fig. C5) which is mapped and correlated with faults in western Elko County. This lineament is also correlated with a narrow zone of aligned magnetic anomalies (Mabey, 1966; Robinson, 1970). It is postulated that this magnetic anomaly results from a swarm of mafic dikes of Tertiary age. Another theory suggests that this zone is a plate-bounding right-lateral transcurrent fault that was tectonically active since late Paleozoic time (Rowan and Wetlaufer, 1975).

North-northwest trending lineaments are well exposed in Tertiary volcanic rocks north of Paradise Valley (fig. C6) and correlate with faults mapped in that area. One lineament can be correlated with a fault in the undivided Pennsylvanian-Permian Pumpernickel and Havallah formation at the north end of the Hot Springs Range. Another northwest trending lineament correlated with a fault in the Pennsylvanian

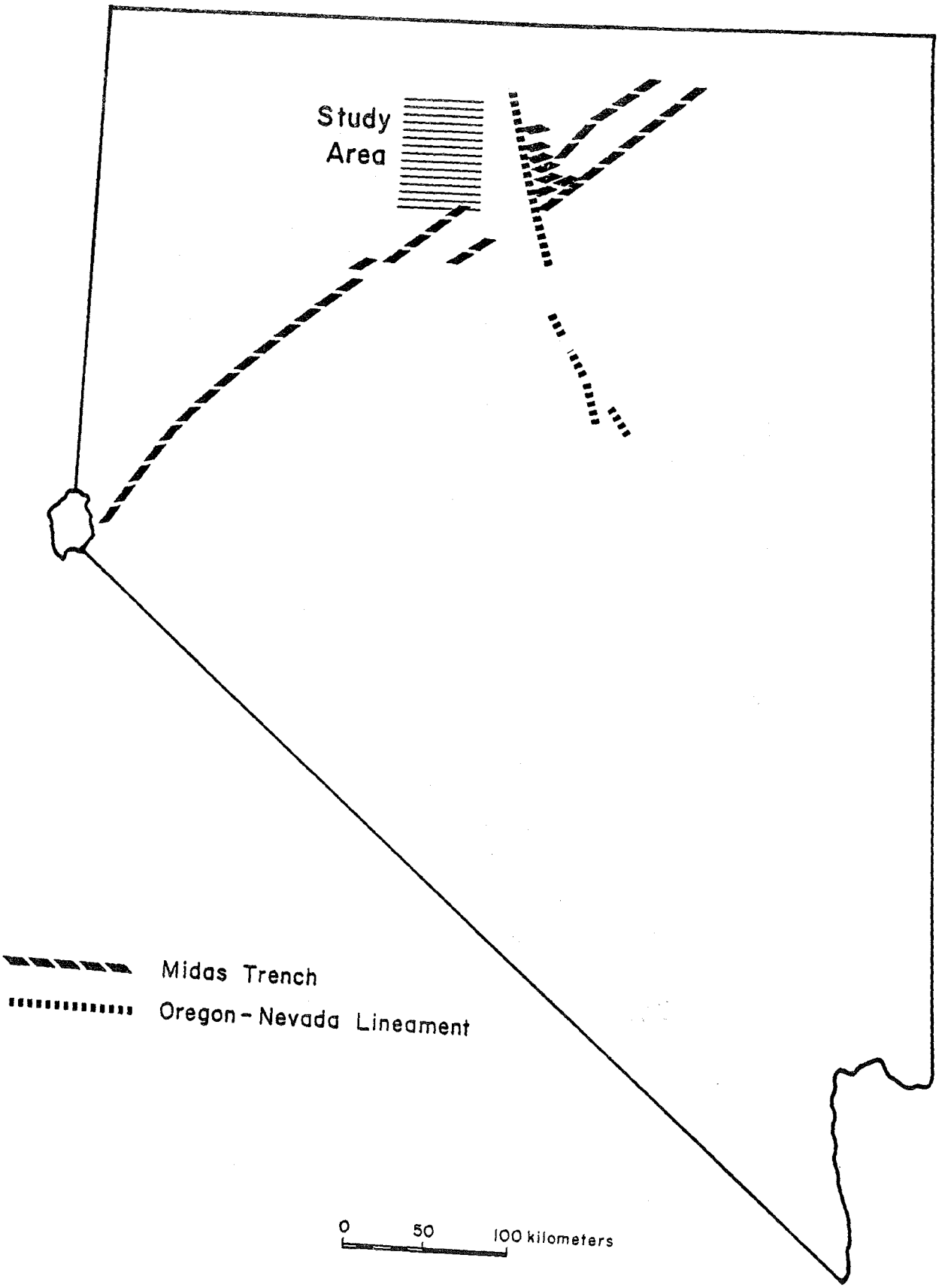

Figure C5. Location and trend of the Midas Trench and Oregon-Nevada Lineament (modified after Rowan and Wetlaufer, 1975).

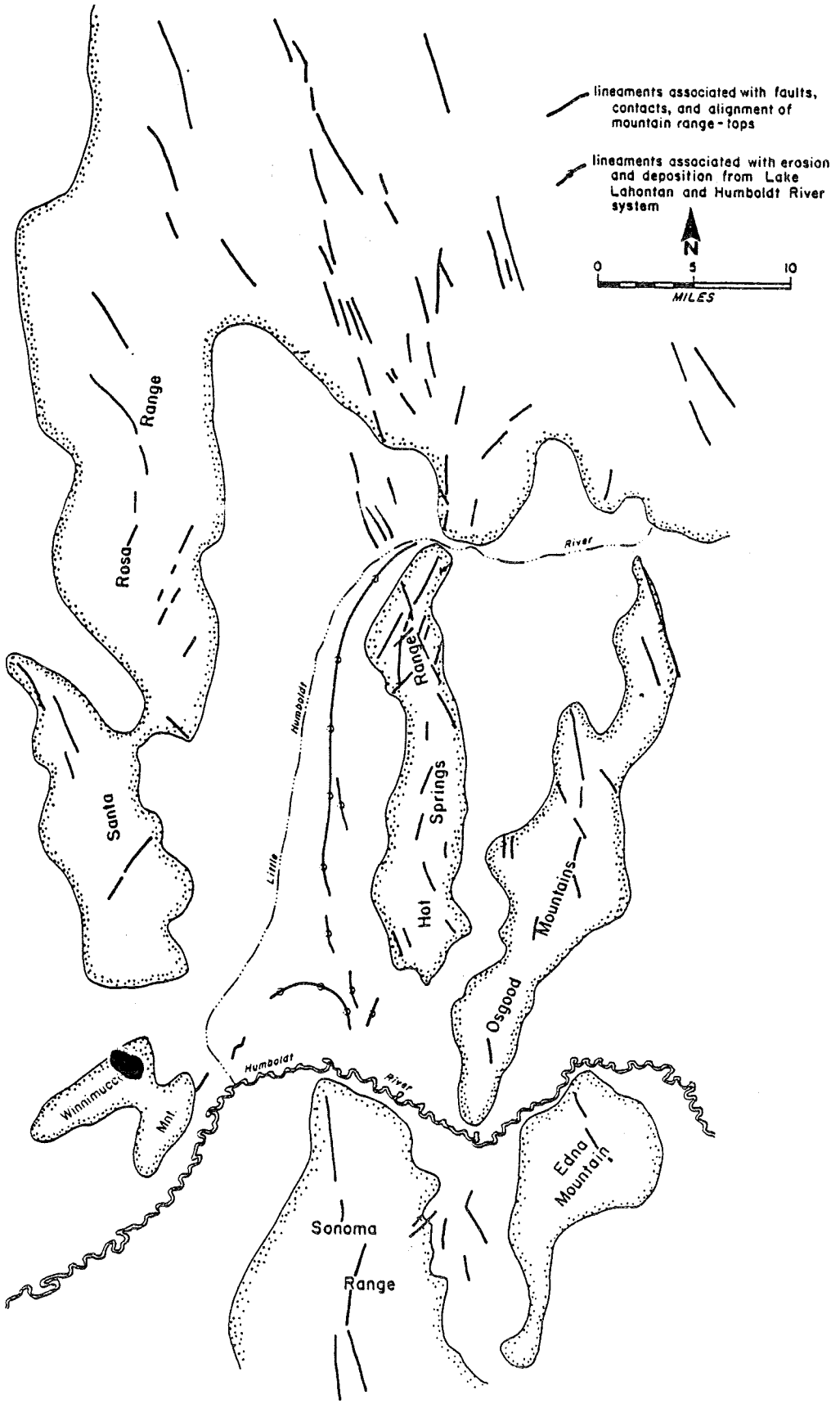

Figure C6. Lineaments identified from satellite imagery and aerial photographs.

Permian Antler Peak limestone near the north end of the Osgood Mountains. Both fault zones are associated with extensive deposits of tungsten, gold and mercury. The origin of these deposits is the result of contact metamorphism and hydrothermal alteration associated with the intrusion of Cretaceous granodiorite (Compton, 1960).

Northeast-trending lineaments are poorly exposed in the study area, but some were identified at the north end of the Hot Springs Range, the Santa Rosa Range and at Golconda Butte. These lineaments are parallel to the Midas Trench (Rowan and Wetlaufer, 1973) which is regarded as a major crustal feature on the basis of anomalous seismic data (Koizumi and others, 1973; Hill and Pakiser, 1967), and high heat flow values (Ryall and others, 1973). If projected beyond the study area, the Midas Trench extends into Yellowstone Park, Wyoming, a former volcanic center which is presently an area of high heat flow.

During the month of October, 1980, selected portions of the Paradise Valley study area were photographed from a fixed-wing aircraft in black and white stereographic pairs at a scale of 1:24,000. The photographs were purposely exposed during low sun-angle illumination to reveal subtle linear and curvilinear topographic features possibly related to recent movement along faults. The air photo survey covered approximately 80 line miles. Flight line selection was based principally on distribution of thermal springs, but flight specifications including planning the date and time of flight relied heavily on the work of Walker and Trexler (1977).

A LSAP taken at the north end of the study area (fig. C7) reveals the subtle trace of a fault scarp (B on photo) between Tertiary volcanic rocks and Paleozoic sedimentary rocks. This fault may be a structural control for Day Warm Springs (D on photo), but appears to be unrelated to the location of The Hot Springs (C on photo). Feature A which is similar in appearance to fault

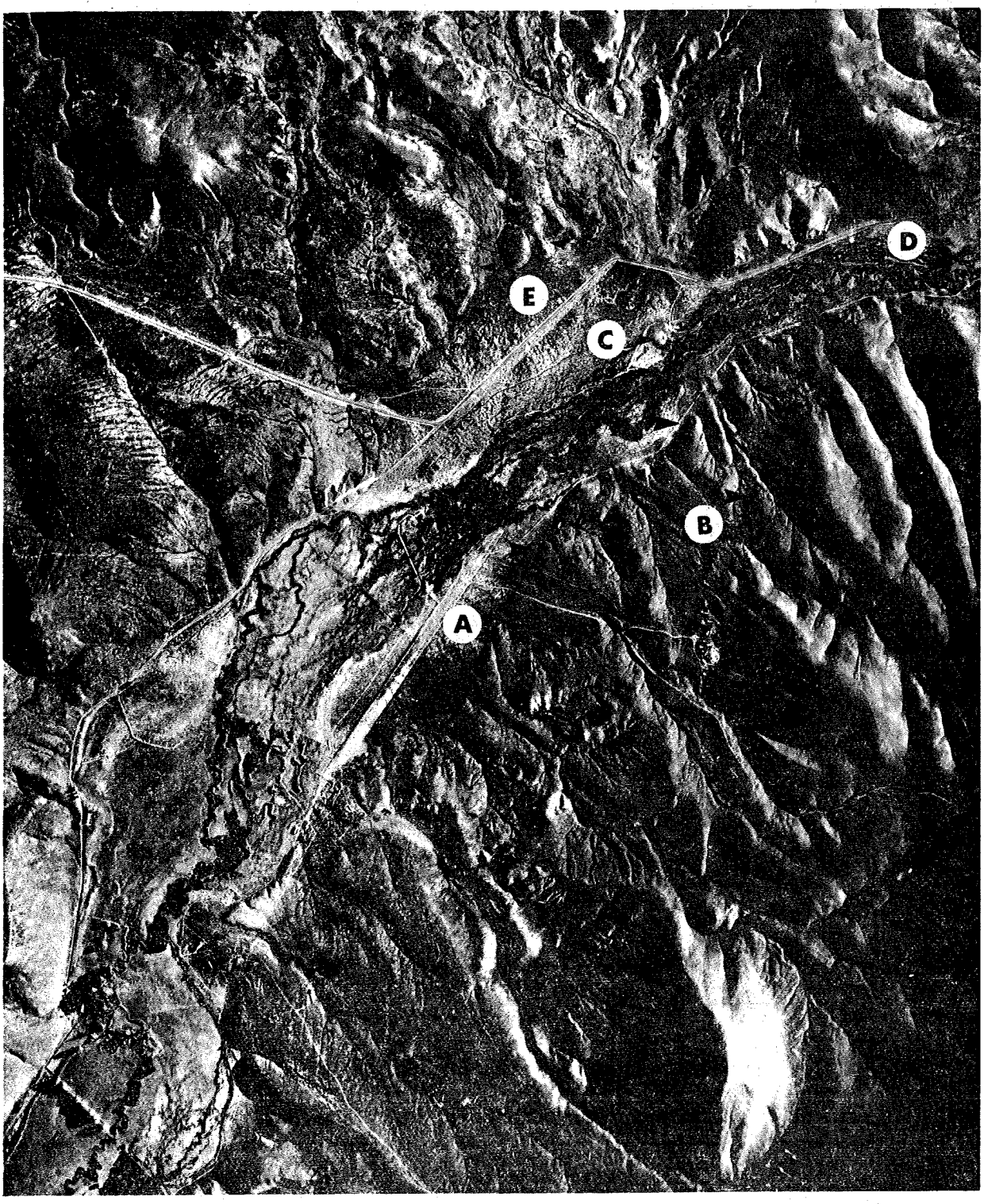

Figure C7. Geomorphic features identified near The Hot Spring: (A) stream-cut bench (B) fault scarp in bedrock (C) The Hot Spring (D) Day Warm Springs (E) irrigation ditch.

scarps is probably a remnant stream-cut channel bank of the Little Humboldt River. Feature E is a hand-dug irrigation ditch.

Further south along the west side of the Hot Springs Range (fig. C8) an extensive fault scarp (A to A1 on photo) is easily recognized cutting older alluvial deposits. Additional faults were identified on the ground immediately east of this fault scarp (B on photo) which is also the location of the Cahill Mercury Mine. Another irrigation ditch appears on the photo at C.

Old shoreline features from Lake Lahontan can be identified at A and B on Figure C9 at the southern end of the Hot Springs Range. These features are common throughout the western Basin and Range province and are often confused with fault scarps. The linear feature at C is probably an older fault scarp in the alluvial fan. Evidence of recent faulting in the southern end of the study area is obscured by an extensive sand dune field (D on photo). This dune field originates in Desert Valley 48 km (30 mi) to the west, and covers an area of approximately 160 km^2 (100 mi^2). Dutch Flat Well is shown at E.

Immediately south of Figure C9, a fault scarp (fig. C10) can be seen at A just west of Golconda Butte (B on photo). This scarp is also recognized as a lineament on the 1:250,000 scale NASA Landsat satellite image. Feature C is another stream-cut channel in the Lahontan lake sediments. More sand dunes can be seen at D, and E marks the location of the artesian hot well.

The last photo (fig. C11) was taken directly over the town of Golconda. Extensive agricultural activity and Humboldt River floodplain deposits probably obscure any traces of recent faulting in this area. The linear feature at A is another stream-cut channel in the alluvial fan at the southern end of the Osgood Mountains. Segerstrom's Hot Springs are located at B, and the Golconda Hot Spring is at C.

Although LSAP helped delineate many faults identified as lineaments on large scale photos, no recent (late Quaternary) faults were revealed. This

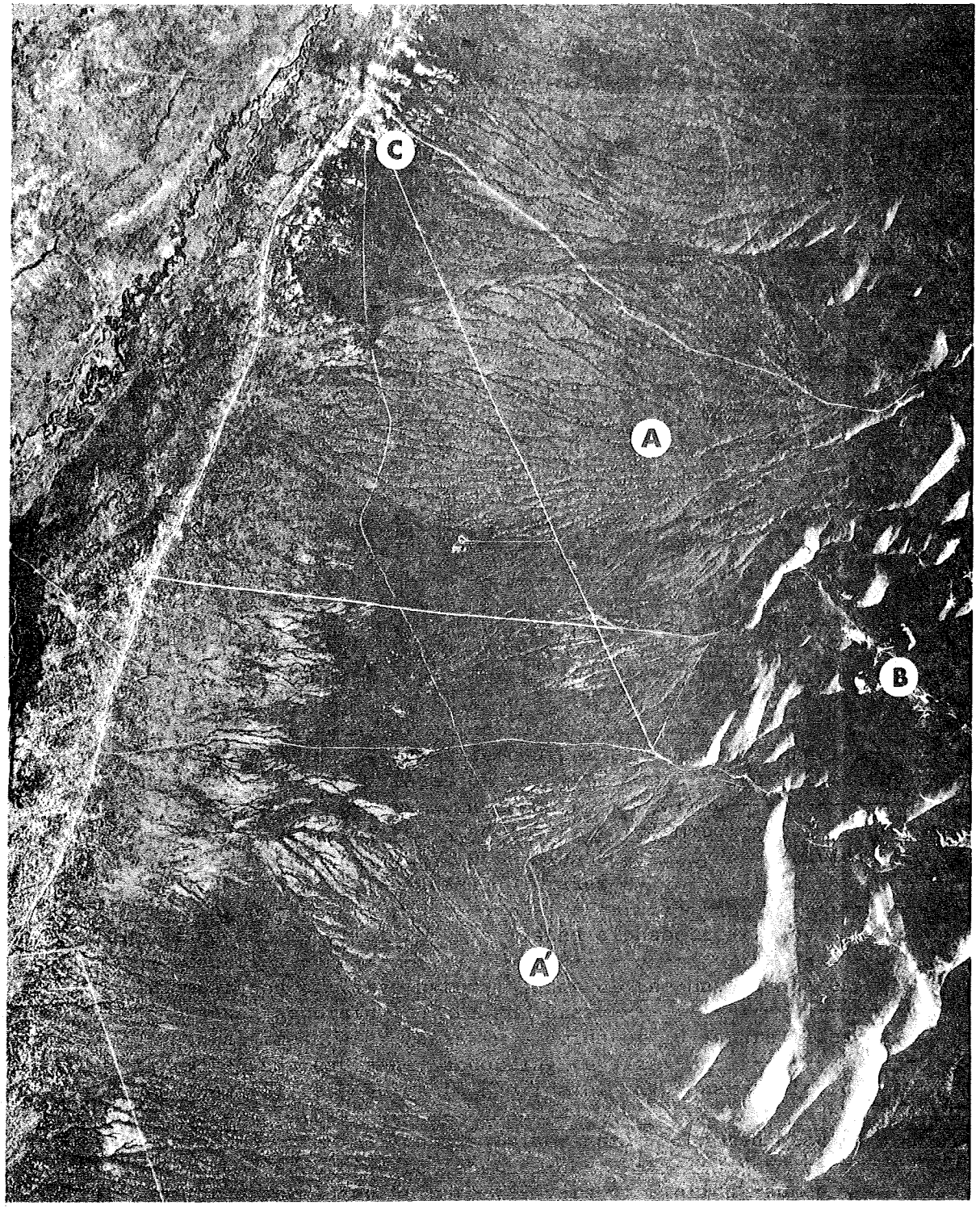

Figure C8 Geomorphic features identified at the northwest end of the Hot Springs Range: (A) fault scarp in alluvium (B) Cahill Mercury Mine (C) irrigation ditch (scale 1:24,000).

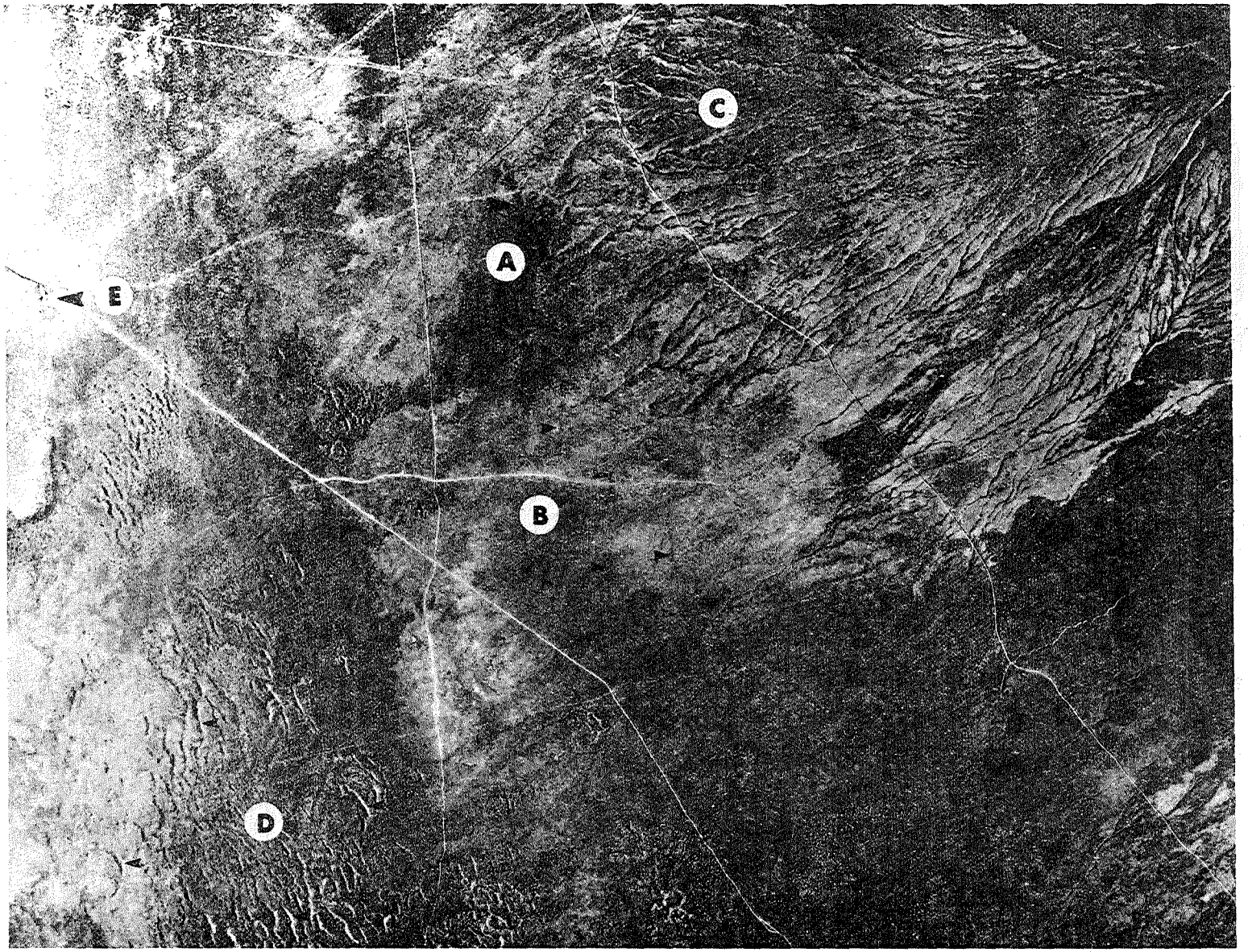

Figure C9. Geomorphic features identified at the southwest end of the Hot Springs Range: (A,B) Lake Lahontan shorelines (C) fault (?) in alluvium (D) sand dune (E) Dutch Flat Well (13°C) (scale 1:24,000).

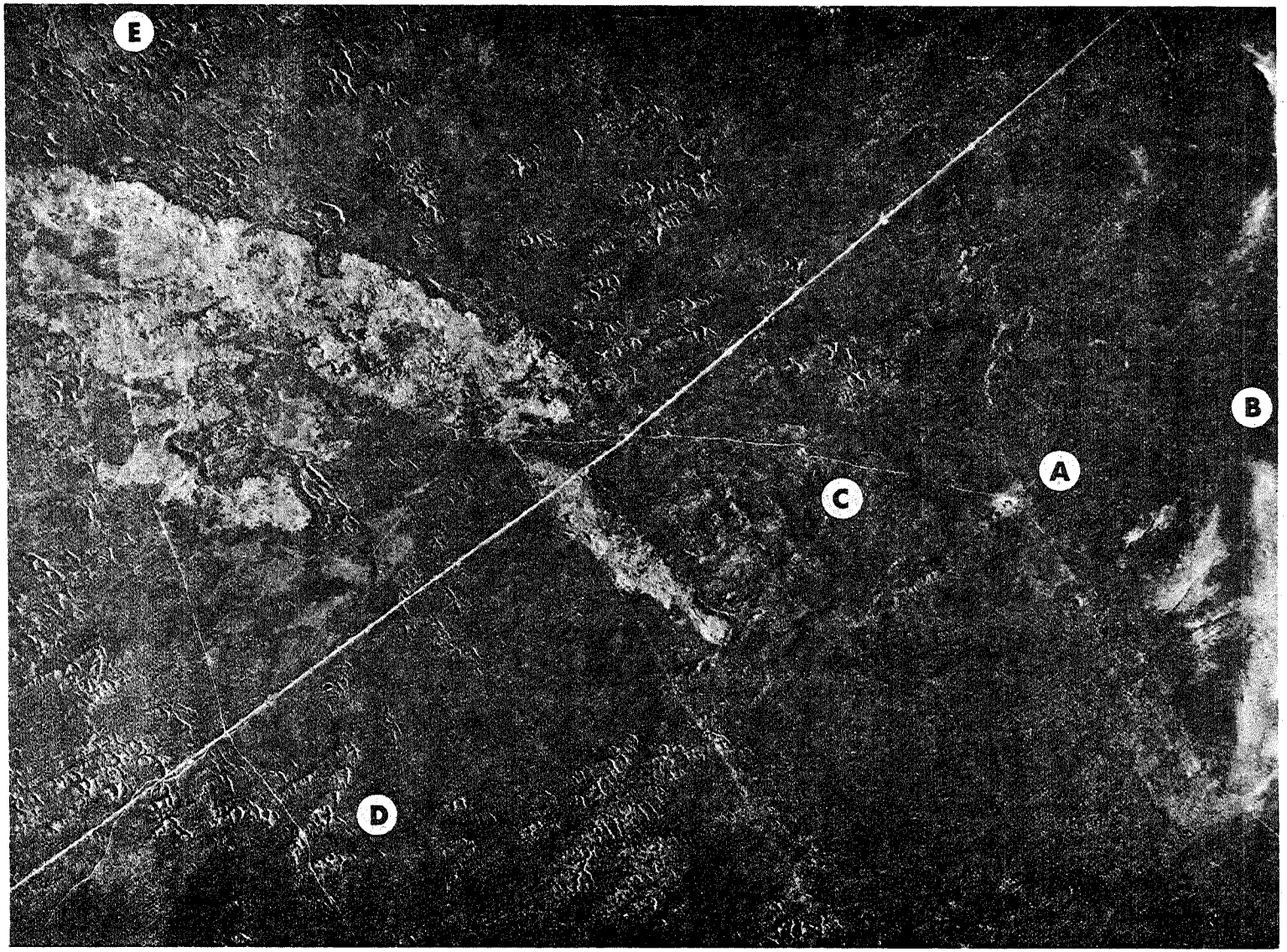

Figure C10. Geomorphic features identified near the artesian hot well: (A) fault scarp (B) Golconda Butte (C) stream cut channel (D) sand dunes (E) artesian well (68°C) (scale 1:24,000).

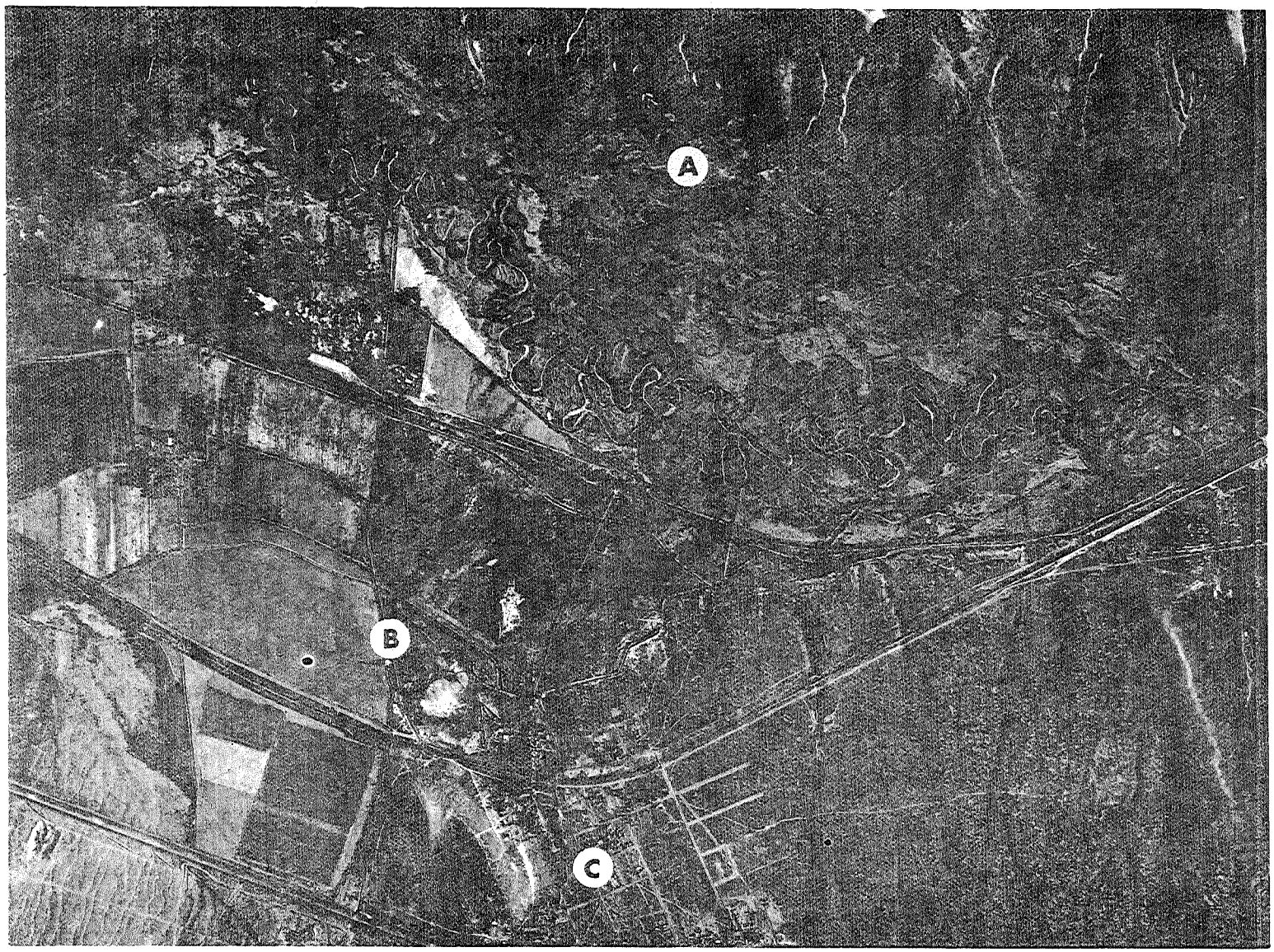

Figure C11. Geomorphic features identified near Golconda: (A) stream-cut channel (B) Segerstom's Hot Springs (C) Golconda Hot Spring (scale 1:24,000).

implies that seismic activity in this area has not included earthquakes of sufficient magnitude to produce measurable surface disruption since the recession of Lake Lahontan.

FLUID GEOCHEMISTRY

Paradise Valley is an important agricultural area. Much existing water chemistry data is derived from water resource inventories designed to support present and future farming needs. One of the earliest reports (Loeltz and others, 1949) describes the extent of existing groundwater supplies and classifies water resources including thermal fluids on the basis of major dissolved constituents. Cohen (1962) extended the survey to include many more water analyses, especially near Winnemucca, and correlates waters containing unusually high concentrations of dissolved species (sodium, boron) with faults and thermal springs. Harill and Moore (1970) discuss the effects of large-scale groundwater withdrawal from 1948 to 1968 in the Paradise Valley area. Thermal fluids in this area are also included in two reconnaissance studies of geochemical characteristics of hot springs throughout northern Nevada (Mariner and others, 1974; Sanders and Miles, 1974).

Eighteen fluid samples from both thermal and non-thermal sources were collected and analyzed for major, minor and trace elements, and for stable isotopes of hydrogen (deuterium) and oxygen (^{18}O). Chemical analyses included the determination of 32 dissolved species, as well as pH and alkalinity. Results of the chemical analyses are listed in Table C2 which includes sample names, numbers, location, and measured temperatures. Many of the analyzed elements are not listed because they fall below detection limits of the analytical equipment. Table C3 lists additional water analyses for thermal and non-thermal fluids in Paradise Valley.

Sample Name	Location	No.	T°C	pH	Ca	Mg	K	Na	Sr	Li	Cl	SO_4	HCO_3	CO_3	F	NO_3	SiO_2	B
Artesian Well	37/39 3 dc	GB-1	68	7.5	26	7.76	23	431	1.33	.77	14	68.2	1170	0	3.2	<.05	23.9	1.42
Dutch Flat well	38/39 22 db	GB-2	13	7.7	54.5	15.1	20	377	.85	.13	232	195	617	0	.61	4.08	36.3	1.91
Golconda Hot Spr.	36/40/32 ac	GB-3	42	6.85	42.7	9.75	26	151	.79	.50	24.4	54.2	521	0	2.47	<.05	20.0	1.50
Segerstrom (5) Spr.	36/40 29 dc	GB-4	61	7.4	36.1	8.37	24	146	.79	.47	22.0	53.4	451	0	2.14	<.05	29.5	1.31
Segerstrom (1) Spr.	36/40 29 dc	GB-5	71	7.1	36.7	7.65	22	128	.745	.37	16.8	48.4	427	0	1.81	<.05	32.2	1.08
Paradise well	40/38 34 ba	GB-6	18	7.2	95.9	19.5	3	66	.936	.04	66.6	109	270	0	.3	4.12	16.3	.16
L. Humboldt R.	41/41 26 ca	GB-7	18	7.35	40.6	7.32	8	42	.304	.03	31.6	27.5	146	0	.7	2.10	33.9	.13
The Hot Spring	41/41 19 aa	GB-8	56	7.1	24.9	7.15	13	298	1.63	.37	26	31.1	660	0	4.92	.24	24.1	2.02
Klauman well	41/40 23 ac	GB-9	18	6.9	19.2	4.05	10	60	.09	.03	24	27.7	166	0	.477	1.98	46.9	.19
Home Ranch well	40/40 19 ba	GB-10	18	7.1	49.6	13.7	13	63	.285	.05	36.3	37.3	275	0	.738	<.05	37.7	.20
Humboldt River	36/41 30 aa	GB-11	18	7.45	52.9	17.6	10	102	.383	.08	66.6	73.8	302	0	.921	.19	17.2	.37
Segerstrom well (1)	36/40 32 aa	GB-12	67	6.95	36.2	7.78	22	132	.749	.37	19.2	49.5	377	0	1,94	<.05	31.4	1.13
Day Warm Springs	41/41 20 ca	GB-13	36	6.75	28.7	7.08	21	461	.77	1.00	18	17.3	1376	0	5.70	.24	16	2.44
Big Cottonwood Ck.	42/39 25 bd	GB-14	15	7.35	50.0	11.1	3	42	.351	.01	11.6	10.5	265	0	.355	<.05	19.8	.16
Segerstrom well (2)	36/40 32 ac	GB-15	42	6.60	39.9	9.3	23	133	.742	.40	21.2	50.7	466	0	2.14	<.05	21.7	1.22
Buckbrush Spr.	41/41 17 aa	GB-16	9	7.65	43.4	15.7	9	71	.255	.03	41.7	42.9	242	0	.593	10.3	33.2	.09
Wash O'Neil Ck.	41/39 30 ca	GB-17	5	7.60	34.7	5.98	1.1	9	.168	.01	4.37	10	124.4	0	.802	.00	7.3	0
Humboldt River	36/40 21 cb	GB-18	5	8.20	57.4	16.6	8	70	.382	.06	3.44	50.8	312.3	0	.523	.38	22.6	.14

Table C-2 Chemical analyses of thermal and non-thermal fluids collected in the Paradise Valley study area.

Sample Name	Well Depth	Location	No.	T°C	pH	Ca	Mg	K	Na	Na+K	Cl	SO_4	HCO_3	CO_3	F	SiO_2	B
Miller well		39/39 3 ba	GB-19	14	8.2	33	3	5.4	33	--	26	24	143	0	0.2	--	.06
Miller well	225 ft.	39/39 3 cb	GB-20	13	7.9	48	1			49	43	34	164	0	--	--	--
Martin-Mickelson	225 ft.	39/39 13 c	GB-21	--	--	38	9.7			70	45	46	214	0	--	--	--
Martin-Mickelson	307 ft.	39/39 15 aa	GB-22	17	8.1	42	10			57	33	32	230	0	--	--	--
Martin-Mickelson	291 ft.	39/39 16 da	GB-23	15	8.0	36	4	6.4	34		27	25	159	0	0.2	--	.06
Garvey well	415 ft.	40/40 18 da	GB-24	14	8.2	24	6	9.8	41		28	28	145	0	0.6	--	.09
Garvey well	405 ft.	40/40 30 bc	GB-25	12	7.6	45	10			65	57	50	197	0	--	--	--
No name well		40/40 31 ca	GB-26	13	7.9	31	6	9.8	46		32	30	176	0	0.7	--	.16
E. Ferraro well	735 ft.	41/39 11 dc	GB-27	16	8.3	29	6	4.7	34		30	20	126	0	0.4	--	.02
G. Miller well		41/39 24 bc	GB-28	16	7.9	30	7			38	32	26	137	0	--	--	--
Garvey well		41/39 36 ac	GB-29	16	8.1	25	4			23	19	8	115	0	--	--	--
E. W. Gondra well	435 ft.	41/40 22 da	GB-30	22	8.4	23	6	13	57		29	31	173	0	0.7	83	.2
Little Humboldt R.		41/40 23 c	GB-31	--	--	33	8			48	27	33	180	0	--	--	.16
Martin Creek		42/40 12b	GB-32	--	--	19	6			28	18	18	110	0	--	--	--
Cottonwood Creek		42/39 25 bd	GB-33	--	--	44	11			63	11	10	323	0	--	--	.19
R. Thomas well	303 ft	41/40 33 ab	GB-34	13	--	33	6	10	54		44	41	161	0	0.8	--	.11
The Hot Spring		41/41 19 ac	GB-35	57	--	26	8.5			334	26	34	920	0	--	--	2.54

Table C3. Chemical analyses of selected waters in the Paradise Valley study area. Data from Table 7 and 7a, Harril and Moore (1970).

Sample Name	Well Depth	Location	No.	T°C	pH	Ca	Mg	K	Na	Na+K	Cl	SO_4	HCO_3	CO_3	F	SiO_2	B
Little Humboldt R.		41/41 19 ac	GB-36	--	--	34	8			40	27	31	165	0	--	--	.09
Pasquale-Rich well	500 ft.	42/39 14 aa	GB-37	--	--	27	7	4.5	38		38	25	116	0	0.5	44	.06
Colony Creek		42/39 34 c	GB-38	--	--	11	4			9	2	3	70	0	--	--	--
Cerri well	51 ft.	42/40 16 ac	GB-39	9	--	52	13			126	66	45	329	0	--	--	.4
Toll House well	79 ft.	37/38 2 aa	GB-40	--	--	27	8			120	67	74	232	0	--	--	.51
USGS well		37/38 21 dd	GB-41	--	8.5	34	7.1	9.6	116		62	52	255	0	--	--	--
USGS well	38 ft.	37/38 24 ac	GB-42	14	7.5	64	25	18	376		311	163	618	0	--	--	2.8
No name well	61 ft.	37/39 3 dc	GB-43	69	7.7	26	11	26	452		16	71	1230	0	--	--	1.4
USGS well	30 ft.	37/39 19 aa	GB-44	11	7.9	22	4.4	9.6	284		86	210	446	0	--	--	.9
No name well		37/39 28 ad	GB-45	14	7.7	32	9.7	9.6	109		69	117	167	0	--	--	.4
No name well		38/39 16 aa	GB-46	17	8.2	27	4	8.7	40		21	23	160	0	0.4	73	.1
W.S. Hill well	78 ft.	38/39 16 cd	GB-47	13	8.0	14	8	5.7	184		95	166	180	0	0.5	67	.15
C.F. Grady well	280 ft.	38/39 21 aa	GB-48	14	8.2	31	6			82	47	54	192	0	--	--	--
G. Etchart well	420 ft.	38/39 28 da	GB-49	--	8.0	56	9.8	11	72		79	91	156	0	0.4	81	.1
No name well	64 ft.	38/39 35 aa	GB-50	17	7.9	40	16	5.8	45		66	16	202	0	--	--	--

Table C-3. (Cont.)

Historical chemical data for thermal fluids were combined with this new data to evaluate changes in chemical composition over a period of 35 years (fig. C12). The data show that within analytical error and with few exceptions, chemical composition of thermal fluids has remained uniform over the period of record (1945 to 1980). Small perturbations may be the result of sampling or analytical irregularities, or may occur from dilution due to heavy precipitation.

Historical data combined with recent data were also plotted on a tri-linear diagram (fig. C13) (Piper, 1944) and are based on major anion and cation compositions. The diagram indicates that fluids can be classified into three groups. Non-thermal fluids constitute the majority of samples and also show the widest range of chemical compositions. Thermal fluids, on the other hand (shaded regions), make up two small groups and have a limited range of chemical compositional variation.

The wide range of chemical compositions for non-thermal fluids may be explained in part by geography. For example, samples 40, 41, 48, 2, 42, 44, and 47 were collected from an area in south-central Paradise Valley. Likewise, samples 24, 26 and 10 were collected in north-central Paradise Valley and are chemically different from previously listed samples. Thermal fluids from the Golconda area (samples 3, 4, 5, 12, and 15) also constitute a distinct chemical group. Remaining thermal fluids (samples 1, 8 and 13) were sampled from two springs that are 40 km (25 mi) apart. Figure C13, however, indicates that these springs are chemically similar to one another and, like the Golconda area springs, are chemically dissimilar to the non-thermal fluids collected from the respective surrounding areas.

The unique chemical composition of thermal fluids relative to non-thermal fluids is also seen in the map of modified Stiff (1953) diagrams (fig. C14).

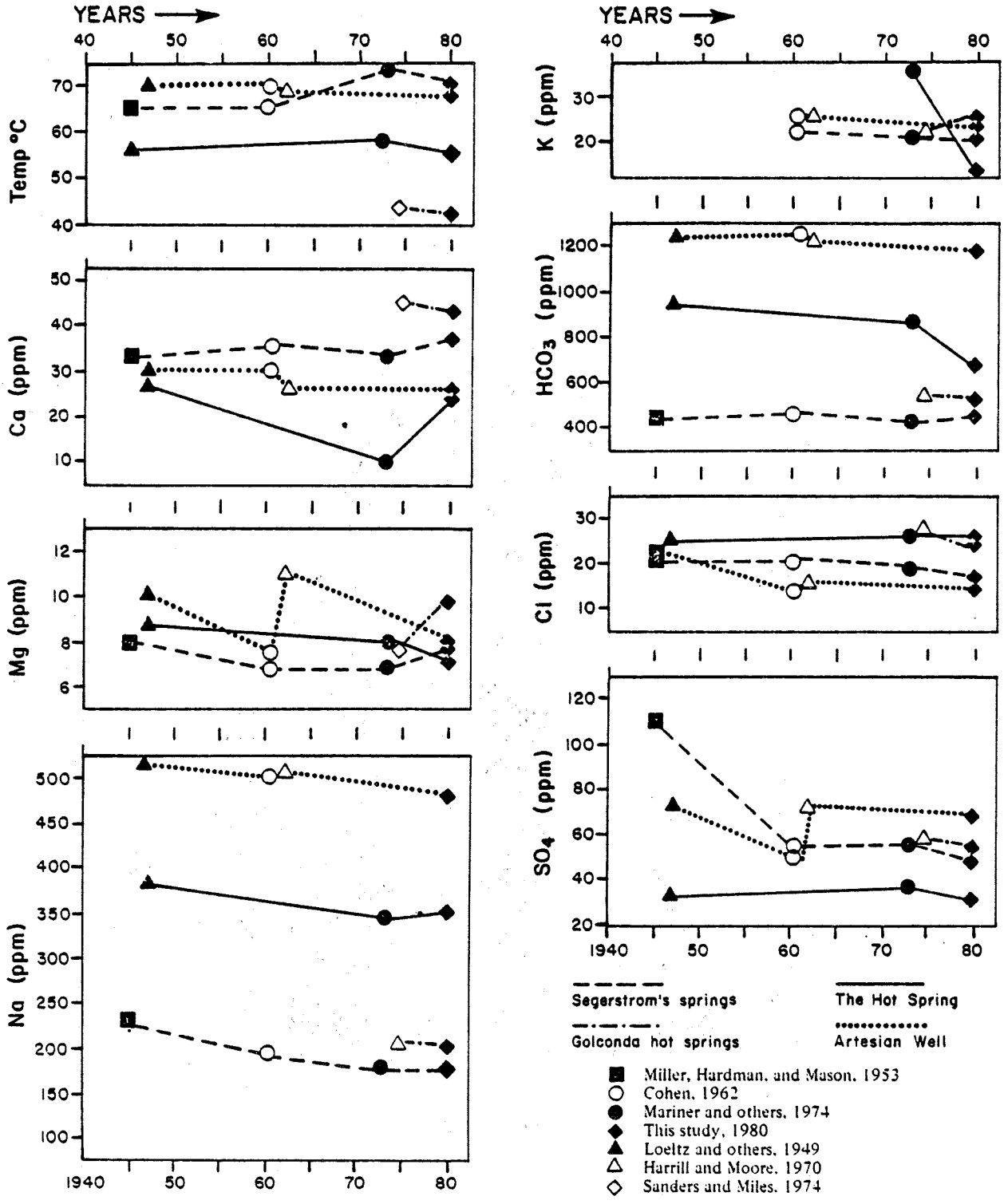

Figure C12. Chemical composition of selected thermal fluids in the Golconda study area, 1945-1980.

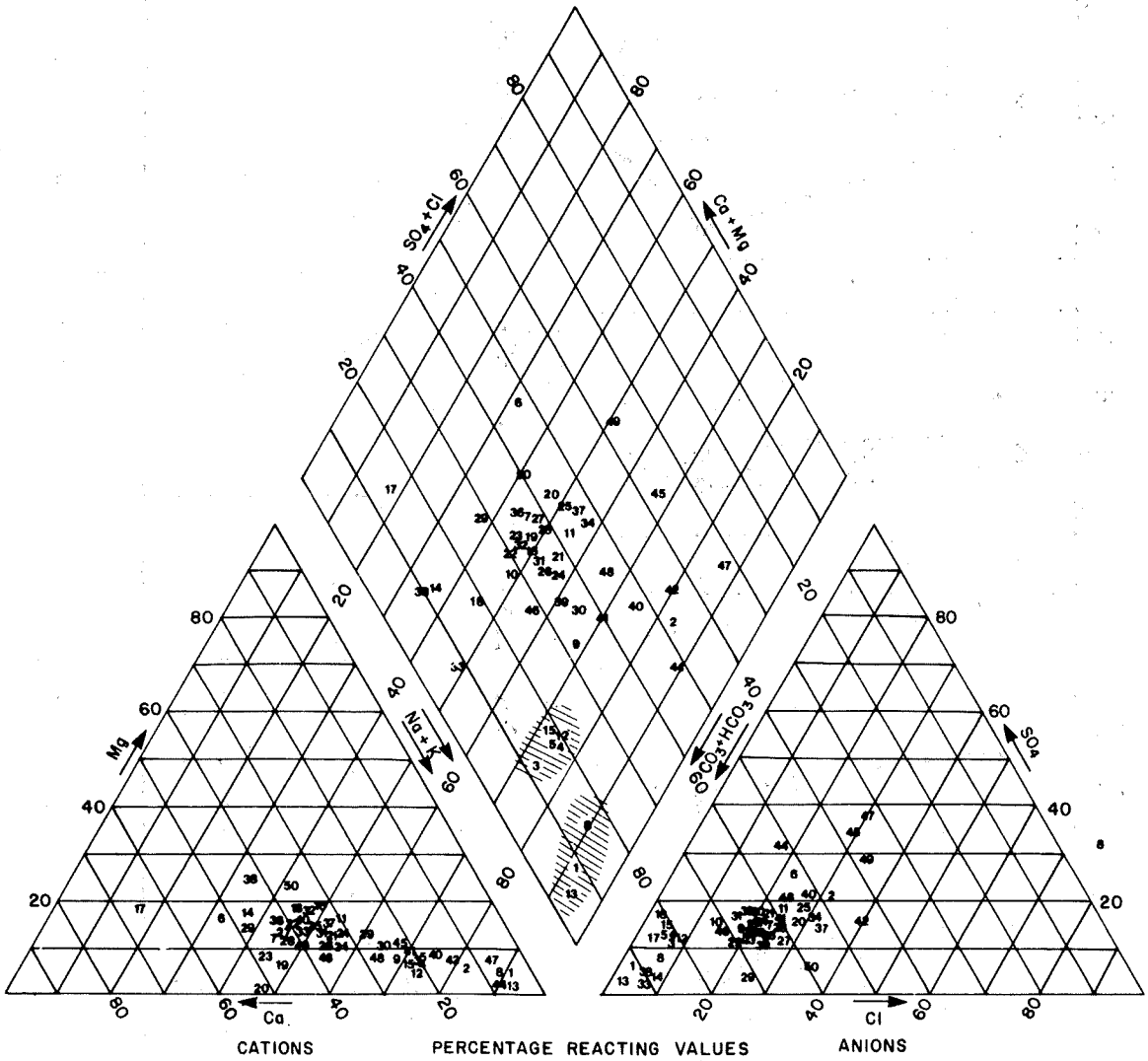

Figure C13. Chemical characteristics of thermal and non-thermal fluids in the Paradise Valley study area.

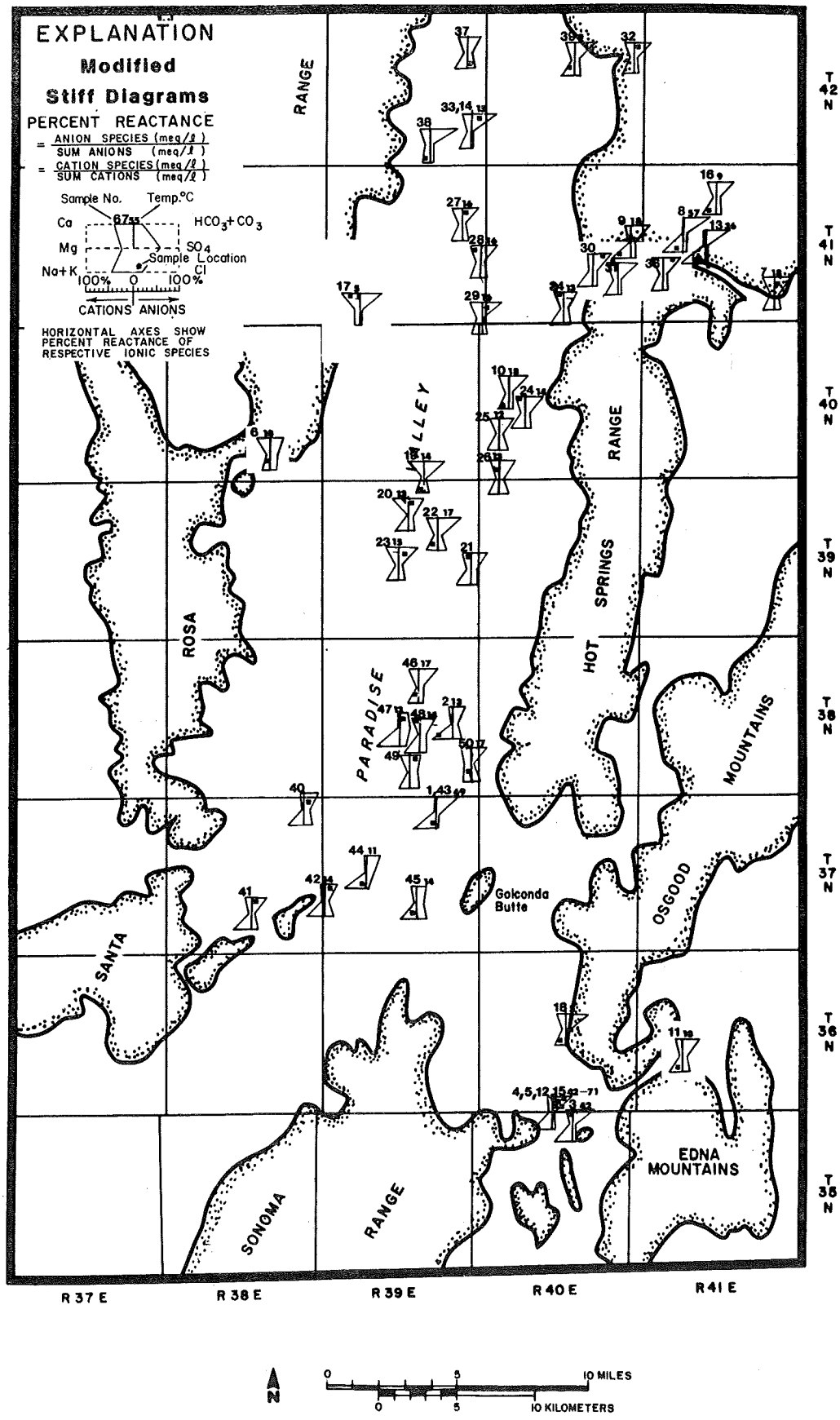

Figure C14. Spatial distribution of water sample sites and chemical characteristics of fluids in the Paradise Valley study area.

All but one of the thermal fluids are chemically dissimilar to the surrounding non-thermal fluids. The only exception is sample 30 (22°C) which is identical to cooler surrounding groundwaters. This sample collected from a deep well (132 m; 435 ft) may represent typical groundwater heated by the average geothermal gradient (32°C/km) in the Basin and Range province.

Chemical analyses of trace and minor elements were largely undiagnostic; the fluids contained such small amounts of these constituents that they fell below equipment detection limits. Only four elements exceeded detection limits. Results for the 18 analyzed samples are shown in Figure C15.

With few exceptions, thermal fluids contain much higher concentrations of Sr, B, Li, and Ba. One exception is sample 2 which has high concentrations of B, Sr, and Ba. It is also similar to thermal waters with respect to cations, but contains much more SO_4 and Cl. This unusual composition may be the result of mixing of thermal and non-thermal fluids. Another explanation is that high trace element content may be derived from dissolution of compounds in mineralized zones in the Dutch Flat Mining District immediately east of the sample site. A third explanation combines both of the above.

Analyses of sample 6 also show anomalously high concentrations of Sr. Figure C13 indicates that this sample contains the highest Ca concentration of all 18 samples. Ca-rich sediments of the Raspberry and Winnemucca formation crop out where this fluid was sampled.

Ca and Sr are chemically similar. Sr is found in great abundance in Ca-rich minerals such as calcite (CCO_3) and anhydrite ($CaSO_4$). It seems likely, therefore, that the Sr anomally for this fluid is related to high concentration of Ca and close association of Ca-rich sediments.

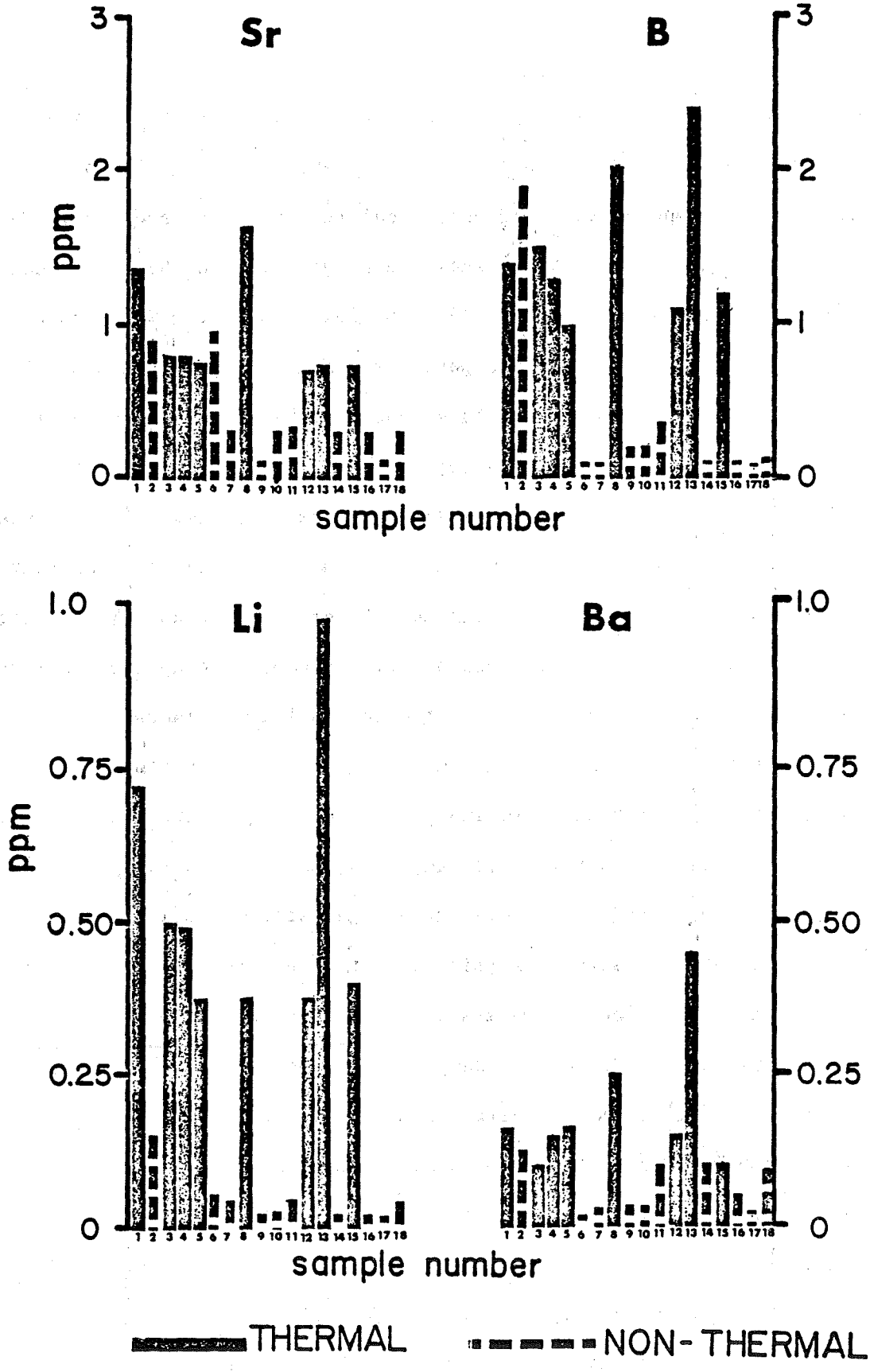

Figure C15. Minor and trace element compositions of fluid samples in the Paradise Valley study area.

Isotopic Analyses

In addition to major, minor and trace element analyses, the 18 fluid samples were also submitted for analysis of deuterium and ^{18}O. Sample names, numbers, measured temperatures, and analytical results are presented in Table C4. Locations of these samples are shown in Figure C13 and the analytical results are plotted against Craig's (1963) worldwide meteoric water data (fig. C16). Duplicate analyses were performed on many samples in order to establish error bars for the data. This procedure resulted in errors of $\pm 3^{o}/11$ for D and $\pm .2^{o}/oo$ for ^{18}O. A separate duplicate of sample 1 (no. 19) was submitted for analyses four months after it was collected. Both samples 1 and 19 were collected the same day. Sample 1 was submitted for immediate analysis but sample 19 remained "on the shelf" for four months. The analyses are within established analytical errors and, therefore, it appears that the wax-sealed bottles effectively preclude the possibility of isotopic re-equilibration with atmospheric D and ^{18}O for at least four months.

Figure C16 shows that isotopic analyses form a continuous line of increasingly heavier fluids from sample 1 to sample 14, parallel to Craig's worldwide meteoric line. The dashed line representing the local meteoric line was derived by a linear regression analysis of surface non-thermal waters. This line has a slope of 4 which is comparable for surface waters in a closed basin. Isotopically lighter fluids such as samples 1, 8 and 13 are generally associated with water derived from precipitation at higher altitudes or from snowmelt. Recharge is probably restricted to precipitation on mountain ranges higher than 2400 m (8000 ft) above sea level and precludes surface waters and groundwaters in the basin.

With the exception of samples 8 and 16, there are no large ^{18}O shifts. This implies that the fluids have not re-equilibrated with rocks at high

Table C4. Hydrogen and Oxygen stable isotope analyses: Paradise Valley study area.

Sample Name	Sample Number	$\delta D^{o}/oo$	$\delta^{18}D^{o}/oo$	$T^{o}C$
Artesian Well	1	-132	-17.0/-17.1	68
(separate duplicate)	19	-136	-17.0	68
Dutch Flat Well	2	-130	-16.5	13
Golconda Hot Spring	3	-119	-15.8	42
Segerstrom (5) Sp.	4	-120	-15.3	61
Segerstrom (1) Sp.	5	-120	-15.8	71
Paradise Well	6	-119/-119	-15.2	18
Little Humboldt River	7	-123/-121	-15.4	18
The Hot Spring	8	-134	-15.8	56
Klauman Well	9	-123	-15.4	18
Home Ranch Well	10	-116	-14.9	18
Humboldt at Preble	11	-107	-12.5	18
Segerstrom Well (1)	12	-126	-15.7	67
Day Warm Springs	13	-131	-16.4	36
Big Cottonwood Creek	14	-110/-109	-13.7	15
Segerstrom Well (2)	15	-128	-15.7	42
Buckbrush Spring	16	-126	-13.9/-13.9	9
Wash O'Neil Creek	17	-112	-14.7	5
Humboldt River	18	-114	-14.2	5

Values separated by a slash (/) indicate duplicate analyses on a single sample.

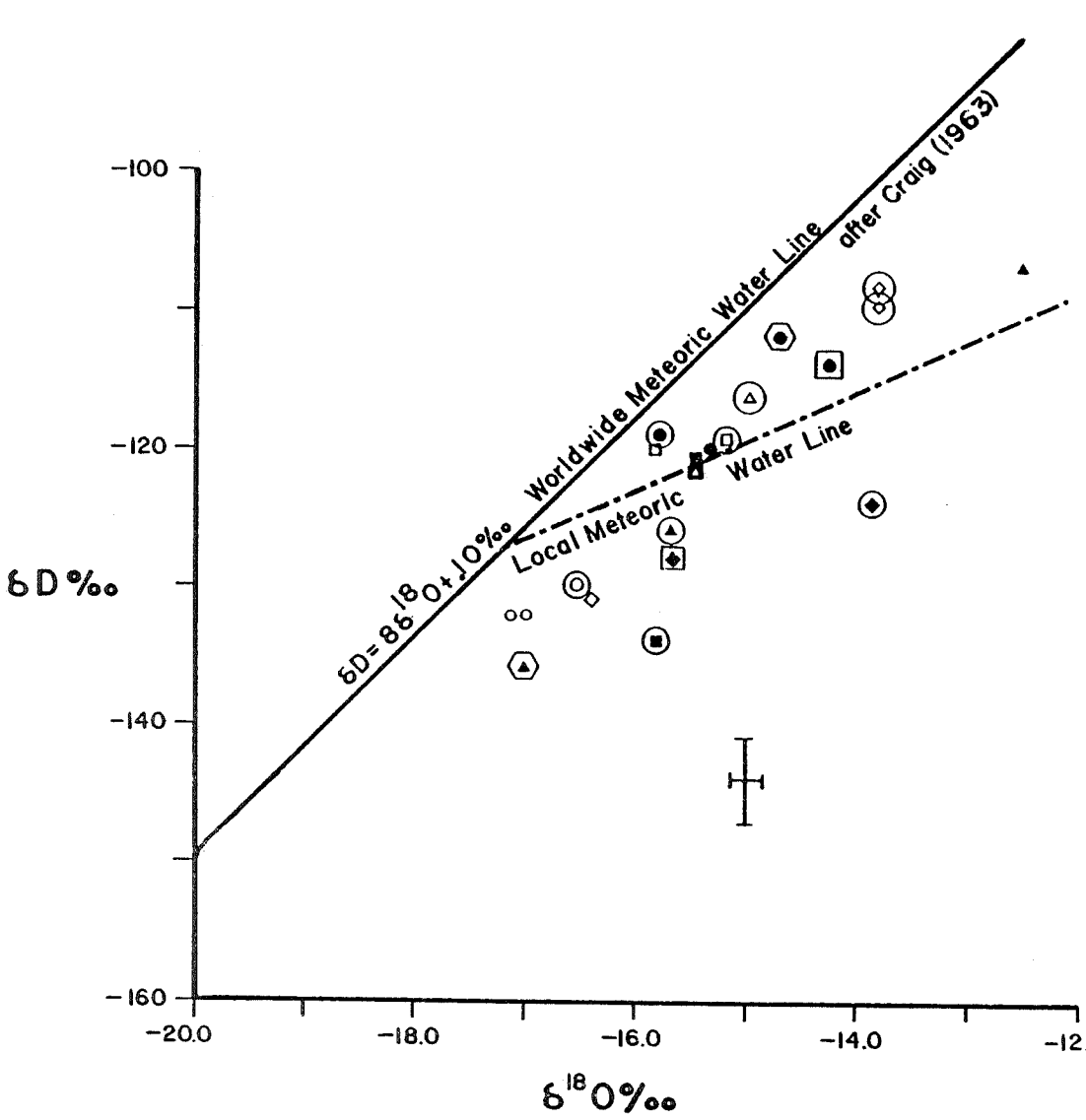

Isotope values for fluids collected from the Paradise Valley study area.

No.	Name	Temp.(°C)	Symbol
1	Artesian well	68°	○
2	Dutch Flat well	13°	◎
3	Golconda Hot Spring	43°	●
4	N. Golconda Spring #5	61°	◉
5	N. Golconda Spring #1	72°	□
6	Paradise well	18°	▣
7	Little Humboldt Bull Head	18°	■
8	The Hot Spring	56°	▣
9	Klauman W.	18°	△
10	Home Ranch well	16°	◬
11	Humboldt at Prebble	18°	▲
12	Segerstrom well #1	67°	◭
13	Day Warm Spring	36°	◇
14	Big Cottonwood Creek	15°	◈
15	Segerstrom well #2	42°	◆
16	Buckbrush Spring	9°	◈
17	Wash O'Neal Creek	4°	⬢
18	Humboldt at Golconda	4°	▣
19	Artesian well (4 mos duplicate	68°)	◭

Figure C16. Stable light isotopes of thermal and non-thermal fluids in the Paradise Valley study area.

temperatures. Samples 8 and 16 are located in areas where carbonate rocks are abundant. Both springs are also presently precipitating calcium carbonate, suggesting that the slight ^{18}O shift could be the result of re-equilibration with carbonates. Clayton and others (1968) have recognized large ^{18}O shifts in oil field waters at temperatures as low as 10°C. These reactions rely on small water-to-rock ratios and long residence times.

Figure C16 indicates that, like the tri-linear chemical composition diagram (fig. C13), waters sampled from the Golconda area have intermediate isotopic compositions. These fluids may represent a mixture of isotopically lighter fluids (samples 1, 8 and 13) and heavier non-thermal fluids. This mixing appears to involve equal volumes of thermal and non-thermal fluids and probably occurs within 100 m (328 ft) of the surface.

Samples collected from hot springs in Golconda (samples 3, 4 and 5) appear to be more enriched in deuterium than samples collected from nearby hot wells. The configuration of data in Figure C16 is probably dependent upon a mechanism that increases the proportion of deuterium in the fluid while maintaining ^{18}O at a uniform level. That mechanism may be explained by introducing slightly higher levels of either hydrogen sulfide gas or more likely, methane gas. Both gases are commonly associated with hot springs. Methane gas is often detected in swamps and river floodplains as a result of decomposition of organic materials.

Hydrostatic pressure on fluids collected from wells 12 to 15 m (40-50 ft) below the surface may be sufficient to trap additional hydrogen sulfide or methane in solution. Samples collected from surface springs may be deficient in these gases as a result of no hydrostatic head and, therefore, may contain higher proportions of deuterium.

Chemical Geothermometers

Chemical geothermometers were calculated for all thermal fluids in the Paradise Valley study area. Calculations were performed on data obtained from water analyses, and included three silica and one cation geothermometers. Results and equations used in the calculations are presented in Table C5.

Silica geothermometers (A, B, C) have calculated values comparable to measured temperatures of the thermal springs and wells. Thermodynamic calculations indicate that fluid samples 1, 8, 4, and 5 are slightly saturated with respect to quartz, and samples 3, 13 and 15 are slightly saturated with respect to chalcedony. These phase relationships should be considered for determining the validity of the calculations, and also for limiting the selection of values. Historical analytical data for silica values from thermal water samples 8 and 4 indicate that present analyses are low by a factor of 2. A temperature estimate of 120° to 125°C results from recalculating the geothermometers on the basis of these data.

Cation geothermometers (column D) for samples 1, 8 and 13 are in agreement with geothermometers calculated from historical silica values. For samples from the Golconda area (samples 3, 4, 5, 12, and 15) a value of 200°C seems high, considering that measured temperatures are less than 75°C. Since these fluids have high magnesium values, a correction factor (Fournier and Potter, 1979) was calculated and new values are presented in column E. These values are still high compared to silica geothermometers from present analyses, but are comparable to values obtained using historical silica values.

Based on combined data sets for chemical geothermometers, the highest expected temperatures for thermal fluids in Paradise Valley area range from 95° to 125°C. Temperature gradients in the vicinity of The Hot Springs suggest that these fluids exist only at depths of .5 to 1 km beneath the valley.

Table C5 Chemical geothermometers for fluids from the Paradise Valley study area.

Sample Name	Sample Number	T°C	A*	B	C	D	E**
Segerstrom Well #1	12	67	81	85	50	199	94
Day Warm Springs	13	36	55	62	23	154	59
Segerstrom Well #2	15	42	66	72	35	200	80
The Hot Spring	8	56	71	75	39	146	56
Artesian Well	1	68	70	75	38	162	67
Golconda Hot Spring	3	42	63	69	31	202	87
Segerstrom Spring #5	4	61	78	82	47	200	85
Segerstrom Spring #1	5	71	82	86	51	200	90

*Equations for calculating chemical geothermometers

A. [1]Quartz-no steam loss $T^{\circ}C = \frac{1309}{5.19 - \log SiO_2} - 273.15$

B. Quartz-maximum steam loss $T^{\circ}C = \frac{1522}{5.75 - \log SiO_2} - 273.15$

C. Chalcedony $T^{\circ}C = \frac{1032}{4.69 - \log SiO_2} - 273.15$

D. Na-K-Ca

$$T^{\circ}C = \frac{1647}{\log (Na/K) + \beta \left[\log (\sqrt{Ca}/Na + 2.06\right] + 2.47} - 273.15$$

$t < 100^{\circ}C, \beta = 4/3 \quad t > 100^{\circ}C, \beta = 1/3$

**Magnesium corrected Na-K-Ca geothermometers; from Fournier and Potter (1979).

1. In Geothermal Systems: Principals and Case Histories; ed. by L. Rybach and L. P. Muffler, 1980, J. Wiley and Sons, p. 109-143.

Mixing Model

A simple mixing model is proposed for thermal and non-thermal fluids in the Golconda area based on chemical and isotopic relationships. The model assumes mixing of two dilute fluids in an inert, near-surface environment. The model also assumes that precipitation of dissolved species as a result of mixing is negligible.

The model is based on the assumption that Golconda thermal waters (numbers 3, 4, 5, 12, and 15) represent fluids derived by mixing thermal fluids (comparable in composition to sample 1) with non-thermal fluids (comparable to sample 18). Chemical data (fig. C13) indicate that Golconda thermal fluid compositions are intermediate when compared to samples 1 and 18. Spatial relationships among the three groups of samples suggest that the Golconda samples may be derived by a respective mixing ratio of 2:1 for thermal and non-thermal fluids. Isotopic data (fig. C16) support a 2:1 thermal to non-thermal fluid mixing ratio for some Golconda samples.

This assumption was tested by generating a hypothetical fluid consisting of 65 percent thermal fluid (composition of sample 1) with 35 percent non-thermal fluid (composition of sample 18). Calculation results are presented in Table C6.

Mixing model results are also graphically illustrated in Figure C17. Based on an assigned mixing ratio of 2:1, model data match analytical data reasonably well with the exception of Na and HCO_3. This may be explained by chemical precipitation of $NaHCO_3$ upon mixing the two fluids which was first thought to be negligible in the model. Soils surrounding Golconda Hot Springs contain massive amounts of a white crystalline substance presumed to be calcium carbonate. Based on these calculations it is reasonable to assume that this substance is largely sodium bicarbonate. The mechanism of deposition for sodium bicarbonate has not yet been established.

Table C6. Chemical compositions of fluids used in mixing model.

Dissolved Species (ppm)	Fluid Samples 1	18	3	Model Fluid
Ca	26	57.4	42.7	37
Mg	7.76	16.6	9.75	11
K	23	8	26	23
Na	431	70	151	330
Sr	1.33	.382	.79	.99
Li	.77	.06	.5	.52
Cl	14	3.44	24.4	10.3
SO_4	68.2	50.8	54.2	62.1
HCO_3	1170	312.3	521	869
F	3.2	.028	2.47	2.09
SiO_2	23.9	22.6	20	23.4
B	1.42	.14	1.5	.96

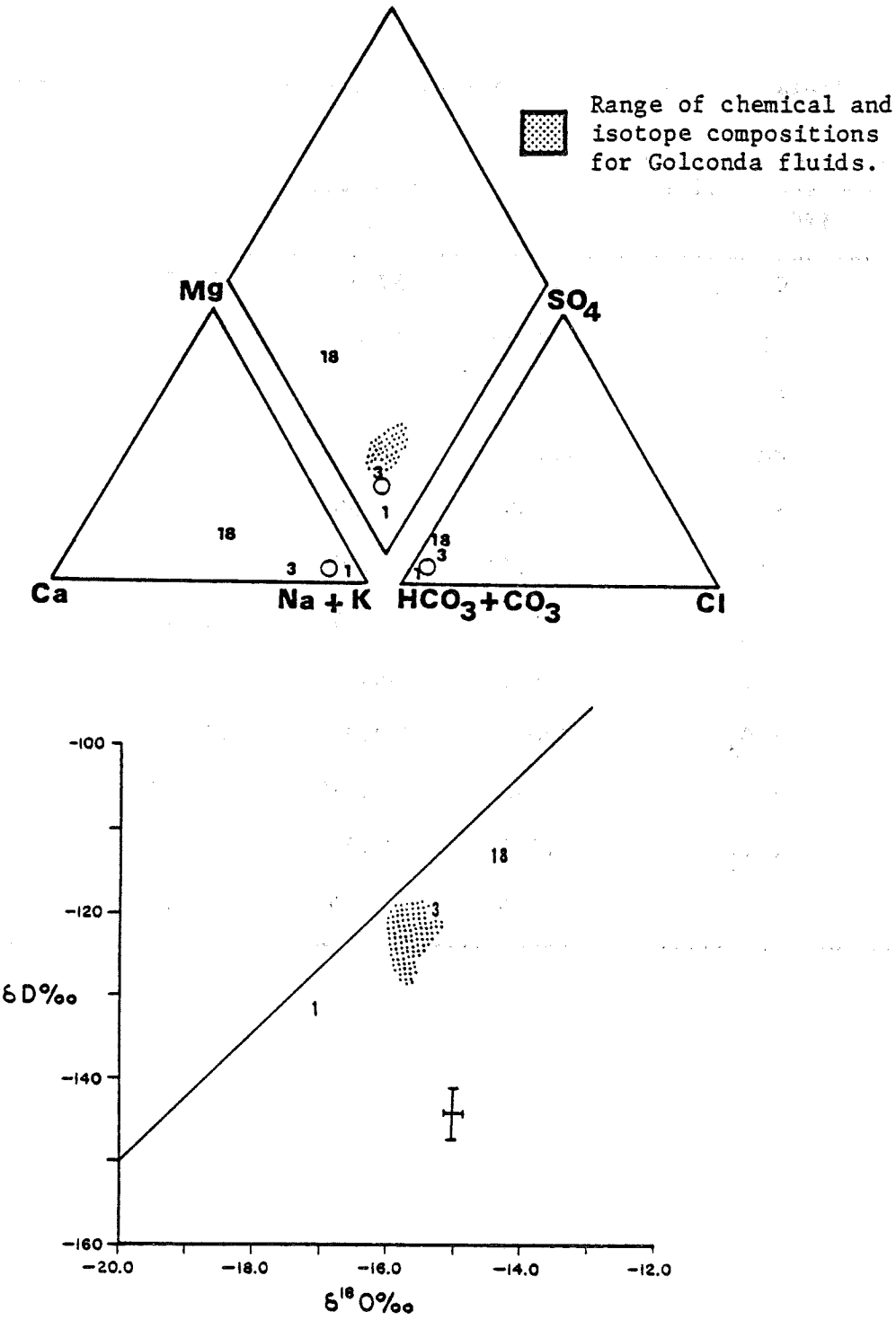

Figure C17. Chemical and isotopic compositions of mixing-model fluid relative to source fluids.

SOIL-MERCURY SURVEY

Approximately 160 soil samples were collected throughout the study area and analyzed for mercury on a gold-film apparatus. Samples were collected at a depth of 25 to 30 cm below the surface, and soil characteristics were recorded at the time of collection.

Sampling strategy consisted of examining both regional and specific site trends in soil-mercury values. Figure C18 illustrates sites sampled in the regional study, and outlines areas selected for specific site studies. Table C7 lists samples and associated values, and gives a brief soil description. Values of mercury in the soil samples range from 0 to 4700 ppb, with an estimated combined operator-apparatus error of 15 percent. A preliminary statistical survey indicated no difference in mercury content among the three major soil types: sand, silt and clay.

In order to identify true soil-mercury anomalies, two important criteria must be established: background values to which anomalous values may be compared, and level of mercury contamination from sources other than geothermal.

Establishing a valid background value for mercury in soil is accomplished using statistical methods for large, uniformly distributed samples. Figure C19 is a histogram plotting frequency of occurrence against mercury content. The diagram shows 76 samples falling in the range 10 to 20 ppb. Frequency drops off quickly on either side of this range. This diagram does not, however, establish background levels. It merely illustrates total range of values and frequency of occurrence within selected limits. Unfortunately, there is no clear-cut boundary between "background" and "anomalous" values. Furthermore, the "background" value is probably a range of values. Therefore, a value of 18 was arbitrarily assigned as the mean background value. In addition, a value three times the mean background value of 18 was established to account for the

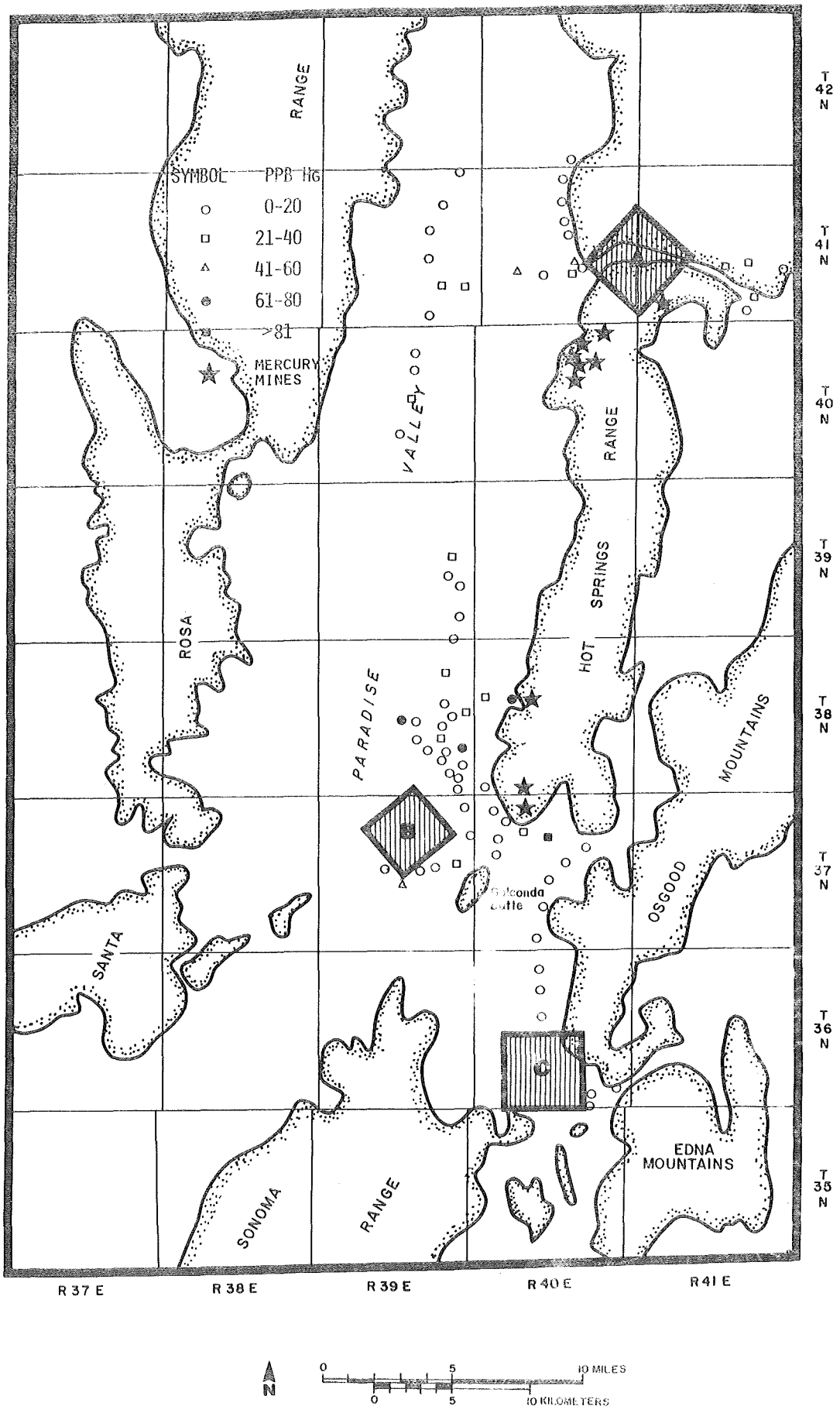

Figure C18. Sample sites for soil-mercury survey showing location of areas sampled near hot springs and location of mercury mining districts.

Table C7. Soil-mercury analyses from the Paradise Valley study area.

Sample No.	Composition of soil	Mercury content (ppb)
G-1	dry fine silt	4.5
G-2	moist clay	24.5
G-3	dry silt	22.8
G-4	dry silt	22.0
G-5	dry silt	23.2
G-6	dry silt	32.9
G-7	dry silt	34.0
G-8	fine moist silt	16.7
G-9	fine moist silt	25.2
G-10	fine dry silt	48.1
G-11	moist clay	24.4
G-12	moist silty clay	6.6
G-13	hard moist clay	50.6
G-14	very hard moist clay	34.4
G-15	dry loose fine silt	24.1
G-16	dry loose silt	17.6
G-17	dry loose silt	13.0
G-18	hard dry clay	19.0
G-19	loose silt	20.1
G-20	dry loose sandy silt	8.0
G-21	loose sandy silt and pebbles	80.3
G-22	dry loose fine silt	34.4
G-23	dry loose fine sandy silt	22.6
G-24	dry loose fine sandy silt	17.1
G-25	dry loose fine silt	15.3
G-26	dry loose fine silt	21.1
G-27	dry loose fine silt	12.5
G-28	hard moist silty clay	14.3
G-29	hard moist silty clay	13.7
G-30	hard moist silty clay	11.7
G-31	hard moist clay	27.4
G-32	dry loose fine silt	15.7
G-33	hard moist clay with pebbles	12.5
G-34	hard moist clay	101.0
G-35	hard dry silty clay	56.0
G-36	loose moist sand with pebbles	16.7
G-37	loose dry silty sand	12.2
G-38	loose dry sand	16.4
G-39	loose dry sand	15.0
G-40	loose dry sandy silt	14.7
G-41	loose dry sand	17.2
G-42	hard moist sandy clay	14.6
G-43	loose dry sand	15.1
G-44	loose dry sandy silt	14.4
G-45	hard dry sandy silt	214
G-46	hard dry sandy silt and clay	21.8
G-47	loose dry sandy silt	18.6
G-48	hard dry sandy silt	15.7
G-49	hard dry sandy silt	8.6
G-50	hard dry sandy silt	12.5
G-51	soft moist clay	17.2
G-52	hard moist clay	2200.0
G-53	moist clay	17.0

Table C7. (Cont.)

Sample No.	Composition of soil	Mercury content (ppb)
G-54	dry silt	20.7
G-55	moist clay	25.8
G-56	dry silt	1100.0
G-57	dry coarse sand and silt	28.3
G-58	hard moist clay	25.8
G-59	hard dry silt	38.6
G-60	hard dry silt with pebbles	19.2
G-61	hard dry silt with pebbles	17.8
G-62	dry silt clay	11.0
G-63	hard dry silt with pebbles	16.3
G-64	hard dry silt	15.4
G-65	soft dry silt	16.5
G-66	hard dry wilt with pebbles	15.0
G-67	hard dry silt with pebbles	11.4
G-68	soft dry silt with pebbles	15.3
G-69	hard sandy silt with pebbles	11.9
G-70	fine dry sand	9.8
G-71	soft dry silt	19.0
G-72	soft dry silt	13.9
G-73	soft dry silt	13.9
G-74	soft dry silt	13.9
G-75	soft dry silt	12.5
G-76	soft dry silt	15.9
G-77	hard clay with pebbles	11.9
G-78	hard clay with pebbles	11.4
G-79	soft silty clay	16.0
G-80	soft moist clay	3.0
G-81	hard dry silt with pebbles	17.4
G-82	soft dry silt	12.1
G-83	soft dry silt	22.6
G-84	soft dry silt	12.2
G-85	soft dry silt	9.7
G-86	hard moist silty clay	0.0
G-87	hard dry silt	29.1
G-88	dry sand	14.3
G-89	dry sand	17.6
G-90	sandy silt	11.0
G-91	hard dry sandy silt	43.3
G-92	hard dry sandy silt	16.2
G-93	dry sand	12.5
G-94	dry sand	24.5
G-95	dry sand/silt	14
G-96	moist silty sand	12.3
G-97	hard dry silt	9.7
G-98	hard dry silty clay	47.7
G-99	moist silt	31.0
G-100	moist silt	20.0
G-101	moist clay	39.0
G-102	soft moist silt	18.0
G-103	soft moist silt	37.0
G-104	dry silt	13.0
G-105	sample lost	
G-106	hard dry sandy clay	30.0

Table C7. (Cont.)

Sample No.	Composition	Mercury content (ppb)
G-107	moist sand	0.0
G-108	moist sand	11.0
G-109	moist sandy clay	0.0
G-110	moist sandy clay	43.0
G-111	hard dry silt	19.0
G-112	sample lost	
G-113	moist silty sand	0.0
G-114	hard moist silty sand	13.0
G-115	hard moist sandy silt	15.0
G-116	hard moist clay	22.0
G-117	moist sandy clay	19.0
G-118	hard sandy clay	89.0
G-119	dry sandy silt	25.0
G-120	dry sandy silt	11.0
G-121	dry silt with pebbles	25.0
G-122	dry silt with pebbles	18.0
G-123	hard dry silty clay	55.0
G-124	hard dry silty clay	212.0
G-125	soft dry silt with pebbles	99.0
G-126	soft moist silty clay	1700.0
G-127	hard dry silty clay	206.0
G-128	soft dry silty clay	38.0
G-129	soft dry silty clay	99.0
G-130	soft dry silt	53.0
G-131	dry silt	63.0
G-132	dry silty clay	17.0
G-133	moist clay	13.0
G-134	moist silty clay	20.0
G-135	dry silt	17.0
G-136	dry silt	17.0
G-137	dry silty sand	8.0
G-138	dry silty clay	15.0
G-139	dry silt	12.0
G-140	moist sand	12.0
G-141	dry silt	23.0
G-142	dry silt	18.0
G-143	dry silt	67.0
G-144	moist silty clay	20.0
G-145	dry silt	13.0
G-146	red clay	0.0
G-147	black sand	85.0
G-148	moist clay	16.0
G-140	moist clay	37.0
G-150	dry silty clay	200.0
G-151	dry silty clay	540.0
G-152	moist clay	4693.0
G-153	dry silt	107.0
G-154	sandy clay	234.0
G-155	moist clay	43.0
G-156	moist clay	795.0
G-157	hard silty clay	313.0
G-158	black sand	58.0
G-159	moist clay	120.0

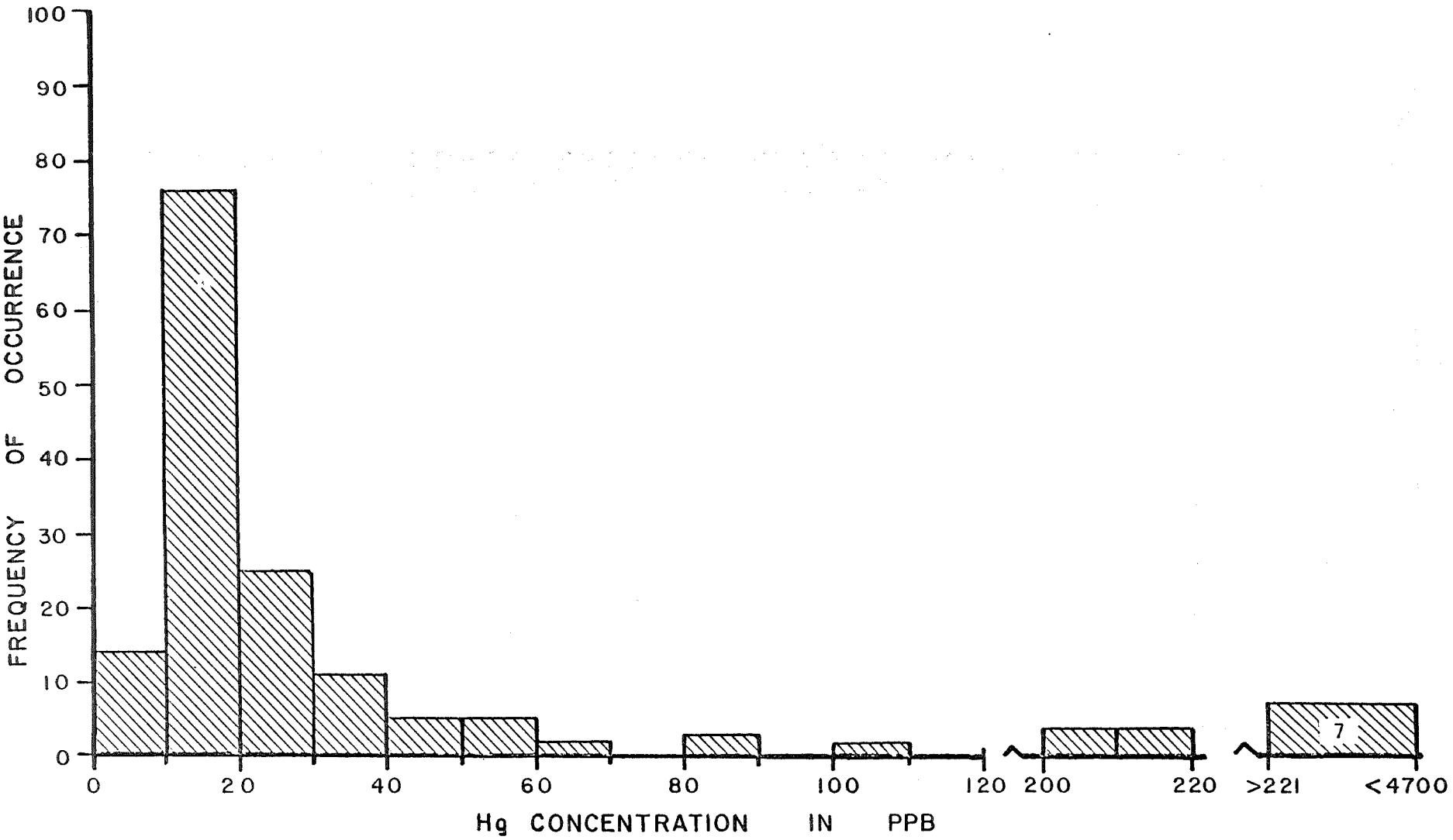

Figure C19. Histogram showing frequency of occurrence for soil-mercury samples.

probable range of background values as well as errors involved in analysis. Therefore, only those values greater than 54 ppb are considered anomalous.

The second criteria is much easier to address. Several possible sources of detrital mercury contamination include nearby mercury sulfide deposits or mercury mining activities, milling activities using mercury amalgamation processes, detonation and explosive devices using mercury fulminate, and agricultural insecticides or fertilizers containing trace amounts of mercury compounds. Of these four sources of contamination, only the first is a likely source in Paradise Valley.

Figure C18 shows locations of several mercury mines in Paradise Valley. All areas containing anomalous soil-mercury values are also co-located with mercury mines. The source of mercury in the soil samples is probably detrital mercury carried downslope during heavy runoff. The area may be further contaminated by wind-transported and river-transported mercury-rich particles.

Three areas containing thermal fluids were selected for intense Hg soil surveys to establish possible trends in the immediate vicinity of the hot springs. Values for the samples are shown in open circles on aerial photographs of the area.

Figure C20 shows distribution of samples around The Hot Spring at the north end of Paradise Valley. All but two samples have values that are considered background. The two exceptions were collected along a highly mineralized fault zone. Figure C18 also indicates that mercury mining was active at one time in this area. These extremely high mercury values are, therefore, considered detrital and not an indication of mercury deposition from recent geothermal activity.

The second area (fig. C21) shows soil-mercury distribution near the artesian hot well. Many of these values are very low, probably due to the sand dune field which has buried clay-rich layers that trap rising mercury

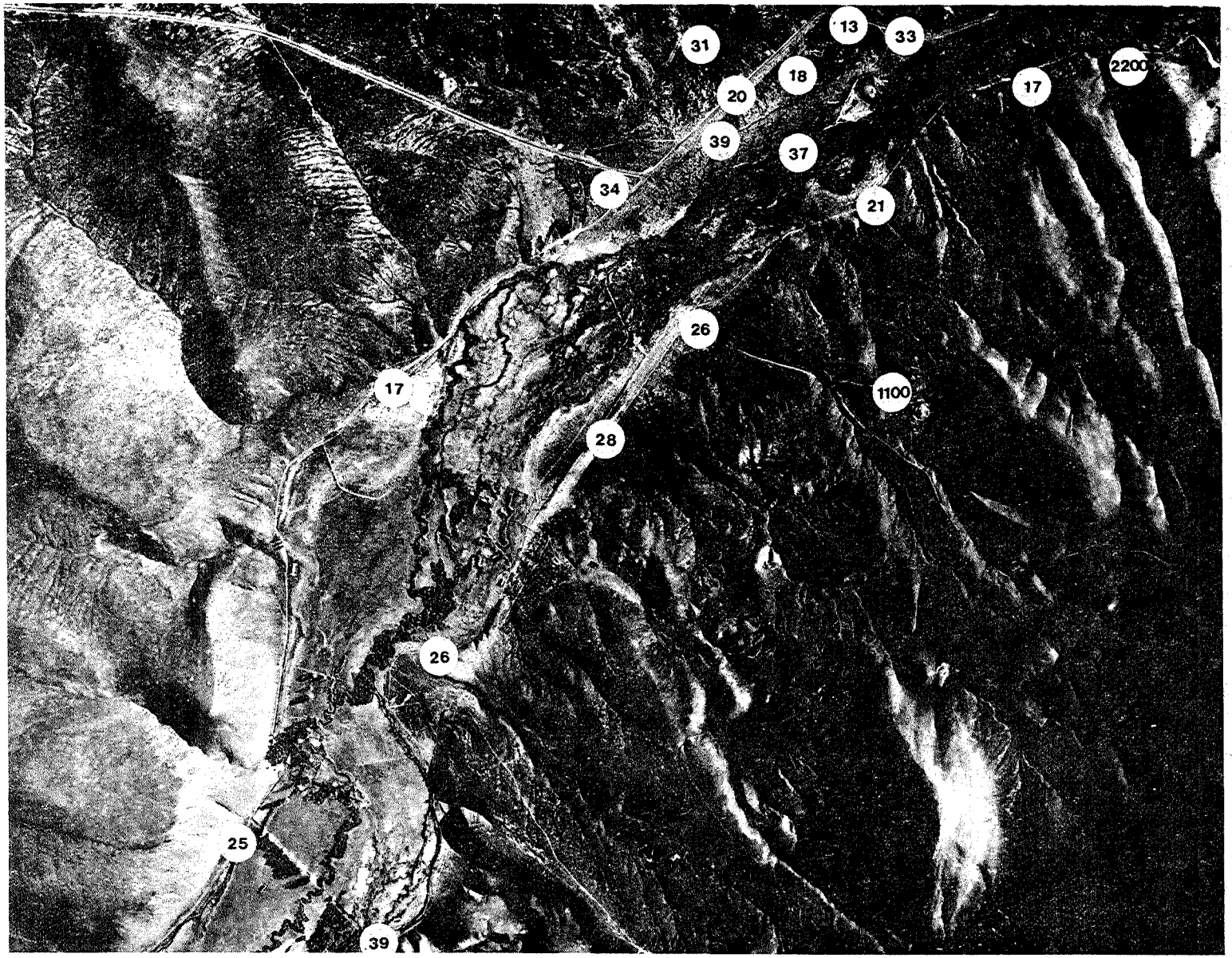

Figure C20. Distribution of mercury (ppb) in soil samples near The Hot Spring; A in figure C18, scale 1:24,000.

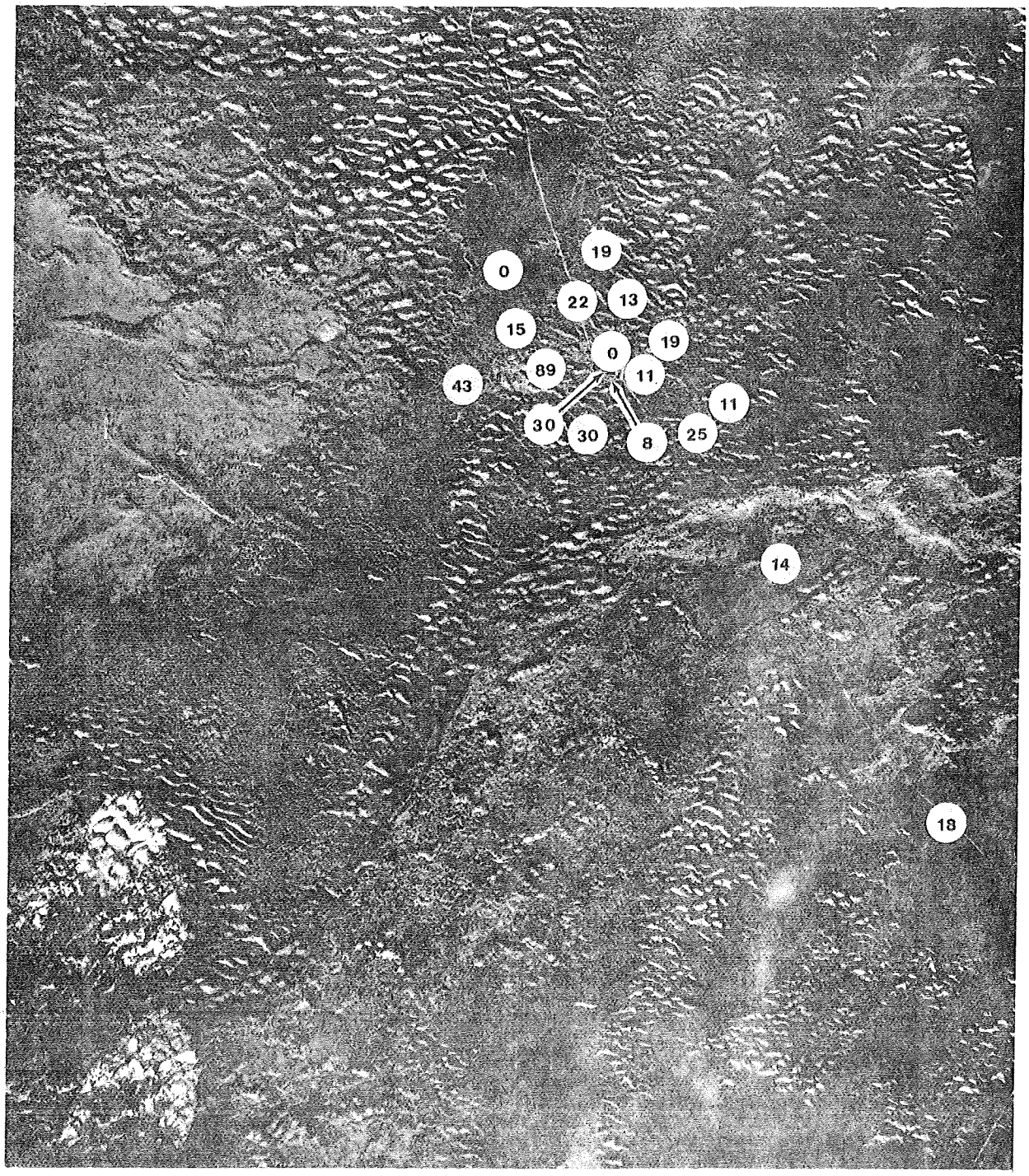

Figure C21. Distribution of mercury (ppb) in soil samples near the artesian hot well; B in figure C18, scale 1:24,000.

vapors. Only one sample is considered anomalous, and no definite trend could be identified in the data.

The final area (fig. C22) illustrates soil-mercury distribution around the town of Golconda. The area outlined in white delineates anomalous soil-mercury values co-located with Segerstrom's Hot Springs. This was also the site of an ore-processing plant, but soil sampled at the plant site is lower in mercury than soil sampled north of the site. Two piles of partially processed tungsten ore occur at the southern end of the outlined area, but neither could account for extremely high values near the center of the area. It is reasonable to assume that this area of anomalous soil-mercury values was produced by condensation of mercury-rich vapors in well-developed soils.

In general, the soil-mercury survey was not very effective in Paradise Valley because of widespread mercury mines and associated contamination. The area around Segerstrom's Hot Springs in Golconda was well-defined by anomalous values. This indicates that the technique can produce legitimate results under the right conditions.

TWO-METER TEMPERATURE PROBE SURVEY

During September, October and November 1980, 50 temperature probes were implanted to a depth of two meters throughout the study area. Figure C23 shows the location of the probe sites and delineates the areas around the hot springs that were surveyed more intensely. Table C8 lists temperature, location and date of reading for all probes.

The survey was planned to include both regional and site-specific temperature distribution analysis. However, failure of rented equipment on three different occasions limited the extent of the regional survey.

In general, the probes were spaced at .5 to 1.5 km (.25-1.0 mi) intervals,

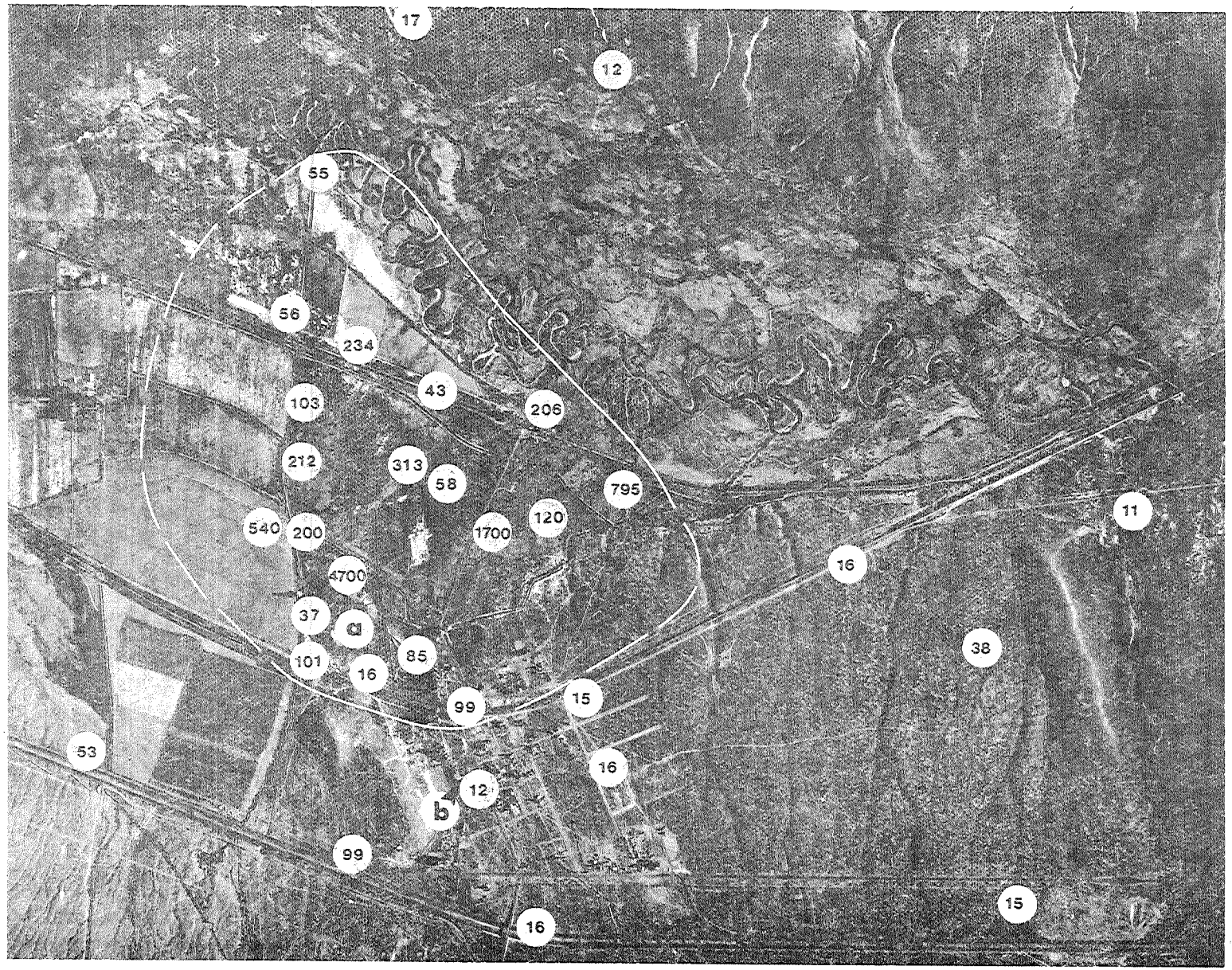

Figure C22. Distribution of mercury (ppb) in soil samples at Golconda (C in figure C18), scale 1:24,000.

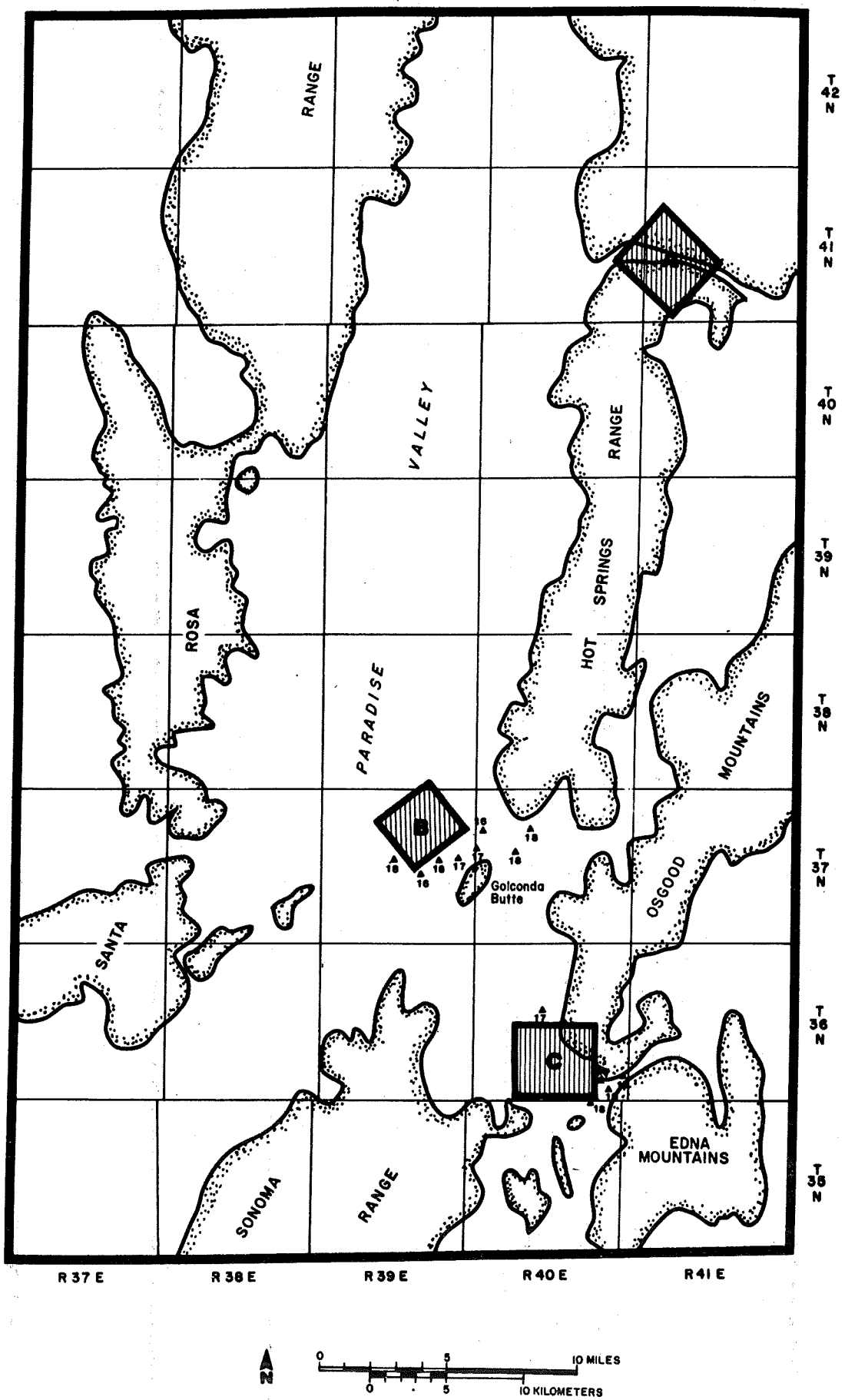

Figure C23. Two-meter depth temperature probe survey sites ($T^{o}C$).

Table C8. Measured temperatures for 2 m depth probes.

Probe No.	Location	Date of Reading	Temperature °C
1	36/40/29 dc	9/18/80	27.
2	36/40/29 aa	9/18/80	17.4
3	36/40 21 ac	9/18/80	19.0
4	36/40 36 ba	9/18/80	19.2
5	36/40 35 db	9/18/80	18.8
6	36/40 34 ad	9/18/80	15.9
7	37/39 3 dc	9/20/80	30.5
8	41/41 19 aa	9/20/80	24.1
9	41/41 19 ad	9/20/80	16.8
10	41/41 20 cd	9/20/80	17.2
11	41/41 18 dd	9/20/80	17.1
12	41/41 18 cd	9/20/80	14.3
13	41/41 13 dc	9/20/80	17.3
14	37/39 3 da	9/20/80	16.5
9A	41/41 19 ad	10/10/80	16.5
15	41/41 20 db	10/10/80	17.1
16	41/41 20 cb	10/10/80	15.4
17	41/41 19 ad	10/10/80	17.3
18	41/41 19 bc	10/10/80	13.5
19	41/40 24 cb	10/10/80	15.5
20	37/39 3 dc	10/10/80	30.2
21	37/39 10 ac	10/10/80	18.6
22	39/39 15 bb	10/10/80	17.7
23	37/39 22 bc	10/10/80	16.5
24	37/39 16 cc	10/10/80	17.6
25	37/39 14 ca	10/10/80	16.7
26	37/39 15 dd	10/10/80	16.5
27	37/39 13 bd	10/10/80	17.4
28	37/39 12 db	10/10/80	16.3
29	37/40 18 ab	10/10/80	18.2
30	37/40 8 cb	10/10/80	17.5
31	36/40 29 ca	10/10/80	16.3
32	35/40 3 ad	10/10/80	17.6
33	35/40 3 bb	10/10/80	17.4
34	36/40 33 bc	10/10/80	17.8
35	36/40 33 ad	10/10/80	17.6
36	36/40 17 ad	10/10/80	17.0
37	41/40 19 ac	11/20/80	11.9
38	41/40 19 ba	11/20/80	13.4
39	41/40 19 aa	11/20/80	13.0
40	41/40 19 ab	11/20/80	13.5
41	41/40 18 dc	11/20/80	13.2
42	41/40 17 dd	11/20/80	16.0
43	37/39 3 cd	11/21/80	29.6
44	37/39 3 dc	11/21/80	17.3
45	37/39 3 ca	11/21/80	30.3
46	37/39 3 bd	11/21/80	21.1
47	38/39 35 cc	11/21/80	13.1
48	37/39 10 ab	11/21/80	16.2
49	37/39 10 ba	11/21/80	18.1
50	37/39 3 dd	11/21/80	14.9

and were allowed two to three days to equilibrate before they were removed. In order to determine the time required for the probes to equilibrate, several readings on different probes were taken over a period of time. Figure C24 shows that all probes reached equilibration within 24 hours of burial.

In the Paradise Valley area, the annual temperature wave can produce a fluctuation of 8 to 10 centigrade degrees at a depth of two meters. This value is estimated from groundwater temperatures over a one-year period and probably accounts for lower temperatures recorded in November (table C8).

Regional data show that background temperatures range from 12 to 19°C, depending on time of year. Temperatures were generally 1 to 2°C warmer in areas where depth to bedrock was shallow. This is probably because such areas contain less pore water which, upon evaporation, produces a significant loss of heat. In areas adjacent to surface water such as the Humboldt or Little Humboldt Rivers, the effects of large volumes of groundwater and surface water of uniform temperature possibly masked any measurable lateral variation in temperature produced by geothermal fluids.

All site-specific surveys conducted near The Hot Spring show that near-surface temperatures drop off rapidly in all directions away from surface thermal fluids. At The Hot Spring (fig. C25), the highest recorded temperature was 24°C. This probe was located approximately 100 m (300 ft) east of The Hot Spring. Temperatures recorded in the Little Humboldt River floodplain were significantly influenced by the shallow groundwater, and show lower temperatures than those recorded near the range front.

Figure C26 also shows a rapid decrease in measured temperatures away from the artesian hot well. A temperature of 21°C was recorded approximately 300m (1000 ft) west of the spring. This is probably due to subsurface flow of thermal fluids down the topographic and hydraulic gradient. This

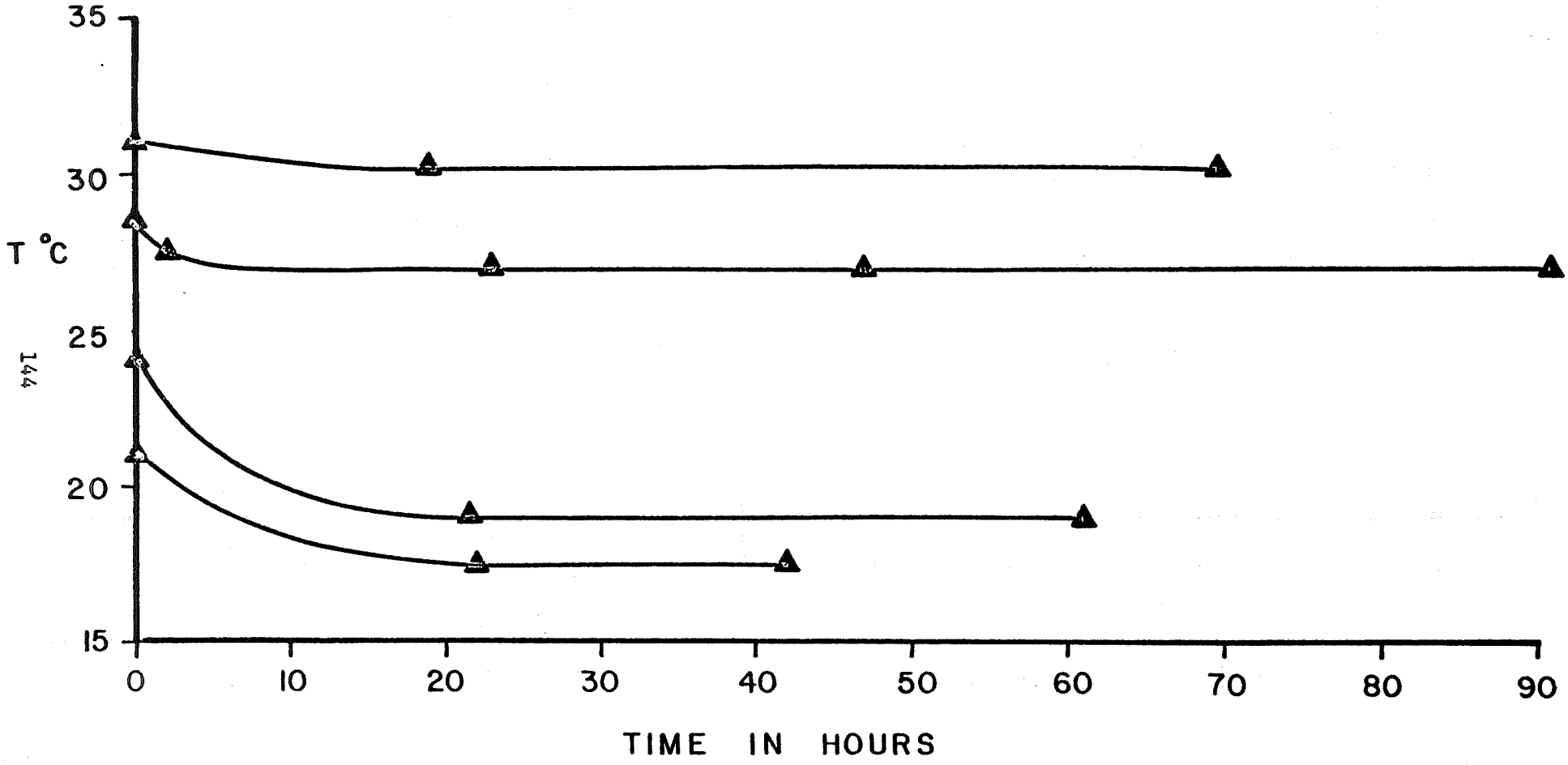

Figure C24. Equilibrium curves for selected two-meter depth temperature probes.

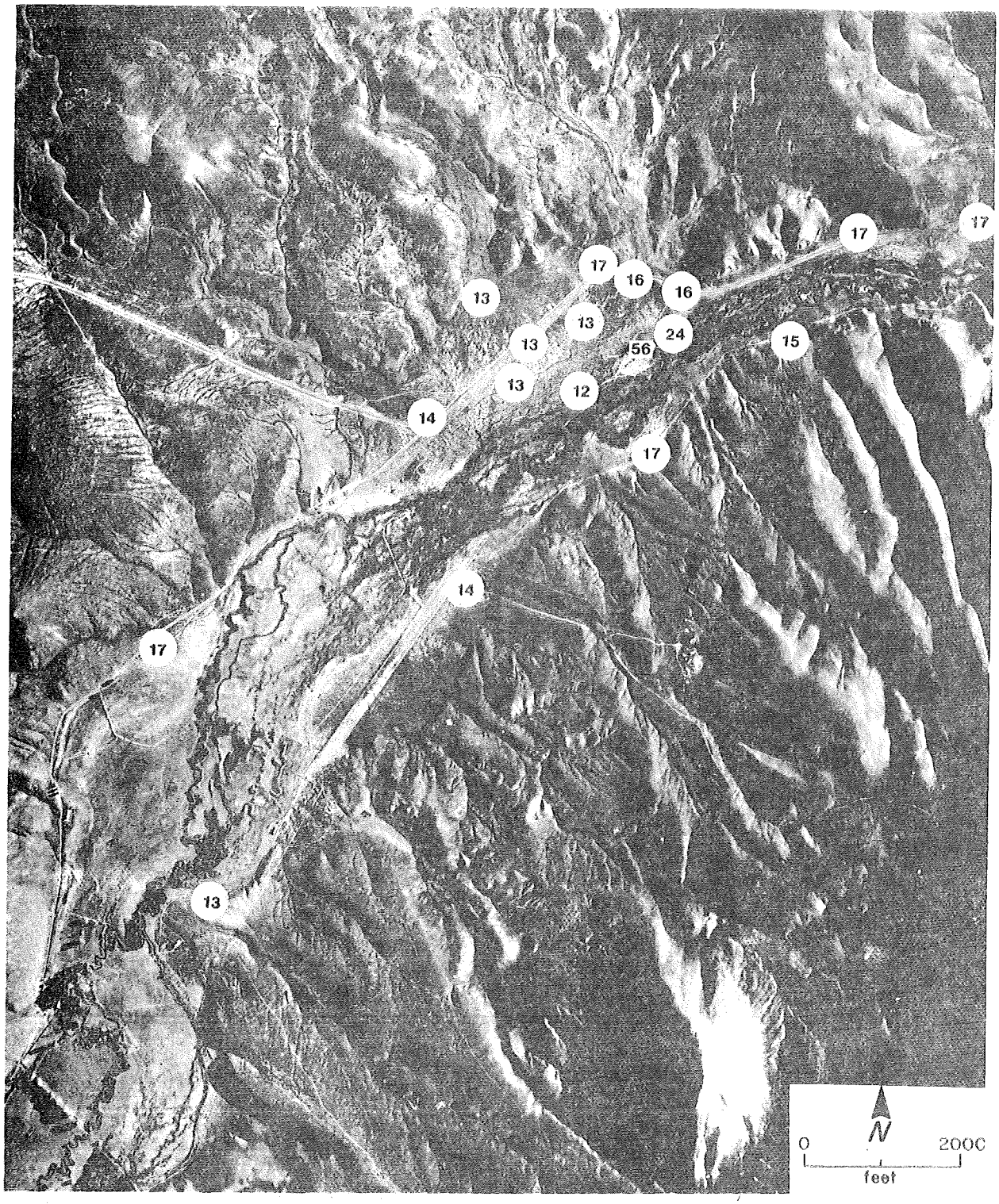

Figure C25. Two-meter depth temperature probe survey results at The Hot Spring (rectangle); A in figure C23, T°C, scale 1:24,000.

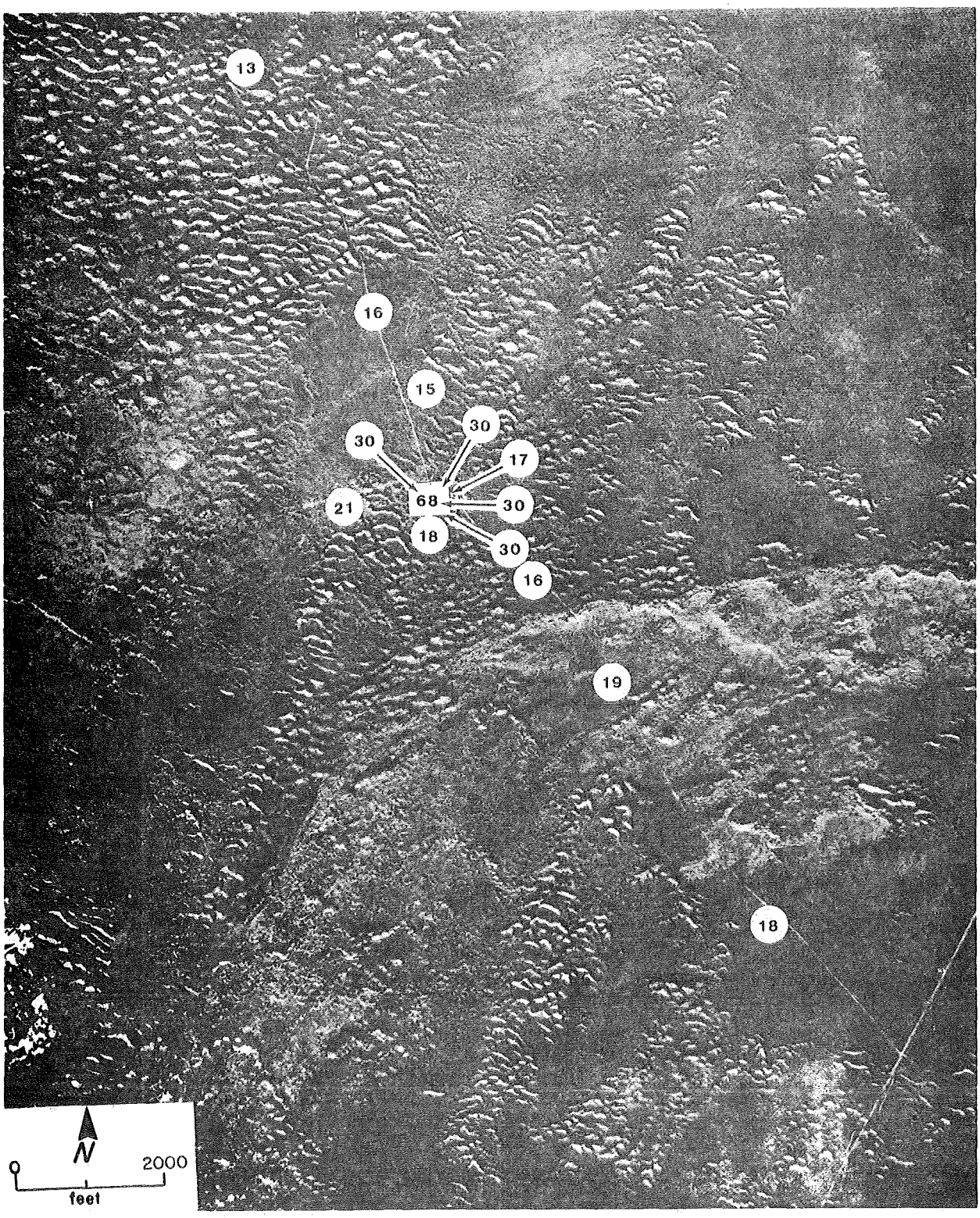

Figure C26. Two-meter depth temperature probe survey results at artesian hot well (rectangle); B in figure C23, T°C, scale 1:24,000.

flow was probably confined to a small restricted zone. A clay-rich layer was encountered in many drill holes at a depth of 1.5 m.

Significant drilling difficulties hampered the survey in the final area (fig. C27). The entire area is underlain by a layer of coarse gravel which could not be penetrated with available drilling equipment. Data show a rapid temperature decrease in all directions away from thermal fluids.

Data from the two-meter temperature probe holes indicate that thermal fluids are not being transported to the surface along recent faults. Since few recent faults are exposed in this area, it is postulated that the fluids are being directed to the surface in narrow pipes. These pipes which appear at the surface as tuffa mounds result from self-sealing chemical precipitation in a seismically quiet area. All springs show evidence of tuffa mounds; it is likely that these narrow pipes extend to great depth and limit the lateral extent of thermal fluids. Data from a seismic survey conducted in this area (Dudley and McGinnis, 1964) suggest that a vertical zone of sediments cemented by hydrothermal material ($CaCO_3$) is enclosed in sediments of lower seismic velocity. Below the pipe structure, fluids probably migrate up faults or sedimentary contacts in lower Paleozoic rocks. Geologic cross-sections of the Santa Rosa Range (Compton, 1960) and the Osgood Mountains and Hot Springs Range (Hotz and Willden, 1964) show that Paleozoic and lower Mesozoic sedimentary rocks were tilted so that bedding planes are nearly vertical.

DRILL SITE SELECTION

Six tentative drill sites were selected on the basis of data analysis and accessibility of the sites. Also, an attempt was made to locate well sites in areas where little subsurface data were available.

Drill site selection depended heavily on three data sets: gravity survey,

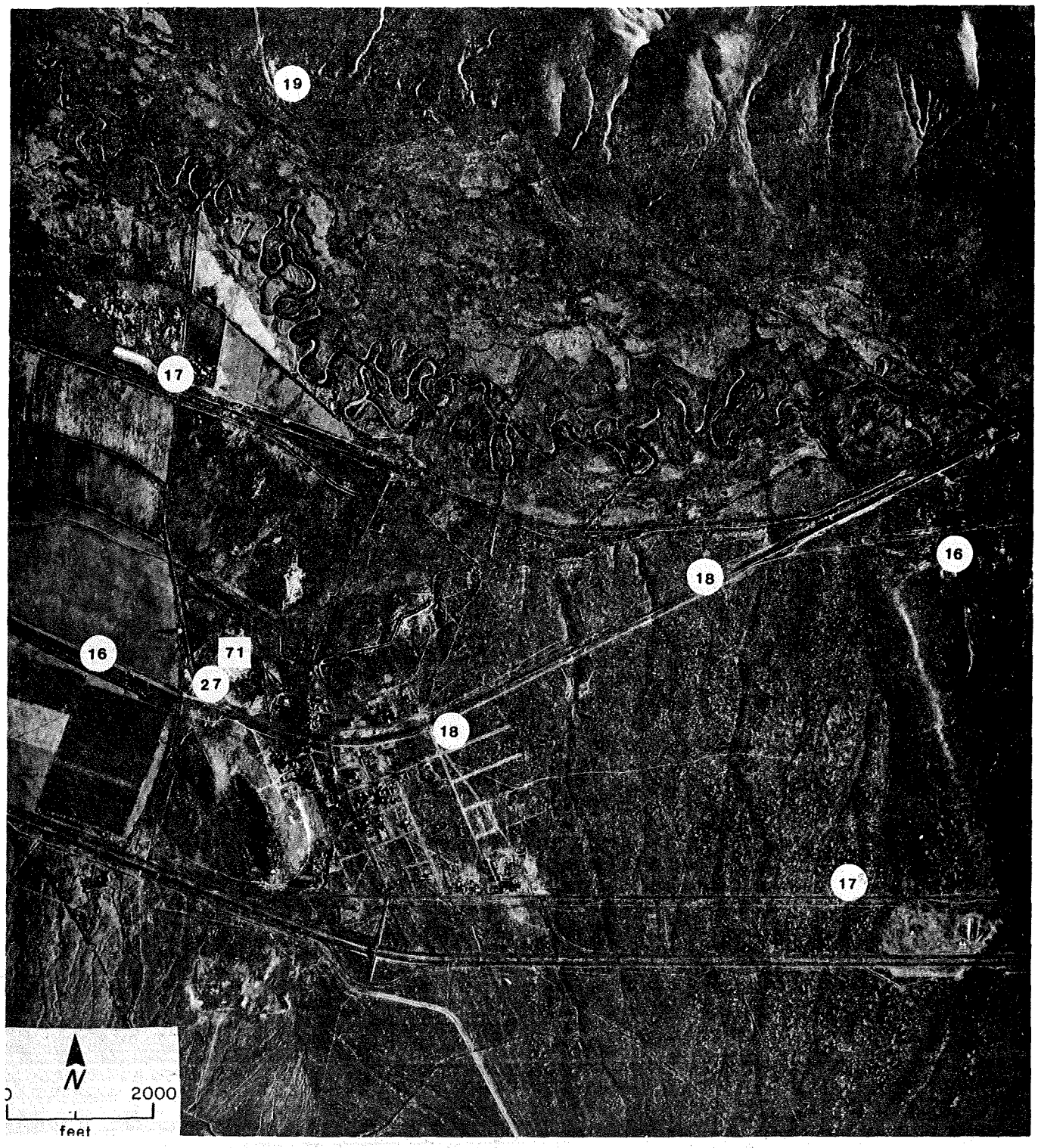

Figure C27. Two-meter depth temperature probe survey results at Golconda (rectangle is Segerstrom's Hot Springs); C in figure C23, T°C, scale 1:24,000.

existing water wells, and air photos and imagery. Data derived from fluid chemistry, soil-mercury or two-meter depth temperature probe surveys were not considered useful in drill site selection. The drill sites were also located on private land in order to expedite drilling and ensure completion within the contract time-frame.

The three selected drill sites (fig. C28) are located on the east side of the study area. Land owner, Nevada First Corporation, was extremely co-operative and helpful throughout the study and granted permission to drill at these sites. An alternate site was also selected in case drilling difficulties precluded completion of the task at the three primary sites. All three sites are co-located with steep gradients in the gravity contours interpreted as normal faults. Limited water-well data were available in these areas, however, geologic and air photo data suggest that these sites are located near faults.

Test Hole Drilling

Drilling in the Golconda area began April 3, 1981 at GDS-1 (fig. C28). The contractor, Aqua Drilling, utilized an Ingersal-Rand rotary air drill rig, 5 in. od. drill pipe in 20 ft sections, and a 6 5/8 in. tri-cone bit. A 10 ft section of 8 in. od. conductor casing was installed and the hole was drilled with air until the water table was encountered. At this point, mud was used to lift drill chips out of the hole and to reduce caving. Drilling was completed April 6, 1981 and the hole was cased with 2 in id. schedule 40 PVC pipe to a depth of 113 m (372 ft). The pipe was fitted with screw-type connections and left open at the bottom. For this hole it was necessary to "jet" the casing into the hole with mud because of caving in the drill hole.

Drill hole GDS-2 was started on April 6, 1981 and was completed April 7,

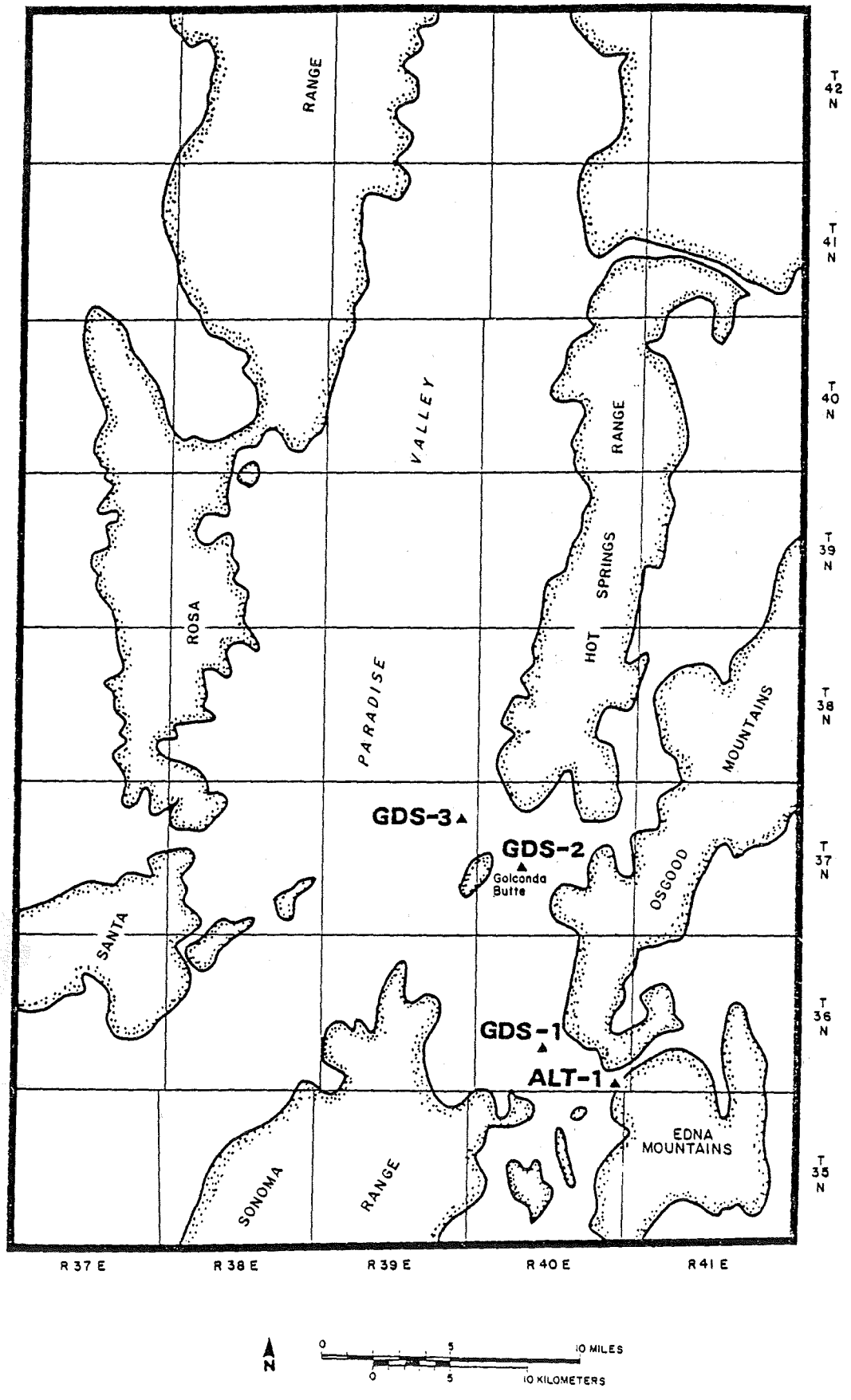

Figure C28. Location of primary and alternate drill sites.

1981. GDS-3 was started and completed April 8, 1981. Both holes were drilled with mud in a portable mud pit, and both were cased with 2 in PVC pipe closed at the bottom. PVC pipe was then filled with water and capped. All casing was cut off below ground level and buried in small vaults to prevent vandalism.

During drilling, chip samples were collected and described at 10 ft. intervals. These samples were next examined with a binocular microscope, and lithologic logs were completed for each hole (fig. C29, C30, and C31).

Completed lithologic logs indicate that drilled strata consisted of interbedded alluvial, fluvial and lacustrine deposits with minor eolian deposits near the surface. There is no indication that bedrock was reached in any hole although sizable boulders were encountered. These logs are similar to logs for some deep wells drilled for irrigation in other parts of the valley.

During drilling, thermistor probes were installed in two locations to monitor mud temperature. One was placed at the annulus between the conductor casing and portable mud pit (for out-temperatures); the other was placed at the far end of the mud pit (for in-temperatures). The difference between these two values represents the amount of heat gained from friction and from any thermal fluids encountered in the drilling. Figure C32 shows the relationship between $\Delta T^{o}C$ (mud out_t - mud in_t) and the drilling depth. The figure does not reveal any significant increases in temperatures as drilling progressed.

Temperature Gradient Measurements

A temperature profile was completed on GDS-2, two days after completion of the well. This measurement was made to determine the amount of time required for the well to reach thermal equilibrium. Approximately one week after completion of GDS-3, all three holes were profiled and the results are shown in

Lithologic log for drill site 1, Golconda study area

Location: T36N, R40E, Sec. 21, SW/4 of the NE/4

Static water level: 30 ft.

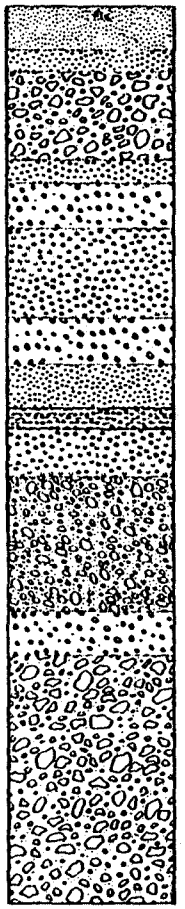

Sample interval (in feet below surface)	lithologic description
0 - 20	coarse, well rounded to angular sand with a matrix of wet clay
20 - 30	very coarse sand and fine gravel (1-2 mm) in a thick gray, water saturated clay matrix; approximately 50% matrix
30 - 70	rounded to angular gravels (1-20 mm) in a clay matrix; approximately 25% matrix, pebbles are mixture of volcanic and metamorphic rocks
70 - 80	clean, well sorted and well rounded to angular gravels (2-3 mm); no sand or clay
80 - 100	clean, well-sorted and well rounded to angular gravels (3-5 mm); no sand or clay
100 - 140	clean, well sorted and well-rounded gravels; some stones slightly angular, some clay in matrix (gravels range from 2 to 7 mm in some samples)
140 - 160	clean, well-sorted, rounded to angular gravels (2-7 mm); some sandy clay in matrix
160 - 180	well sorted, rounded to angular gravels (2-7 mm) with 25% sandy clay matrix
180 - 190	coarse sand and fine gravel (1-2 mm) in clay matrix; approximately 50% matrix.
190 - 210	rounded to angular gravels (2-5 mm) in sandy-clay matrix
210 - 270	clean, well sorted, rounded to angular gravels (2-4 mm) in a sparse matrix of sandy-clay
270 - 290	clean, rounded to angular gravels (2-7 mm) in a sparse sandy clay matrix
290 - 400	clean, rounded to, angular gravels in a sandy clay matrix (approximately 10% matrix); occasional pebble may be as large as 10 mm

Figure C29. Lithologic log for GDS-1.

Lithologic log for drill site 2, Golconda study area

Location: T37N, R40E Sec 20, SE/4 of the SE/4

Static water level: 100 ft.

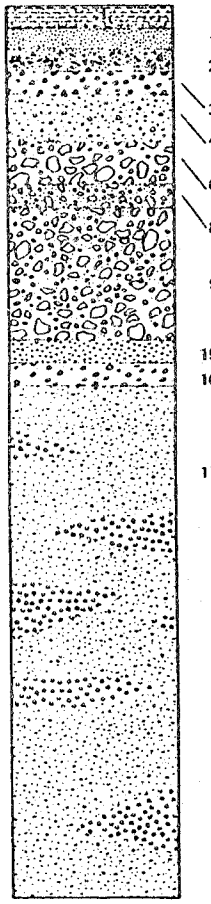

Sample interval (in feet below surface)	lithologic description
0 - 10	coarse most sandy clay with some mica flakes
10 - 20	dry, coarse and fine sands, some silt and clay
20 - 30	mostly coarse sand (70%), some fines, with gravel mixture (2 30 mm); sand and gravels are rounded to angular
30 - 40	rounded to angular gravels (2 - 20 mm) consisting of quartzite and volcanics; no sand or clay
40 - 60	well-rounded to angular gravels (2 - 10 mm); volcanics show red mineralization which may be either hematite or cinnabar; some clay and silt in the matrix
60 - 80	rounded to angular gravels (2 - 30 mm), sandy clay in matrix, volcanics continue to show red mineralization
80 - 90	clean, largely volcanic gravels (2 - 20 mm), rounded to angular with minor sand and clay in the matrix
90 - 150	clean, rounded to angular gravels (2 - 20 mm), minor sand and clay in the matrix, pebbles mostly volcanics and continue to show red mineralization, vesicular basalt and scoria common
150 - 160	coarse, rounded to well rounded sand in 10% clay matrix, minor pea gravel
160 - 170	clean well-rounded to angular gravels (2 - 20 mm) mostly volcanics with some quartzite and sandstone
170 - 400	clean, rounded to angular gravels (2 - 5 mm) with minor sand and clay; pebbles are both volcanics and quartzite

Figure C30. Lithologic log for GDS-2.

Figure C33. Solid triangles represent the preliminary profile for GDS-2.

Gradients for all three wells have similar slopes. The highest temperatures range from 19 to 21°C. Although these temperatures are technically "thermal" (T>20°C), they represent the normal geothermal gradient in the Basin and Range province (30 to 35°C/km). Temperatures obtained for both profiles in GDS-2 are within 2°C of one another indicating that thermal equilibrium is quickly attained.

Profiles near the top of the wells show relatively high gradients (235°C/km). This is probably due to evaporative cooling in upper, more porous layers. Below 30 m, the gradients attain values typical for the Basin and Range. There is no indication that any fluids related to surface thermal fluids were encountered.

SUMMARY AND CONCLUSIONS

Normal faults associated with Basin and Range deformation have been identified as the major controlling geologic structures for rising geothermal fluids in various parts of Nevada (Trexler and others, 1980). In the Paradise Valley area it is likely that such faults are the ultimate control of geothermal fluid flow, but data gathered in this investigation may support additional hypotheses. Thermal fluids co-located with major lineament intersections may be channeled along vertically-oriented bedding planes, and probably are confined to narrow pipes of tuffa-cemented sediments exposed at the surface.

Fault scarps associated with Basin and Range deformation are widespread throughout northern Nevada, but are not well exposed in the Paradise Valley study area. The gravity survey conducted throughout the valley revealed steep gravity gradients in many areas, an indication of vertical displacement along faults. However, few surface features could be identified as fault

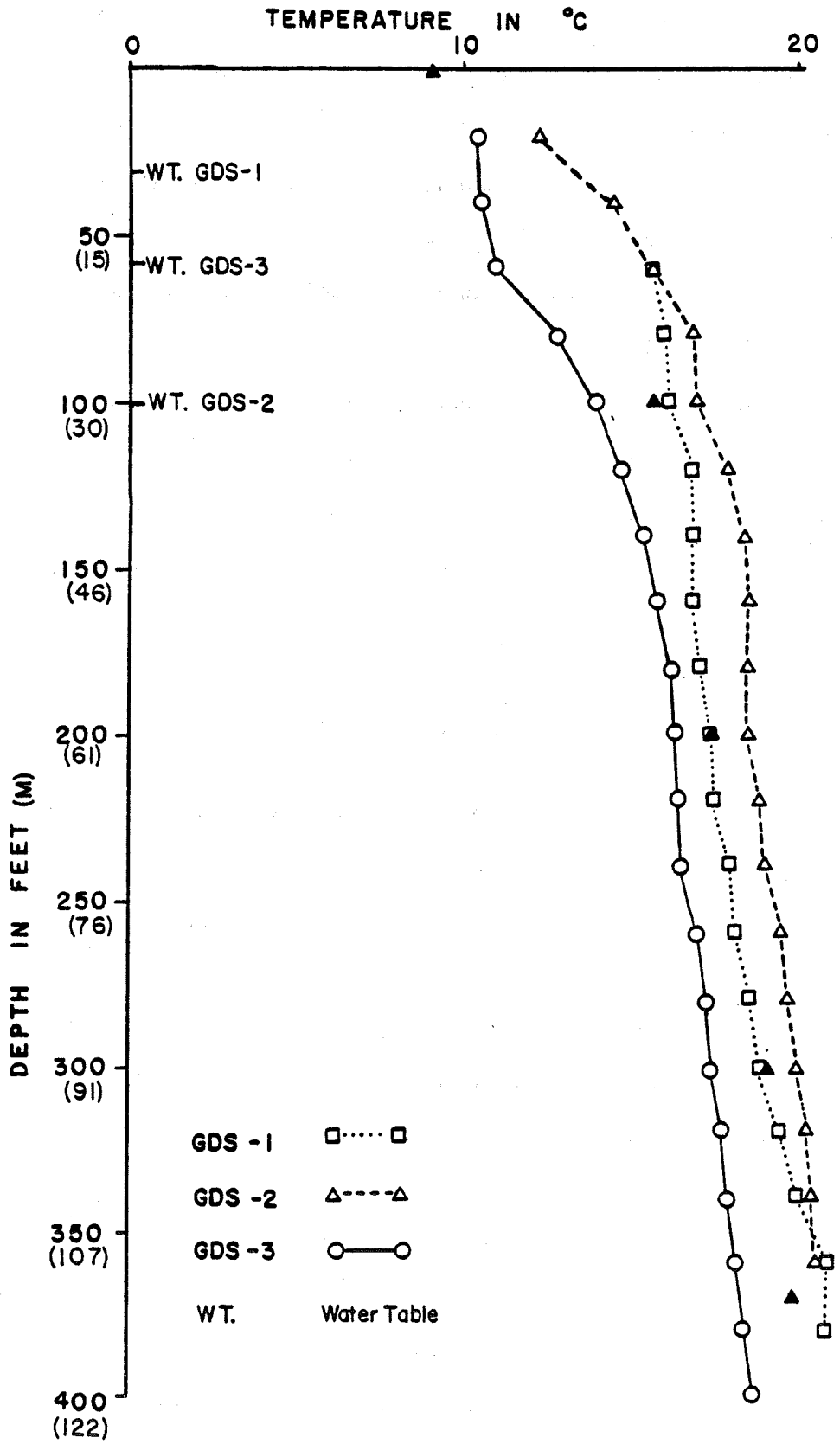

Figure C33. Temperature gradient profiles for GDS 1,2,3.

related on low sun-angle aerial photographs and could not be co-located with gravity anomalies. In addition, thermal fluids did not discharge from a recognizable fault scarp.

Linear and curvilinear features identified on Landsat images, however, can be correlated to some trends in the gravity contour map. These data indicate that all thermal fluids are located at or near the intersection of lineaments related to the Midas Trench and the Oregon-Nevada lineament. These intersections are probably zones of relatively high permeability which enhance the initial flow of rising thermal fluids.

Two-meter temperature probe surveys indicate that thermal fluids in Paradise Valley do not influence the temperature regime outside the immediate area of fluid discharge. It appears that thermal fluid-flow is restricted to a relatively narrow vertical zone of cemented sediments. These cemented sediments crop out as tuffa mounds at the surface, but probably extend deep into the subsurface. Such situations are common throughout Nevada where thermal fluids precipitate chemical compounds like $CaCO_3$ and $NaHCO_3$, and become "sealed off" from the non-thermal environment.

Soil-mercury surveys conducted in this area were largely inconclusive because of the interference from sources of detrital mercury. The survey did, however, identify an unusual mercury anomaly in the Golconda area although it is difficult to draw any general conclusions from this one example.

Results of the fluid isotope study demonstrate that thermal fluids do not originate as valley-level surface waters or groundwaters. They are isotopically lighter than non-thermal fluids collected in the study area, and probably originated as rain or snow at elevations exceeding 2450 m (8000 ft) above sea level. Fluids must sink directly into the earth from this point because re-equilibration with atmospheric oxygen and hydrogen is rapid and

different isotopic values were measured in a single stream-flow at different elevations (Koenig, this report).

Thermal fluids are also chemically distinct from surrounding non-thermal fluids. Chemical characteristics for both major and minor dissolved constituents suggest that thermal fluids are in chemical equilibrium with rock types different from those for surface, non-thermal fluids. Graphic analysis demonstrates that thermal fluids fall into two small groups with limited compositional variation. Non-thermal fluids, however, show a wide compositional variation which probably reflects local surface conditions.

A continuum exists in both isotopic and chemical compositions for all sampled fluids. Thermal fluids for the Golconda area appear to lie between local non-thermal fluids and remaining thermal fluids with respect to chemical and isotopic composition. A simple mixing model produced reasonably successful results for a mixing ratio of 2:1 for thermal to non-thermal fluids.

Temperature gradients are isothermal for wells in the vicinity of thermal springs. Such gradients do not suggest the presence of a hotter reservoir in the near-subsurface. Temperature gradients in the wells outside areas of thermal fluid discharge show a positive geothermal gradient of approximately $32^{o}C/km$, a typical value for the Basin and Range province.

Combined data sets suggest that low-to-moderate temperature geothermal fluids in the Paradise Valley study area are discharging from narrow, vertical pipes of cemented sediments extending deep into the subsurface. Thermal fluids originate as rain or snow on range-tops and are heated by the normal geothermal gradient. These fluids quickly sink to an estimated total depth of 2 to 4 km (1.5 - 3 mi) and probably begin their ascent near the intersection of faults associated with major lineament systems in this area. Mixing of thermal and non-thermal fluids in the near subsurface is probably responsible for the intermediate chemical and isotopic compositions of some thermal fluids.

SOUTHERN CARSON SINK STUDY AREA

by JAMES L. BRUCE

INTRODUCTION

A geothermal assessment study of the southern Carson Sink was initiated in response to a U.S. Navy proposal to establish a demonstration space heating system at the Fallon Naval Air Station (N.A.S.) using geothermal fluids.

The study area is located approximately 100 km (60 mi) east of Reno, Nevada and is part of a much larger area known as the Carson Sink. Figure D1 shows the extent of the study area (approximately 600 sq. km; 360 sq. mi), and its relationship to the Carson Sink.

Roughly triangular in shape, the Carson Sink is a large basin covering over 3000 square km (1800 sq. mi). It is bordered by several mountain ranges which range in elevation from 1500 m to 2500 m (5000 - 8200 ft). The basin is actually a large playa and fluvial plain which has only a few meters of topographic relief over most of its surface.

The southern Carson Sink became an agricultural center during the 1920's after the Newlands irrigation system was built. Later, the U.S. Navy established the Fallon Naval Air Station as a support facility for several air-to-ground target ranges.

Geothermal resource development began in the early 1920's when people drilling for water to irrigate their lands encountered hot water aquifers. Figure D2 shows the locations of these anomalous regions including Lee Hot Springs, the only surface occurrence of geothermal fluids in the study area located at the northwestern end of the Blow Sand Mountains.

Today, the southern Carson Sink is widely recognized as an area of great geothermal resource potential, and several geothermal exploration companies are presently drilling here. Unfortunately, this data is not published. However, the Geothermal Utilization Division of the Naval Weapons Center, China Lake, California recently conducted a geothermal assessment of Navy

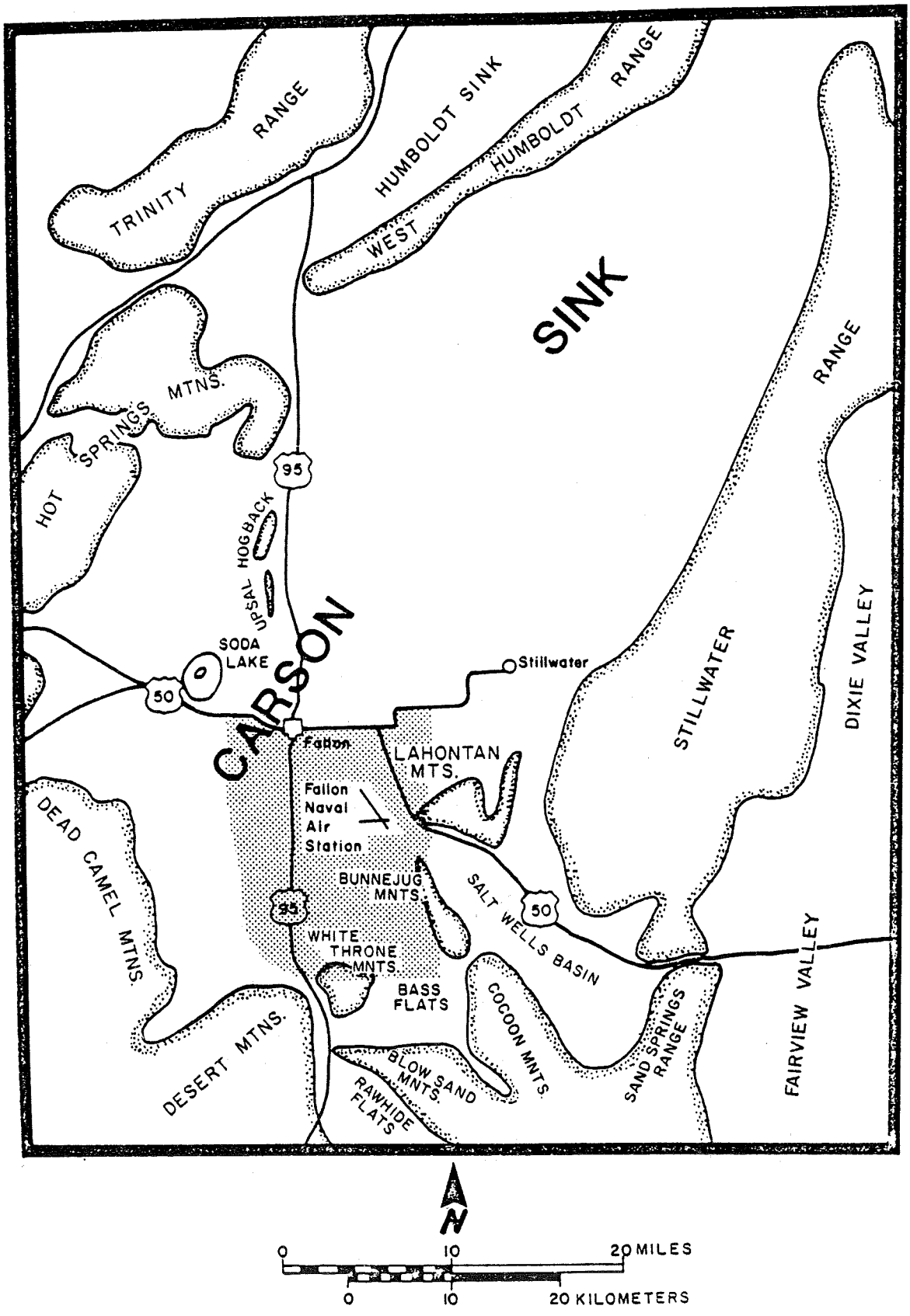

Figure D1. Map of the Carson Sink region, study area designated by shading.

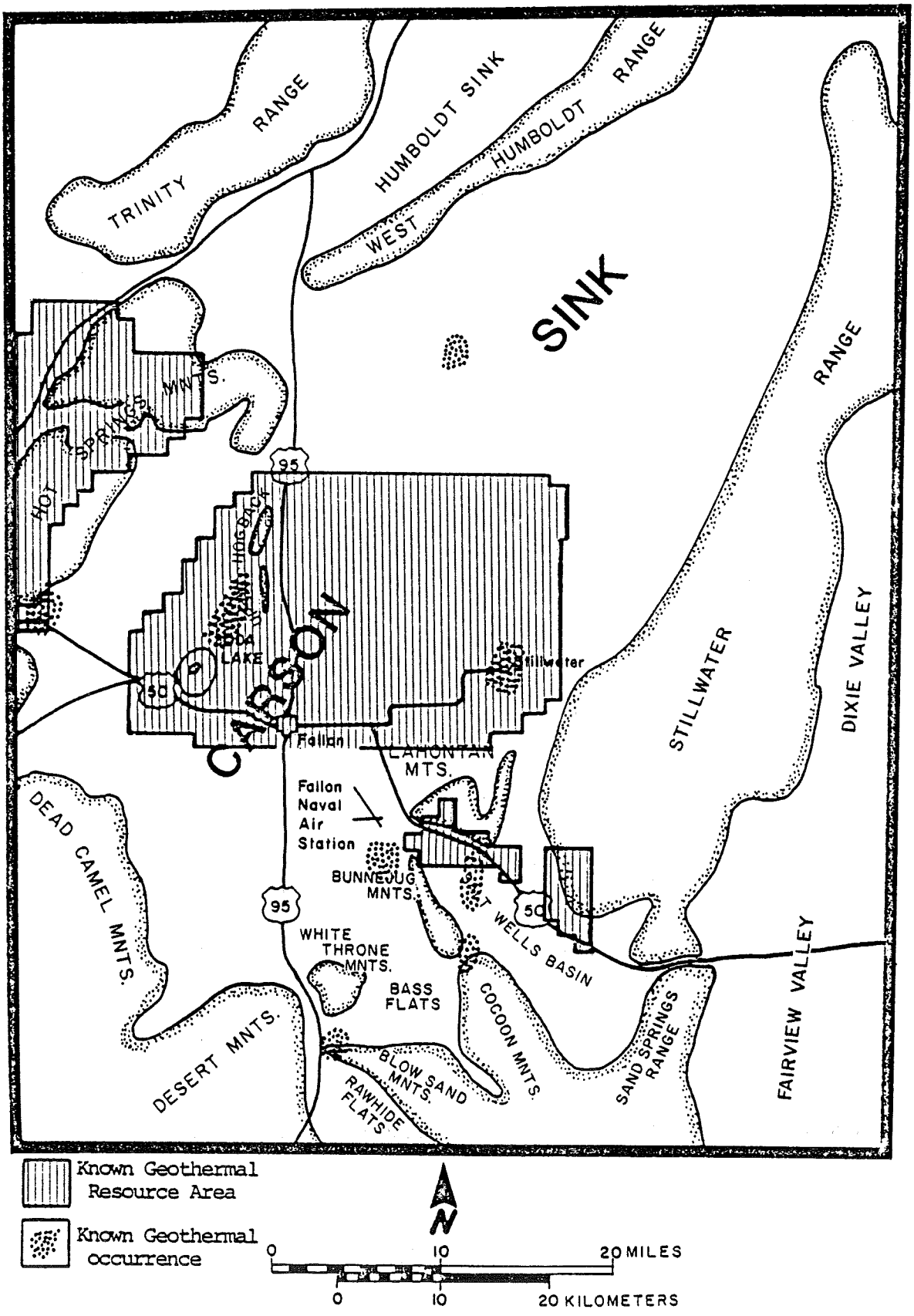

Figure D2, Geothermal occurrences in the southern Carson Sink.

properties in the study area (Bruce, 1979) and their findings are incorporated into this report.

GEOLOGY, STRUCTURE AND TECTONICS

Complex geologic structures and lithology are found within and adjacent to the Carson Sink. Crustal extension during the late Cenozoic Era (Hastings, 1979; Stewart, 1980) created a large basin which then was filled with several thousand meters of clastic material (Morrison, 1964). Extensive extrusive volcanic units are also found in the southern ranges bordering the Sink (Willden and Speed, 1974).

Intersecting structural trends create a complex of horsts and grabens in the southern Carson Sink. Volcanic rocks are also widespread in this area. The oldest rocks are middle to late Mesozoic sediments and metasediments including limestones and argillaceous rocks (Willden and Speed, 1974). These rocks occur as septa or roof pendants in the core of the Stillwater and Sand Spring mountain ranges. Larger outcrops are shown in Figure D3.

Late Mesozoic granodiorites and quartz monzonites of Cretaceous or Tertiary age intrude into these older Mesozoic sediments (Stewart and Carlson, 1978; Willden and Speed, 1974). Small isolated occurrences of Mesozoic sediments are found further west at the intersection of the Sand Springs and Cocoon ranges (Willden and Speed, 1974); most are found further east.

Extensive volcanism occurred during the Teriary age and covered the older Mesozoic units (Willden and Speed, 1974). These thick volcanic rocks range in composition from basalt to rhyolite and may also consist of several volcaniclastic and tuffaceous units. The volcanic rocks are also used to define the basement layer of the Carson Sink (Hastings, 1979).

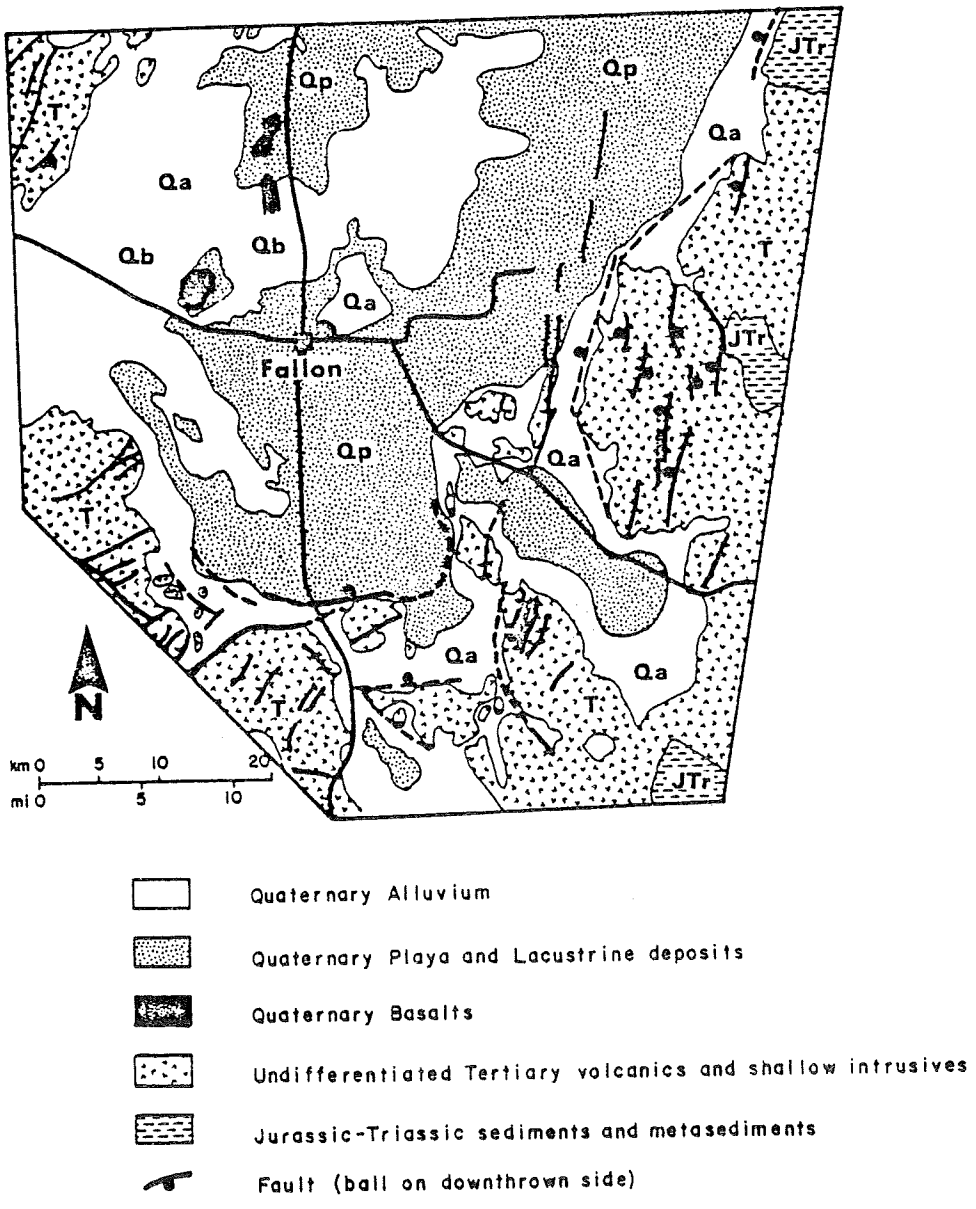

Figure D3. Generalized geologic map of the southern Carson Sink.

Olivine basalts over 500 meters thick are the most abundant volcanic units in the southern Carson Sink (Willden and Speed, 1974). Acidic volcaniclastic units with interbedded basalts are used to correlate the age of sediments in the Carson Sink (Hastings, 1979; Morrison, 1964).

Occurrences of Quaternary basalt in the region of Soda Lake, Upsal Hogback and Rattlesnake Butte indicate that volcanism shifted from the ranges that border the southern Carson Sink to the central portion of the Sink (Morrison, 1964; Willden and Speed, 1974). Volcanic bombs and clastic debris radiating from Upsal Hogback and Soda Lake suggest an explosive origin (Morrison, 1964; Willden and Speed, 1974). Well logs from Rattlesnake Butte show that sediments are interbedded with basalt flows, suggesting a series of flow type eruptions (Bruce, 1979). Pillow structures are also found in the Rattlesnake Butte units indicating a subaqueous origin. Basalt lapilli tuffa and basaltic sands from Quaternary basalt flows are thought to be coeval with Lake Lahontan (Willden and Speed, 1974).

The basaltic character of Upsal Hogback and Soda Lake, and the alignment of these two volcanic centers suggest a rift type origin (Trexler and others, 1978). Hill and others (1979) and Stark and others (1980) further substantiate this theory and suggest that a shallow heat source is present. Geophysical studies indicate that a highly altered zone or magma body exists 5-10 km northeast of Soda Lake at a depth of 2500-3000 m based upon low seismic velocities (Hill and others, 1979). A resistivity survey conducted in the area indicates anomalously low resistivities (Stark and others, 1980).

As the Carson Sink evolved, Tertiary sediments, clastic debris, and volcaniclastic flows, tuffs and ash falls filled the depression (Morrison, 1964). At higher levels in the sedimentary section, the units are a finer grain representing a change from a fluvial to lacustrine environment.

Apparently, these fine silts and sands were deposited by lakes and deltas in the large basin existing during the late Pliocene and early Pleistocene ages.

Lake Lahontan was the largest and the last major inter-basin lake. This lake covered much of northwestern Nevada and was the termination point for several drainage systems (Morrison, 1964). The Carson River emptied into Lake Lahontan in what is now the southern Carson Sink, and created an extensive delta region extending across the basin (Morrison, 1964). The sands and silts brought in by the Carson River and deposited in the delta are not much coarser than the lake sediments deposited further north in the Carson Sink. These late Quaternary sediments are sands and silts which alternate with coarser sands in the older river channels (Morrison, 1964). As Lake Lahontan receded, many shorelines were created. Wave cut terraces and gravel bars are the most striking features and can be easily mistaken as structural rather than geomorphic features.

The three major structural trends found in the Carson Sink in northwest Nevada are the northwest trending Walker Lane, the northeast trending Carson lineament - Midas Trench trend, and the north to north-northeast trending Basin and Range structures (Rowan and Wetlaufer, 1973).

The northwest trend of Salt Wells Basin and the area west of the Bunejug and Cocoon Mountains parallel the northwest trend of the Walker Lane, the western edge of the Stillwater Range deflects toward the Lahontan Mountains and parallels the Carson Lineament - Midas Trench trend (fig. D4). Overlapping both features is the north-northeast trending Basin and Range faulting.

The Walker Lane appears to be the transition zone between the more rigid western provinces and the Basin and Range province due to a strike-slip component in that zone (Rowan and Wetlaufer, 1973). The Carson lineament - Midas

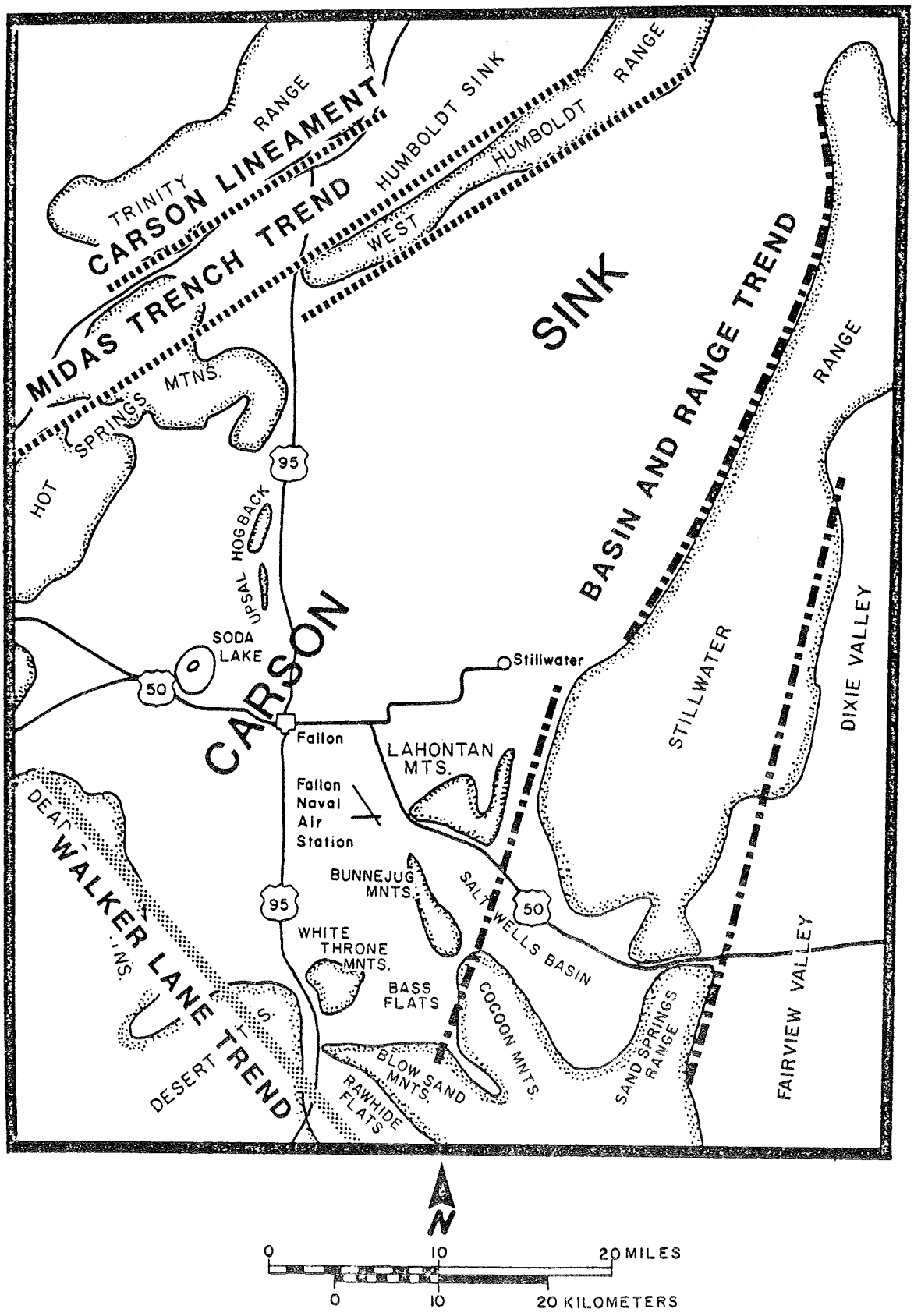

Figure D4. Major structural trends associated with the Carson Sink.

Trench trend may represent an earlier axis of Basin and Range extension (Trexler and others, 1978) which rotated to a more north-northeast alignment. The Carson Sink reflects both trends and may be the transition zone between the two Basin and Range alignments. Buried structures aligned in the northern Carson Sink show a change in alignment from northeast to north-northeast (Hastings, 1979) as shown in Figure D5.

AERIAL IMAGE INTERPRETATION

As part of the regional structure analyses, aerial images were analyzed for linear and curvilinear features using 1:250,000 scale computer-enhanced false color Landsat images, 1:60,000 scale black and white air photos, and 1:40,000 scale black and white low sun-angle air photos. Linear and curvilinear features were then compared with features on these different scales to check the accuracy of the survey. Well-defined lineaments were field checked as potential structural features. Weakly-defined linear and curvilinear features were compared with regional geophysical data to check if they represented a structural trend. Major lineaments are shown in Figure D6, and appear to parallel one of the three major structural trends discussed in the previous section. Geothermal anomalies lie along these major lineaments. Yet many of these anomalous regions do not appear as localized linear features on the larger scale air photos. Geothermal anomalies which occur along the northeast trending lineament across the central portion of Figure D6 may result from a deep-seated structural control, but not enough data is available to substantiate this theory.

Figure D7 is a fault map based upon the air photo study. The absence of fault traces within the basin fill of the southern Carson Sink probably represents a cultural disturbance of the area (i.e., agricultural development, etc.).

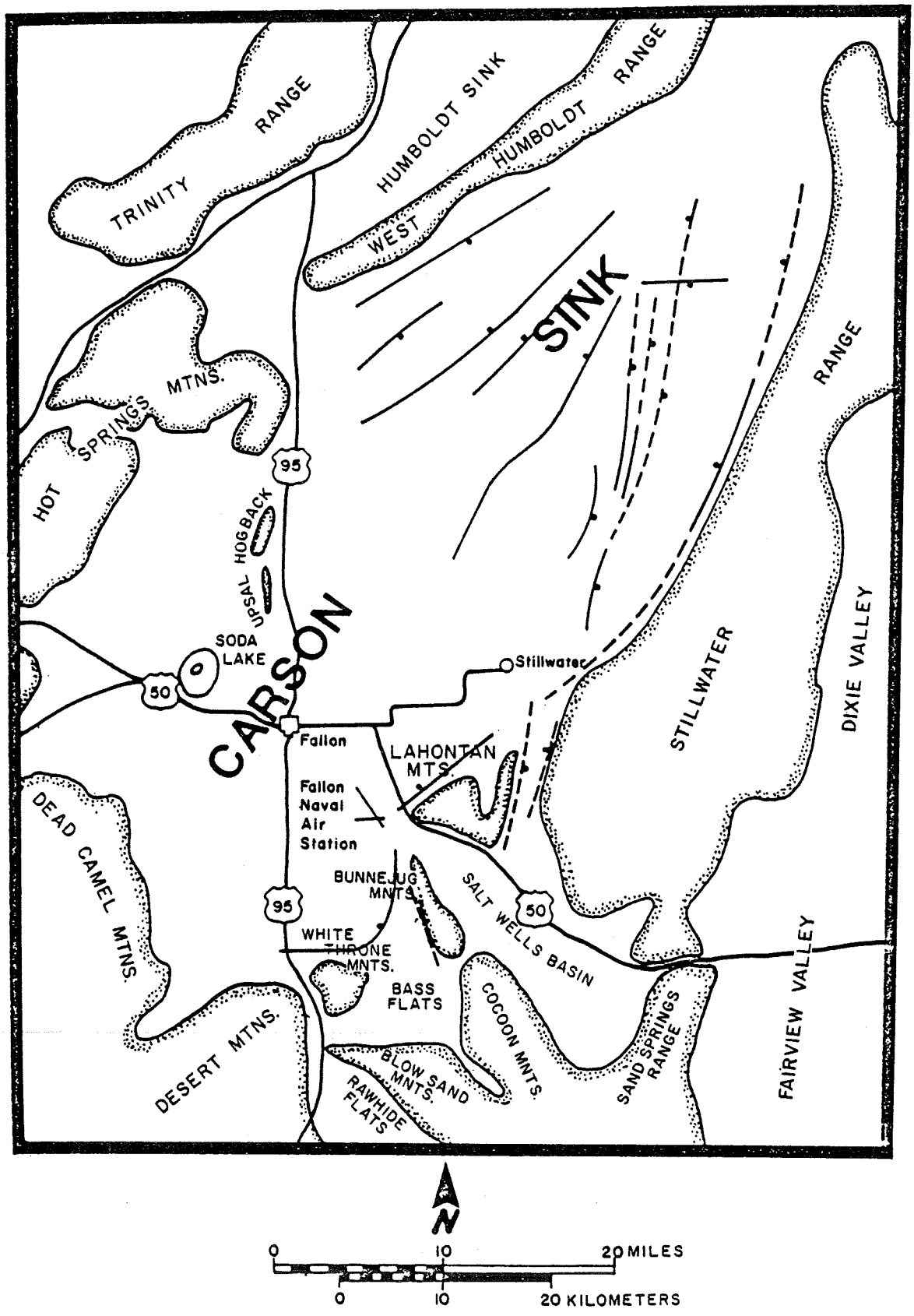

Figure D5. Basement structural trends in the Carson Sink (modified from Hastings, 1979).

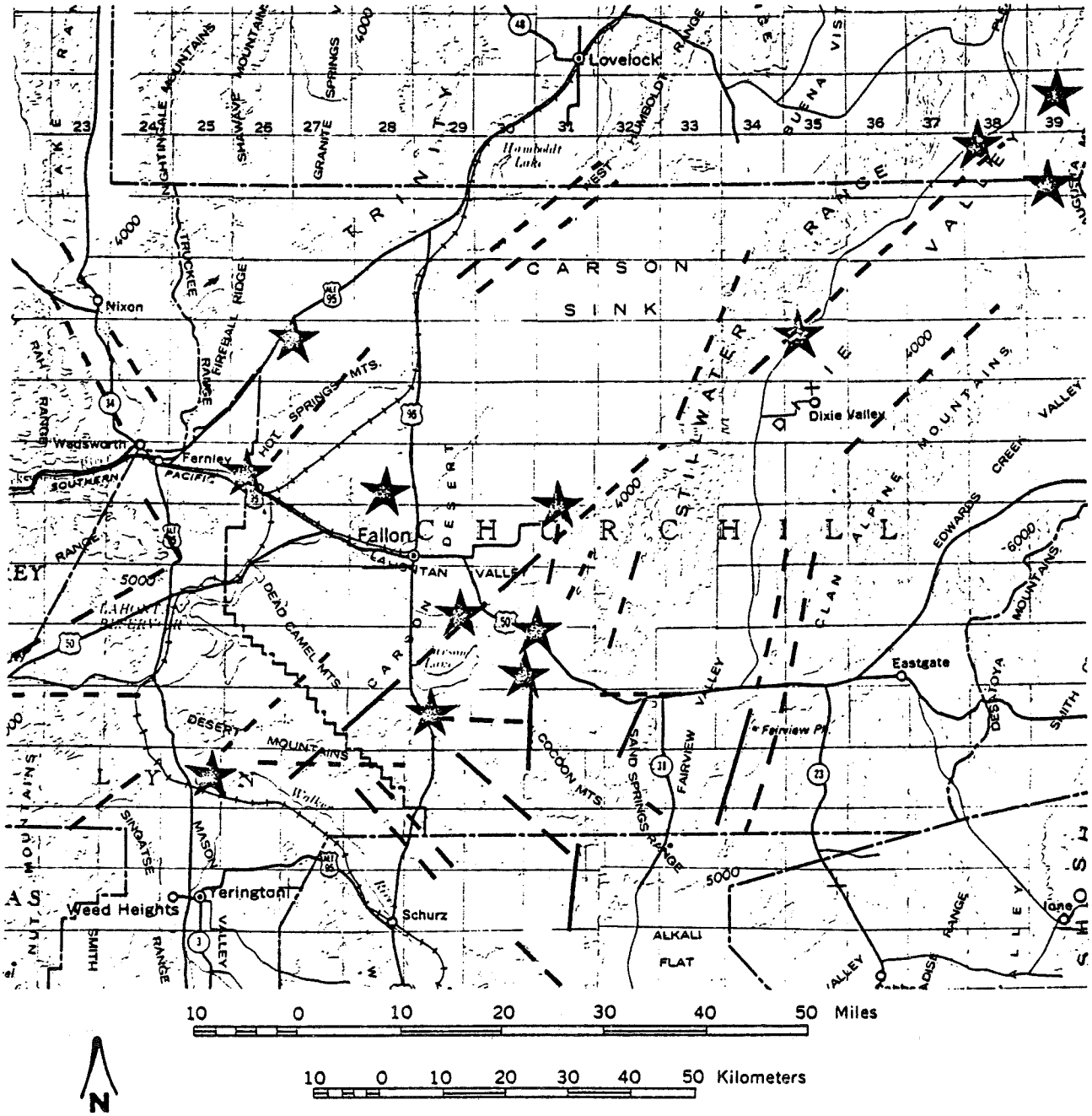

Contour interval 1000 feet

Figure D6. Regional lineaments (dashed where inferred); geothermal occurrences designated by stars.

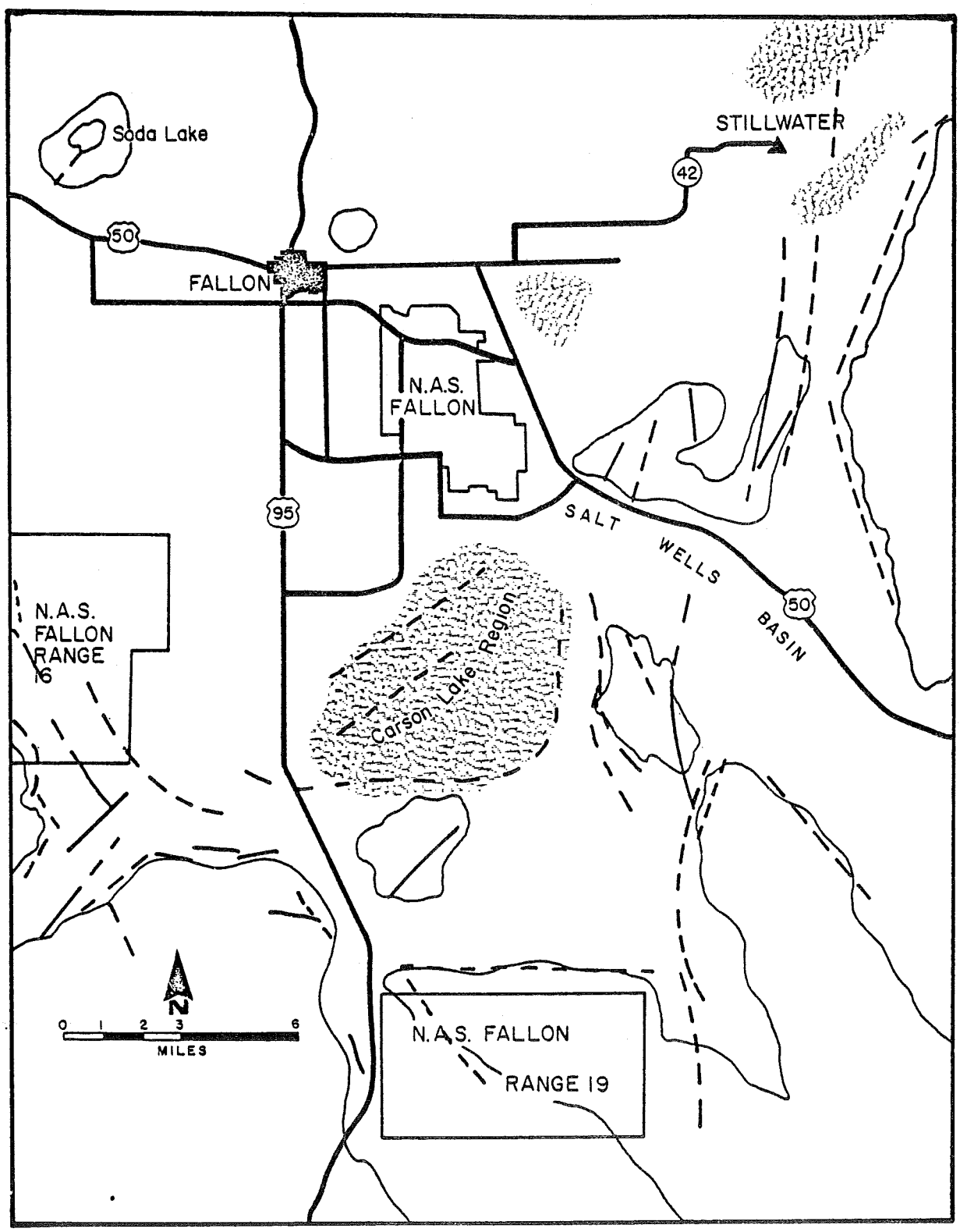

Figure D7. Fault map of the southern Carson Sink (dashed where inferred).

Most surface evidence of movement was obliterated by the recession of Lake Lahontan. Therefore, fault traces in this area are shown on the figure as dashed lines.

Several fault traces show evidence of recent movement such as the Wildcat Scarp, the curvilinear feature south and east of the Carson Lake region (personal communication, Bell, 1981), and the Rainbow Mountain fault trace in the Lahontan Mountains south of the Stillwater range. The Rainbow Mountain fault shows ground rupture and limited vertical offset which occurred during a series of earthquakes from July to December, 1954 (Slemmons, 1957).

Most geothermal anomalies in the southern Carson Sink are only a few hundred meters deep and appear to be associated with one or more fault traces (figs. D7, D8). Three anomalous regions east of the study area have a north-south alignment. This alignment may represent a basement structural trend which acts as a conduit for ascending geothermal fluids.

Olmstead and others (1975) theorize that the Stillwater anomaly is created by geothermal fluids which ascend upward along buried fault zones and migrate in a lateral direction in permeable sandy units of the basin fill. Lee Hot Springs appears to migrate up a fault zone and is one exception to this lateral spreading of geothermal fluids.

FLUID CHEMISTRY

Thermal and non-thermal fluid analyses were compiled for several locations in and adjacent to the study area. Data sources include published data (Garside and Schilling, 1979), the State Consumer Protection Office, and samples collected in the field and analyzed by BC Laboratories in Bakersfield, California (table D1).

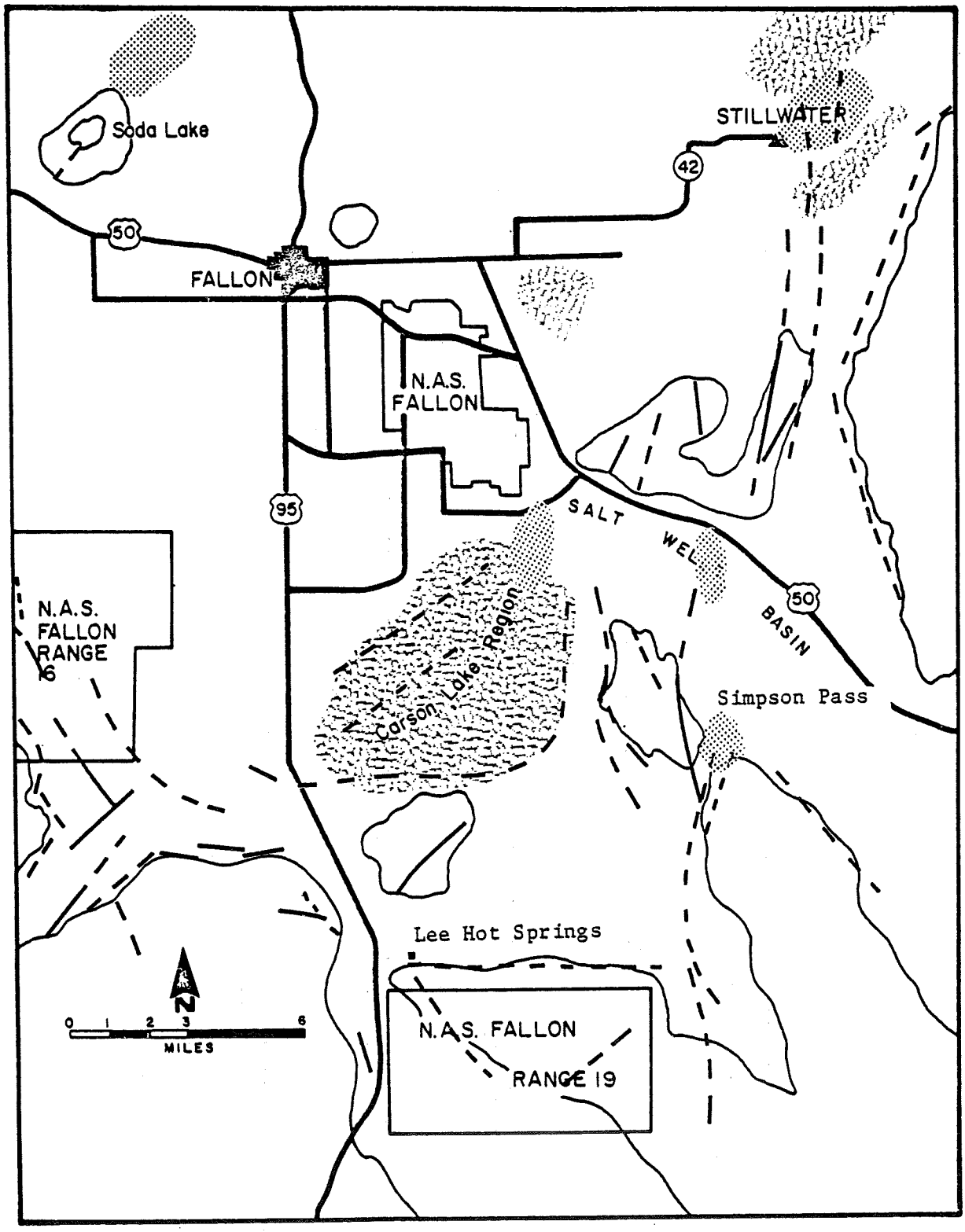

Figure D8. Relationship of faults to geothermal occurrences. Geothermal anomalies indicated by stippling pattern.

Table D-1 Selected Fluid Analyses for Thermal and Non-Thermal Fluids in the Southern Carson Sink.

Sample No.	Location	Depth (ft.)	pH	TDS	Temp (°C)	Ca	Mg	Na	K	Al	Li	NH_4	F	Cl	SO_4	NO_3	HCO_3	CO_3	Data Source	Notes
CRDC	19N27E 19ad	Surface	8.5	412	C	32	8.6	69	4.0	<0.1	0.08	<1.0	0.32	33	80	1.8	154	6.8	S	B 0.22, SiO_2 23.0: Carson River Sample
F1	17N29E 6a	--	8.3	945	C	69	18.5	179	14	<0.1	0.07	<1.0	0.44	105	196	6.7	307	21	S	B 0.52, SiO_2 30.0
F2	18N29E 33a	--	8.8	1337	C	1	0.42	410	8	<0.1	0.02	<1.0	2.80	220	35	5.8	577	41	S	B 1.7, SiO_2 34
F3	18N29E 27c	--	8.5	1491	C	1.5	0.39	445	10	<0.1	0.02	<1.0	3.40	133	26	3.1	764	75	S	B 1.8, SiO_2 28
F4	18N29E 34dd	--	8.7	3002	C	1.4	0.37	1000	19.5	<0.1	0.03	3.0	2.7	850	15	0.9	1007	68	S	B 4.5, SiO_2 36
F5	18N29E 36b	--	8.6	4359	C	2.3	2.8	1460	40.5	<0.1	0.10	9.0	2.2	1473	15	0.4	1239	75	S	B 5.1, SiO_2 41
F10	16N30E 10	310	7.35	1000	C	56	26	-410-		-	-	-	0.80	320	480	92.5	139	0	NCPD	Fe 0.32
F11	16N28E 6ca	440	7.30	4410	C	175	97	-1321		-	-	-	-	1950	600	20	388	0	NCPD	Fe 0.32
F40	17N29E 10b	97.5	8.7	2546	C	3	1	923	21	-	-	-	4.12	730	8	0.8	1171	0	NCPD	As 0.41, Fe 0.5, Mn 0.01
F60	18N30E 35d	280	7.88	3814	C	34	10	-1404-		-	-	-	7.0	1620	454	22.2	490	0	NCPD	As 0.13, Fe 0.13
F72	18N28E 27	54	7.99	695	C	41	12	184	12	-	-	-	0.83	46	178	1.2	376	0	NCPD	As 0.07, Fe 0.03, Mn 1.10
F76	18N29E 5d	127	8.98	397	C	1	0	161	3	-	-	-	1.43	13	44	0.7	249	36	NCPD	As 0.58, Fe 0.67, Mn 0.03
F79	18N29E 28d	180	8.38	1168	C	2	1	459	7	-	-	-	3.14	275	24	0.7	695	28	NCPD	As 0.13, Fe 0.1, Mn 0.02
F80	18N29E 35a	120	8.35	1791	C	2	1	706	16	-	-	-	3.13	375	6	0.4	1142	32	NCPD	As 0.29, Fe 0.08, Mn 0101

Sample No.	Location	Depth (ft.)	pH	TDS	Temp (°C)	Ca	Mg	Na	K	Al	Li	NH_4	F	Cl	SO_4	NO_3	HCO_3	CO_3	Data Source	Notes
F91	18N30E 35	100	7.93	3442	C	32	7	-1268-		-	-	-	7.8	1500	373	8.2	432	0	NCPD	As 0.04, Fe 0.37
F92	18N30E 29	103	8.24	4964	C	13	5	-1580-		-	-	-	-	1890	398	6.0	493	0	NCPD	Fe 0.66
F6	17N30E 6cc	172	8.0	3966	72.8	70	3.1	1350	41.5	<0.1	2.3	2.2	1.4	2138	58	<0.4	190	0	S	B 5.3, SiO_2 104
SL1	20N28E 22ba	87	-	-	31.0	26	9	940	100	-	1.7	-	0.8	1400	22	0.2	354	0	G&S	B 6.1, SiO_2 56
SL2	20N28E 28bc	45	-	-	57.4	360	46	1800	160		2.0		0.6	1800	2500	0.1	305	0	G&S	B 3.4
SL3	20N28E 28cb	133	-	-	39.0	100	2.4	1100	50		1.7		0.6	1400	480	0	181	0	G&S	B 5.3, SiO_2 130
SL4	20N28E 28dc	523	-	-	62.0	170	0.8	1650	50		3.0		1.9	2800	68	-	106	0	G&S	B 13.5, SiO_2 170
ST1	19N31E 76	-	-	-	96.0	108	1.7	1480	42				5.0	2200	190	-	90	0	G&S	B 15.0, SiO_2 170
ST2	19N21E 7bc	204	-	-	100.0	91	1	-1400-					-	2080	190	-	104	0	G&S	
LHS	16N29E 34ba	Spring	8.2	1622	100.0	42	0.4	460	30	0.1	0.68	.06	8.7	406	430	0.5	103.1	19.6	USN	B 1.3, SiO_2 120

S = Collected Sample
NCPD = Nevada Consumer Protection Division, Health Dept. Files
G&S = Garside and Schilling, 1979
USN = Geothermal Utilization Division data, Naval Weapons Center, China Lake, California.

Table D-1. (Contiued)

Figure D9 is a trilinear plot showing the chemical distribution of the analyses. There is no real separation between thermal and non-thermal fluids, possibly due to dilution by local groundwaters. The fluids are deficient in calcium, magnesium, carbonate, and bicarbonate ions; they are enriched in sodium, potassium and chloride ions. This phenomenon may be explained by ionic exchange between the fluids and clay-rich sediments within the basin.

Concentrations of lithium in thermal waters are an order of magnitude greater than those of non-thermal fluids. Many of the non-thermal fluid analyses did not include an analysis for lithium, therefore, this data is not conclusive.

Geographic distribution and chemical characteristics are shown in Table D1 and Figure D10. Non-thermal fluids represented in the top left section of the diagram are sodium bicarbonate; sodium chloride is predominant in the bottom left section. This transition represents a change in the hydrologic environment of the area. Sodium bicarbonate fluids are found in the coarser deltaic sediments, while sodium chloride fluids are found in the finer clay-rich deltaic and lake sediments.

Sample CRCD is a surface water sample taken at the head of the irrigation canal. It was hypothesized that changes in groundwater chemistry might be due to leaky irrigation canals in the area. However, it is now believed that lithologic variations control the fluid chemistry more than local groundwater.

Lee Hot Springs may represent the regional geothermal fluids. Located a short distance from the basin, the fluids at Lee Hot Springs ascend upward and do not migrate through an extensive sedimentary section. Therefore, there is no ionic exchange between clays and fluids. To further develop this hypothesis, it is necessary to obtain fluid samples from deep within the sedimentary basin which have retained their original chemical characteristics.

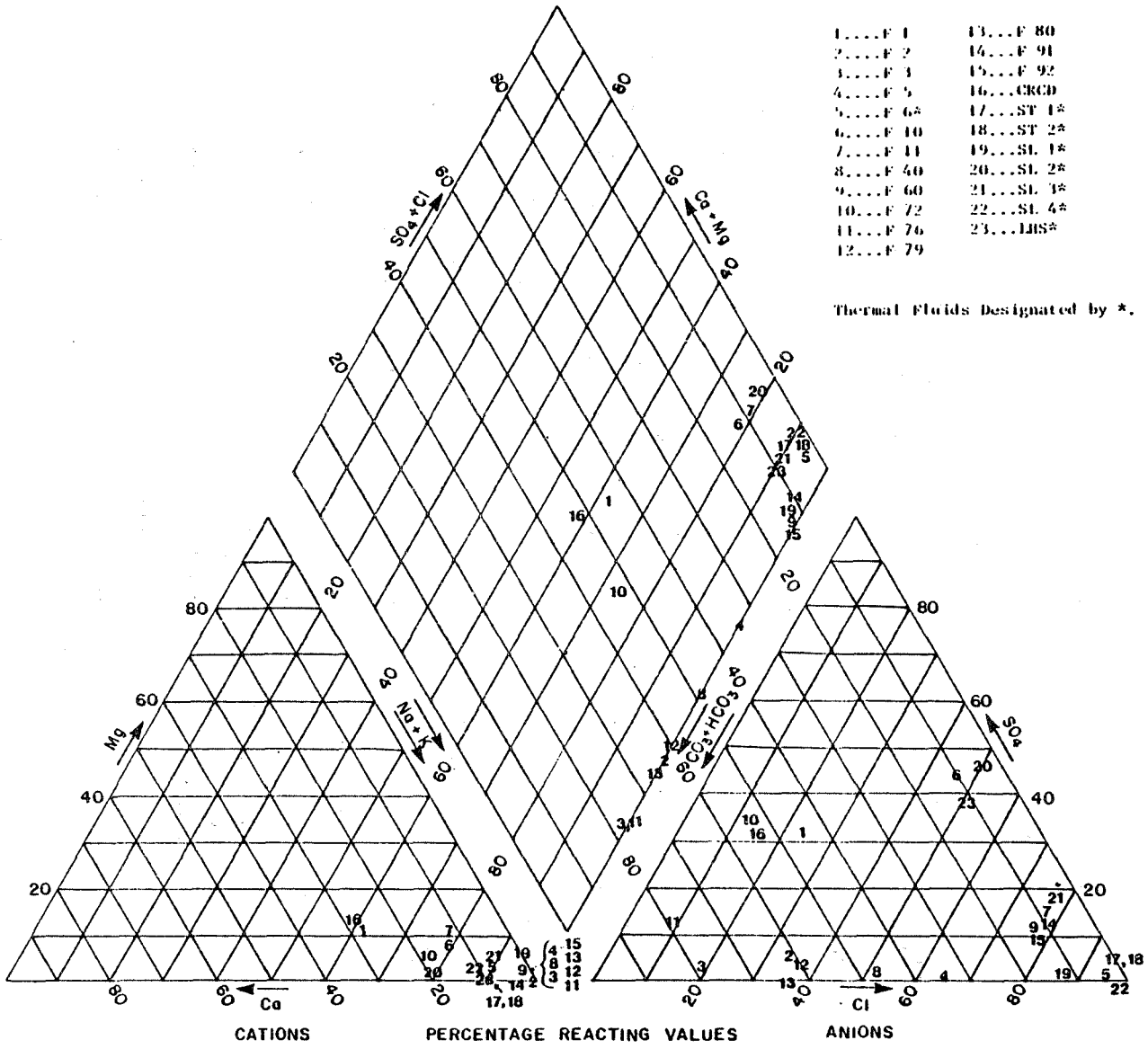

Figure D9. Trilinear plot of selected fluid samples.

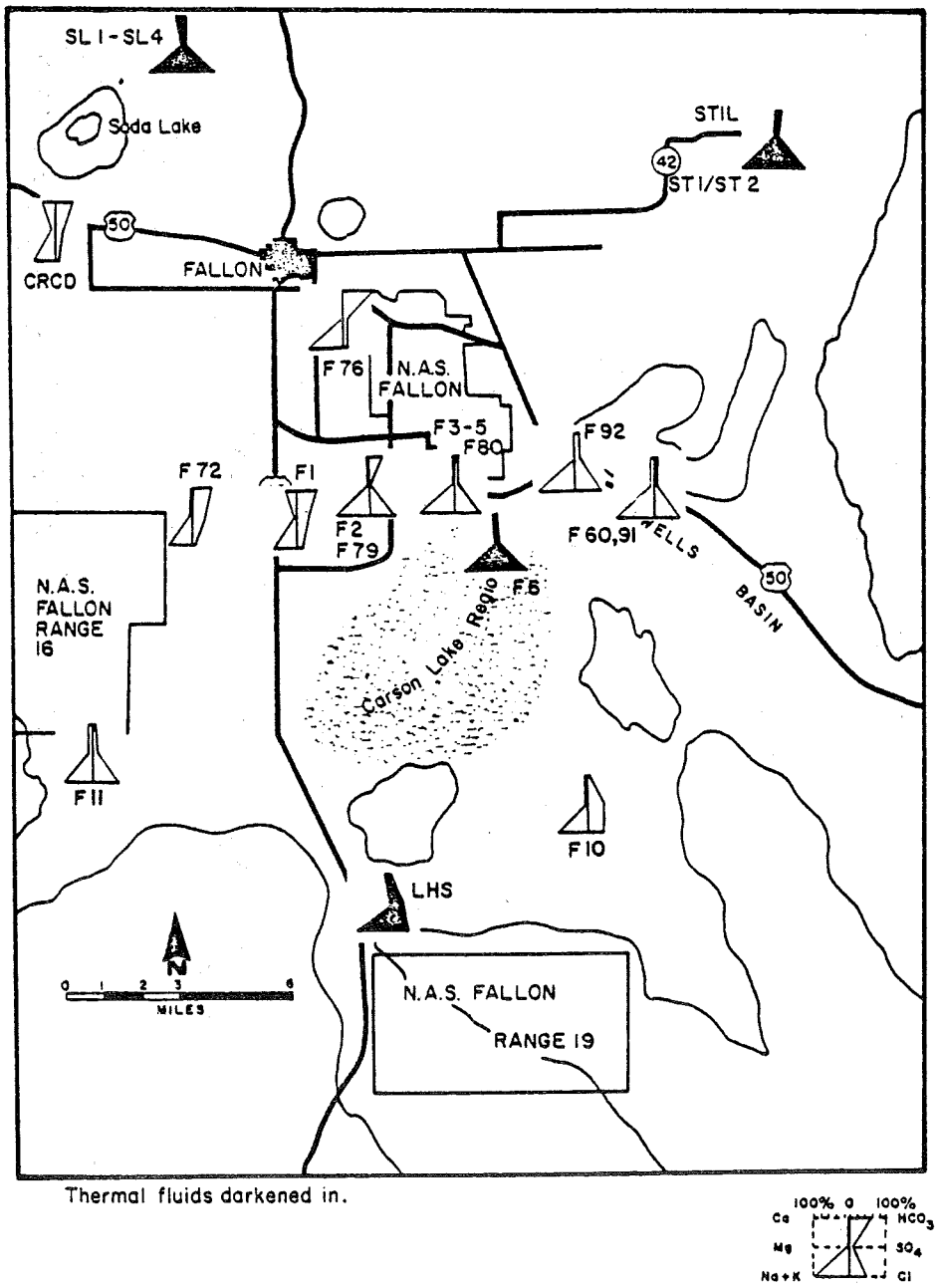

Thermal fluids darkened in.

Figure D10. Geographic distribution of fluid samples and their general composition.

SOIL-MERCURY SURVEY

A detailed soil survey for mercury concentrations was undertaken to augment a similar survey completed on Navy lands (Bruce, 1979). Approximately 125 samples were collected for analysis. Several samples were collected from previous study sites (Bruce, 1979) and contained comparable concentrations of mercury, although no direct relationship could be established between the two surveys. Figure D11 is a composite map of anomalous trends found in the two surveys. Major anomalies parallel major structural trends, however, it appears that these mercury anomalies are not directly associated with a major structural feature. A minor deflection in basement material (see "Gravity Survey") parallels the large northeast trending anomaly south of the Fallon Naval Air Station. Furthermore, the small southern extension of this northeast trending anomaly is located over the geothermal anomaly south of the Fallon Naval Air Station, and parallels a trend in the basement structure.

Mercury concentrations found in soil samples in the study area range from less than 10 ppb to greater than 6000 ppb. The mean value ranged from 500 to 700 ppb, and background values were less than 50 ppb.

Although the lithologies are essentially the same, soil samples collected immediately outside the study area during a previous study (Bruce, 1979) contained lower mercury concentrations than soil samples collected during this study. There is no explanation for this phenomenon.

GRAVITY SURVEY

During the detailed gravity survey, approximately 300 stations were set up in a 1.6 km X 0.8 km (1 mi X 1/2 mi) rectangular grid system. Due to access problems, the subcontractor performing the survey occupied only 290 gravity

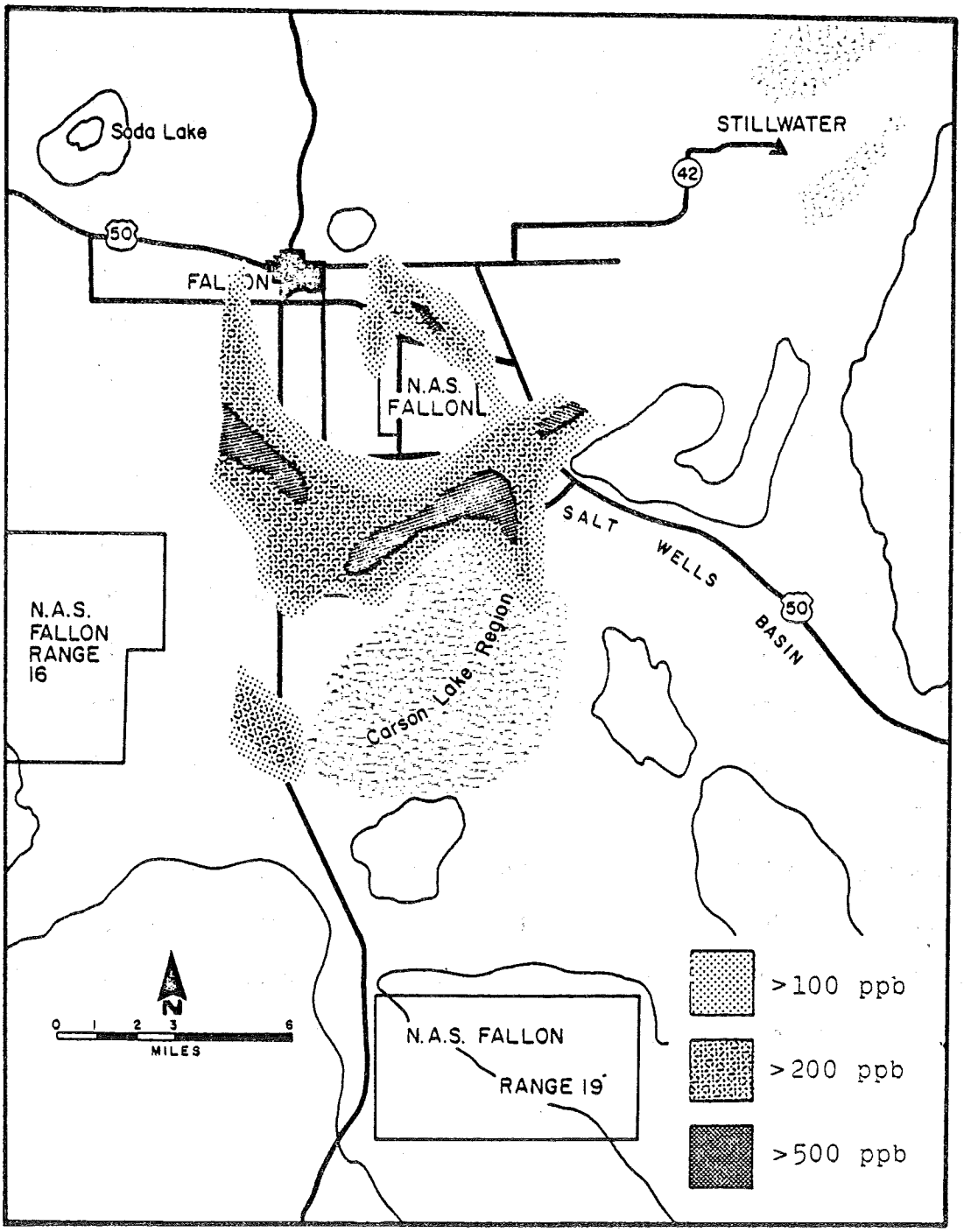

Figure D11. Soil-mercury anomalies.

stations. Furthermore, he did not occupy any existing gravity stations. Therefore, this gravity survey only shows basement configuration. Depth-to-basement calculations and regional corrections could not be made.

Figure D12 is the terrain-corrected Bouguer gravity map of the study area. The gravity low corresponds to the structural low identified by Wahl (1965) in the southern Carson Sink. The north-south trend of the 290 milligal contour along the eastern portion of the figure represents the north-south trending Basin and Range fault which separates the Bunejug Mountains' horst from the Carson Lake graben.

A modified version of the formula T = A/0.013S (Thompson and Sandberg, 1958) was used to estimate depth-to-basement where "T" is the thickness of sedimentary fill measured in feet, "A" is the difference between the highest and lowest survey values, "0.013" is the attraction of an infinite slab in milligals per foot, and "S" is the difference in specific gravity between geologic units. At the gravity low south of Fallon, calculations using S = 0.5 or 0.6 g/cm^3 produced an estimated depth-to-basement of 500 meters (1500 ft). This corresponds to calculations made by Wahl (1965).

Profiles of sections A-A' and B-B' (fig. D13) show that the Carson Lake graben is a south dipping block bounded by normal faults to the south and east. The step in profile B-B' probably represents step-faulting beneath the basin fill. A shallow, hot artesian well (Well 6) is located south of the Fallon Naval Air Station where profile B-B" on the map crosses the tip of a nose-like feature at the 290 milligal contour. This deflection in the north-south trend of the gravity contours probably represents an offset caused by another fault in the basement unit. These intersecting fault zones may provide conduits for ascending geothermal fluids. No other geothermal anomalies are found along this trend.

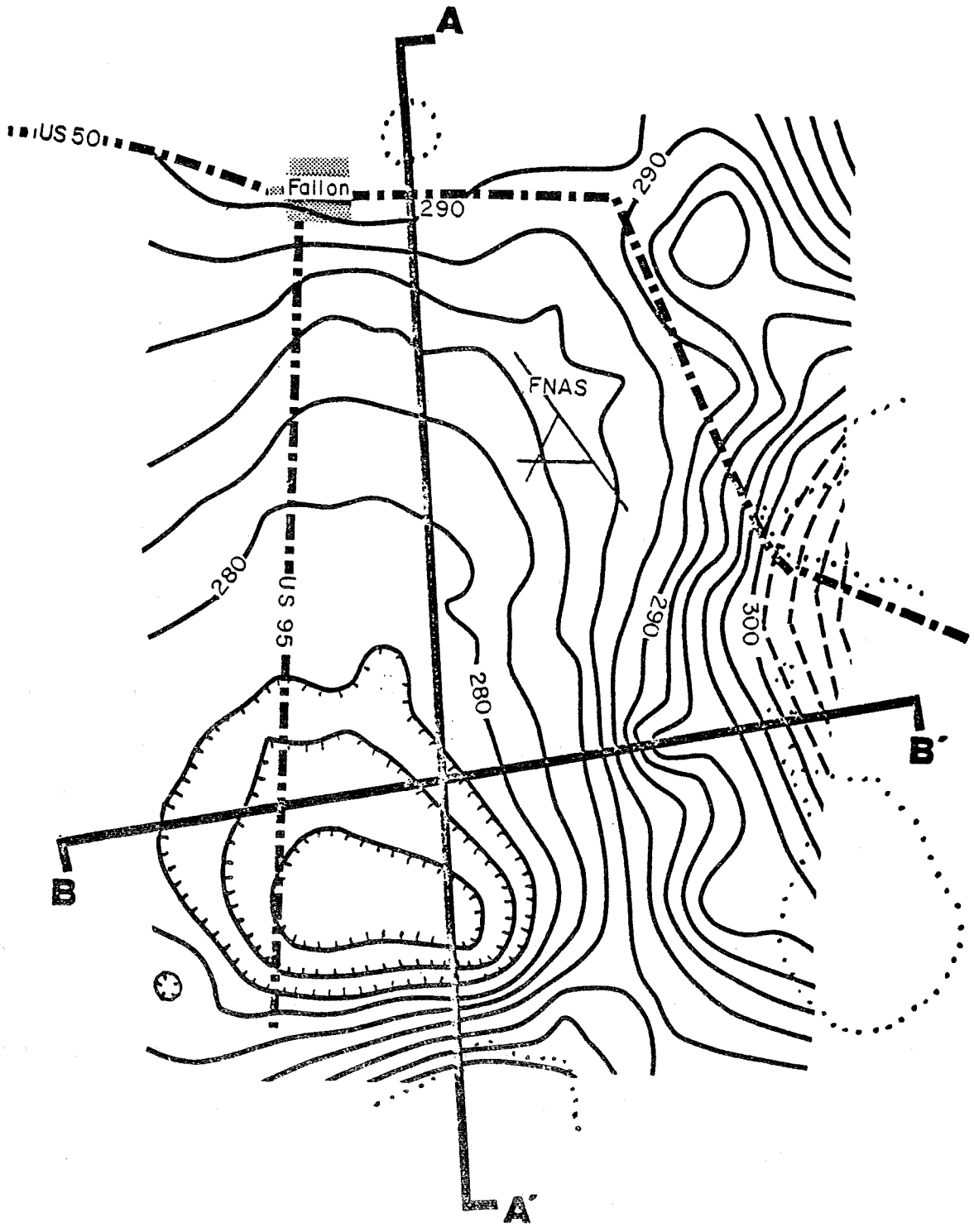

Figure D12. Terrain-corrected Bouguer gravity map of the southern Carson Sink (not corrected for regional gravity).

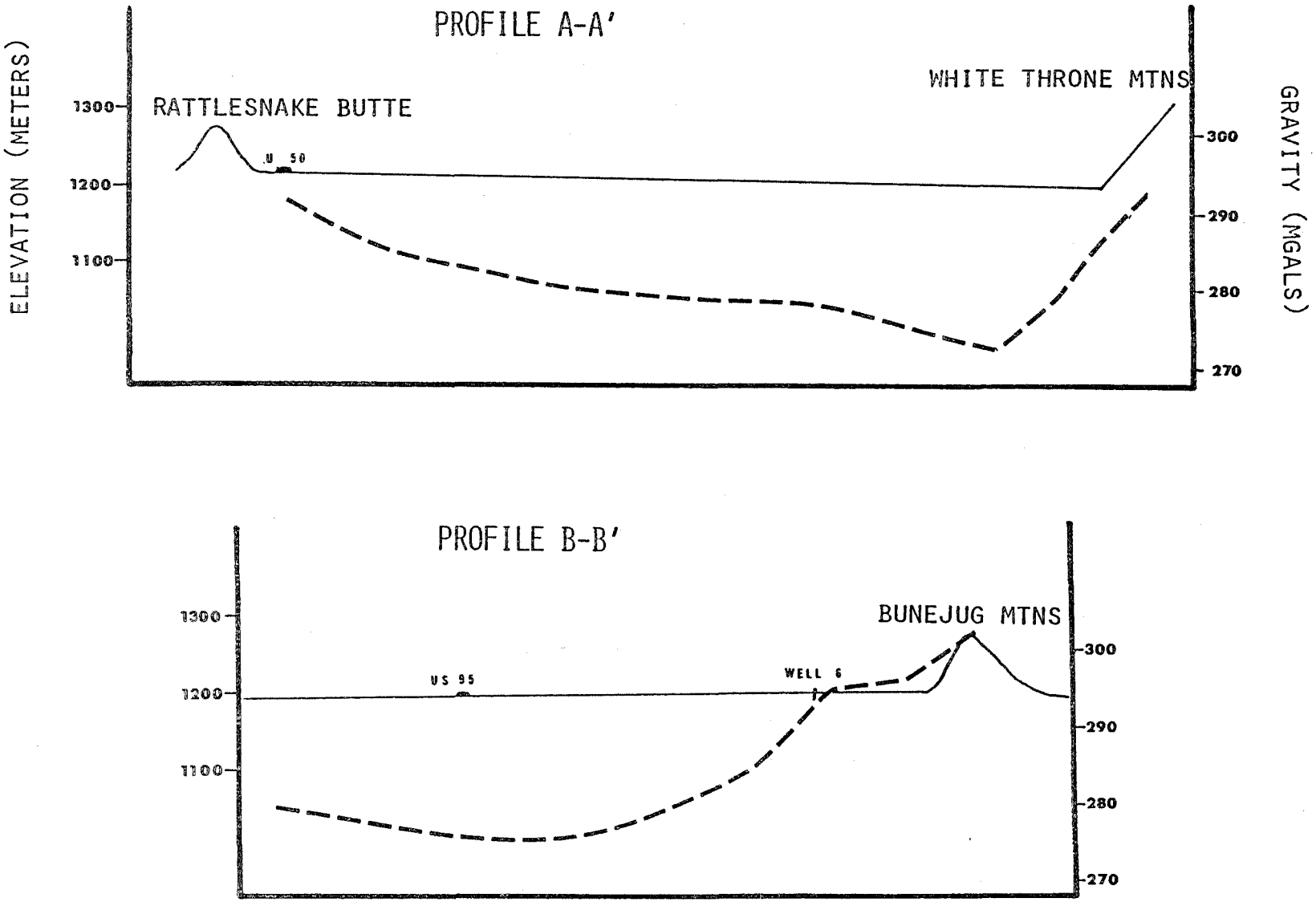

Figure D13. Gravity Profiles across the Southern Carson Sink.

Northeast trending gravity contours east and west of the Fallon Naval Air Station may be related to the Carson Lineament - Midas Trench trend (fig. D12). The deflection of gravity contours in the southeast corner of the diagram may be associated with Walker Lane structures located a few kilometers west of this area.

TEMPERATURE GRADIENT STUDIES

Data from temperature gradient holes drilled in the study area was made available by the Geothermal Utilization Division of the Naval Weapons Center, China Lake, California (fig. D14).

Aquifer test wells NTH 1, 2 and 3 were drilled by the Navy to test various anomalous trends around the Fallon Naval Air Station. Well 0 is a deep aquifer test well over 500 meters (1500 ft) deep. Well 6 is a small stock watering well with an artesian flow of 72°C. Temperature gradient holes (TGH) 23 through 26 were drilled by the Navy around well 6, and TGH 27 through 30 were drilled to test a geothermal anomaly beneath the large soil-mercury anomaly in the northeastern part of the basin (Bruce, 1979).

The isotherm characteristics of the region are based upon temperature data combined with bottom hole temperatures (profile A-A^1, fig. D15). The decrease in depth of the geothermal anomaly at the southern end of the profile probably represents a fault zone or a hot water aquifer which is bringing geothermal fluids closer to the surface. Temperature gradient plots from these wells are shown in Figure D16. Temperature estimates of 120° to 150°C (225° - 300°F) at 400 to 600 meter depths (1300 - 6000 ft) are based upon gradient data and are lower than geothermometer temperatures of 140°C (SiO_2) and 200°C (Na-K-Ca) (Bruce, 1979).

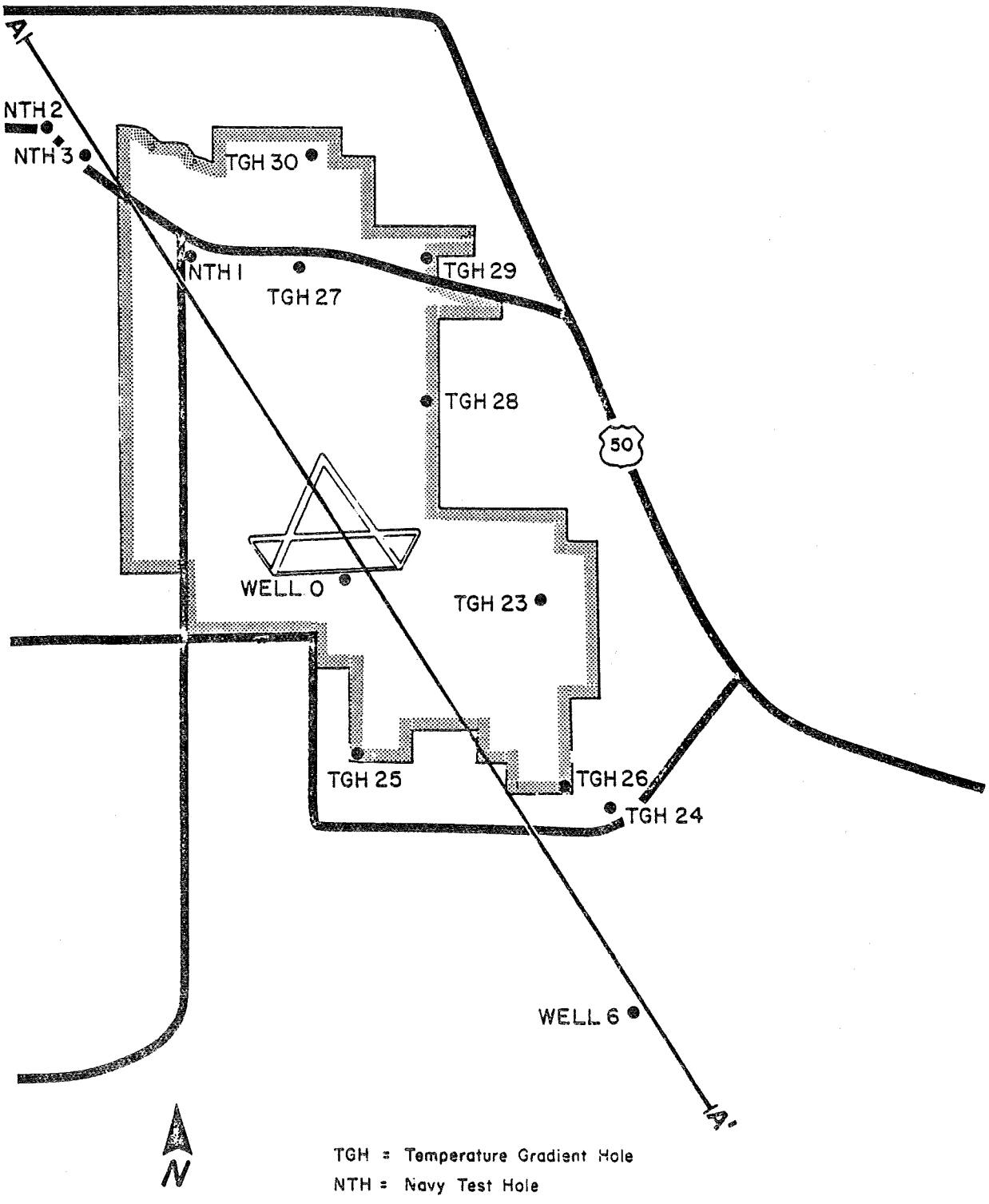

Figure D14. Location map of thermal wells and temperature gradient holes.

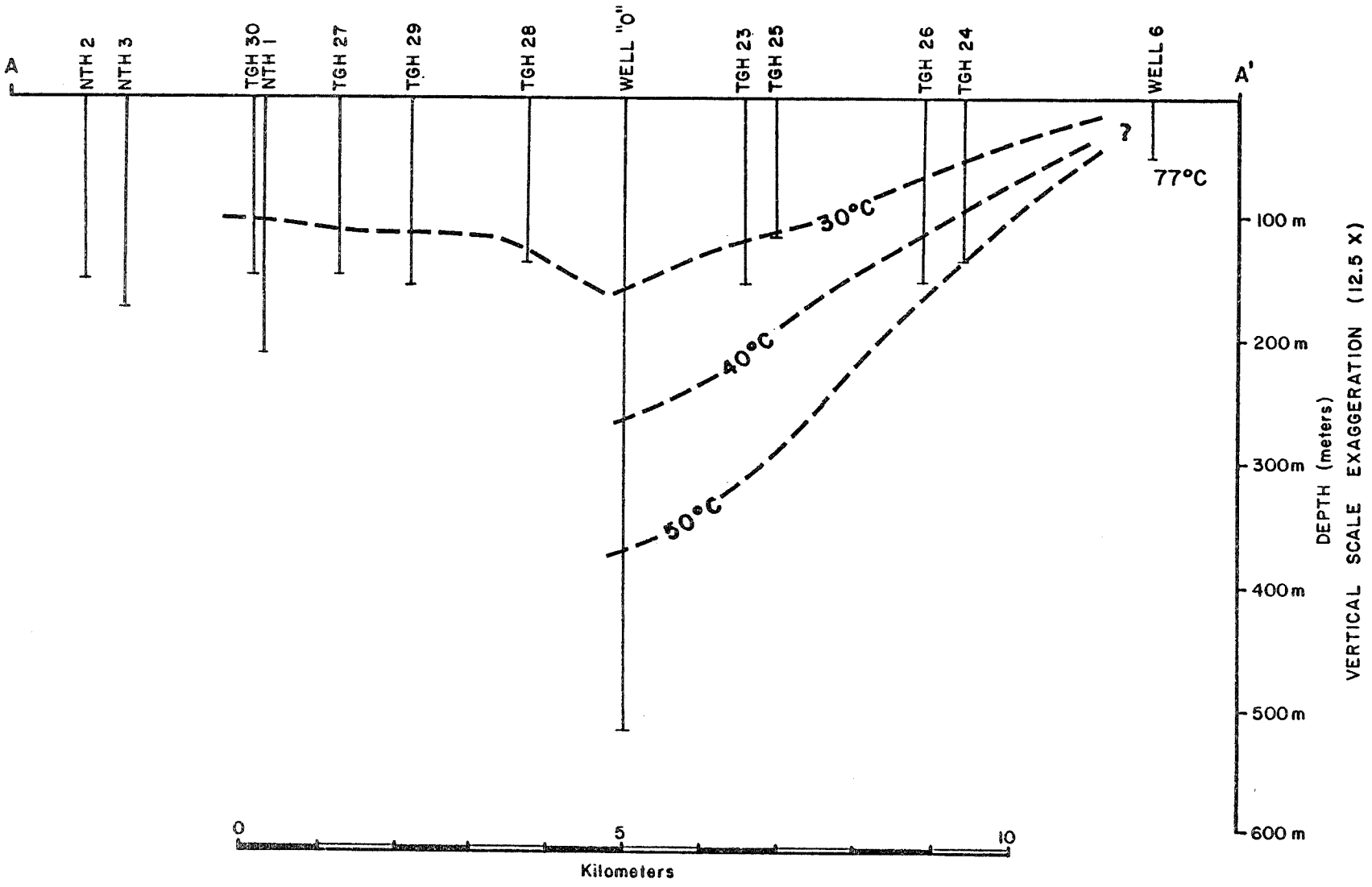

Figure D15. Interpretive isotherm cross-section from bottom hole temperature and gradient data. (See Figure D14 for locations of wells and temperature gradient holes).

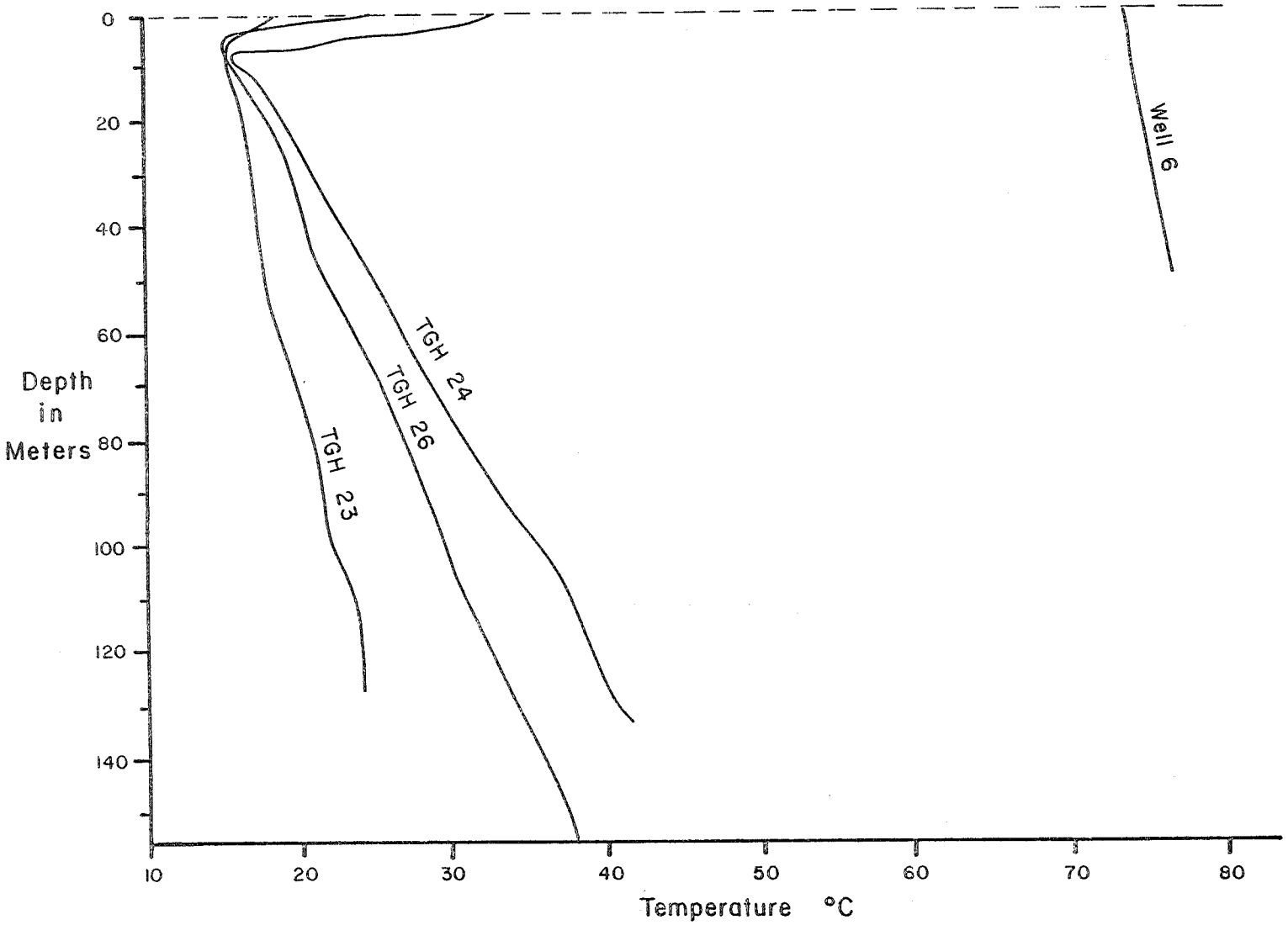

Figure D16. Selected temperature gradient plots.

SUMMARY AND CONCLUSIONS

A relatively shallow geothermal anomaly may exist along the eastern edge of the southern Carson Sink which could be developed for space heating.

Additional wells at least 500 m (1500 ft) deep must be drilled in the area to determine its lateral extent and to determine if the temperature gradients are maintained. Production test wells must be flow-tested to determine if the hydrologic system of the resource contains enough fluids to sustain the resource over several years of use.

Investigative techniques used during geothermal assessment of the southern Carson Sink are aerial image interpretation to delineate regional and localized lineaments and fault zones which could be conduits for ascending geothermal fluids; a soil-mercury survey to delineate regions of high mercury concentrations associated with buried structures or geothermal anomalies; a micro-gravity survey to identify basement structures; and temperature gradient data to interpret subsurface thermal conditions. Fluid chemistry did not provide any useful information except it indicated that lithium is present in thermal waters. A shallow temperature survey was not conducted because a very shallow, cold aquifer overlies warm aquifers in the southern Carson Sink.

STATEWIDE GEOTHERMAL RESOURCE ASSESSMENT

by GEORGE GHUSN

STATEWIDE GEOTHERMAL ASSESSMENT PROGRAM

In 1979, the State-Coupled Geothermal Assessment Team published a map entitled "Geothermal Resources of Nevada and their Potential for Direct Utilization" (Trexler and others, 1979) which presents information on the location, temperature and chemistry of 298 springs and warm wells with temperatures in excess of 20°C. In addition, the map shows areas with potential for direct heating applications.

In an effort to update this resource data base for 1980, a number of earlier tasks were repeated including a literature search, field checking and fluid sampling and chemical analysis. During the literature search, well logs were reviewed at the State Engineer's office, geology and geothermal publications were researched, and bibliographic references were re-examined. Also, various individuals contributed important suggestions and information during personal interviews.

Field checking consisted of temperature measurements of selected thermal wells and springs, and in situ pH and specific conductance measurements. Also, two fluid samples were collected at each of 20 sites; one sample was a 250 ml volume and the second, a 80-100 ml aliquot. The larger sample was topped-off to reduce atmospheric interaction and preserved in a raw state for the analysis of anions. To ensure reliable cation data, the smaller sample was filtered to remove particulate matter larger than 5 microns, and reagent grade nitric acid was added to bring the pH to a value of approximately two.

Table E1 presents chemical data from the samples sites; Figure E1 gives the locations of these sites.

Map No.[1]	Name and Location	Map Index No.[2]	T°C	Ca	Mg	K	Na	Li	Cl	SiO_2	SO_4	CO_3/HCO_3	F	pH	Conductance Micromhos/cm	Collection Data
1	Bartine Ranch Area Springs T19N,R50SE,S4,5	#100	44.3°	69.0	17.3	12.1	37.1	0.113	8.96	37.0	24.5	334	0.889	7.47	634	5/80
2	Geococchea, Simonsen Warm Springs NE¼,NE¼,S1,T22N,R56E	#290	22.6°	41.5	20.1	6.73	17.6	0.01	6.68	20.1	34.5	6.49/217	0.319	8.65	472	5/80
3	Collar and Elbow Spring S27,T26N,R65E	#286	22.0°	49.3	17.2	3.95	8.43	0.01	5.05	24.4	20.1	226	0.334	7.74	418	5/80
4	Shelbourne Springs S12,T22N,R64E	#291	24.6°	56.4	16.7	1.38	4.28	0.01	3.58	22.8	18.8	232	0.235	8.29	420	5/80
5	Moon River Spring NW¼,S25,T6N,R60E	#222	29.5°	52.2	19.8	4.59	19.7	0.05	9.13	31.1	39.9	267	0.704	8.17	552	5/80
6	Williams Hot Springs NE¼,S33,T13N,R60E	#296	51.8°	.723	0.06	1.52	51.5	0.04	10.4	70.0	14.3	28.8/43.3	4.75	9.98	286	6/80
7	Preston Springs SW¼,NE¼,S2,T12,R61E	#297	22.7°	39.7	17.9	3.32	11.7	0.015	16.0	22.4	37.9	185	0.22	8.06	434	6/80
8	Mosquito Ranch Area Spring SE¼,NE¼,S6,T11N,R47E	#204	31.6°	7.16	0.512	1.90	42.8	0.03	7.66	68.3	17.8	9.28/83.0	0.889	9.12	229	5/80
9	Hall Mine Well Anaconda Molybdenum Project S8,T5N,R42E	--	27.7°	15.3	0.924	12.8	57.4	0.06	11.6	108	43.7	130	0.738	8.23	383	5/80
10	MacFarlane's Bath House Spring NW¼,S27,T37N,R29E	#133	61.6°	21.9	11.9	33.3	1180	0.511	831	99.6	196	1906	2.39	7.42	6210	6/80
11	Mound Spring S7,T28N,R44E	#151	30.0°	69.5	25.2	29	111	.43	18.3	19.1	87.3	492	3.04	7.1	1100	7/80
12	Dann Hot Spring NW¼,NW¼,NE¼,S10,T28N,R49E	# 92	85°	12.1	1.33	53.2	261	2.40	84.8	99.0	134	507	10.8	7.8	1100	7/80
12	Dann Ranch Well S2,T28N,R49E	--	28°	43.8	13.7	2.67	39	.06	15.8	19.6	28.4	225	0.378	7.2	420	7/80

[1] Map included in this report.

[2] Map index number for "Geothermal Resources of Nevada and their Potential for Direct Utilization". Trexler and others (1979).

Table E1. Chemistry of sampled sites for statewide assessment.

Map No.[1]	Name and Location	Map Index No.[2]	T°C	Ca	Mg	K	Na	Li	Cl	SiO_2	SO_4	CO_3/HCO_3	F	pH	Conductance Micromhos/cm	Collection Data
13	Hot Creek Springs S34,T43N,R60E	# 54	38.2°	67.2	21.6	20.0	24	.09	3.34	13.6	56.8	293	0.758	7.2	650	7/80
14	Rowland Hot Springs SE¼,NW¼,S14,T46N,R56E	# 43	58.7°	7.83	0.17	5.32	129	.88	12.6	51.5	49.8	254	12.8	8.0	1020	7/80
15	Hot Springs Ranch Springs S24,T37N,R43E	#135	25.3°	19.1	3.09	4.96	72	.10	18.6	33.3	26.9	185	6.16	7.4	350	7/80
16	Reveille Valley Mill Spring S28,T2N,R50E	#228	27.5	7.0	.23	.29	31	.047	6.5	47.7	12.5	/86.5	.859	7.23	188	8/80
17	Gunderson Well SE¼,SE¼,S19,T3S,R55E	#166	28°	15.7	1.75	7.02	43.8	.03	11.9	102	34.7	-/124	2.48	7.87	309	9/80
18	Walker Warm Spring SW¼,SE¼,S4,T7N,R27E	#184	34.5°	27.9	.66	3.0	212	.40	4.44	21.3	68.2	-/43.9	7.89	7.2	---	1/81
19	Gondra Well NE¼,SE¼,S22,T41N,R40E	#122	22°	23.	6.	57.	13	---	29.	83.	31.	-/173.	.7		510	1/81
20	McCoy Ranch Hot Springs S33,T26N,R39E	#261	50°	94.	36.5	10.	218.	0.00	286.	32.5	216.	-/312.	1.37	7.31	---	*
21	Hyder Cone Hot Springs SW¼,S28,T25N,R38E	#262	72°	43.	10.	20.2	334.	1.59	47.5	69.	111.	-/869.	8.1	7.22	---	*
22	Gabbs Area Wells S22,27,28,33,T12N,R36E	#199	63°	28.	0.00	6.	233.	---	40.	---	442.	8/17	9.25	8.42	---	*
23	Well No. 6 SW¼,SW¼,S6,T17N,R30E	---	72.8°	70.	3.1	41.5	1350.	2.3	2138.	104.	58.	-/189.7	1.40	8.0	6600	2/81
24	T.C.I.D. No. 1 SE¼,NW¼,NW¼,S15,T22N,R30E	---	70.4°	17.	3.1	73.	3000.	1.9	4531.	74.	120.	27.3/182.8	2.4	8.3	11500	2/81
25	Cheveron Kosmos 1-9 Well S9,T29N,R23E	#273	120.0	81.	.06	79.	1200.	1.7	2280.	---	300.	16/110	5.5	---	---	++

*Bohm, Burkhard W. (1980)
‡Booth, Martin (1981)
++Nevada Bureau of Mines and Geology Geothermal Open File.

Table El. (Continued)

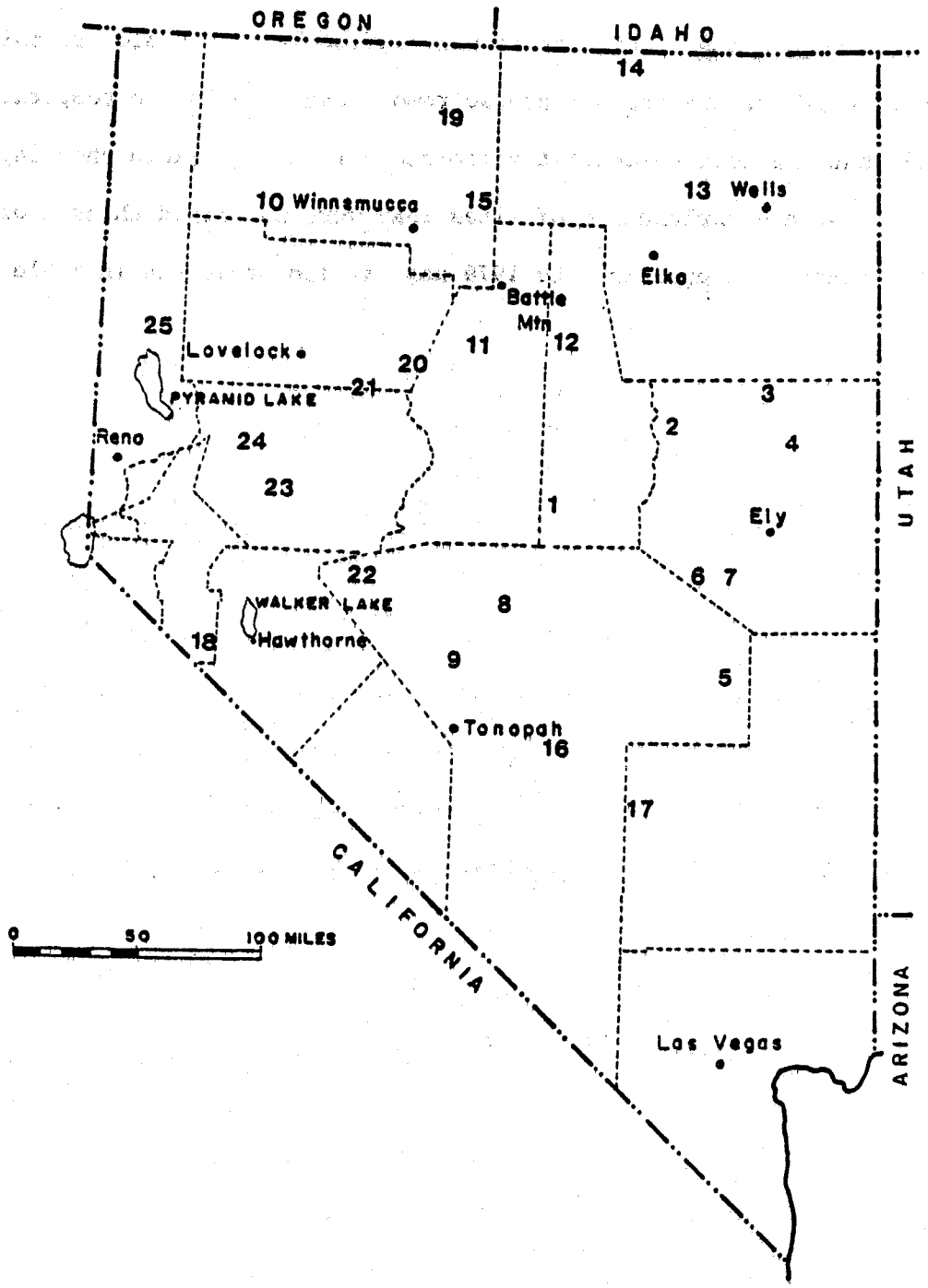

Figure E1. Locations of sample sites for statewide assessment.

It was not possible to obtain complete field information for all locations which lacked data in the 1979 compilation. In some cases either the well or spring could not be found, or it was physically impossible to collect samples. A few of the springs are so remote and marginal in temperature (20° - 25°C) that the cost-to-benefit ratio did not warrant field checking. Table E2 is a list and explanation of sites that were not field-checked or sampled. An errata list updating the 1979 map is also presented in Table E2.

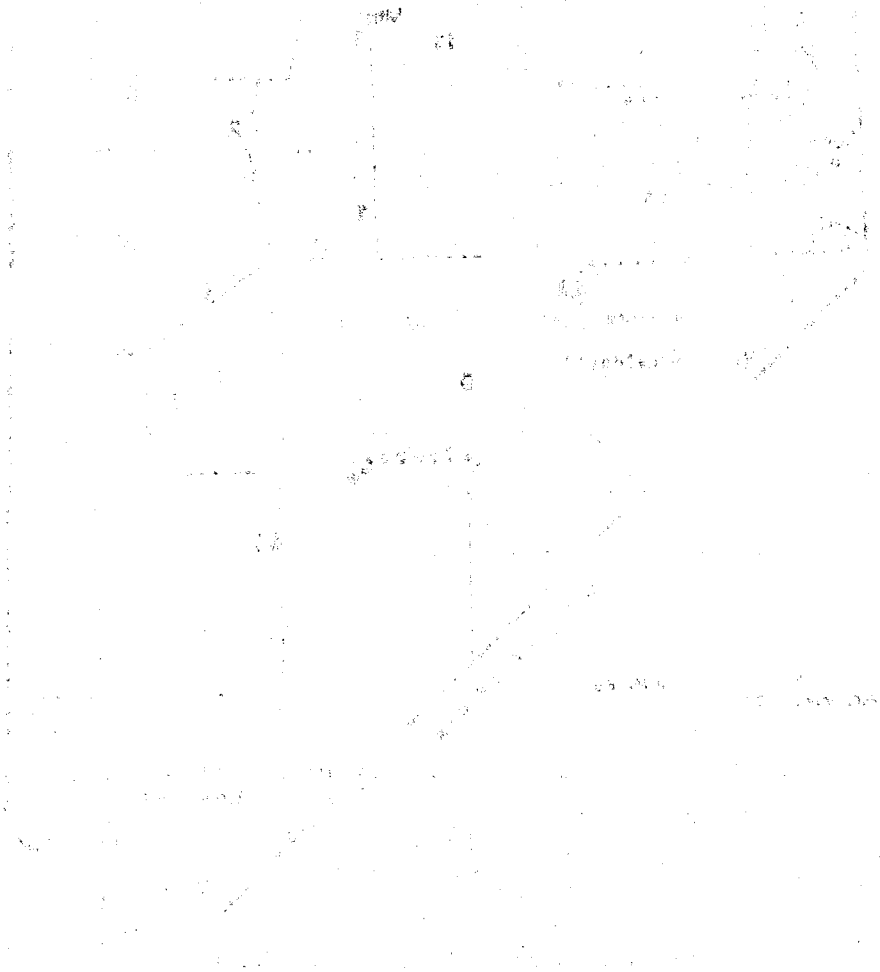

Table E2. List of unsampled sites and errata from "Geothermal Resources of Nevada and their Potential for Direct Utilization" (Trexler et al, 1979).

Map Index #	Name	Reason For Not Being Sampled
227	Warm Springs Valley Spring	Thought to be solar-heated.
265	Squaw Valley Springs	Unfavorable cost-to-benefit ratio.
98	Sulfur Springs	Unable to locate.
61	Well in Big Smoky Valley	No longer warm.
220	Hot Creek Valley Spring	Unable to locate.
83	Pearl Hot Springs	Dry.
84	Silver Peak Hot Springs	Dry.
162	Hammond Spring	Unfavorable cost-to-benefit ratio.
86	Spring	Unfavorable cost-to-benefit ratio.
29	Brown's Spring	Unfavorable cost-to-benefit ratio.
39	Doud Spring	Unfavorable cost-to-benefit ratio.
173	Magma Power Co. Hazen #1	Unable to locate.
12A	Fallon Naval Air Station Well	Unable to sample.
12B	Fallon Naval Air Station Well	Unable to sample.
11	Eight Mile Flat Borax Spring	Unable to locate.
247	Buffalo Valley Area Springs	Unable to locate.
58	Thousand Springs	Unable to locate; possibly dry.
66	Ralph's Warm Springs	Unable to sample.
215	Emigrant Spring	No longer warm.
81	Well	Unable to sample.
287	Well	Unable to sample.
148	Spring	Unable to sample.

Errata

60 Does not exist; probably a mislocation of #61.

37 Should have symbol for 1500 ppm TDS.

32 Name should not read Black Canyon area. The reference number should be 38.

110 The McGee Mtn. Area Springs are cold (10°C). The listing on the map is an exploration well 200 ft deep. It is doubtful this hole still exists.

12A and 12B are mislocated on the map. 12A should be SE¼, NW¼, Sec. 4, T18N, R29E. 12B should be NE¼, SW¼, Sec. 23, T18N, R29E.

BIBLIOGRAPHY

BIBLIOGRAPHY

Adams and Bishop , 1844, The Pacific Tourist: New York.

Birman, J. H., 1969, Geothermal exploration for ground water: Geol. Soc. America Bull., v. 80, p. 617-630.

Bohm, B. W. and Jacobson, R. L., 1977, Preliminary investigation of geothermal resources near Hawthorne, Nevada: Water Resources Center, Desert Research Institute, Proj. Rpt. No. 50, 30 p.

Bohm, B. W., Jacobson, R. L., Campana, M. E. and Ingraham, N. L., 1980, Ch. 5 Hydrology and Hydrogeochemistry in Geothermal Reservoir Assessment Case Study--Northern Dixie Valley, Nevada, Southland Royalty Co., Forth Worth, Texas DOE/ET/27006-1.

Booth, G. M. III, 1981, Preliminary plan for development of geothermal energy in the town of Gabbs, Nevada. Work performed for U.S. DOE Contract No.DE-FC03-80RA50075.

Bruce, J. L., 1979, Fallon Exploration Project, Naval Air Station, Fallon, Nevada. Technical publication No. 6194, Naval Weapons Center, China Lake, California.

Burchfiel, B. C. and Davis, G. A., 1972, Structural framework and evolution of the southern part of the Cordilleran orogen, western United States: Am. Jour. of Sci. v. 272, p.79-118.

Cartwright, Keros, 1966, Thermal prospecting for shallow glacial and alluvial aquifers in Illinois (abs.): Geol. Soc. America Abs. with program, 1966 annual meeting, p. 36.

Clayton, R. N., Muffler, L. P. J. and White, D. E., 1968, Oxygen isotope study of calcite and silicates of the River Ranch No. 1 Well,Salton Sea Geothermal Field, California. Am. J. Sci. v 266, p. 968.

Cohen, Philip, 1962, Preliminary results of hydrogeochemical studies in the Humboldt River Valley near Winnemucca, Nevada: Nevada Dept. of Cons. and Nat. Resources, Water Resources Bull. 19.

Compton, R. R., 1960, Contact metamorphism in the Santa Rosa Range, Nevada: Geol. Soc. America Bull., v. 71 p. 1383-1416.

Craig, H., 1963, The isotopic geochemistry of water and carbon in geothermal areas: Proc. Sploeto Conf. on Nuclear Geology, Tongiorgi, ed. p. 17-53.

Cusicanqui, H., Mahon, A. J. and Ellis, A. J., 1975, The geochemistry of the El Tatio geothermal field, Northern Chile: Proc. Second UN Symp., San Francisco, California, 20-29 May.

Dudley, W. W. and McGinnis, L. D., 1964, Seismic-refraction and earth resistivity investigation of hydrogeologic problems in Humboldt River Basin, Nevada, in geophysical studies in Nevada relating to hydrogeology: Nevada Dept. Cons. and Nat. Resources. Water Resources Bull. 25, (Univ. of Nevada Desert Research Inst. Tech. Report 2) p. 7-23.

Ekren, E. B., Bucknam, R. C., Carr, W. J., Dixon, G. L. and Quinlan, W. D., 1976, East-trending structural lineaments in central Nevada: U. S. Geol. Survey, Prof. Paper 986, 16 p.

Ellis, A. J. and Mahon, W. A. J., 1977, Chemistry and geothermal systems: Academic Press, New York, 392 p.

Erickson, R. L. and Marsh, S. P., 1971a, 1972, Geochemical, aeromagnetic and generalized geologic maps showing distribution and abundance of lead and silver, Golconda and Iron Point quadrangles, Humboldt County, Nevada: U. S. Geol. Survey Mineral Inv. Field Studies Map MF-315, scale 1:24,000, 2 sheets.

Erickson, R. L. and Marsh, S. P., 1971b, 1972, Geochemical, aeromagnetic and generalized geologic maps showing distribution and abundance of gold and copper, Golconda and Iron Point quadrangles, Humboldt County, Nevada: U. S. Geol. Survey Mineral Inv. Field Studies Map MF-314, scale 1:24,000, 2 sheets.

Erickson, R. L. and Marsh, S. P., 1971c, Geochemical, aeromagnetic and generalized geologic maps showing distribution and abundance of mercury and arsenic, Golconda and Iron Point Quadrangles, Humboldt County, Nevada: U. S. Geol. Survey Misc. Field Stud. Map No. MF-312, maps, scale 1:24,000.

Erickson, R. L. and Marsh, S. P., 1972, Geochemical, aeromagnetic and generalized geologic maps showing distribution and abundance of molybdenum and zinc, Golconda and Iron Point quadrangles, Humboldt County, Nevada: U. S. Geol. Survey Mineral Field Studies Map MF-345, scale 1:24,000, 2 sheets.

Erwin, J. W., 1974, Bouguer gravity map of Nevada, Winnemucca sheet: Nevada Bureau of Mines and Geology Map 47.

Erwin, J. W. and Berg, J. C., 1977, Bouguer Gravity Map of Nevada, Reno Sheet Nevada Bureau of Mines and Geology, Map 58.

Everett, D. E. and Rush, F. E., 1967, A brief appraisal of the water resources of the Walker Lake area, Mineral, Lyon and Churchill Counties, Nevada: Dept. Conservation Nat. Resources, Water Resources - Reconnaissance Series, Rpt. 40, 44 p.

Ferguson, H. G. and Muller, S. W., 1949, Structural geology of the Hawthorne and Tonopah Quadrangles, Nevada: U. S. Geol. Survey Prof. Paper 216, 53 p.

Ferguson, H. G., Roberts, R. J. and Muller, S. W., 1951, Geologic map of the Winnemucca quadrangle, Nevada: U. S. Geol. Survey Quad Map GQ-11.

Ferguson, H. G., Roberts, R. J. and Muller, S. W., 1952, Geology of the Golconda quadrangle: U. S. Geol. Survey Quadrangle Map. scale 1:1250,000.

Flynn, Thomas, Koenig, B. A., Trexler, D. T. and Bruce, J. L., 1980, Area-specific investigations of three low-to-moderate temperature geothermal resource areas in Nevada: Geothermal Resource Council Transactions, Vol. 4, p. 41-44.

Fournier, R. O. and Potter, R. W. II, 1979, Magnesium correction to the Na-K-Ca chemical geothermometer: Geochim. Cosmochim. Acta, v. 43, p. 1543-1550.

Fournier, R. O. and Rowe, J. J., 1966, Estimation of underground temperatures from silica content of water from hot springs and wet-steam wells: Am. J. Sci., v. 264, p. 685-697.

Fournier, R. O. and Truesdell, A. H., 1973, An empirical Na-K-Ca geothermometer for natural waters: Geochim. Cosmochim. Acta, v. 37, p. 1255-1275.

Garside, L. J. and Schilling, J. H., 1979, Thermal waters of Nevada, Nevada Bureau of Mines and Geology, Bulletin 91.

Goldstein, N. E., 1977, Northern Nevada geothermal exploration strategy analysis: Report prepared for U. S. DOE under contract W-7405-ENG-48, 55 p.

Goldstein, N. E. and Paulsson, B., 1979, Interpretation of gravity surveys in Grass and Buena Vista Valleys, Nevada: Geothermics, v. 7, p. 29-50.

Harrill, J. R. and Moore, D. O., 1970, Effects of groundwater regime at Paradise Valley, Humboldt County, Nevada, 1948-1968, and hydrologic reconnaissance of the tributary areas: Nevada Dept. of Cons. and Nat. Resources, Water Resources Bull. 39.

Hastings, D. D., 1979, Results of exploratory drilling, northern Fallon basin, western Nevada. RMAG-UAG, 1979 Basin and Range Symposium Guidebook, p. 515-522.

Healy, D. L, Wahl, R. R. and Currey, F. E., 1980, Complete Bouguer gravity map of the Nevada part of the Walker Lake 2° sheet: U. S. Geol. Survey Open File Rpt. 80-519, p. w/map at 1:250,000 scale.

Hill, D. G., Layman, E. B. Swift, C. M., Yungul, S. H., 1979,Soda Lake, Nevada thermal anomaly: Geothermal Resources Council, Annual Meeting Transaction, v. 3.

Hill, D. P. and Pakiser, L. C., 1967, Seismic-refraction study of crustal structure between the Nevada Test Site and Boise, Idaho: Geol. Soc. Am. Bull. v. 78, No. 6, p. 685-704.

Hotz, P. E. and Willden, Ronald, 1964, Geology and mineral deposits of the Osgood Mountains quadrangle, Humboldt County, Nevada: U. S. Geol. Survey Prof. Paper 431.

Kappelmeyer, O., 1957, The use of near-surface temperature measurements for discovering anomalies due to causes at depths: Geophysical prospecting, v. 5, No. 3, p. 239-258.

Ketner, K. B., 1977, Deposition and deformation of lower Paleozoic western facies rocks, northern Nevada, in Stewart, J. H., Stevens, C. H., Fritsche, A. E. eds., Paleozoic paleogeography of the western United States: Soc. Econ. Paleontologists and Mineralogists, Pacific Sec., Pacific Coast Paleogeography Symposium 1, p. 251-258.

Kintzinger, P. R., 1956, Geothermal survey of hot ground near Lordsburg, New Mexico: Science, v. 124, p. 629.

Koizumi, C. J., Ryall, A. S. and Priestley, K. F., 1973, Identification of a paleosubduction zone under Nevada. (abs): Earthquake Notes, v. 44, no. 1-2 p. 76.

Locke, Augustus, Billingsley, P. R. and Mayo, E. B., 1940, Sierra Nevada tectonic patterns: Geol. Soc. Am. Bull., v. 51, p. 513-540.

Loeltz, O. S., Phoenix, D. A. and Robinson, T. W., 1949, Groundwater in Paradise Valley, Humboldt County, Nevada: State of Nevada, Office of the State Engineer Water Resources Bull. 10.

Mabey, D. R., 1966, Regional gravity and magnetic anomalies in part of the Eureka County, Nevada, in Mining Geophysics - v. 1, Case Histories: Tulsa, Oklahoma, Soc. Explor. Geophysicists p. 77-83.

Mariner, R. H., Rapp, J. B., Willey, L. M. and Presser, T. S., 1974, Chemical composition and estimated minimum thermal reservoir temperatures of the principal hot springs of northern and central Nevada: U. S. Geol. Survey open-file report.

Marsh, S. P. and Erickson, R. L., 1974, Integrated geologic and geochemical studies, Edna Mountain, Nevada: International Geochemical Exploration Symp. Proc. No. 5, p. 29-30.

Miller, M. R., Hardman, George and Mason, H. G., 1953, Irrigation waters in Nevada: Nevada Univ. Agr. Exp. Sta. Bull. 187.

Moore, J. G., 1969, Geology and mineral deposits of Lyon, Douglas and Ormsby Counties, Nevada, with a section on industrial minerals by N. L. Archbold: Nevada Bureau of Mines Bull. 75, 44 p.

Morrison, R. B., 1964, Lake Lahontan, Geology of the Southern Carson Desert, Nevada. USGS Prof. Paper 401.

Muller, S. W. and Ferguson, H. G., 1936, Triassic and lower Jurassic formations of west central Nevada: Geol. Soc. Am. Bull, V. 47, p. 241-251.

Nevada Bureau of Mines and Geology, 1977, Aeromagnetic map of Nevada, Reno Sheet Nevada Bureau of Mines and Geology Map 54.

Olmsted, F. H., 1977, Use of temperature surveys to a depth of 1 meter in thermal exploration in Nevada: U. S. Geol. Survey Prof. Paper 1044-B.

Olmstead, F. H., Glancy, P. A., Harrill, J. R., Rush, F. E. and Van Denburgh, A. S., 1975, Preliminary hydrogeologic appraisal of selected hydrothermal systems in northern and central Nevada. USGS open file report 75-56.

Piper, A. M., 1944, A graphic procedure in the geochemical intrepretation of water-analyses: Transactions, American Geophysical Union Papers, Hydrology.

Poole, F. G., 1974, Flysch deposits of the Antler foreland basin, western United States, in Dickinson, W. R. ed, Tectonics and Sedimentation: Soc. Econ. Paleontologists and Mineralogists Spec. Pub. No. 22, p. 58-82.

Robinson, E. S., 1970, Relations between geological structure and aeromagnetic anomalies in central Nevada: Geol. Soc. America Bull. v. 81 p. 2045-2060.

Ross, D. C., 1961, Geology and mineral deposits of Mineral County, Nevada: Bull. 58, Nevada Bur. of Mines and Geol., 98 p.

Rowan, L. C. and Wetlaufer, P. H., 1973, Structural geologic analyses of Nevada using ERTS-1 images: A preliminary report: symp. of significant results obtained from ERTS-1, March 5-9, 1973, NASA/Goddard Space Flight Center, p. 413-423.

Rowan, L. C. and Wetlaufer, P. H., 1975, Iron-absorption band analysis for the discrimination of iron-rich zones: U. S. Geol. Survey, Final Rpt., prepared for NASA/Goddard Space Flight Center, under contract S-70243-AG, 152 p.

Ryall, A. S., Priestley, K. F., Savage, W. U. and Koizumi, C. J., 1973, Cenozoic tectonics related to a paleosubduction zone under northern Nevada (abs): Earthquake Notes, v. 44, No. 1-2, p. 76.

Rybach, L. and Muffler, L. P., 1980, Geothermal Systems: Principles and Case Histories: John Wiley and Sons, Ltd., p. 109-143.

Sanders, J. W. and Miles, M.J., 1974, Mineral content of selected geothermal waters: Nevada Univ., Reno, Desert Research Inst., Center for Water Resources Research Proj. Report 26.

Silberling, N. J., 1975, Age relationships of the Golonda thrust fault, Sonoma Range, north-central Nevada: Geol. Soc. Am. Spec. Paper No. 163, 28 pp.

Singer, I. A. and Brown, R. M., 1956, The annual variation of sub-soil temperatures about a 600-foot diameter circle: Am. Geophys. Union Transaction, v. 37, p. 743.

Slemmons, D. B., 1957, Geological effects of the Dixie Valley - Fairview Peak, Nevada, earthquakes of December 16, 1954. Seismol. Soc. Amer. Bull. v. 47, No. 4, p. 353-375.

Speed, R. C., 1977, Island-arc and other paleogeographic terrains of the late Paleozoic age in the western Great Basin, in Stewart, J. H., Stevens, C. H. and Fritsche, A. E., eds., Paleozoic Paleogeography of the western United States: Soc. Econ. Paleontologists and Mineralogist, Pacific. Sec., Pacific Coast Paleogeography Symp. 1, p. 349-362.

Speed, R. C., 1977b, Excelsior formation, west-central Nevada: Stratigraphic appraisal, new divisions, and paleogeographic interpretations: in Stewart, J. H., Stevens, C. H. and Fritche, A. E., eds., Paleozoic Paleogeography of the western United States: Soc. Econ. Paleontologists and Mineralogists, Pacific Sec., Pacific Coast Paleogeography Symposium, p. 349-362.

Stark, M., Wilt, M., Haught, J. R. and Goldstein, N., 1980, Controlled source electromagnetic survey at Soda Lakes geothermal area, Nevada. Final report, U. S. DOE contract W-7405-ENG-48, Lawrence Berkeley Laboratory, Univ. of California, Berkeley., Report No. LBL-11221.

Stewart, J. H., 1971, Basin and Range structure - a system of horsts and grabens produced by deep-seated extension: Geol. Soc. America Bull. v. 82. p. 1019-1044.

Stewart, J. H., 1980, Geology of Nevada: Nevada Bur. of Mines and Geol., Special Publication No. 4, 136 p.

Stewart, J. H. and Carlson, J. E., 1974, Preliminary geologic map of Nevada: U. S. Geol. Survey, Misc. Field Studies Map MF-609.

Stewart, J. H. and Carlson, J. E., 1978, Geologic map of Nevada, USGS, scale 1:500,000.

Stewart, J. H., Walker, G. F. and Kleinhampl, F. J., 1975, Oregon-Nevada lineament, Geology v. 5, p. 265-268.

Stiff, H. S., 1953, The interpretation of chemical water analyses by means of patterns. Jour. of Petroleum Technology, pp. 15-17.

Thompson, G. A., 1959, Gravity measurements between Hazen and Austin. A study of Basin and Range structure: Jour. Geophys. Res., v. 64, p. 217-229.

Thompson, G. A., 1960, Late Cenozoic structure of the Basin and Range, in XXI International Geologic Congr. Proceedings, Copenhagen, v. 18, p. 62-68.

Thompson, G. A. and Sandberg, C. H., 1958, Structural significance of gravity surveys in the Virginia - Mt. Rose area, Nevada and California: Bull. Geol. Jor. America, V. 69, p. 1269-1282.

Trexler, D. T., Bell, E. J. and Roquemore, G. R., 1978, Evaluation of lineament analysis as an exploration technique for geothermal energy, western and central Nevada: Final report of work performed for the U. S. Dept. of Energy under contract No. EY-76-5-08-0671, 78 p.

Trexler, D. T., Flynn, T. and Koenig, B. A., 1979, Assessment of low-to-moderate temperature geothermal resources of Nevada: Final report, NVO/01556-1.

Trexler, D. T., Koenig, B. A., Flynn, T. and Bruce, J. L., 1980, Assessment of the geothermal resources of Carson-Eagle Valleys and Big Smoky Valley, Nevada: First Annual Report, DOE/NV/10039-2.

U. S. Geological Survey, 1971, Aeromagnetic map of parts of the Walker Lake, Reno, Chico, and Sacramento 1° by 2° quadrangles, Nevada-California: Geophys. Invest. Map GP-751, scale 1:250,000.

Van Denburgh, A. S. and Rush, F. E., 1975, Source of nitrate in water from supply well 8, Hawthorne Naval Ammunition Depot, Nevada: U. S. Geol. Survey, Admin. Rpt., in cooperation with U. S. Navy, 23 p.

Van Wormer, J. D. and Ryall, A. S., 1980, Sierra Nevada-Great Basin boundary zone: Earthquake hazard related to structure, active tectonic processes, and anomalous patterns of earthquake occurrence: Bull. Seismological Soc. Am., v. 70, No. 5, p. 1557-1572.

Wahl, R. R., 1965, An interpretation of gravity data from the Carson Sink area, Nevada. Stanford University, unpubl. student paper.

Walker, P. M. and Trexler, D. T., 1977, Interpretive technique, uses and flight planning considerations for low sun-angle photography: Photogram. Eng. and Remote Sensing, v. XLIII, No. 4, p. 493-505.

White, D. E., 1968, Hydrology, activity, and heat flow of the Steamboat Springs thermal system, Washoe County, Nevada: U. S. Geol. Survey Prof. Paper 458-C, 109 p.

Willden, Ronald, 1964, Geology and mineral deposits of Humboldt County, Nevada: Nevada Bureau of Mines Bull. 59, 154 p.

Willden, R. and Speed, R. C., 1974, Geology and mineral deposits of Churchill County, Nevada. Nevada Bureau of Mines and Geology, Bull. 83.

☆U.S. GOVERNMENT PRINTING OFFICE: 1981-740-145/2443